CANOPIES IN AQUATIC ECOSYSTEMS: INTEGRATING FORM, FUNCTION, AND BIOPHYSICAL PROCESSES

EDITED BY: Virginia B. Pasour, Brian L. White, Marco Ghisalberti, Matthew Philip Adams, Matthew H. Long, Matthew A. Reidenbach, Uri Shavit and Julia E. Samson

PUBLISHED IN: Frontiers in Marine Science

frontiers Research Topics

frontiers

ISSN 1664-8714
ISBN 978-2-88963-340-1
DOI 10.3389/978-2-88963-340-1

About Frontiers

Frontiers is more than just an open-access publisher of scholarly articles: it is a pioneering approach to the world of academia, radically improving the way scholarly research is managed. The grand vision of Frontiers is a world where all people have an equal opportunity to seek, share and generate knowledge. Frontiers provides immediate and permanent online open access to all its publications, but this alone is not enough to realize our grand goals.

Frontiers Journal Series

The Frontiers Journal Series is a multi-tier and interdisciplinary set of open-access, online journals, promising a paradigm shift from the current review, selection and dissemination processes in academic publishing. All Frontiers journals are driven by researchers for researchers; therefore, they constitute a service to the scholarly community. At the same time, the Frontiers Journal Series operates on a revolutionary invention, the tiered publishing system, initially addressing specific communities of scholars, and gradually climbing up to broader public understanding, thus serving the interests of the lay society, too.

Dedication to Quality

Each Frontiers article is a landmark of the highest quality, thanks to genuinely collaborative interactions between authors and review editors, who include some of the world's best academicians. Research must be certified by peers before entering a stream of knowledge that may eventually reach the public - and shape society; therefore, Frontiers only applies the most rigorous and unbiased reviews.
Frontiers revolutionizes research publishing by freely delivering the most outstanding research, evaluated with no bias from both the academic and social point of view. By applying the most advanced information technologies, Frontiers is catapulting scholarly publishing into a new generation.

What are Frontiers Research Topics?

Frontiers Research Topics are very popular trademarks of the Frontiers Journals Series: they are collections of at least ten articles, all centered on a particular subject. With their unique mix of varied contributions from Original Research to Review Articles, Frontiers Research Topics unify the most influential researchers, the latest key findings and historical advances in a hot research area! Find out more on how to host your own Frontiers Research Topic or contribute to one as an author by contacting the Frontiers Editorial Office: researchtopics@frontiersin.org

CANOPIES IN AQUATIC ECOSYSTEMS: INTEGRATING FORM, FUNCTION, AND BIOPHYSICAL PROCESSES

Topic Editors:
Virginia B. Pasour, Army Research Office, United States
Brian L. White, University of North Carolina at Chapel Hill, United States
Marco Ghisalberti, University of Western Australia, Australia
Matthew Philip Adams, University of Queensland, Australia
Matthew H. Long, Woods Hole Oceanographic Institution, United States
Matthew A. Reidenbach, University of Virginia, United States
Uri Shavit, Technion Israel Institute of Technology, Israel
Julia E. Samson, Consultant, Amsterdam, Netherlands

Citation: Pasour, V. B., White, B. L., Ghisalberti, M., Adams, M. P., Long, M. H., Reidenbach, M. A., Shavit, U., Samson, J. E., eds. (2020). Canopies in Aquatic Ecosystems: Integrating Form, Function, and Biophysical Processes. Lausanne: Frontiers Media SA. doi: 10.3389/978-2-88963-340-1

Table of Contents

frontiers in Marine Science

EDITORIAL
published: 15 November 2019
doi: 10.3389/fmars.2019.00697

Editorial: Canopies in Aquatic Ecosystems: Integrating Form, Function, and Biophysical Processes

Julia E. Samson[1], Marco Ghisalberti[2], Matthew Philip Adams[3], Matthew A. Reidenbach[4], Matthew H. Long[5], Uri Shavit[6] and Virginia B. Pasour[7]*

[1] Department of Biology, University of North Carolina at Chapel Hill, Chapel Hill, NC, United States, [2] Oceans Graduate School, University of Western Australia, Perth, WA, Australia, [3] School of Earth and Environmental Sciences, School of Biological Sciences, and School of Chemical Engineering, University of Queensland, Brisbane, QLD, Australia, [4] Department of Environmental Sciences, University of Virginia, Charlottesville, VA, United States, [5] Department of Marine Chemistry & Geochemistry, Woods Hole Oceanographic Institution, Woods Hole, MA, United States, [6] Department of Civil and Environmental Engineering, Technion Israel Institute of Technology, Haifa, Israel, [7] Army Research Office, Durham, NC, United States

Keywords: fluid dynamics, ecosystem engineering, coral, algae, canopy, mass transport, light availability, nutrient cycling

Editorial on the Research Topic

Canopies in Aquatic Ecosystems: Integrating Form, Function, and Biophysical Processes

This Research Topic presents new research investigating the coupling between physical (fluid dynamics, mass transport, and light availability) and biological (nutrient cycling, particle transport, ecosystem structure, and biodiversity) processes in aquatic canopies. The starting point for this topic was the observation that our notion of "canopy" in the aquatic sciences, in contrast to that of our terrestrially-focused colleagues, remains underdeveloped. Forest canopy studies have been considered a new field of science (Nadkarni et al., 2011) and the concept of forest canopy research is clearly documented in the literature (Barker and Pinard, 2001; Nadkarni, 2001; Lowman, 2009); we have not found similar mentions of the canopy concept in aquatic studies. Over the past decade, however, there has been an increase in the number of studies on underwater canopies, as well as a shift toward more multidisciplinary studies that consider more than just the physical impacts of the canopy's presence (Ackerman, 2007; Nepf et al., 2007; O'Brien et al., 2014).

Through this Research Topic, we provide a platform to explore the various physical and ecological impacts of aquatic canopies on the broader environment. We considered a fairly broad definition of canopy and did not restrict the concept to macroscale algae and corals. Any biological or physical entity displaying canopy-like characteristics (notably resistance to flow in the water column) is of interest for understanding canopy impacts. Additionally, we acknowledge that underwater canopies are not usually static structures but display dynamic behavior and can change over time and space.

An important goal of this Research Topic was to start integrating different (methodological) approaches and discipline-specific viewpoints to develop a more holistic view of how canopies shape their ecosystems. Oftentimes, studies have focused on a single aspect of the canopy, creating a one-dimensional view of its function in a given ecosystem, for example as a flow regulator (Nepf and Vivoni, 2000; Ghisalberti and Nepf, 2009) or as a photosynthetic structure (Binzer et al., 2006). Understanding the strong and inherent coupling between a canopy's physical and biological impacts, however, would provide much more insight into the importance and function of canopies in aquatic ecosystems.

The manuscripts we received were diverse in the topics they treated as well as their aims and approaches. Several papers in our collection investigated canopies from a mechanistic point of view, looking at the effects of canopy structure on flow and the resulting ecosystem impacts.

OPEN ACCESS

Edited and reviewed by:
Angel Borja,
Technological Center Expert in Marine and Food Innovation (AZTI), Spain

****Correspondence:***
Julia E. Samson
juliasamson@mac.com

Specialty section:
This article was submitted to Marine Ecosystem Ecology, a section of the journal Frontiers in Marine Science

Received: *28 September 2019*
Accepted: *29 October 2019*
Published: *15 November 2019*

Citation:
Samson JE, Ghisalberti M, Adams MP, Reidenbach MA, Long MH, Shavit U and Pasour VB (2019) Editorial: Canopies in Aquatic Ecosystems: Integrating Form, Function, and Biophysical Processes. Front. Mar. Sci. 6:697. doi: 10.3389/fmars.2019.00697

Starting at the sub-meter scale, van Rooijen et al.'s work on predicting drag forces in canopies offers a detailed understanding of canopy-flow interactions. The authors provide a robust tool to quantify canopy flow resistance across a range of canopy types (emergent or submerged, rigid or flexible). Their model will prove to be useful in further studies requiring accurate drag quantification in canopy environments, for example when studying reduced in-canopy flow environments or measuring the impact of the canopy on sedimentation.

At the canopy level, Fonseca et al. considered the interactions between canopy-forming organisms and their environment (both biotic and abiotic factors). They examined the importance of shoot flexibility and shoot density in seagrass beds that are exposed to flow and how these parameters influence hydrodynamics, turbulence, sedimentation, and light penetration within the seagrass bed.

Moving up from the seagrass bed to the meadow scale, Reidenbach and Thomas show that seagrass canopies exert significant control over both wave height and hydrodynamic conditions at the sediment-water interface. Their findings suggest that the role of seagrass canopies in sedimentation and the (re-)suspension of sediment particles in the water column is not confined to the seagrass bed, but extends beyond and above it, impacting the ecosystem more generally.

A couple of papers in the Research Topic looked directly at the functional effects a canopy can have at the ecosystem level. An important impact of the canopy that was highlighted is the influence of algal canopies on local recruitment. As shown by Umanzor et al., low canopy densities favor the recruitment of more seaweeds whereas high canopy densities displayed a higher abundance of microphytobenthic (benthic diatoms and cyanobacteria) recruits. They conclude that small-scale biophysical interactions linked to seaweed morphologies and densities can have profound effects on the recruitment and settlement of new primary producers. These interactions are often overlooked but can have significant consequences on the dynamics of the overall ecosystem.

Shifting ecosystem dynamics have been observed in the seagrass beds of the Chesapeake Bay, where one seagrass species, *Zostera marina*, is being replaced in some locations by *Ruppia maritima*. French and Moore investigated how seagrass species, biomass, and density affected invertebrate communities and sediment properties. They found correlations between seagrass species and sediment coarseness, shoot density and invertebrate biodiversity, and between seagrass biomass and both invertebrate biodiversity and abundance. Although seagrass species might not directly influence which invertebrate species are found, changes in sediment coarseness and seagrass biomass could well-affect the fauna abundance as well as the physical conditions under which they thrive.

Other papers highlighted the importance of going beyond the existing boundaries between research communities. In their perspective article, Stevens and Plew call for more connection and exchange between biophysicists focusing on natural marine canopies and those concentrating on "built" canopies (i.e., suspended aquaculture canopies) commonly used in (shell)fish farms. Though their purposes might differ (answering ecological vs. economic questions), both groups of researchers would benefit from learning more about each other's approaches and insights.

Taking a higher-level view, Folkard's comprehensive review provides guidelines for future exploration (including a request for physicists and ecologists to move toward each other in terms of methodology, reminding us of Stevens and Plew's call for more connection between research communities) and urges researchers to make the leap to the landscape-scale. Putting biophysical processes happening in aquatic canopies back in their landscape-wide context is crucial to support and inform management and conservation efforts since most of them take place at this scale.

In fact, a few papers in this collection have already taken up this call. Follett et al.'s contribution shows how seagrass bed parameters such as shoot density affect local hydrodynamics, which in turn affect pollen dispersion in the bed, and thus genetic variation in offspring (seeds) based on location height within the canopy. This paper also illustrates how modeling and experimental/field approaches can complement each other and lead to a more robust understanding of canopy systems.

Finally, on the largest scale, Ørberg et al. investigated the role of canopy-forming algae in the subarctic intertidal. *Ascophyllum* seaweeds were shown to facilitate higher species richness and recolonization by increasing habitat surface and complexity and modifying environmental stressors such as extreme temperature or desiccation. In the context of climate change, *Ascophyllum nodosum*'s distribution range is expected to shift northwards, thus promoting the northward colonization of intertidal fauna in the Arctic.

From microscale hydrodynamic forces affecting sedimentation to allelic variation, invertebrate biodiversity, and the colonization of new habitats, the many impacts of aquatic canopies on the broader environment constitute a burgeoning area of research. Our understanding of what these canopies are, how they function, and how they influence entire ecosystems is rapidly expanding. Cross-disciplinary initiatives, including those presented in this topic, will continue feeding this momentum and lead us to new and important insights.

AUTHOR CONTRIBUTIONS

JS, MG, MA, MR, ML, and VP contributed input for the editorial. JS wrote the editorial. MG and MA gave extensive feedback on the draft. MG, MA, MR, ML, US, and VP gave feedback on the finalized version.

FUNDING

MA acknowledges funding support from Australian Research Council (ARC) Linkage Grant LP160100496 and the National Environmental Science Programme (NESP) Tropical Water Quality Hub. Funding to MR provided by the National Science Foundation (DEB-1237733 and DEB-1832221) and by a NSF CAREER grant (OCE-1151314). ML was supported by NSF OCE grant 1633951.

REFERENCES

Ackerman, J. D. (2007). Diffusivity in a marine macrophyte canopy: implications for submarine pollination and dispersal. *Am. J. Bot.* 89, 1119–1127. doi: 10.3732/ajb.89.7.1119

Barker, M. G., and Pinard, M. A. (2001). "Forest canopy research: sampling problems, and some solutions," in *Tropical Forest Canopies: Ecology and Management, Forestry Sciences, Vol. 69,* eds K. E. Linsenmair, A. J. Davis, B. Fiala, and M. R. Speight (Dordrecht: Springer), 23–38.

Binzer, T., Sand-Jensen, K., and Middelboe, A.-L. (2006). Community photosynthesis of aquatic macrophytes. *Limnol. Oceanogr.* 51, 2722–2733. doi: 10.4319/lo.2006.51.6.2722

Ghisalberti, M., and Nepf, H. M. (2009). Shallow flows over a permeable medium: the hydrodynamics of submerged aquatic canopies. *Trans. Porous Med.* 78:309. doi: 10.1007/s11242-008-9305-x

Lowman, M. D. (2009). Canopy research in the twenty-first century: a review of arboreal ecology. *Trop. Ecol.* 50, 125–136.

Nadkarni, N. M. (2001). Enhancement of forest canopy research, education, and conservation in the new millennium. *Plant Ecol.* 153, 361–367. doi: 10.1023/A:1017546225607

Nadkarni, N. M., Parker, G. G., and Lowman, M. D. (2011). Forest canopy studies as an emerging field of science. *Ann. For. Sci.* 68:217. doi: 10.1007/s13595-011-0046-6

Nepf, H. M., Ghisalberti, M., White, B., and Murphy, E. (2007). Retention time and dispersion associated with submerged aquatic canopies. *Water Resour. Res.* 43:W04422. doi: 10.1029/2006WR005362

Nepf, H. M., and Vivoni, E. R. (2000). Flow structure in depth-limited, vegetated flow. *J. Geophys. Res.* 105, 28547–28557. doi: 10.1029/2000JC900145

O'Brien, J. M., Lessard, J. L., Plew, D., Graham, S. E., and McIntosh, A. R. (2014). Aquatic macrophytes alter metabolism and nutrient cycling in lowland streams. *Ecosystems* 17, 405–417. doi: 10.1007/s10021-013-9730-8

Conflict of Interest: The authors declare that the research was conducted in the absence of any commercial or financial relationships that could be construed as a potential conflict of interest.

frontiers in Marine Science

ORIGINAL RESEARCH
published: 03 September 2018
doi: 10.3389/fmars.2018.00296

Intertidal Seaweeds Modulate a Contrasting Response in Understory Seaweed and Microphytobenthic Early Recruitment

Schery Umanzor[1†], *Lydia Ladah*[1*] *and José A. Zertuche-González*[2]

[1] *Department of Biological Oceanography, CICESE, Ensenada, Mexico,* [2] *Departamento de Oceanografía Biológica, Instituto de Investigaciones Oceanológicas, Universidad Autónoma de Baja California, Ensenada, Mexico*

Recruitment is a fundamental step upon which all subsequent interactions within a community occur. We explored how the attenuation of physical conditions by seaweed plots comprised of either *Chondracanthus canaliculatus*, *Pyropia perforata*, *Sylvetia compressa* or a mixed aggregation, at varying densities (average 1,199, 816, and 408 in. m^{-2}), affected recruitment of seaweeds and microphytobenthic organisms in the understory, and if physical factors modulate their abundance and distribution. We outplanted macroscopic seaweeds in the intertidal and measured changes in understory irradiance, particle retention, and bulk water flow. Both factors influenced physical conditions below the canopy. However, only canopy density had a significant effect on recruitment. The low-density canopy treatments had a greater abundance of seaweed recruits, with the opposite found for microphytobenthic organisms. The recruitment processes of seaweeds and microphytobenthic organisms, however, appeared to be independent of each other and were not due to competition. We conclude that it is crucial to consider microscale biological interactions, which are rarely addressed when assessing recruitment processes of benthic primary producers.

Keywords: bioengineers, rocky intertidal, seaweed spores, sporophytes, understory settlement

OPEN ACCESS

Edited by:
Marco Ghisalberti, University of Western Australia, Australia

Reviewed by:
Anna R. Armitage, Texas A&M University at Galveston, United States
David Ian Taylor, Cawthron Institute, New Zealand

***Correspondence:**
Lydia Ladah
lladah@cicese.mx

***Present Address:**
Schery Umanzor, Department of Ecology and Evolutionary Biology, University of Connecticut, Stamford, CT, United States

Specialty section:
This article was submitted to Marine Ecosystem Ecology, a section of the journal Frontiers in Marine Science

Received: *05 February 2018*
Accepted: *03 August 2018*
Published: *03 September 2018*

Citation:
Umanzor S, Ladah L and Zertuche-González JA (2018) Intertidal Seaweeds Modulate a Contrasting Response in Understory Seaweed and Microphytobenthic Early Recruitment. Front. Mar. Sci. 5:296. doi: 10.3389/fmars.2018.00296

INTRODUCTION

Abiotic factors can affect both the distribution and abundance of organisms, thus modulating community structure (Crain and Bertness, 2006). In a recent contribution, Umanzor et al. (2017) explored how different seaweed aggregations influenced the abundance and distribution of understory microphytobenthic (MPB) organisms (benthic diatoms and cyanobacteria) on an exposed rocky intertidal. Results showed that the settlement of microphytobenthic organisms was modulated by the interaction between the species composition and the density of the seaweed aggregations, with branched morphologies at higher densities having higher particle retention and greater abundance of MPB organisms underneath their canopies. Authors also reported recruitment (here defined as early post- settlement *sensu* Vadas et al., 1992) of seaweeds, although there was no further analysis on recruitment patterns of seaweed spores across the treatments. Therefore, in this contribution, we repeated the experiment assessing the effect that macroscopic seaweeds as ecosystem engineers had on the recruitment of the microscopic stages of seaweeds (spores, gametophytes, and early sporophytes). We then evaluated the factors that could be affecting the patterns of distribution and abundance of seaweed recruits underneath manipulated canopies in the intertidal compared to MPB settlement.

Positive interactions and stress attenuation can play an important role in determining the establishment and survival of seaweed recruits (Bertness et al., 1999; Choi and Norton, 2005; Bennett and Wernberg, 2014). Overall, recruitment is the key process upon which all subsequent interactions within a community will occur. As such, variations in successful recruitment events can substantially influence the dynamics of adult populations (Woodin, 1991; Vadas et al., 1992). Evidence shows that there are multiple factors, both inherent and external to the species, that can influence successful settlement and recruitment of early stages. Inherent factors can include the number of propagules produced, growth rates and size of settling cells, germination and spore viability, and even the strength of adhesion by early propagules (Vadas et al., 1992).

On the other hand, external factors such as particle movement resulting in sedimentation, siltation, scour or increased turbidity might affect early settlers by either preventing or enhancing their survival. On the Great Barrier Reef, for example, increased sedimentation has significantly decreased the rates of recruitment, survival, growth, and regeneration of *Sargassum* sp. (Umar et al., 1998). Also, in a laboratory experiment, Watanabe et al. (2016) found that the adhesion rate of spores and the gametophyte survival and growth rates of *Eisenia* sp. (now *Ecklonia*) declined noticeably with increasing sedimentation rates. Particle movement resulting in complete burial or sand scour can, however, also have a positive outcome for some algal species such as *Rhodomela, Penicillus,* and *Halimeda*, allowing their colonization of areas where other species would not thrive (Hurd et al., 2014).

Moreover, substrate properties such as its topography and stability can also greatly enhance or reduce successful seaweed recruitment. In a controlled experiment, Callow et al. (2002) tested how varying microtopographies affected the settlement of *Enteromorpha* sp. spores. They found that lower profile topographies significantly reduced the abundance of settled spores. Contrarily, Schumacher et al. (2007) found that smooth surfaces enhanced spore settlement of *Ulva* sp. In fact, Linskens (1966) reported that algae propagules will either settle on smooth or rugose surfaces, depending on the species. Coupled with the substrate properties, water motion is another factor that has long been studied as critical in influencing settlement and survival of seaweed propagules (Vadas et al., 1992). Seaweed zygotes use a range of adhesive mechanisms for attachment, allowing them to either thrive in low or high wave-energy environments. Through field and laboratory experiments, Taylor and Schiel (2003) demonstrated that the "stickability" of *Durvillaea antarctica* zygotes allowed the species to attach immediately and firmly to surfaces exposed to different wave regimes, resulting in high rates of survival when compared to zygotes of *Hormosira banksii* and *Cystophora torulosa*.

For intertidal seaweeds, desiccation stress due to aerial exposure can also cause increased mortality of early stages. Brawley and Johnson (1991) showed that without the protection against water loss provided by parental canopies, a large percentage of seaweed early settlers would inevitably die. However, pre-existing canopies can also represent a stressful biotic force, which can also potentially influence recruitment success. Canopies can cause shading, sweep propagules away or prevent settlement entirely, outcompete them for space and nutrients, or cause chemical interferences (Sousa, 1979; McCourt, 1984; Brawley and Johnson, 1991), that in the short term will trigger high mortality rates of potential new settlers. Evidence for canopy inhibition of early-post settlement or recruitment has been recorded in succession and reproductive ecology studies in the intertidal zone, with overall recruitment increasing due to the attrition of canopy cover (Sousa, 1979; Robertson, 1987).

Together, seaweed aggregations and microphytobenthic biofilms can interact directly or indirectly by modifying biophysical parameters (Fong et al., 1993; Hardison et al., 2013), and thus a influence the recruitment of associated organisms. For example, Hardison et al. (2013) measured the independent and interactive effect that both the MPB and benthic macroalgae can have on the quality and quantity of sediment organic matter (SOM). They concluded that while the MPB increased the SOM liability, benthic macroalgae tend to decrease it. They also found that both groups influenced bacterial build-up that could have a further effect on hypoxia events, sulfide accumulation, mineralization or denitrification of shallow water systems. Bacterial build up can also be important in determining the abundance and distribution of a variety of organisms, as for many benthic invertebrates, larval settlement occurs in response to bacterial cues (Freckelton et al., 2017).

Despite the many contributions related to seaweed recruitment in the intertidal zone, few studies have simultaneously explored the recruitment and development of seaweeds and the MPB. In part, this could be attributed to the difficulty in obtaining *in situ* measurements from organisms of such small size, but also could be due to the complexity of characterizing the microenvironment they inhabit. However, because seaweed recruits and MPB colonize similar areas, we expect the abundance of their early stages to be limited or enhanced by the same physical factors. Consequently, we tested the following hypotheses: (1) seaweed recruitment shows a similar abundance and distribution underneath intertidal canopies of different species and densities and (2) seaweed recruitment follows the same pattern of distribution as the microphytobenthos underneath seaweed canopies. We constructed experimental quadrats consisting of *Pyropia perforata* (Agardh, 1883), *Silvetia compressa* (Agardh, 1848), *Chondracanthus canaliculatus* (Harvey, 1840), and a mixed assemblage comprised of the former three, at three densities. We then determined if seaweed recruitment was correlated to the attenuation of bulk water flow, particle transport, and irradiance driven by the experimental canopies.

MATERIALS AND METHODS

Study Site

Experiments were conducted for a 15-day period on a rocky shore in Baja California (31° 51′ 41.6″ N and 116° 39′ 58.1″ W) during spring (2016) when the selected seaweeds *(C. canaliculatus, Silvetia compressa,* and *P. perforata*) were abundant. These species were selected because they are among the most common species in local intertidal sites, often forming dense beds or patches. This area has a semidiurnal tidal cycle with two low tides and two high tides of different heights per day (Umanzor

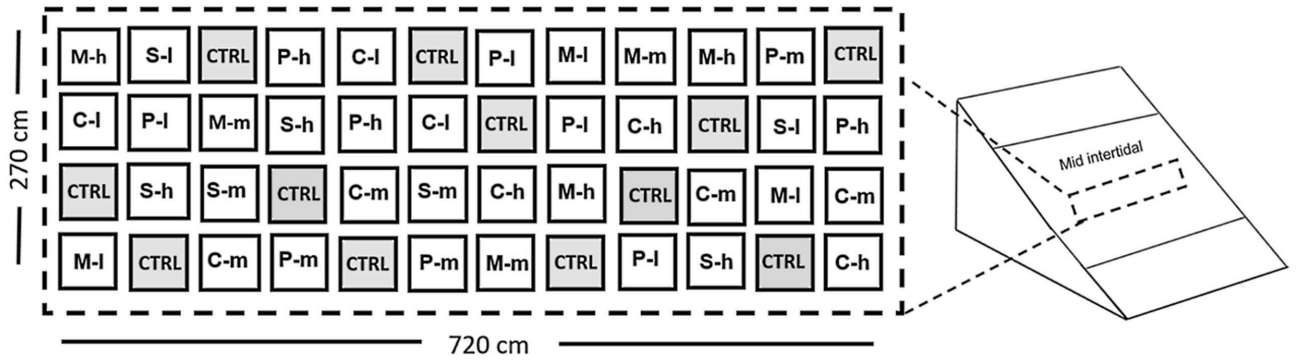

FIGURE 1 | Experimental design comprising 48 randomly distributed quadrats including either *Chondracanthus canaliculatus* (C), *Silvetia compressa* (S), *Pyropia perforata* (P), or the mixed assemblage (M) at a given density: high (h), medium (m), low (l), or control (CTRL). Quadrats were assembled with ropes cultured with fragments of the selected seaweeds.

TABLE 1 | Plaster bar erosion, irradiance, particle retention, and abundance of microphytobenthic organisms and microscopic stages of seaweeds based on species composition, density, and their interaction, using a two-factor crossed ANOVA.

	df treatments (df error)	*F*	*p*
BULK WATER FLOW			
Species composition	3 (32)	1.5	NS
Density	3 (32)	297	<0.001
Interaction	9 (32)	1.2	NS
IRRADIANCE			
Species composition	3 (32)	9.3	<0.001
Density	3 (32)	16.8	<0.001
Interaction	9 (32)	1.3	NS
PARTICLE RETENTION			
Species composition	3 (32)	8.6	<0.001
Density	3 (32)	46.4	<0.001
Interaction	9 (32)	2.3	<0.05
MICROPHYTOBENTHOS			
Species composition	3 (32)	1.9	NS
Density	3 (32)	63.4	<0.001
Interaction	9 (32)	2.2	NS
SEAWEED MICROSCOPIC STAGES			
Species composition	3 (32)	0.6	NS
Density	3 (32)	8.6	<0.001
Interaction	9 (32)	1.7	NS

et al., 2017). The experimental quadrats were fixed in the mid-intertidal zone, where seaweeds are generally abundant, but in a clear section allowing us to minimize effects caused by natural stands of seaweed. All quadrats remained submerged during high tides and the less extreme low tides.

Targeted Seaweeds

Chondracanthus canaliculatus is a corticated red alga, abundant from the mid to low rocky intertidal zones in Baja California. Although the species is perennial, it is particularly abundant during spring and summer when growth peaks (García-Lepe et al., 1997). The fucoid *Silvetia compressa* is a leathery brown alga, abundant in the upper and mid intertidal. It is a perennial species, which produces eggs ranging from 80 to 100 μm, showing peak recruitment periods throughout the year (Johnson and Brawley, 1998). Finally, *P. perforata* is a foliose red algae, abundant in the upper and mid intertidal, with peak abundance during spring and summer (Zertuche-González et al., 2000). In Baja California, the macroscopic stages of *P. perforata* can persist throughout the year. Both red algae can produce spores larger than 20 μM (Knight and Nelson, 1999; Maggs and Callow, 2003; Avila et al., 2011). At the time of the experiment, at least 50% of all blades were reproductive.

Experimental Design

To determine the effect that different canopies had on the recruitment of seaweeds compared to recruitment of MPB cells, we installed experimental quadrats in the intertidal zone. Quadrats consisted of monocultures of the selected species or a mixed tri-culture (including all three species) at three densities each. We assembled each quadrat using seaweed fragments of approximately 10 cm in lenght collected from the intertidal zone. Densities were assigned based on the maximum density of these species per square meter on a nearby rocky shore, quantified *in situ* before sample collection. In addition, control treatments with no algae were included. Quadrats were checked daily, and seaweeds showing any damage were immediately replaced by fresh ones to maintain the appropriate density for each treatment.

As each treatment included three replicates, the design comprised 48 quadrats total (**Figure 1**), following an orthogonal approach (Underwood, 1997). Quadrats consisted of 30 x 30 cm steel frames covered with plastic netting to which seaweeds and data collection devices were attached. Quadrats were individually secured to the intertidal using 2.5 kg lead weights. Settlement slides, particle collectors, light meters, and plaster cylinders were fixed underneath the canopy in each quadrat.

Physical Variable Sampling

Relative measurements of light levels were obtained using light meters (ONSET™ computer corp., Ma, USA) attached below the canopies and programmed to record every 15 min for a 7-day period. We calculated particle retention below the canopies by dry weight differences of two synthetic fiber pads (25 × 75 mm, initial weight 1.362 ± 0.003 g) per quadrat. Pads were collected after a 48 h period underneath the canopies. After collection, fiber pads were oven dried at 70°C for 60 h and then weighed three times (Sartorius, Germany ± 0.0001 g) to obtain the average weight per day per quadrat. A proxy measure of the relative bulk water flow underneath the canopies was acquired using the dissolution of plaster. Two cylindrical plaster bars (1 × 8 cm, initial weight 10.422 ± 0.005) were installed per quadrat and subsequently removed after 48 h. The bars were then oven dried at 70°C for 72 h before weighing them three times to obtain an average per quadrat. The difference in dry weight before and after deployment allows a relative estimate of bulk water flow based on the dissolution of plaster in a given area over a standardized time when compared to a control with no water motion (Komatsu and Kawai, 1992).

Microscopic Seaweed and Microphytobenthic Recruitment

To assess recruitment by seaweed microscopic stages and the microphytobenthos, a transparent polycarbonate slide (25 × 75 × 3 mm) was fixed underneath every canopy treatment and collected after a 15-day period. After collection, slides were placed individually in Petri dishes containing filtered (1 μM) seawater and immediately fixed with Lugol's solution (1%) for direct cell counting at 400x with an inverted microscope (Zeiss AxioObserver, Germany). We divided each slide into 10 equally sized sections from which a photograph was taken. We used all photographs for recruitment quantification and identification. For seaweed recruitment, we considered spores, gametophytes, and early sporophytes, regardless of size. When possible, we further classified them as red, brown or green. For the MPB, we only considered cells bigger than 20 μm because we could not photograph smaller cells with enough detail to ensure their correct identification.

Data Analysis

Density (high, medium, low, and control) and species composition (*S. compressa, C. canaliculatus, P. perforata,* and mixed culture) were considered categorical and independent factors. Natural log transformations were conducted as required to satisfy the assumptions (Underwood, 1997). Normality (Shapiro-Wilk test), independence of variables (Durvin-Watson test) and homogeneity of variances (Cochran's test) were confirmed per factor and level.

The iterative effect of the two categorical factors on bulk water flow, particle retention, irradiance, and seaweed and MPB recruitment was used in an ANOVA by least mean squares at an alpha value of 0.05. *Post-hoc* (Tukey test) comparisons were conducted where differences were found. Also, simple and multiple regressions were performed to identify which environmental factor or combined factors resulted in significant

TABLE 2 | Measures of plaster bars final weight, irradiance, and particle retention as a function of species composition, density and their interaction.

Level of factor	Level of factor	Plaster bar final weight (g)		Irradiance (μm quanta m^{-2} s^{-1})		Particle retention (g m^{-2})	
		Mean	± S.E.	Mean	± S.E.	Mean	± S.E.
C. canaliculatus				110.2	13.8		
P. perforata				131.9	17.8		
S. compressa				74.5	18.5		
Mixed culture				135.6	12.7		
High		9.2	0.05	62.3	13.2		
Medium		9.2	0.04	84.8	10.3		
Low		8.2	0.05	132.9	12.4		
C. canaliculatus	High					2341.8	142.2
C. canaliculatus	Medium					1263.4	93.6
C. canaliculatus	Low					720.6	133.7
P. perforata	High					1161.8	56.1
P. perforata	Medium					842.7	161.7
P. perforata	Low					506.8	92.8
S. compressa	High					2323.2	67.5
S. compressa	Medium					1548.7	158.7
S. compressa	Low					618.5	139.2
Mixed culture	High					1472.3	65.6
Mixed culture	Medium					999.2	94.9
Mixed culture	Low					621.5	108.0
Control		7.3	0.06	272.2	9.7	662.4	63.1

predictors of the abundance of both groups and to determine if any correlation existed between them. Outputs and raw data of the variables measured in this manuscript are available through the figshare repository (http://figshare.com), doi: 10.6084/m9.figshare.5797137.

RESULTS

Overall, the differences in the ability of the canopies to attenuate intertidal physical conditions seemed to influence the abundance of seaweed recruitment underneath the canopies directly. In general, higher abundances of seaweed recruits occurred underneath canopy treatments with the least attenuated physical conditions, whereas the MPB showed the lowest abundance under these conditions.

Algal species and canopy density influenced the measured physical parameters below the canopies. There was no significant effect of species composition on water bulk flow. There was, however, a significant effect of density on water flow ($p < 0.001$; **Table 1**). Plaster bars underneath the high and medium density treatments had significantly lower dissolution than the low density and control treatments (Tukey $p < 0.001$), suggesting there was significantly less bulk water flow underneath the canopies of higher densities (**Table 2**).

Furthermore, there was no significant interaction effect between species and density on the attenuation of irradiance below the canopies, yet there was an effect driven separately by each factor ($p < 0.001$; **Table 1**). The species *Silvetia compressa* and overall the high and medium density treatments attenuated irradiance the most (Tukey $p < 0.05$; **Table 2**). There was also a significant interaction between species composition and density on particle retention below the canopy ($p < 0.05$ **Table 1**). Synthetic fiber pads below the *S. compressa* and *C. canaliculatus* canopies at high densities retained more particles than other treatments (Tukey $p < 0.001$; **Table 2**).

On the other hand, only density treatments showed a significant effect on the abundance of seaweed and MPB recruitment underneath the canopies ($p < 0.001$, **Table 1**). However, both groups had contrasting distributions. Diatoms were abundant underneath higher density treatments (**Figure 2**), while seaweed recruits were abundant underneath lower density treatments (**Figure 3**).

Early sporophytes of brown seaweeds were the most abundant seaweed microscopic stage found and often grew close to one another. Red algal spores were second in abundance and showed a more isolated distribution, with few to no other seaweeds or microphytobenthic organisms settled next to them (**Figure 4**). Conversely, benthic diatoms were the dominant organism within the MPB with *Cocconeis* spp. representing 89% of the settlers and often forming biofilm mats. Fewer representatives of other benthic diatoms, such as *Navicula* sp. (10%), *Climacosphenia* sp. (<1%), and cyanobacteria, such as *Chroococcus* sp. (<1%), were present at lower abundances (**Figure 5**).

Surprisingly, none of the physical factors used in the regression analyses explained the variability in the abundance of seaweed recruits (**Table 3**) ($r^2 = 0.047$, p = NS). However, the regression analyses did show that particle retention by the seaweed canopy aggregations explained 64% of the variability in the abundance of MPB cells in the understory ($n = 48$, $p < 0.001$).

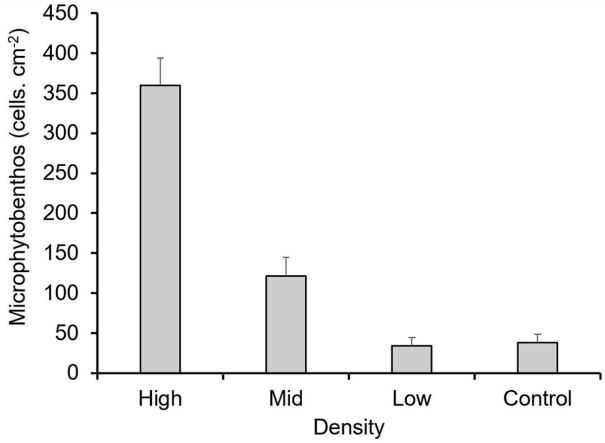

FIGURE 2 | Abundance of microphytobenthic organisms settled underneath the experimental canopies. Mean values ± one standard error.

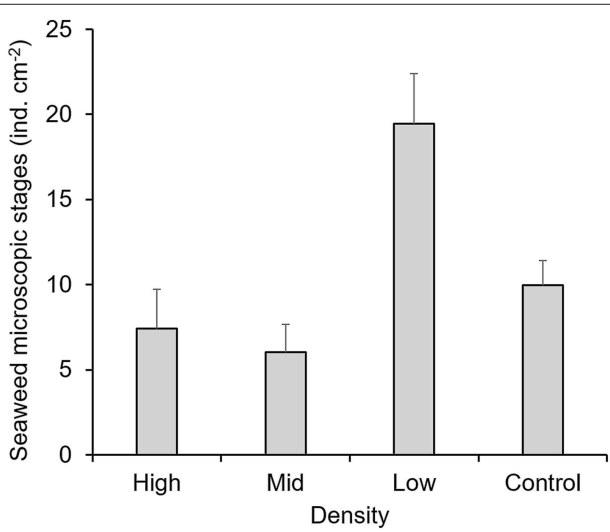

FIGURE 3 | Abundance of microscopic stages of seaweeds settled underneath the canopy treatments. Mean values ± one standard error.

DISCUSSION

Overall, our results indicate that the attenuation of physical factors driven by macroscopic seaweeds influences the abundance and distribution of seaweed and MPB recruits differently. We found a greater abundance of MPB cells underneath the most attenuated canopies and a greater abundance of seaweed settlers underneath the least attenuated canopies. In contrast to the MPB, particle retention did not appear to affect seaweed recruitment significantly. Moreover,

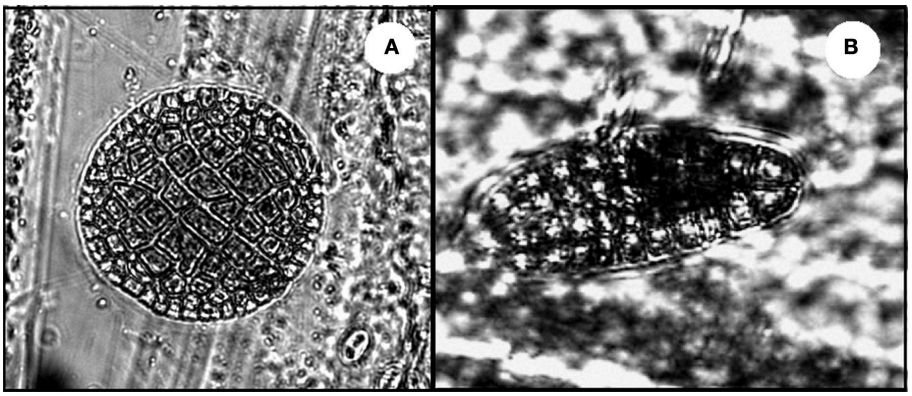

FIGURE 4 | Microscopic stages of seaweeds settled underneath the canopies. **(A)** Spore of red seaweed and **(B)** sporophyte of brown seaweed.

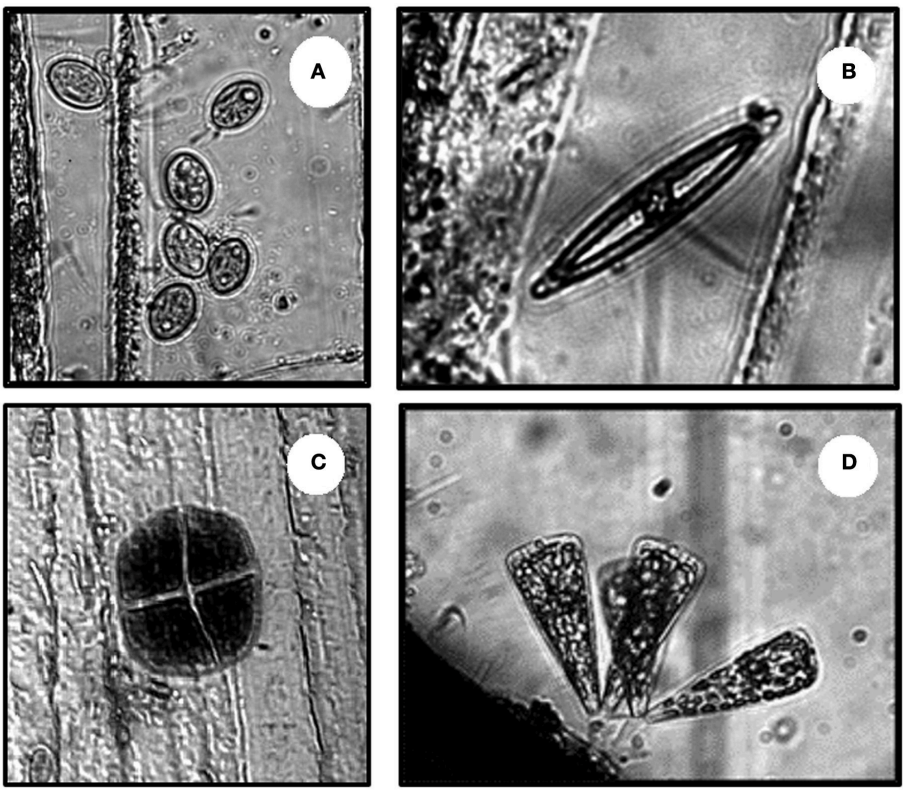

FIGURE 5 | Microphytobenthic organisms settled underneath the canopies. **(A)** *Cocconeis* sp., **(B)** *Navicula* sp., **(C)** *Chroococcus* sp., and **(D)** *Climacosphenia* sp.

no relationship with the physical factors measured herein explained the abundance of seaweed recruits. We neither find any relationship between the distribution patterns of MPB cells and seaweed recruits. The distribution and abundance patterns might suggest competition for space, light or nutrients, due to their apparently inverse, but not significantly related distribution, however no relationship was found to evidence this. Huang and Boney (1984) experimentally demonstrated that although MPB cells can outcompete juvenile brown and red seaweeds, both groups could also coexist with no competition between them, which seems to be the case in our study.

At least 50% of the blades in our experimental quadrats were fertile during the study period, coinciding with the reproductive periods described for these species in the region (Pacheco-Ruiz et al., 1989; García-Lepe et al., 1997; Johnson and Brawley, 1998; Zertuche-González et al., 2000). Many of the germlings or spores measured in this study could have

TABLE 3 | Regression summary for the recruitment of seaweed microscopic stages (p = NS) and microphytobenthic cells ($r^2 = 0.64$, $p < 0.001$) and underneath the canopy.

	Beta	S.E.	B	S.E.	$t_{(44)}$	p
SEAWEED MICROSCOPIC STAGES						
Particle retention	−0.19	0.20	−5.09	5.23	−0.9	NS
Bulk water flow	−0.08	0.19	−0.96	2.13	−0.4	NS
Irradiance	0.03	0.19	0.0004	0.003	0.1	NS
MICROPHYTOBENTHOS						
Particle retention	0.62	0.12	271.70	55.39	4.9	<0.001
Bulk water flow	0.07	0.12	13.460	22.57	0.5	NS
Irradiance	−0.17	0.12	−0.047	0.03	−1.4	NS

resulted from self-seeding in our quadrats, which might be related to the relatively high abundance of brown and red seaweed microscopic stages underneath the canopies. The non-motile eggs of the fucoid seaweeds are within the largest reproductive cells among seaweeds. Although spores released from our outplants might sink relatively faster into the water than the MPB (Okuda and Neushul, 1981), thus facilitating colonization of available substrate, many could have been lost to mortality (Santelices, 1990; Hurd et al., 2014) or could have been impeded from settling by the high canopy densities of our treatments. In fact, a number of studies have reported settlement of recruits to be inhibited by previously established seaweeds; either due to the physical barrier thalli represent (McCourt, 1984), a sweeping effect (Fletcher and Callow, 1992; Johnson and Brawley, 1998), or by particular traits of the canopies (Brawley and Johnson, 1991). *C. canaliculatus*, for example, can form dense mats that can trap enough sediment which prevents subsequent settlement by algal spores (Sousa, 1979; Sousa et al., 1981). Moreover, studies show that seaweed recruits also respond to the chemical properties of the microenvironment. For instance, flagellated spores can detect and respond to a variety of inorganic and organic nutrients, swimming toward or away from microhabitats with nutrients at concentrations that enhance or inhibit growth (Amsler et al., 1992; Maggs and Callow, 2003; Hurd et al., 2014). It is possible that inhibitory cues by our experimental canopies could have deterred green motile spores from settling, therefore explaining their relatively low abundance in our experimental treatments.

Early colonizers play a key role in ecology because they can modify the physicochemical conditions of their environment. In turn, they can furthermodulate settlement of other organisms (Dobretsov, 2008; Orvain et al., 2015). In fact, benthic diatoms are among the first algae to settle on new substrate, and it is suggested that they may affect the settlement of later successional organisms (Amsler et al., 1992). Research shows that together, the MPB and bacteria can form biofilms that can influence the adhesion of seaweed spores by modifying the chemical characteristics of the settlement surface (Callow and Callow, 2006; Ma et al., 2010). This effect, however, is not always consistent, as the strength of adhesion depends on the species of seaweeds tested, their stage of development and the physicochemical properties of the substrate (Mieszkin et al., 2013). Although this study was repeated a year later, similarly to Umanzor et al. (2017), we found that diatoms of the genus *Cocconeis* almost solely colonized all understories. This result provides further evidence of the relevance of particle retention for the settlement of benthic organisms, as particle transport and deposition significantly influence their establishment, survival, and development (Eckman and Duggins, 1991; Morrow and Carpenter, 2008). Even though we only considered diatoms and cyanobacteria within these films, bacteria were also most likely abundant.

It is possible that MPB organisms were already attached to the seaweed canopies as epiphytes, and that the transfer to the seabed occurred directly underneath the high-density treatments. In contrast to seaweed propagules, the MPB can grow exponentially and cover a large area in a relatively short time, from a few founding cells (Blanchard et al., 2001), facilitating rapid colonization of new substrate. Such developmental and colonization attributes could have resulted in the differences in the abundance and distribution of the MPB and seaweed recruits measured underneath the canopies. It is also possible that grazers could have influenced the recruitment process of both the MPB and seaweed microscopic stages. Experimental studies show that grazers and filter feeders can ingest and digest algal spores, affecting the pattern of dispersal and settlement on rocky shores (Buschmann and Santelices, 1897; Eckman and Duggins, 1991). Also, Coleman et al. (2006) showed that limpet grazers affected diversity and biomass of intertidal seaweeds across a latitudinal gradient. However, in this study, we did not witness any grazers on our settlement slides. Nonetheless, our experiment did not consider any exclusion caging, therefore, selective feeding underneath the treatment canopies could have potentially influenced the outcome of the experiment, though we do believe this to be unlikely.

We conclude that although both seaweed microscopic stages and MPB cells inhabit similar microhabitats, microscale processes appear to affect their recruitment in different ways. As shown here, the presence of macroscopic seaweeds can greatly influence the settlement and distribution of a variety of benthic organisms. Microscale changes promoted by seaweeds with different morphologies and at different densities can have profound effects on the settlement of associated organisms and these effects could trigger changes at a larger scale that should not be underestimated. Although intertidal seaweed aggregations seem to modulate a contrasting response in understory microphytobenthic and seaweed recruitment, more experimental work considering longer periods and control environments is required to determine the reciprocal effects that the MPB and seaweed microscopic stages might have on each other. Determining the identity of the recruits and if there is an effect by bacterial films and chemical cues is also recommended. Complex interactions in intertidal dynamics, the small size of the target organisms, and the characteristics of the microenvironment they inhabit all make it difficult to obtain *in situ* measurements of the potential

feedback loops between seaweeds and microphytobenthic communities. Nonetheless, the interactions between seaweed aggregations and other benthic microorganisms need further focus as the ecological effects driven by changes in the recruitment of primary producers can have significant further consequences on the dynamics of the overall ecosystem.

AUTHOR CONTRIBUTIONS

SU was responsible for data collection and processing. LL contributed to the experimental design and writing of the manuscript. JZ-G contributed with intellectual inputs and data processing.

FUNDING

This project was supported by CONACYT under Grant 221662 to LL and a scholarship from CONACYT (CVU 576942) to the first author. The Coastal Complexity Crew: Towards a paradigm shift for the near-shore ocean by exploring the biophysical complexity of spatial-temporal scales in coastal productivity.

ACKNOWLEDGMENTS

We would like to thank Dr. David Siqueiros and Alberto Galvez for their feedback in identifying and photographing the microorganisms. We also appreciate the contributions by J. Manuel Guzman and the volunteers who helped to set up the experiment in such a challenging intertidal.

REFERENCES

Amsler, C. D., Reed, D. C., and Neushul, M. (1992). The microclimate inhabited by macroalgal propagules. *Br. Phycol. J.* 27, 253–270. doi: 10.1080/00071619200650251

Avila, M., Piel, M. I., Caceres, J. H., and Alveal, K. (2011). Cultivation of the red alga *Chondracanthus chamissoi*: sexual reproduction and seedling production in culture under controlled conditions. *J. Appl. Phycol.* 23, 529–536. doi: 10.1007/s10811-010-9628-1

Bennett, S., and Wernberg, T. (2014). Canopy facilitates seaweed recruitment on subtidal temperate reefs. *J. Ecol.* 102, 1462–1470. doi: 10.1111/1365-2745.12302

Bertness, M. D., Leonard, G. H., Levine, J. M., Schmidt, P. R., and Ingraham, A. O. (1999). Testing the relative contribution of positive and negative interactions in rocky intertidal communities. *Ecology* 80, 2711–2726.

Blanchard, G. F., Guarini, J. M., Orvain, F., and Sauriau, P. G. (2001). Dynamic behaviour of benthic microalgal biomass in intertidal mudflats. *J. Exp. Mar. Bio. Ecol.* 264, 85–100. doi: 10.1016/S0022-0981(01)00312-4

Brawley, S. H., and Johnson, L. E. (1991). Survival of fucoid embryos in the intertidal zone depends upon developmental stage and microhabitat. *J. Phycol.* 27, 179–1991.

Buschmann, A. H., and Santelices, B. (1897). Micrograzers and spore release in Iridaea laminarioides Bory (Rhodophyta: Gigartinales). *J. Exp. Biol. Ecol.* 108, 171–179.

Callow, J. A., and Callow, M. E. (2006). "Progress in molecular and subcellular biology: marine molecular bio- technology," in *Progress in Molecular and Subcellular Biology: Marine Molecular Bio- Technology*, eds N. Fusetani and A. S. Clare (Berlin: Springer-Verlag), 141–169.

Callow, M. E., Jennings, A. R., Brennan, A. B., Seegert, C. E., Gibson, A., Wilson, L., et al. (2002). Microtopographic cues for settlement of zoospores of the green fouling alga enteromorpha. *Biofouling* 18, 229–236. doi: 10.1080/08927010290014908

Choi, H. G., and Norton, T. A. (2005). Competition and facilitation between germlings of *Ascophyllum nodosum* and *Fucus vesiculosus*. *Mar. Biol.* 147, 525–532. doi: 10.1007/s00227-005-1593-x

Coleman, R. A., Underwood, A. J., Benedetti-Cecchi, L., Aberg, P., Arenas, F., Arrontes, J., et al. (2006). A continental scale evaluation of the role of limpet grazing on rocky shores. *Oecologia* 147, 556–564. doi: 10.1007/s00442-005-0296-9

Crain, C. M., and Bertness, M. D. (2006). Ecosystem engineering across environmental gradients: implications for conservation and management. *Bioscience* 56, 211–218. doi: 10.1641/0006-3568(2006)056[0211:EEAEGI]2.0.CO;2

Dobretsov, S. (2008). "Inhibition and induction of marine biofouling by biofilms," in *Marine and Industrial Biofouling*, eds H C. Flemming, P.S. Murthy, R. Venkatesan, and K. Cooksey (Berlin: Springer), 293-313. doi: 10.1007/7142_2008_10

Eckman, J. E., and Duggins, D. O. (1991). Life and death beneath macrophyte canopies: effects of understory kelps on growth rates and survival of marine, benthic suspension feeders. *Oecologia* 87, 473–487.

Fletcher, R. L., and Callow, M. E. (1992). The settlement, attachment and establishment of marine algal spores. *Br. Phycol. J.* 27, 303–329. doi: 10.1080/00071619200650281

Fong, P., Donohoe, R. M., and Zedler, J. B. (1993). Competition with macroalgae and benthic cyanobacterial mats limits phytoplankton abundance in experimental microcosms. *Mar. Ecol. Prog. Ser.* 100, 97–102. doi: 10.3354/meps100097

Freckelton, M. L., Nedved, B. T., and Hadfield, M. G. (2017). Induction of invertebrate larval settlement; different bacteria, different mechanisms? *Sci. Rep.* 7:42557. doi: 10.1038/srep42557

García-Lepe, M. G., Ballesteros-Grijalva, G., Zertuche-González, J. A., and Chee-Barragán, A. (1997). Annual variation in size and reproductive phenology of the red alga *Chondracanthus canaliculatus* (Harvey) Guiry at Punta San Isidro, Baja California, Mexico. *Ciencias Mar.* 23, 449–462.

Hardison, A. K., Canuel, E. A., Anderson, I. C., Tobias, C. R., Veuger, B., and Waters, M. N. (2013). Microphytobenthos and benthic macroalgae determine sediment organic matter composition in shallow photic sediments. *Biogeosciences* 10, 5571–5588. doi: 10.5194/bg-10-5571-2013

Huang, R., and Boney, A. D. (1984). Growth interactions between littoral diatoms and juvenile marine algae. *J. Exp. Mar. Bio. Ecol.* 81, 21–45. doi: 10.1016/0022-0981(84)90222-3

Hurd, C. L., Harrison, P. J., Bischof, K., and Lobban, C. S. (2014). *Seaweed Ecology and Physiology*, *2nd Edn*. Cambridge: Cambridge University Press.

Johnson, L. E., and Brawley, S. H. (1998). Dispersal and recruitment of a canopy-forming intertidal alga: the relative roles of propagule availability and post-settlement processes. *Oecologia* 117, 517–526. doi: 10.1007/s004420050688

Knight, G. A., and Nelson, W. A. (1999). An evaluation of characters obtained from life history studies for distinguishing New Zealand Porphyra species. *J. Appl. Phycol.* 11, 411–419. doi: 10.1023/A:1008175226816

Komatsu, T., and Kawai, H. (1992). Measurements of time-averaged intensity of water motion with plaster balls. *J. Oceanogr.* 48, 353–365.

Linskens, H. F. (1966). Adhesion of reproductive cells of Benthontic algae. *Algae* 68, 99–110.

Ma, Y., Liu, P., Zhang, Y., Cao, S., Li, D., and Chen, W. (2010). Inhibition of spore germination of Ulva pertusa by the marine bacterium Pseudoalteromonas haloplanktis CI4. *Acta Oceanol. Sin.* 29, 69–78. doi: 10.1007/s13131-010-0009-z

Maggs, C. A., and Callow, M. E. (2003). "Algal spores," in *Encyclopedia of Life Sciences* (Nature Publishing Group), 1–6. doi: 10.1038/npg.els.0000311

McCourt, R. M. (1984). Seasonal patterns of abundance, distributions and phenology in relation to growth strategies of three Sargassum species. *J. Exp. Biol. Ecol.* 74, 171–156.

Mieszkin, S., Callow, M. E., and Callow, J. A. (2013). Interactions between microbial biofilms and marine fouling algae: a mini review. *Biofouling* 29, 1097–1113. doi: 10.1080/08927014.2013.828712

Morrow, K. M., and Carpenter, R. C. (2008). Macroalgal morphology mediates particle capture by the corallimorpharian *Corynactis californica*. *Mar. Biol.* 155, 273–280. doi: 10.1007/s00227-008-1023-y

Okuda, T., and Neushul, M. (1981). Sedimentation of red algal spores. *J. Phycol.* 17, 113–118.

Orvain, F., Martinez, A.-S., Desoche, E., and Claquin, P. (2015). "Chemical interaction between epilitic microphytobenthic biofilm and larval development of the sea urchin Paracentrotus lividus," in *Proceedings of Congress on Artificial Reefs: From Materials to Ecosystems* (Caen), 239–247.

Pacheco-Ruiz, I., García-Esquivel, Z., and Aguilar-Rosas, L. E. (1989). Spore discharge in the carragenophyte Gigartina canaliculata Harvey (Rhodophyta, Gigartinales). *J. Exp. Mar. Bio. Ecol.* 126, 293–299. doi: 10.1016/0022-0981(89)90194-9

Robertson, B. L. (1987). Reproductive ecology and canopy structure of *Fucus spiralis L*. *Bot. Mar.* 30, 475–482.

Santelices, B. (1990). Patterns of reproduction, dispersal and recruitment in seaweeds. *Oceanogr. Mar. Biol. Ann. Rev.* 28, 177–276.

Schumacher, J. F., Carman, M. L., Estes, T. G., Feinberg, A. W., Wilson, L. H., Callow, M. E., et al. (2007). Engineered antifouling microtopographies – effect of feature size, geometry, and roughness on settlement of zoospores of the green alga Ulva. *Biofouling* 23, 55–62. doi: 10.1080/08927010601136957

Sousa, W. P. (1979). Experimental investigations of disturbance and ecological succession in a rocky intertidal algal community. *Ecol. Monogr.* 49, 227–254. doi: 10.2307/1942484

Sousa, W. P., Schroeter, S. C., and Gaines, S. D. (1981). Latitudinal variation in intertidal algal community structure: the influence of grazing and vegetative propagation. *Oecologia* 48, 297–307. doi: 10.1007/BF00346486.

Taylor, D. I., and Schiel, D. R. (2003). Wave-related mortality in zygotes of habitat-forming algae from different exposures in southern New Zealand: the importance of "stickability". *J. Exp. Mar. Bio. Ecol.* 290, 229–245. doi: 10.1016/S0022-0981(03)00094-7

Umanzor, S., Ladah, L., and Zertuche-González, J. A. (2017). The influence of species, density, and diversity of macroalgal aggregations on microphytobenthic settlement. *J. Phycol.* 53, 1060–1071. doi: 10.1111/jpy.12565

Umar, M. J., Mc Cook, L. J., and Price, I. R. (1998). Effects of sediment deposition on the seaweed Sargassum on a fringing coral reef. *Coral Reefs* 17, 169–177.

Underwood, A. (1997). *Experiments in Ecology: Their Logical Design and Interpretation Using Analysis of Variance*, *1st Edn*. Cambridge: Cambridge University Press.

Vadas, R. L., Johnson, J. S., and Norton, T. A. (1992). Recruitment and mortality of early post-settlement stages of benthic algae. *Br. Phycol. J.* 27, 331–351. doi: 10.1080/00071619200650291

Watanabe, H., Ito, M., Matsumoto, A., and Arakawa, H. (2016). Effects of sediment influx on the settlement and survival of canopy-forming macrophytes. *Sci. Rep.* 6:18677. doi: 10.1038/srep18677

Woodin, S. A. (1991). Recruitment of infauna: positive or negative cues? *Integr. Comp. Biol.* 31, 797–807. doi: 10.1093/icb/31.6.797

Zertuche-González, J. A., Pacheco-Ruiz, I., Cabello-Pasini, A., Chee-Barragan, A., Guzman, J. M., Galvez, A., et al. (2000). *In situ* growth and reproduction of Porphyra perforata in the Pacific Coast of Baja California. *J. Phycol.* 36, 72. doi: 10.1046/j.1529-8817.1999.00001-214.x

Conflict of Interest Statement: The authors declare that the research was conducted in the absence of any commercial or financial relationships that could be construed as a potential conflict of interest.

frontiers in Marine Science

ORIGINAL RESEARCH
published: 19 September 2018
doi: 10.3389/fmars.2018.00332

Canopy-Forming Macroalgae Facilitate Recolonization of Sub-Arctic Intertidal Fauna and Reduce Temperature Extremes

Sarah B. Ørberg[1,2], Dorte Krause-Jensen[1,2], Kim N. Mouritsen[3], Birgit Olesen[3], Núria Marbà[4], Martin H. Larsen[5], Martin E. Blicher[6] and Mikael K. Sejr[1,2]*

[1] Department of Bioscience, Aarhus University, Silkeborg, Denmark, [2] Arctic Research Centre, Aarhus University, Aarhus, Denmark, [3] Department of Bioscience, Aarhus University, Aarhus, Denmark, [4] Global Change Research Group, IMEDEA (CSIC-UIB), Institut Mediterrani d'Estudis Avançats, Esporles, Spain, [5] Danish Centre for Wild Salmon, Randers, Denmark, [6] Greenland Climate Research Centre, Greenland Institute of Natural Resources, Nuuk, Greenland

Ice can be an important structuring factor physically removing intertidal flora and fauna. At high latitudes in particular, the removal of canopy-forming algae by ice scour may be important as their canopy may serve to modify the extreme environment for marine organisms at low tide. We simulated the effect of ice scouring by manipulating the biomass of the canopy-forming algae *Ascophyllum nodosum* in a sub-Arctic fjord ["Full canopy," "Reduced canopy," "Bare (start)," "Bare (annual)"]. Over a three-year period, we quantified key physical parameters and the recolonization of flora and fauna to test the hypothesis that *A. nodosum* and rock rugosity facilitate recolonization of sub-Arctic intertidal fauna and that potential facilitation could rely on an ability of *A. nodosum* canopy to modify air temperature and ice scour. Finally, we estimated the recovery period of *A. nodosum* canopy height to pre-disturbance levels based on estimated early growth rates. We found that *A. nodosum* canopy facilitated higher species richness and recolonization of dominating faunal species (*Littorina saxatilis, Littorina obtusata, Mytilus edulis,* and *Semibalanus balanoides)*, and also significantly reduced the high temperatures in summer and raised the low temperatures in winter. The abundance of *M. edulis* and *A. nodosum* recolonization increased significantly with rock rugosity and the recovery of *A. nodosum* canopy height was estimated to a minimum of 15 years. We conclude that algal canopy and rock rugosity play key roles in structuring sub-Arctic intertidal communities, likely by modifying environmental stress such as extreme temperature, desiccation, and by increasing the settling surface and the habitat complexity. As the distribution of canopy-forming algae is expected to shift northward, they may act as a key habitat facilitating a northward colonization of intertidal fauna in the Arctic. We highlight the importance of considering scales relevant to biological communities when predicting impacts of climate change on distributional patterns and community structure in the Arctic intertidal.

Keywords: biotic interactions, physical disturbance, rocky intertidal, community recovery, recruitment, Greenland

OPEN ACCESS

Edited by:
Matthew H. Long,
Woods Hole Oceanographic Institution, United States

Reviewed by:
Stein Fredriksen,
University of Oslo, Norway
Jan Marcin Weslawski,
Institute of Oceanology (PAN), Poland

****Correspondence:***
Sarah B. Ørberg
sao@bios.au.dk

Specialty section:
This article was submitted to Marine Ecosystem Ecology, a section of the journal Frontiers in Marine Science

Received: *25 June 2018*
Accepted: *28 August 2018*
Published: *19 September 2018*

Citation:
Ørberg SB, Krause-Jensen D, Mouritsen KN, Olesen B, Marbà N, Larsen MH, Blicher ME and Sejr MK (2018) Canopy-Forming Macroalgae Facilitate Recolonization of Sub-Arctic Intertidal Fauna and Reduce Temperature Extremes. Front. Mar. Sci. 5:332. doi: 10.3389/fmars.2018.00332

INTRODUCTION

In intertidal ecosystems, air temperature, exerting a major control on biological processes, can be modified by a number of factors acting at scales that are relevant to biological communities (Helmuth, 1998; Helmuth et al., 2010). For example, sea ice modifies air temperature directly (Scrosati and Eckersley, 2007) and ice scouring may indirectly influence air temperature through the removal of canopy-forming algae (Gutt, 2001; Petzold et al., 2014). Algal canopies may also insulate organisms from extreme temperatures in the high intertidal as typically seen in temperate regions (Beermann et al., 2013; Watt and Scrosati, 2013a) and, thereby, influence community structure locally (Crowe et al., 2013). Ice, either in the form of sea ice or glacial ice, is a characteristic feature of high latitude coastal systems such as those found in Greenland, where export of glacial ice into the coastal ocean is increasing (Howat et al., 2007). In the Godthåbsfjord, West Greenland, for example, the loss rate of glacial ice has doubled within a decade, likely increasing the output of icebergs and thereby the risk of ice scouring in benthic communities (Motyka et al., 2017).

Here, we aim to understand the interplay of biotic and abiotic factors in structuring sub-Arctic rocky intertidal communities that can also improve predictions for climate change-induced range shifts (Gilman et al., 2010; HilleRisLambers et al., 2013). Several studies have shown the impact of canopy-forming algae on the understory community and patterns of recolonization as they alter the physical environment (Dayton, 1971; Hawkins, 1983; Jenkins et al., 1999a, 2004; Cervin et al., 2004). However, these studies are mostly restricted to the temperate intertidal as we found only one example from the sub-Arctic intertidal, mainly focusing on biotic factors (Ingólfsson and Hawkins, 2008).

The literature reports differential responses of intertidal organisms to canopy cover, also depending on the environmental stress level (McCook and Chapman, 1991; Bertness et al., 1999; Broitman et al., 2009; Crowe et al., 2013; Watt and Scrosati, 2013b). For instance, algal canopy cover enhances the survival of newly-settled barnacles only in the high intertidal zone (Dayton, 1971; Hawkins, 1983; Jenkins et al., 1999b). Moreover, species richness and diversity increase with algal canopy cover in the high and mid intertidal zone, again underlining the importance of the bioengineering effects of a canopy mainly in stressful environments (Watt and Scrosati, 2013a,b). Most likely canopies create an interplay of negative and positive interspecific interactions (Jenkins et al., 1999b; Beermann et al., 2013). As an example, barnacle recruitment may be negatively affected by whiplashes from algal fronds, but positively affected by lowered water loss and buffering of temperature, together resulting in a neutral effect of algal canopy cover on barnacles in the mid- and high intertidal (Beermann et al., 2013).

In a highly stressful environment, such as the sub-Arctic intertidal zone, the positive effects of algal canopy likely exceed the negative as suggested by the stress gradient hypothesis (Bertness and Callaway, 1994). However, we lack field studies from the sub-Arctic intertidal to support this hypothesis. In particular, the ability of algal canopies to buffer extreme air temperatures may be important in shaping high latitude intertidal communities. Variation in air temperature is a key stressor for intertidal organisms, impacting a range of biochemical and physiological processes (Helmuth, 1998; Denny and Harley, 2006). Water loss and thereby the risk of desiccation is also affected by air temperature (Helmuth, 1998), and even a few degrees temperature change can markedly impact mortality rates in the intertidal, especially for newly-settled organisms (Foster, 1971b). Ice scouring is another key stressor for intertidal organisms, and crevices in the rocky shore may, like canopy-forming algae, offer microhabitats, that shield organisms from destruction by ice scouring as well as other physical stressors (Foster, 1971b; McCook and Chapman, 1991; Walters and Wethey, 1996; Helmuth et al., 2010).

Sub-Arctic communities are considered to be shaped by large-scale climate variables and physical exposure, but clearly there is a potential for small scale variation induced by canopy-forming algae and rock roughness that may greatly affect the local physical regime, supporting community recovery after a disturbing event such as ice scouring. Therefore, the ability and speed of recovery of algal canopies may greatly affect the recovery process of the intertidal faunal community after ice scouring and potentially limit their northern distribution range.

Kobbefjord is a sheltered Greenlandic fjord in the sub-Arctic region, i.e., immediately south of the Arctic Circle. However, according to the AMAP definition, Kobbefjord is considered to be in the Arctic. We chose this study area as parts of this rocky intertidal are characterized by high biomass of the long-lived fucoid canopy-forming alga *Ascophyllum nodosum* (Olsen et al., 2010), and the level of mechanical stress from sea ice is considered low. Yet, patches of the community may be in a recovering state after mechanical stress caused by scouring sea ice that form seasonally in the area. *Ascophyllum nodosum* has a wide geographical distribution extending to 69.7°N on the coast of Greenland (Lüning, 1990) and the growth rate of the Greenland populations respond positively to a warming climate (Marbà et al., 2017).

Here, we present a first attempt at disentangling the multiple factors that influence small-scale variation in physical regimes experienced by sub-Arctic intertidal organisms. First, we test the hypothesis that *A. nodosum* canopy facilitates the recolonization of sub-Arctic intertidal fauna. We do so by quantifying faunal recolonization rates at different manipulated levels of canopy cover over a 3-year period. Secondly, we measure the temperature and ice scouring intensity experienced by the intertidal organisms at different levels of algal canopy cover. Thirdly, we consider the physical properties of the rock as a settlement surface and microhabitat during recolonization. Finally, we quantify the early growth rates of *A. nodosum* recruits, and attempt to estimate the recovery period to pre-disturbance canopy height after dislodgement by mechanical disturbance, such as ice scouring. The recovery period of *A. nodosum* canopy height is expected to be rather slow due to the colder climate as growth rates are lowered at low temperatures (Steen and Rueness, 2004; Keser et al., 2005).

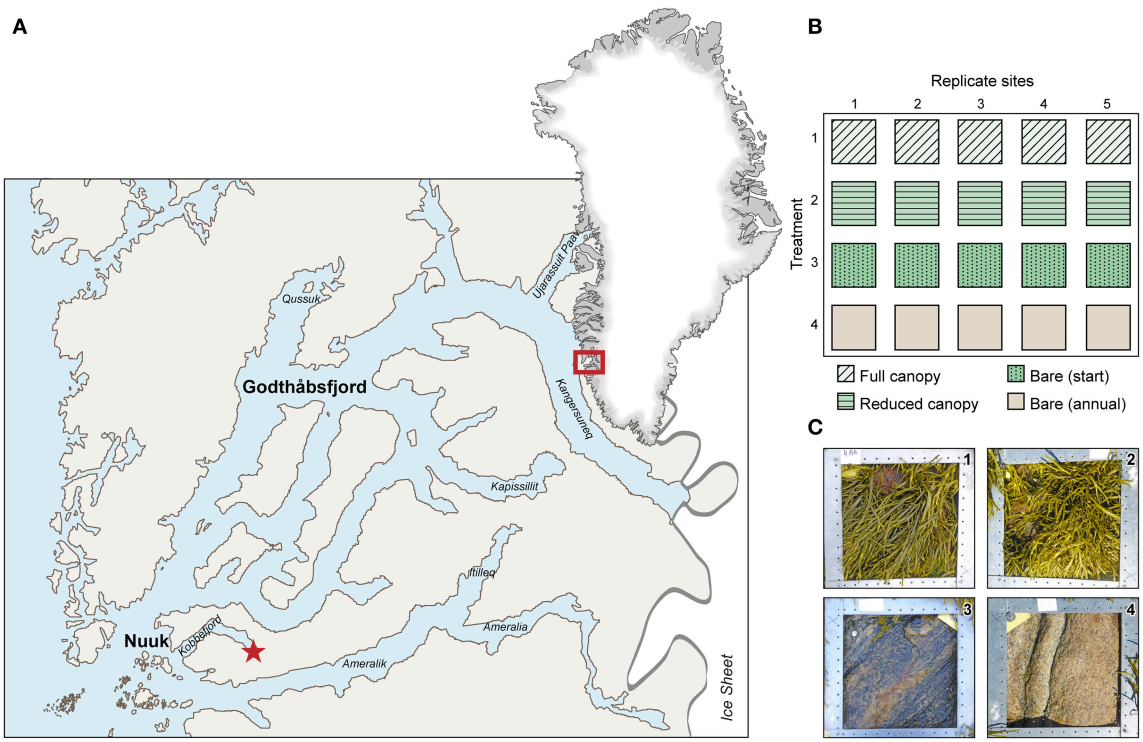

FIGURE 1 | Study area and experimental setup. **(A)** Godthåbsfjord system, SW Greenland with indication of the study site in inner Kobbefjord (★ 64°08N, 51°23W). **(B)** Experimental setup applied in inner Kobbefjord mid intertidal, with the four treatments applied at each of the five replicate sites. **(C)** Examples of experimental quadrats from each treatment by August 2014 (the end of experimental period) [1: Full canopy, 2: Reduced canopy, 3: Bare (start), 4: Bare (annual) (**Table 1**)].

MATERIALS AND METHODS

Study Area

The study was conducted in the sub-Arctic Kobbefjord, a branch of the Godthåbsfjord system in south-west Greenland (64°08N, 51°23W) (**Figure 1A**). The shoreline is largely dominated by bedrock, and the mountains surrounding Godthåbsfjord and Kobbefjord are dominated by granites and granitoid gneiss (Mosbech et al., 2000; Nutman and Friend, 2009). The fjord is 17 km long and 0.8–2 km wide with a maximum depth of 150 m. It is influenced by daily tidal amplitudes of 1–5 m (Richter et al., 2011) and sea surface temperatures ranging from −1 to 9°C (Versteegh et al., 2012). Air temperature ranges from a minimum of −25°C in winter to a maximum of 20°C in summer, measured in Nuuk (Blicher et al., 2013). From April to October, the fjord receives freshwater run-off from several rivers in the innermost part of the fjord, resulting in a salinity gradient in the surface water. From December to May, sea ice usually covers the inner part of the fjord (Mikkelsen et al., 2008). This results in a system characterized by large seasonal variation in key physical parameters such as light, temperature, salinity, and mechanical stress (ice scouring).

Field Experiment

The experiment was conducted in the inner part of the fjord at a rocky intertidal area covered by canopy-forming fucoid algae (predominantly *A. nodosum* with occasional presence of *Fucus vesiculosus*) and spanned a 3-year period from August 2011 to August 2014. Additional quantification of algal recolonization was conducted in August 2016. We used an experimental design with five replicate sites located along 200 m of the shoreline having similar overall vertical rock slope, similar compass direction (all S-SW facing) and evenly developed *A. nodosum* canopy. At each of the five replicate sites, four experimental treatments were established in 25 × 25 cm quadrats (**Table 1**, **Figures 1B,C**) ["Full canopy," "Reduced canopy," "Bare (start)" and "Bare (annual)"] and the horizontal sequence of the four treatments was fully randomized within each replicate site. All quadrats were laid out just below the mean tidal level (determined during a full tidal cycle). The slope of the rock within the resulting 20 quadrats varied between 5 and 30°. In "Full canopy," macroalgae were left untouched whereas fauna was removed from both canopy and rock face at the initiation of the experiment (August 2011). In "Reduced canopy," macroalgae were cut to a height of 15 cm to imitate a moderate impact of mechanical disturbance from ice scouring still allowing macroalgae to recover (Gendron et al., 2017), and fauna was removed from both the remaining canopy and the rock face at the initiation of the experiment (August 2011). In "Bare (start)," the entire quadrat was cleared at the initiation of the experiment (August 2011) for all macroalgae including their holdfasts and all fauna to imitate maximum ice scouring impact.

TABLE 1 | The four treatments applied at each of five replicate sites in the inner Kobbefjord mid intertidal, August 2011.

Treatment	Action	*N*
1: Full canopy	Canopy untouched, fauna removed	5
2: Reduced canopy	Canopy cut to 15 cm height, fauna removed	5
3: Bare (start)	Canopy and fauna fully cleared in August 2011, only	5
4: Bare (annual)	Canopy and fauna fully cleared annually (August)	5

In "Bare (annual)," the quadrat was cleared annually in a similar way (i.e., August 2011, 2012, and 2013) in order to estimate the variation in annual settling and hence the recolonization potential. We used a metal brush for the clearing of rock surfaces and ensured that all depressions and crevices were thoroughly cleared for organisms. Macroalgae were cleared by hand for macroscopic invertebrate fauna, by working through the canopy, algal individual by individual. In a buffer zone of approximately 10 cm surrounding each quadrat, macroalgae were scraped from the rock and the canopies of algae further away were cut up to levels that prevent them from overlaying the quadrats. In order to quantify and analyze the algal and faunal community at the start of the experiment (August, 2011), referred to as the "Pre-experimental" community, all the organisms cleared from "Bare (start)" quadrats were collected and subsequently counted according to species or taxa, weighed (drained wet weight after being kept in wire mesh sieves) and measured at their maximum dimension (e.g., shell length of mussels, carapace diameter of barnacles, and height of macroalgae). The average minimum age of *A. nodosum* "Pre-experimental" canopy was evaluated for all individuals longer than 10 cm by counting the number of air bladders (vesicles) on the longest axis, assuming one bladder is formed annually (Åberg, 1996). This method renders a minimum age since it does not account for the age of the shoot before production the first bladder and also does not account for possible breakage of shoots. All values for minimum age, weights and lengths are given as mean ($x \pm SE$).

In August 2012, 2013, and 2014 all fauna and macroalgae in "Bare (start)" and "Bare (annual)" were counted and measured at their maximum dimension (e.g., shell length of mussels, carapace diameter of barnacles, and height of macroalgae) to account for inter-annual settling and to estimate the early growth rate of *A. nodosum* recruits. At the termination of the experiment in August 2014, all quadrats were harvested for both macroalgae and fauna using the same method as in "Bare (start)" August 2011. Retrieved organisms were identified by taxa, counted, weighed, and their maximum dimensions were measured. Macroalgae without bladders were counted as recruits. The vast majority of recruits was below 10 cm length, and as bladders (used to age adult shoots) typically occurred only in individuals >10 cm length, this length limit coarsely separated individuals, here defined as recruits and adults. For each quadrat we quantified the faunal species richness (S) as the number of species and/or taxa present. Finally, in August 2016, 2 years after the final harvest, we quantified the number and length of *A. nodosum* individuals recruited into all 20 quadrats, adding to the estimate of early growth rates after maximum disturbance.

Between August 2011 and 2014, we quantified a range of physical variables in selected quadrats to characterize the habitat and potential differences between "Bare (start)" and "Full canopy" treatments. The temperature was logged every 1.5 h by sensors (Thermochron iButtons®) placed at site 4. The sensors were placed inside spherical brass housing, to protect them from ice scour and attached to a rock surface cleared of macroalgae and below *A. nodosum* canopy, respectively. To verify extreme temperatures measured in the intertidal, we compared with air temperature data from a nearby climate station, obtained from the Greenland Ecosystem Monitoring database (GEM). The overall extent of sea ice during the three winters of 2011–2014 was evaluated from photos taken automatically by a camera mounted on the mountain above the experimental area. The photos were taken daily in the period from January to May each year as part of the GEM monitoring program. Additionally, the ice scouring intensity was quantified at each of the five replicate sites by the degree of bending of steel screws inserted into the rock. The screws were standard commercial stainless steel screws having a height of 45 mm, a head diameter of 8 mm and a shaft diameter just below the head of 4 mm. Two screws protruding 2 cm from the rock surface were placed above each quadrat during the winters 2011–12, and 2013–14 (i.e., a total of 80 screws), and the maximum angle of bending (0–90°) of the two screws from each quadrat was used as a proxy for ice scouring intensity. To measure the roughness of the rock surface, i.e., rugosity, within the quadrats when cleared for algae and fauna, we used a profile gauge tool that captured the surface profile of the rock, which was then photographed for later image analysis using the "measure" tool in ImageJ. The ratio of the true surface profile to the linear surface profile gave an estimate of substrate rugosity (Luckhurst and Luckhurst, 1978; Zawada et al., 2010). The unit of analysis was the mean rugosity across the two diagonal profiles in each sample quadrat.

Statistical Analysis

Status of Main Treatments at the End of the Study Period

We compared the macroalgal biomass in each of the main treatments ["Full canopy," "Reduced canopy," "Bare (start)"] at the end of the study period (August 2014) with the "Pre-experimental" biomass using Two-sample *t*-tests. Similarly, macroalgal adult (> 10 cm) and recruit (< 10 cm) densities were compared to the "Pre-experimental" densities.

Algal Canopy and Faunal Recolonization

To assess the effect of the main treatments [three level factor; "Full canopy," "Reduced canopy," "Bare (start)"] on biomass of each species and faunal species richness at the end of the study period (2014), we performed one-way ANOVAs with biomass or faunal species richness as response variable and treatment as dependent variable. Biomass data was log-transformed (adding 1 before the transformation) to improve normality and homogeneity of variance assessed visually by Q-Q plots and

box plots. To assess the effect of treatment on the density of each species, we performed one-way ANOVAs (GLM) assuming density to follow a Poisson distribution. Before performing the ANOVAs, we confirmed that there was no significant interaction between replicate sites and treatment. Least square means *post hoc* analyses were performed to test the pairwise difference between treatments. Finally, in order to account for probable inter-annual variation in faunal recolonization, a one-way ANOVA was conducted to compare faunal density between years in the "Bare (annual)" treatment.

The Effect of Canopy-Forming Algae on Temperature and Ice Scouring

For the comparison of extreme temperatures measured in "Full canopy" and "Bare (start)," expected to reflect air temperatures during low tide, the 5th and 95th percentiles of temperature measurements were calculated for each month, year and the entire 3-year period. Means of the percentiles in each month, each year and the entire 3-year period between the "Full canopy" and "Bare (start)" were compared using a two-sample *t*-test.

To assess the variation in ice scouring intensity across replicate sites between years, the relationship between the maximum degree of the bending of screws from 2011 to 2012 and 2013 to 2014 was examined by linear regression. Then, to assess the effect of the main treatments on ice scouring, we performed a one-way ANOVA with the maximum degree of the bending of screws (2013–14) as the response variable. Similarly, a one-way ANOVA was performed to assess whether rock rugosity differed between the main treatments. Assumptions of normality and homogeneity of variance were assessed visually by Q-Q plots and box plots.

Rock Rugosity and Recolonization

In the following analysis, we treated the 15 quadrats in the main treatments from 2014 as independent data points since rock rugosity did not differ between treatments (**Table 4C**). Relationships between faunal recolonization (densities or biomasses) and rock rugosity were assessed with linear regression and multiple linear regression (MLR). Similarly, the relationship between *A. nodosum* recruitment density and rock rugosity was assessed by linear regression. All above analyses were performed using SAS statistical software 9.4 (SAS Institute Inc. Cary, NC, USA).

Recovery Period and Early Growth Rate of *Ascophyllum nodosum*

The early growth rate of *A. nodosum* recruited during the study period was quantified based on yearly length measurements of recruits in "Bare (annual)" and "Bare (start)." In total, 30 quadrat measurements (10 quadrat measures × 3 years) were used for the cohort analysis. Since we expected recruit lengths in "Bare (start)" to reflect multiple age groups of 2–3 years after experiment start, we applied Hartigan's diptest (Hartigan, 1985), testing the presence of multiple age groups with the R (R Core Team, 2017) package diptest (Maechler, 2016). By comparing the maximum difference between the observed distribution and a unimodal distribution, which minimizes this difference, Hartigan's diptest statistically tests the null hypothesis of unimodality. If $p < 0.05$, the alternative hypothesis of bi- or multimodality is accepted, i.e., the presence of multiple age groups. Subsequently, the Expectation-Maximization (EM) algorithm (Redner and Walker, 1984) was used to estimate the mean length of recruits within each age group with the R package mixtools (Benaglia et al., 2009). This algorithm uses the maximum likelihood method to find the value of each peak in a multimodal distribution. Here, we looked for three peaks, because we expected new recruits each year in "Bare (start)," i.e., three age groups.

Finally, the growth rate of *A. nodosum* was calculated with linear regression based on the estimated mean lengths within each age group of individuals recruited in the period August 2011 - August 2014. Additional quantification of algal recruit lengths was conducted in August 2016, i.e., 2 years after the final harvest of all quadrats, providing 20 additional estimates similar to the treatment "Bare (start)." This almost doubled the sample area (30 quadrat measurements + 20 quadrat measurements = 50 quadrat measurements), strengthening the overall estimate of early growth rates of algal recruits in inner Kobbefjord. We used the estimated early growth rates for *A. nodosum* recruits to evaluate the time it takes from initial settling to the recovery of the "Pre-experimental" canopy mean length in Kobbefjord. This was based on the growth pattern for *A. nodosum* found by Viana et al. (2014), showing linear growth during the first 2 years and, thereafter, exponential growth until a certain length set by abrasion. We calculated the length of *A. nodosum* after 2 years of linear growth with our early growth rate, and inserted this (as b) in a natural exponential function, which we solved for x (years):

$$y = b \cdot e^{(a \cdot x)},$$

where y is the mean length of "Pre-experimental" canopy, a is the adult relative growth rate of *A. nodosum* from inner Kobbefjord, calculated as the mean linear growth rate (4.92 cm yr^{-1}, Marbà et al., 2017) relative to the intermediate shoot length after starting exponential growth (i.e., length after 2 years + mature length)/2. Finally, we added the first 2 years to achieve the estimate of years it takes to reach the mean length of "Pre-experimental" canopy.

RESULTS

Canopy-Forming Algae in Inner Kobbefjord

Based on the pre-experimental monitoring in August 2011 ["Bare (start)"], the mid intertidal zone of the inner part of Kobbefjord was dominated by the canopy-forming fucoid, *A. nodosum*, with the occasional presence of *F. vesiculosus*. The average length of the *A. nodosum* canopy (> 10 cm) was 46.9 ± 6.0 cm and the minimum age was 5.9 ± 1.3 years for the "Pre-experimental" community ($n = 5$).

Figure 2 shows the combined biomass and densities of *A. nodosum* and *F. vesiculosus* in each treatment, noting that *A. nodosum* represented over 99% of the total observed biomass and adult density, and over 80% of the observed recruit density. The macroalgal biomass in the "Pre-experimental" community was on average 31 kg m^{-2}, which was not significantly different from the macroalgal biomass found in either "Full canopy" and

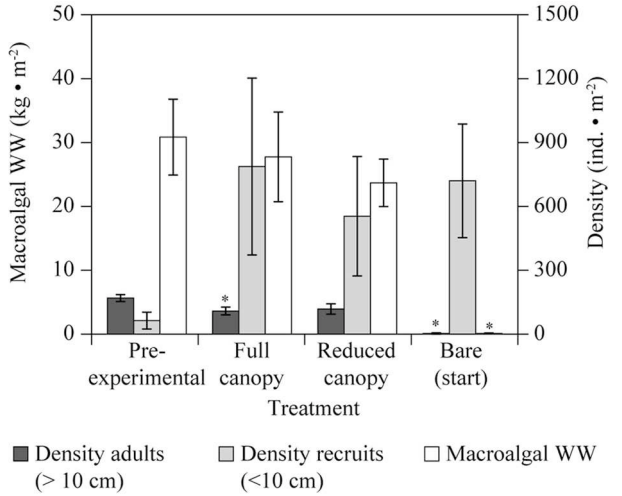

FIGURE 2 | Mid intertidal macroalgal biomass (wet weight, WW) and density of algal recruits and adults, i.e., for *A. nodosum* and *F. vesiculosus* combined, in the main treatments "Full canopy," "Reduced canopy," and "Bare (start)" in Kobbefjord at the end of the experiment (August 2014). "Pre-experimental" was a baseline measurement based on the material cleared from "Bare (start)" at the start of the experiment (August 2011). *Annotates a significant difference of $p < 0.05$ for each treatment compared to "Pre-experimental" by a two-sample *t*-test. $N = 5$ for all mean values. Error bars are SE.

TABLE 2 | Summary of two-sample *t*-tests comparing "Pre-experimental" macroalgal biomass, adult and recruit density to each treatment.

	t_8	*p*
BIOMASS		
Full canopy	0.34	0.75
Reduced canopy	−1.02	0.34
Bare (start)	−5.18	<0.001***
ADULT DENSITY		
Full canopy	−2.45	0.04*
Reduced canopy	−1.76	0.12
Bare (start)	−9.92	<0.001***
RECRUIT DENSITY		
Full canopy	1.73	0.12
Reduced canopy	1.73	0.12
Bare (start)	2.43	0.07

*$p < 0.05$, ***$p < 0.001$.

TABLE 3 | Faunal taxa of "Pre-experimental" community in the mid intertidal zone of inner Kobbefjord, SW Greenland, August 2011.

Taxa	
Littorina obtusata *Littorina saxatilis* *Mytilus edulis* *Semibalanus balanoides*	98.5% of faunal biomass
Platyhelminthes	
Nematoda	
Oligochaeta	
Isopoda	
Gammaridae	
Chironomidae	
Acarina	

The combined biomass (WW) of dominating fauna is given.

"Reduced canopy" in August 2014, three years after experiment start (**Table 2**, **Figure 2**). In contrast, the "Bare (start)" treatment, which was fully cleared at the beginning of the experiment, revealed minimal recovery in macroalgal biomass compared to "Pre-experimental," supporting only 0.11 kg m^{-2} by August 2014 (**Table 2**, **Figure 2**). In addition, the density of macroalgal adults (>10 cm) in "Bare (start)" showed minimal recovery by August 2014 compared to "Pre-experimental," while "Full canopy," "Reduced canopy" and "Pre-experimental" displayed a similar level of adult density (**Table 2**, **Figure 2**). However, as the adult density in "Pre-experimental" was slightly higher than in "Full canopy" (**Table 2**, **Figure 2**), this was not reflected in the biomass. The density of recruits (<10 cm) at the end of the experiment tended to be higher in all treatments than in "Pre-experimental" (**Figure 2**), yet differences were not significant (**Table 2**).

Algal Canopy and Faunal Recolonization

In total, we observed 11 faunal taxa in the study area (**Table 3**). Four species, *S. balanoides, M. edulis, L. obtusata* and *L. saxatilis*, contributed with 98.5% of the faunal biomass (wet weight). Three years after removal, the recovery of total faunal biomass relative to "Pre-experimental" was 26.1% for "Full canopy," 28.5% for "Reduced canopy" and 1.4% for "Bare (start)." The recovery of faunal density was considerably faster than biomass for the dominant taxa, being 45.5% for "Full canopy," 53.8% for "Reduced canopy" and 4.4% for "Bare (start)." Total faunal biomass nor density differed significantly from the "Pre-experimental" total faunal biomass or density.

In terms of biomass, *L. obtusata*, *L. saxatilis* and *M. edulis* were affected by canopy cover (**Figure 3A**, **Table 4A**), with *L. obtusata* showing a significantly higher biomass in both "Full canopy" and "Reduced canopy" compared to "Bare" (*post-hoc* LS test, Bare-Full canopy: $p = 0.007$, Bare-Reduced canopy: $p = 0.004$) and *L. saxatilis* showing a significantly higher biomass in "Reduced canopy" compared to both "Bare" and "Full canopy" (*post-hoc* LS test, Reduced canopy-Bare: $p = 0.001$, Reduced canopy-Full canopy: $p = 0.042$). *Mytilus edulis* displayed a significantly higher biomass in both "Full canopy" and "Reduced canopy" compared to "Bare" (*post-hoc* LS test, Bare-Full canopy: $p < 0.001$, Bare-Reduced canopy: $p < 0.001$). The density of all four species were affected by canopy cover (**Figure 3B**, **Table 4A**). *Littorina obtusata* displayed a significantly higher density in both "Full canopy" and "Reduced canopy" compared to "Bare" (*post hoc* LS test, Bare-Full canopy: $p = 0.007$, Bare-Reduced canopy: $p = 0.004$) and *L. saxatilis* showed significantly higher density in "Reduced canopy" compared to "Bare" and "Full canopy" (*post-hoc* LS test, Reduced canopy-Bare: $p < 0.001$, Reduced

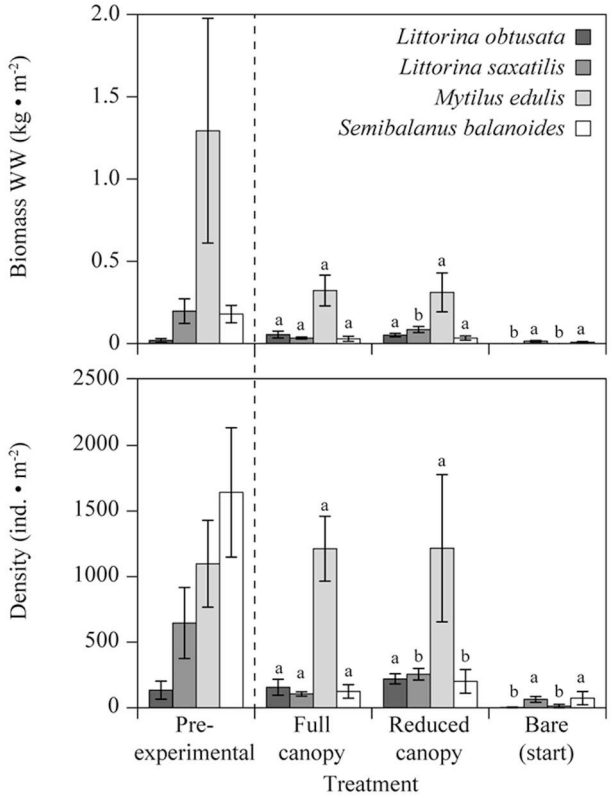

FIGURE 3 | (A) Biomass and **(B)** density of dominating intertidal faunal species in Kobbefjord across the treatments "Full canopy." "Reduced canopy" and "Bare (start)" measured in August 2014 and the "Pre-experimental" community measured in August 2011. Letters annotate significant differences of $p < 0.05$ by a *post-hoc* test between main treatments for each species, i.e., excluding "Pre-experimental." $N = 5$ for all mean values. Error bars are SE.

TABLE 4 | Summary statistics of one-way ANOVAs **(A)** assessing the effect of treatment ["Full canopy," "Reduced canopy" and "Bare (start)"] on biomass and density of dominating intertidal faunal species in Kobbefjord August 2014.

Species	Dependent variable	$F_{(2, 12)}$	p
(A)			
Semibalanus balanoides	Biomass	1.32	0.302
	Density	9.15	0.004**
Mytilus edulis	Biomass	45.07	< 0.001***
	Density	41.23	< 0.001***
Littorina obtusata	Biomass	10.96	0.002**
	Density	9.98	0.003**
Littorina saxatilis	Biomass	12.56	0.001**
	Density	19.96	< 0.001***
(B)			
	Species richness	7.678	0.007**
(C)			
	Rugosity	1.21	0.333
	Ice scour	0.12	0.872

(B) *Assessing effect of treatment ["Full canopy," "Reduced canopy" and "Bare (start)"] on faunal species richness in Kobbefjord August 2014.* ***(C)*** *Assessing effect of treatment ["Full canopy," "Reduced canopy" and "Bare (start)"] on rock rugosity and ice scour intensity. **$p < 0.01$, ***$p < 0.001$.*

canopy-Full canopy: $p = 0.003$) (**Figure 3B**). *Mytilus edulis* displayed a higher density in both "Full canopy" and "Reduced canopy" compared to "Bare" (*post-hoc* LS test, Bare-Full canopy: $p < 0.001$, Bare-Reduced canopy: $p < 0.001$) (**Figure 3B**) and *S. balanoides* displayed a higher density in "Reduced canopy" compared to "Bare" (*post-hoc* LS test, Reduced canopy-Bare: $p = 0.004$) (**Figure 3B**). Moreover, faunal species richness was significantly affected by canopy cover (**Table 4B**), displaying a higher species richness in "Full canopy" and "Reduced canopy" compared to "Bare" (*post-hoc* LS test, Bare-Full canopy: $p = 0.008$, Bare-Reduced canopy: $p = 0.026$). The inter-annual recolonization of *M. edulis* density, based on measurements in "Bare (annual)," was not significantly different between years [ANOVA, $F_{(2, 12)} = 0.45$, $p = 0.65$]. However, *S. balanoides* density was twice as high in 2012 as in the following 2 years [ANOVA, $F_{(2, 12)} = 5.39$, $p = 0.021$].

Modifying Properties of the Canopy-Forming Algae

Sea ice presence varied between years, with just 2 months of sea ice cover in the inner fjord in 2013, compared to 4–5 months of sea ice cover in 2012 and 2014 (**Figure 4**). We were unable to quantify the ice scouring intensity at site 1 and 2 in 2011–2012 due to loss of screws. However, the maximum value of the two screws in each quadrat, showed a similar pattern across sites in 2011-2012 and 2013-2014 [LR, $R^2 = 0.30$, $F_{(1, 13)} = 5.556$, $p = 0.035$], indicating that the variation in ice scouring intensity was consistent across sites between years. Therefore, we used the more complete dataset from 2013–2014 as a proxy for ice scouring intensity in the inner Kobbefjord. The maximum ice scouring intensity in terms of screw bending ranged between 0 and 75° across all quadrats, and maximum ice scouring intensity (2013–2014) did not differ significantly between treatments (**Table 4C**).

The running mean temperature measured in "Full canopy" and "Bare (start)," along with the running mean air temperature (AT) measured in Nuuk city from August 2011 to August 2014 are illustrated in **Figure 4**. Here, we show a slight difference between the mean temperatures in "Full canopy" compared to "Bare (start)." However, in order to uncover and compare the extreme temperatures measured in "Full canopy" and "Bare (start)," we extracted the 5th and 95th percentiles (**Table 5**, see **Supplementary Table 1** for monthly comparisons). We expect these to reflect air temperatures during low tide since the 5th percentiles in winter and the 95th percentiles in summer are below and above the typical range of sea surface temperatures in this area (Versteegh et al., 2012). The means of the percentiles across the 3-year period differed significantly between "Full canopy" and "Bare (start)," suggesting that algal cover buffers the temperature variations (**Table 5**). Testing the percentiles of years separately also showed that the extreme temperatures of

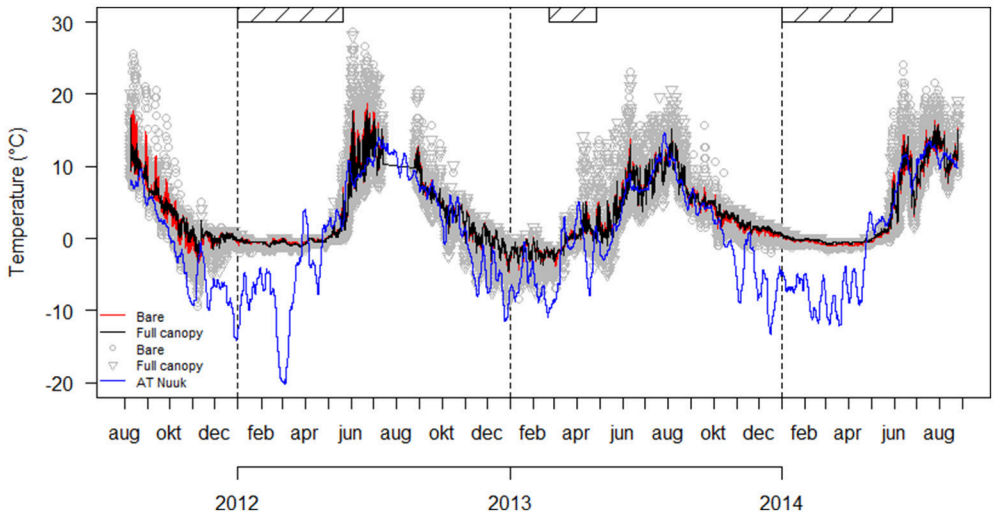

FIGURE 4 | Temperature with running mean (10 observations) recorded in mid intertidal at inner Kobbefjord for the two treatments "Full canopy" and "Bare (start)" from August 2011 through August 2014 (data not available for July 14th–Aug 24th 2012). Air temperature (AT) with running mean (336 observations) recorded in Nuuk by the Greenland Ecosystem Monitoring program in the same period. Hatched bars represent periods of sea ice cover in inner Kobbefjord based on automatized photographing (data only available for January through May).

TABLE 5 | 5th (extreme low) and 95th (extreme high) percentiles of yearly temperatures (°C) in treatment "Full canopy" and "Bare (start)" in inner Kobbefjord mid intertidal from August 2011 to August 2014.

Treatment:	***Bare (start)***		***Full canopy***	
Percentile:	**5th**	**95th**	**5th**	**95th**
Period	**°C**			
Aug 2011–Aug 2012	−0.935	13.112	0.915***	12.619***
Sep 2012–Aug 2013	−2.945	11.107	−2.922	11.116
Sep 2013–Aug 2014	−0.935	13.112	−0.433***	13.112***
Grand total	−1.437	12.611	−1.416***	12.611***

Monthly percentiles are shown in ***Supplementary Table 1****. *Marks level of p-value from two-sample t-test contrasting "Bare (start)" and "Full canopy" mean percentiles. ***$p < 0.001$.*

2011–2012 and 2013–2014 differed significantly between the two treatments, while this was not the case for 2012–2013 (**Table 5**). Testing the percentiles of each month separately showed that mainly summer and winter months differed between treatments, especially so for colder months (see **Supplementary Table 1**). In some summer months, canopy cover reduced the 5% highest temperatures by a maximum of 5.5°C and during winter months the 5% lowest temperatures were raised by a maximum of 0.5°C, again with canopy-forming algae reducing temperature extremes.

Rock Rugosity and Recolonization

Rock rugosity did not differ significantly between the three main treatments (**Table 4C**). Therefore, we chose to combine all 15 quadrats in a linear regression to test the relation between recruitment and rugosity. As opposed to all other invertebrate taxa, the total density of *M. edulis* showed a positive linear relationship with rock rugosity [LR, $R^2 = 0.551$, $F_{(1,13)} = 18.21$, $p < 0.001$] [see **Supplementary Table 2** in Supplementary Material for full (M)LR details]. With a multiple linear regression, we show that both canopy biomass and rock rugosity influenced the total *M. edulis* density positively [MLR, $R^2 = 0.726$, $F_{(2,12)} = 19.53$, $p < 0.001$]. When corrected statistically for canopy biomass, rock rugosity explained 62% of the variation in mussel density ($R^2 = 0.62$, $p < 0.001$) and when corrected statistically for rock rugosity, canopy biomass explained 44% ($R^2 = 0.44$, $p = 0.010$). In addition, *A. nodosum* recruit density showed a positive linear relationship with rock rugosity [LR, $R^2 = 0.419$, $F_{(1,13)} = 11.11$, $p = 0.005$].

Recovery Period of *Ascophyllum nodosum*

We estimated the early growth rate of *A. nodosum* recruits in the period August 2011–August 2014 to be 1.4 cm yr^{-1}. This was based on Hartigan's diptest (HD) that showed the distribution of recruit lengths to be multimodal, representing three age groups (HD, $n = 76$, $D = 0.06$, $p = 0.042$), for which we estimated mean lengths with the Expectation-Maximization algorithm. The addition of the algal recruit length data from 20 quadrats, cleared in August 2014 and quantified in August 2016, increased the sample size 9 times. This strengthened analysis (HD, $n = 673$, $D = 0.04$, $p < 0.001$) identified a similar early growth rate of 2.0 cm yr^{-1}. Based on the strengthened estimate of early growth rate, resulting in 4 cm long shoots after 2 years of linear growth, and assuming an exponential growth pattern thereafter with an estimated growth rate of 0.19 % yr^{-1} [4.92 cm yr^{-1}/(4 + 46.9 cm)/2], we estimated that it would take ca 15 years (including the first 2 years of linear growth) for *A. nodosum* recruits to reach the mean length of the "Pre-experimental" canopy in inner Kobbefjord.

DISCUSSION

Macroalgal Canopy Cover Facilitates Faunal Recolonization

The recolonization of *M. edulis, S. balanoides* and the two snails *L. obtusata* and *L. saxatilis* displayed a positive response to macroalgal canopy cover (predominately *A. nodosum*) at the mid intertidal level in inner Kobbefjord. These findings support the hypothesis that algal canopy has an overall facilitating effect on faunal recolonization in a sub-Arctic intertidal. This is opposed to findings from a temperate intertidal, where an overall neutral response in barnacle recruitment to *A. nodosum* canopy cover was observed at both mid- and high intertidal levels (Beermann et al., 2013). Other studies find positive biotic responses to algal canopy cover confined to the high intertidal (Dayton, 1971; Hawkins, 1983; Jenkins et al., 1999b). In relation to the stress gradient hypothesis, we have already suggested that in a stressful environment like the sub-Arctic, the positive effects of canopy cover in modifying the environment are likely to overrule the negative effects such as space competition and whiplashes from algal fronds. To further verify this hypothesis, we explored the effect of algal canopy in modifying the key stressors in the sub-Arctic intertidal, i.e., extreme air temperature and sea ice scouring.

Macroalgal Canopy Cover Modifies Extreme Temperatures

While earlier studies from Greenland have reported marked diurnal and seasonal temperature variation in the sub-Arctic intertidal (Høgslund et al., 2014), our results take a step further and document that the *A. nodosum* canopy created significant small-scale spatial variation in temperature by acting as an insulating cover. The macroalgal cover in inner Kobbefjord reduced the highest 5% temperatures in summer by up to 5.5°C and raised the lowest 5% in winter by up to 0.5°C (see **Supplementary Table 1**). Thus, *A. nodosum* canopy buffers extreme air temperatures experienced by organisms in a sub-Arctic rocky intertidal. This pattern is consistent with studies from the temperate intertidal where the daily maximum temperature, measured over a month, was lowered by the canopy cover in the mid- and high intertidal zone (Beermann et al., 2013; Watt and Scrosati, 2013a). Therefore, we suggest that the ability of algal canopy to buffer extreme temperatures, likely contributes to the overall positive biotic response to canopy cover found at this study site. In contrast, the canopy-forming algae had no effect on ice scouring intensity, indicating that the canopy did not markedly protect the understory community from the mechanical disturbance of sea ice scouring, which is consistent with previous studies describing *A. nodosum*'s low capacity to withstand ice scouring (Åberg, 1992).

The extreme temperatures measured in this study were within the mean lower and upper thermal limits of the dominating intertidal faunal species, *L. saxatilis*, *L. obtusata*, *S. balanoides,* and *M. edulis*, documented in Scotland (−16.4–35°C, Davenport and Davenport, 2005). However, the current measures of thermal lethal limits in southern populations may not be the same as for sub-Arctic populations. As an example, *M. edulis* populations in Canada (Bourget, 1983) displayed lower, mean lower lethal limits than the populations in Scotland (Davenport and Davenport, 2005). Moreover, mortality rates at increasing temperatures may differ depending on life stage (Foster, 1971a; Bourget, 1983) and most studies include only adult life stages.

In inner Kobbefjord mid intertidal, the minimum 5th percentile temperature was −6.0°C and the maximum 95th percentile was 22°C (see **Supplementary Table 1** in Supplementary Material). These temperatures are expected to increase in the future, based on a warming trend in mean annual air temperatures in west Greenland (Thyrring et al., 2017). In a nearby climate station, the air temperatures have increased by 0.13 ± 0.02°C per year over the last three decades together with an increase in the duration of annual ice-free cover along the Greenland west coast (Marbà et al., 2017). Thus, in future scenarios, the ability of algal canopy to buffer temperature extremes may become more important in preventing increased mortality in understory faunal communities, both with regard to warmer air temperatures in summer and colder air temperatures in winter, as the annual sea ice cover decreases. For example, it was evident that sea ice was buffering cold air temperatures during winter at the studied site, as we observed a marked difference between air temperatures (AT) and temperatures measured in the intertidal during winter compared to the other seasons. During the winter 2013, with only 2 months of sea ice cover in Kobbefjord, the temperatures from the intertidal also showed greater variation than in the other two winters with 5 months of sea ice cover (2012, 2014, **Figure 4**).

Multiple other physico-chemical stress factors, not included in our study, such as desiccation, water flow, wave action, salinity and pH, may also be altered by canopy-forming algae, contributing to the overall positive biotic response to canopy cover (Helmuth, 1998; Jenkins et al., 1999a; Beermann et al., 2013; Wahl et al., 2018).

Rock Rugosity Facilitates Recolonization

The coupling between rock roughness and the colonization of intertidal species has been noted before (Guidetti et al., 2004; Skinner and Coutinho, 2005; Chase et al., 2016). In the studied area, *M. edulis* is, in general, confined to cracks and crevices in the intertidal zone (Blicher et al., 2013) and here, we show that the total recolonization of *M. edulis* across the main treatments was positively related to both rock rugosity and macroalgal biomass. Moreover, *A. nodosum* canopy may contribute to an additional level of rugosity, in that holdfasts attached to the rock, as well as the canopies above, form multiple crevices for settlement. This type of rugosity, habitat complexity and increased surface area for colonization may contribute to the overall positive effect that the *A. nodosum* canopy has on faunal recolonization. In addition, we found that recolonization of *A. nodosum* was positively related to rock rugosity, suggesting that rock roughness is important for the settlement and early development of germlings, likely explained by an increase in settling surface and protection from ice scouring

and other physical stressors in the small crevices (Heaven and Scrosati, 2008; Gerwing et al., 2015; Musetta-Lambert et al., 2015).

Recovery Time of the Intertidal Community

In a sub-Arctic intertidal, where mechanical disturbance such as ice scouring may dislodge the entire community, we show that, for both fauna and macroalgae, the subsequent recovery in density is faster than in biomass. Thus, while the organisms recolonize relatively fast after maximum disturbance, it takes longer to recover the biomass of the intertidal community. On the other hand, when *A. nodosum* individuals prevail and the canopy is simply sliced by ice scouring, the algal biomass fully recovers after 3 years, and the recolonization rates resemble those found in an untouched canopy.

The early growth rate of newly-settled *A. nodosum* in the studied intertidal community averaged 1.4–2 cm yr^{-1}. Comparably, the growth rate of adult *A. nodosum* measured in the same macroalgal community is 4.92 cm yr^{-1} (Marbà et al., 2017). Early growth rates of *A. nodosum* recruits ($\leq$2 years old) from the Isle of Man and south west Spain are reported at 7.2 cm yr^{-1} and 9.6 cm yr^{-1}, respectively (Cervin et al., 2005; Viana et al., 2014). However, in Maine, USA, Keser and Larson (1984) reported an early growth rate of 1.6 cm yr^{-1}, which is similar to what we found. Based on existing growth patterns for this species (Viana et al., 2014), but modified for the local conditions, we estimated that *A. nodosum* in inner Kobbefjord would reach its full length, averaging 46.9 cm, ca 15 years after removal by mechanical disturbance. Correspondingly, we found the macroalgal biomass to be very low, even after 3 years of recovery. The estimated recovery period, in height, is higher than the minimum mean age (6 years) of unbroken branches *of A. nodosum* found in this study, bearing in mind that holdfasts of *A. nodosum* have been suggested to be 50–70 years old, and the community has been referred to as "marine trees" (Olsen et al., 2010), displaying similar patterns of slow population growth as terrestrial trees (Capdevila et al., 2016). However, it is close to the minimum age of the longest individuals, assessed as the presence of 13 full years of consecutive growth, of *A. nodosum* individuals also observed in Kobbefjord (Figure 3 in Marbà et al., 2017). A long recovery period of *A. nodosum* height corresponds to findings in north temperate regions (Printz, 1956; Cervin et al., 2005; Ingólfsson and Hawkins, 2008). However, they largely assign a delay in *A. nodosum* biomass recovery to the competition from other fucoid species. In inner Kobbefjord, algal recruits on bare rock were dominated by *A. nodosum*, with a few *F. vesiculosus,* suggesting that recovery of *A. nodosum* in inner Kobbefjord was not delayed by interspecific competition. Rather, the slow recovery of *A. nodosum* canopy height may be largely due to the constraints of the abiotic environment. Whereas our study assessed the recovery time of canopy height, a complete study of recovery of canopy biomass should also include quantification of population dynamics in terms of recruitment and mortality. Recruitment and mortality rates in the studied *A. nodosum* population, assessed through the Greenland Ecosystem Monitoring program, showed that the vast majority of the biomass was quite persistent with loss rates of individuals of only 1.6–6.2% per year, whereas the pool of new shoots add markedly to the population dynamics, resulting in overall recruitment rates of 6–111% and mortality rates of 1.6–60% for the period 2012–2015. However, the overall population growth ensured a biomass increase of the population of 1–50% yr^{-1} during the assessment period 2012–15, which, by far, outweighed the biomass of lost individuals (Juul-Pedersen et al., 2015).

Ascophyllum nodosum mainly dominates in wave-sheltered areas (Scrosati and Heaven, 2008), while other fucoid species, such as *F. vesiculosus* and *F. distichus*/*F. evanescens* takes over at more exposed sites as well as above the northern distributional range of *A. nodosum*. Like *A. nodosum*, we expect these other fucoid species to display a similar buffering effect on extreme temperatures and facilitate the colonization of intertidal species. However, buffering capacity most likely depends on the level of canopy biomass, which was high in the studied area.

Based on future projections on climate change, the distributional ranges of both *A. nodosum* and *F. vesiculosus* are expected to shift northward (Jueterbock et al., 2013). A northward shift in other high latitude intertidal macroalgal communities have already been documented (Weslawski et al., 2010), and a recent study found that warming tends to enhance the growth of *A. nodosum* at its northern distribution limit (Marbà et al., 2017). In comparison, the southern distribution limits of dominant intertidal fauna, *M. edulis* and *S. balanoides,* are also moving northward (Jones et al., 2010, 2012), and based on our results, algal canopies may be a key habitat in facilitating the northward colonization and abundance of these intertidal species at their northern distribution limit (Gilman et al., 2010).

CONCLUSION

This study emphasizes the role of *A. nodosum* canopy and rocky rugosity in structuring high latitude intertidal communities. We show that intertidal canopy-forming macroalgae have an overall facilitating effect on faunal species richness and recolonization, likely by reducing temperature variations and increasing settling surfaces and habitat complexity. We show that the canopy modifies the small-scale variation in temperature experienced by intertidal fauna, but fails to reduce ice scouring at the rock surface, underlining the complexity in how a physical stressor can vary depending on scale. The facilitating properties of algal canopies are important to consider when predicting future distributional patterns of high latitude intertidal fauna. To fully comprehend the community-structuring role of algal canopies, we need to study whether and how they modify other key stressors, such as salinity, pH, water loss and flow, including different intertidal levels. Finally, we estimated that the full establishment and recovery period of the intertidal community may take at least 15 years while biomass and height of *A. nodosum* canopy builds up, which is important to consider when predicting latitudinal range shifts in the sub-Arctic and Arctic intertidal community.

DATA AVAILABILITY STATEMENT

The raw data supporting the conclusions of this manuscript will be made available by the authors, without undue reservation, to any qualified researcher. The air temperature data from Nuuk was obtained from Greenland Ecosystem Monitoring program (GEM). Requests to access these datasets should be directed to http://data.g-e-m.dk/. The long time series of photos documenting the sea ice in Kobbefjord was obtained from the Andreas Westergaard-Nielsen and request to access these photos should be directed to Andreas Westergaard-Nielsen, (awn@ign.ku.dk).

AUTHOR CONTRIBUTIONS

All authors have approved the submission version. MS, DK-J, KM, and BO conceived and planned the experiment. DK-J, KM, BO, NM, SØ, MB, and ML conducted the field work. Data analysis was led by SØ with input from DK-J, MS, KM, and BO. SØ produced all figures and wrote the first draft with contributions and comments from all the authors.

ACKNOWLEDGMENTS

This project was funded by the Danish Environmental Protection Agency's Arctic initiative (DANCEA) and by the Arctic Research Centre at Aarhus University. We are thankful to Anissa Merzouk for helping with the fieldwork sampling, and we are thankful to Jakob Thyrring and Søren Larsen for support on data analysis. We thank Andreas Westergaard-Nielsen for providing photos of the sea ice cover in Kobbefjord, and we thank the Greenland Ecosystem Monitoring program (www.G-E-M.dk) for providing weather data from Nuuk city. We are also grateful to the Greenland Institute of Natural Resources (GINR), Nuuk, Greenland, and their staff for providing excellent working conditions.

SUPPLEMENTARY MATERIAL

The Supplementary Material for this article can be found online at: https://www.frontiersin.org/articles/10.3389/fmars.2018.00332/full#supplementary-material

REFERENCES

Åberg, P. (1992). A demographic study of two populations of the seaweed *Ascophyllum nodosum*. *Ecology* 73, 1473–1487. doi: 10.2307/1940691

Åberg, P. (1996). Patterns of reproductive effort in the brown alga *Ascophyllum nodosum*. *Mar. Ecol. Prog. Ser.* 138, 199–207. doi: 10.3354/meps138199

Beermann, A. J., Ellrich, J. A., Molis, M., and Scrosati, R. A. (2013). Effects of seaweed canopies and adult barnacles on barnacle recruitment: the interplay of positive and negative influences. *J. Exp. Mar. Biol. Ecol.* 448, 162–170. doi: 10.1016/j.jembe.2013.07.001

Benaglia, T., Chauveau, D., Hunter, D. R., and Young, D. (2009). Mixtools: an R package for analyzing finite mixture models. *J. Stat. Softw.* 32, 1–29. doi: 10.18637/jss.v032.i06

Bertness, M. D., and Callaway, R. (1994). Positive interactions in communities. *Trends Ecol. Evol.* 9, 187–191. doi: 10.1016/0169-5347(94)90087-6

Bertness, M. D., Leonard, G. H., Levine, J. M., Schmidt, P. R., and Ingraham, A. O. (1999). Testing the relative contribution of positive and negative interactions in rocky intertidal communities. *Ecology* 80, 2711–2726. doi: 10.2307/177252

Blicher, M. E., Sejr, M. K., and Hogslund, S. (2013). Population structure of *Mytilus edulis* in the intertidal zone in a sub-Arctic fjord, SW Greenland. *Mar. Ecol. Prog. Ser.* 487, 89–100. doi: 10.3354/Meps10317

Bourget, E. (1983). Seasonal variations of cold tolerance in intertidal mollusks and relation to environmental conditions in the St. Lawrence Estuary. *Can. J. Zool.* 61, 1193–1201. doi: 10.1139/z83-162

Broitman, B. R., Szathmary, P. L., Mislan, K. A. S., Blanchette, C. A., and Helmuth, B. (2009). Predator-prey interactions under climate change: the importance of habitat vs. body temperature. *Oikos* 118, 219–224. doi: 10.1111/j.1600-0706.2008.17075.x

Capdevila, P., Hereu, B., Llu, J., and Linares, C. (2016). Unravelling the natural dynamics and resilience patterns of underwater Mediterranean forests: insights from the demography of the brown alga *Cystoseira zosteroides*. *J. Ecol.* 104, 1799–1808. doi: 10.1111/1365-2745.12625

Cervin, G., Åberg, P., and Jenkins, S. R. (2005). Small-scale disturbance in a stable canopy dominated community: implications for macroalgal recruitment and growth. *Mar. Ecol. Prog. Ser.* 305, 31–40. doi: 10.3354/meps305031

Cervin, G., Lindegarth, M., Viejo, R. M., and Åberg, P. (2004). Effects of small-scale disturbances of canopy and grazing on intertidal assemblages on the Swedish west coast. *J. Exp. Mar. Biol. Ecol.* 302, 35–49. doi: 10.1016/j.jembe.2003.09.022

Chase, A. L., Dijkstra, J. A., and Harris, L. G. (2016). The influence of substrate material on ascidian larval settlement. *Mar. Pollut. Bull.* 106, 35–42. doi: 10.1016/j.marpolbul.2016.03.049

Crowe, T. P., Cusson, M., Bulleri, F., Davoult, D., Arenas, F., Aspden, R., et al. (2013). Large-scale variation in combined impacts of canopy loss and disturbance on community structure and ecosystem functioning. *PLoS ONE* 8:e6623. doi: 10.1371/journal.pone.0066238

Davenport, J., and Davenport, J. L. (2005). Effects of shore height, wave exposure and geographical distance on thermal niche width of intertidal fauna. *Mar. Ecol. Prog. Ser.* 292, 41–50. doi: 10.3354/meps292041

Dayton, P. K. (1971). Competition, disturbance, and community organization: the provision and subsequent utilization of space in a rocky intertidal community. *Ecol. Monogr.* 41, 351–389. doi: 10.2307/1948498

Denny, M. W., and Harley, C. D. G. (2006). Hot limpets: predicting body temperature in a conductance-mediated thermal system. *J. Exp. Biol.* 209, 2409–2419. doi: 10.1242/jeb.02257

Foster, B. A. (1971a). Desiccation as a factor in the intertidal zonation of barnacles. *Mar. Biol.* 8, 12–29. doi: 10.1007/BF00349341

Foster, B. A. (1971b). On the determinants of the upper limit of intertidal distribution of barnacles (*Crustacea*: *Cirripedia*). *J. Anim. Ecol.* 40, 33–48. doi: 10.2307/3328

Gendron, L., Merzouk, A., Bergeron, P., and Johnson, L. E. (2017). Managing disturbance: the response of a dominant intertidal seaweed *Ascophyllum nodosum* (L .) Le Jolis to different frequencies and intensities of harvesting. *J. Appl. Phycol.* 30, 1–16. doi: 10.1007/s10811-017-1346-5

Gerwing, T. G., Drolet, D., Barbeau, M. A., Hamilton, D. J., and Allen Gerwing, A. M. (2015). Resilience of an intertidal infaunal community to winter stressors. *J. Sea Res.* 97, 40–49. doi: 10.1016/j.seares.2015.01.001

Gilman, S. E., Urban, M. C., Tewksbury, J., Gilchrist, G. W., and Holt, R. D. (2010). A framework for community interactions under climate change. *Trends Ecol. Evol.* 25, 325–331. doi: 10.1016/j.tree.2010.03.002

Guidetti, P., Bianchi, C. N., Chiantore, M., Schiaparelli, S., Morri, C., and Cattaneo-Vietti, R. (2004). Living on the rocks: substrate mineralogy and the structure of subtidal rocky substrate communities in the Mediterranean Sea. *Mar. Ecol. Prog. Ser.* 274, 57–68. doi: 10.3354/meps274057

Gutt, J. (2001). On the direct impact of ice on marine benthic communities, a review. *Polar Biol.* 24, 553–564. doi: 10.1007/s003000100262

Hartigan, P. M. (1985). The dip test of unimodality. *Ann. Stat.* 13, 70–84. doi: 10.1214/aos/1176346577

Hawkins, S. J. (1983). Interactions of Patella and macroalgae with settling *Semibalanus balanoides* (L.). *J. Exp. Mar. Bio. Ecol.* 71, 55–72. doi: 10.1016/0022-0981(83)90104-1

Heaven, C. S., and Scrosati, R. A. (2008). Benthic community composition across gradients of intertidal elevation, wave exposure, and ice scour in Atlantic Canada. *Mar. Ecol. Prog. Ser.* 369, 13–23. doi: 10.3354/meps07655

Helmuth, B. (1998). Intertidal mussle microclimates: predicting the body temperature of a sessile invertebrate. *Ecol. Monogr.* 68, 51–74. doi: 10.2307/2657143

Helmuth, B., Broitman, B. R., Yamane, L., Gilman, S. E., Mach, K., Mislan, K. A. S., et al. (2010). Organismal climatology: analyzing environmental variability at scales relevant to physiological stress. *J. Exp. Biol.* 213, 995–1003. doi: 10.1242/jeb.038463

HilleRisLambers, J., Harsch, M. A., Ettinger, A. K., Ford, K. R., and Theobald, E. J. (2013). How will biotic interactions influence climate change-induced range shifts? *Ann. N. Y. Acad. Sci.* 1297, 112–125. doi: 10.1111/nyas.12182

Høgslund, S., Sejr, M. K., Wiktor, J., Blicher, M. E., and Wegeberg, S. (2014). Intertidal community composition along rocky shores in South-west Greenland: a quantitative approach. *Polar Biol.* 37, 1549–1561. doi: 10.1007/s00300-014-1541-7

Howat, I. M., Joughin, I., and Scambos, T. A. (2007). Rapid changes in ice discharge from Greenland outlet glaciers. *Science* 315, 1559–1561. doi: 10.1126/science.1138478

Ingólfsson, A., and Hawkins, S. J. (2008). Slow recovery from disturbance: a 20 year study of *Ascophyllum* canopy clearances. *J. Mar. Biol. Assoc.* 88, 689–691. doi: 10.1017/S0025315408001161

Jenkins, S. R., Hawkins, S. J., and Norton, T. A. (1999a). Direct and indirect effects of a macroalgal canopy and limpet grazing in structuring a sheltered inter-tidal community. *Mar. Ecol. Prog. Ser.* 188, 81–92. doi: 10.3354/meps188081

Jenkins, S. R., Norton, T. A., and Hawkins, S. J. (1999b). Settlement and post-settlement interactions between *Semibalanus balanoides* (L.) (*Crustacea*: *Cirripedia*) and three species of fucoid canopy algae. *J. Exp. Mar. Bio. Ecol.* 236, 49–67. doi: 10.1016/S0022-0981(98)00189-0

Jenkins, S. R., Norton, T. A., and Hawkins, S. J. (2004). Long term effects of *Ascophyllum nodosum* canopy removal on mid shore community structure. *J. Mar. Biol. Assoc.* 84, 327–329. doi: 10.1017/S0025315404009221h

Jones, S. J., Lima, F. P., and Wethey, D. S. (2010). Rising environmental temperatures and biogeography: poleward range contraction of the blue mussel, *Mytilus edulis* L., in the western Atlantic. *J. Biogeogr.* 37, 2243–2259. doi: 10.1111/j.1365-2699.2010.02386.x

Jones, S. J., Southward, A. J., and Wethey, D. S. (2012). Climate change and historical biogeography of the barnacle *Semibalanus balanoides*. *Glob. Ecol. Biogeogr.* 21, 716–724. doi: 10.1111/j.1466-8238.2011.00721.x

Jueterbock, A., Tyberghein, L., Verbruggen, H., Coyer, J. A., Olsen, J. L., and Hoarau, G. (2013). Climate change impact on seaweed meadow distribution in the North Atlantic rocky intertidal. *Ecol. Evol.* 3, 1356–1373. doi: 10.1002/ece3.541

Juul-Pedersen, T., Arendt, K., Mortensen, J., Krawczyk, D., Retzel, A., Nygaard, R., et al. (2015). "Nuuk basic - the marinebasic programme," in *Nuuk Ecological Research Operations 9th Annual Report*, ed.T. R. Topp-Jørgensen, E. Hansen, and J. Christensen. Aarhus University, DCE – Danish Centre for Environment and Energy, 46–66.

Keser, M., and Larson, B. R. (1984). Colonization and growth of *Ascophyllum nodosum* in Maine. *J. Phycol.* 20, 83–87. doi: 10.1111/j.0022-3646.1984.00083.x

Keser, M., Swenarton, J. T., and Foertch, J. F. (2005). Effects of thermal input and climate change on growth of *Ascophyllum nodosum* (*Fucales*, *Phaeophyceae*) in eastern Long Island Sound (USA). *J. Sea Res.* 54, 211–220. doi: 10.1016/j.seares.2005.05.001

Luckhurst, B. E., and Luckhurst, K. (1978). Analysis of the influence of substrate variables on coral reef fish communities. *Mar. Biol.* 49, 317–323. doi: 10.1007/BF00455026

Lüning, K. (1990). *Seaweeds: Their Environment, Biogeography, and Ecophysiology*. New York, NY: John Wiley and Sons, Inc.

Maechler, M. (2016). *Diptest: Hartigan's Dip Test Statistic for Unimodality - Corrected*. Available online at: https://cran.r-project.org/package=diptest

Marbà, N., Krause-Jensen, D., Olesen, B., Christensen, P. B., Merzouk, A., Rodrigues, J., et al. (2017). Climate change stimulates the growth of the intertidal macroalgae *Ascophyllum nodosum* near the northern distribution limit. *Ambio* 46, 119–131. doi: 10.1007/s13280-016-0873-7

McCook, L. J., and Chapman, A. R. O. (1991). Community succession following massive ice-scour on an exposed rocky shore: effects of *Fucus* canopy algae and of mussels during late succession. *J. Exp. Mar. Biol. Ecol.* 154, 137–169. doi: 10.1016/0022-0981(91)90161-O

Mikkelsen, D. M., Rysgaard, S., and Glud, R. N. (2008). Microalgal composition and primary production in Arctic sea ice: a seasonal study from Kobbefjord (Kangerluarsunnguaq), West Greenland. *Mar. Ecol. Prog. Ser.* 368, 65–74. doi: 10.3354/meps07627

Mosbech, A., Anthonsen, K. L., Blyth, A., Boertmann, D., Buch, E., Cake, D., et al. (2000). *Environmental Oil Spill Sensitivity Atlas for the West Greenland Coastal Zone*. Available online at: http://www.ens.dk

Motyka, R. J., Cassotto, R., Truffer, M., Kjeldsen, K., Van As, D., Korsgaard, N. J., et al. (2017). Asynchronous behavior of outlet glaciers feeding Godthåbsfjord (Nuup Kangerlua) and the triggering of Narsap Sermia's retreat in SW Greenland. *J. Glaciol.* 63, 1–21. doi: 10.1017/jog.2016.138

Musetta-Lambert, J. L., Scrosati, R. A., Keppel, E. A., Barbeau, M. A., Skinner, M. A., and Courtenay, S. C. (2015). Intertidal communities differ between breakwaters and natural rocky areas on ice- scoured Northwest Atlantic coasts Intertidal communities differ between breakwaters and natural rocky areas on ice-scoured Northwest Atlantic coasts. *Mar. Ecol. Prog. Ser.* 539, 19–31. doi: 10.3354/meps11484

Nutman, A. P., and Friend, C. R. L. (2009). New 1:20,000 scale geological maps, synthesis and history of investigation of the Isua supracrustal belt and adjacent orthogneisses, southern West Greenland: a glimpse of Eoarchaean crust formation and orogeny. *Precambrian Res.* 172, 189–211. doi: 10.1016/j.precamres.2009.03.017

Olsen, J. L., Zechman, F. W., Hoarau, G., Coyer, J. A., Stam, W. T., Valero, M., et al. (2010). The phylogeographic architecture of the fucoid seaweed *Ascophyllum nodosum*: an intertidal "marine tree" and survivor of more than one glacial-interglacial cycle. *J. Biogeogr.* 37, 842–856. doi: 10.1111/j.1365-2699.2009.02262.x

Petzold, W., Willers, M. T., and Scrosati, R. A. (2014). Visual record of intertidal disturbance caused by sea ice in the spring on the Atlantic coast of Nova Scotia. *F1000Research* 3:112. doi: 10.12688/f1000research.4439

Printz, H. (1956). Recuperation and recolonisation in *Ascophyllum nodosum*. *Proc. Int. Seaweed Symp.* 2, 194–197.

R Core Team (2017). *A Language and Environment for Statistical Computing*. Available online at: https://www.r-project.org/

Redner, R. A., and Walker, H. F. (1984). Mixture densities, maximum likelihood and the EM algorithm. *Soc. Ind. Appl. Math.* 26, 195–239. doi: 10.1137/1026034

Richter, A., Rysgaard, S., Dietrich, R., Mortensen, J., and Petersen, D. (2011). Coastal tides in West Greenland derived from tide gauge records. *Ocean Dyn.* 61, 39–49. doi: 10.1007/s10236-010-0341-z

Scrosati, R., and Eckersley, L. K. (2007). Thermal insulation of the intertidal zone by the ice foot. *J. Sea Res.* 58, 331–334. doi: 10.1016/j.seares.2007.08.003

Scrosati, R., and Heaven, C. (2008). Trends in abundance of rocky intertidal seaweeds and filter feeders across gradients of elevation, wave exposure, and ice scour in eastern Canada. *Hydrobiologia* 603, 1–14. doi: 10.1007/s10750-007-9160-8

Skinner, L. F., and Coutinho, R. (2005). Effect of microhabitat distribution and substrate roughness on barnacle *Tetraclita stalactifera* (Lamarck, 1818) settlement. *Brazilian Arch. Biol. Technol.* 48, 109–113. doi: 10.1590/S1516-89132005000100014

Steen, H., and Rueness, J. (2004). Comparison of survival and growth in germlings of six fucoid species (*Fucales*, *Phaeophyceae*) at two different temperature and nutrient levels. *Sarsia* 89, 175–183. doi: 10.1080/00364820410005818

Thyrring, J., Blicher, M. E., Sørensen, J. G., Wegeberg, S., and Sejr, M. K. (2017). Rising air temperatures will increase intertidal mussel abundance in the Arctic. *Mar. Ecol. Prog. Ser.* 584, 91–104. doi: 10.3354/meps12369

Versteegh, E. A. A., Blicher, M. E., Mortensen, J., Rysgaard, S., Als, T. D., and Wanamaker, A. D. (2012). Oxygen isotope ratios in the shell of *Mytilus*

edulis: Archives of glacier meltwater in Greenland? *Biogeosciences* 9, 5231–5241. doi: 10.5194/bg-9-5231-2012

Viana, I. G., Bode, A., and Fernández, C. (2014). Growth and production of new recruits and adult individuals of *Ascophyllum nodosum* in a non-harvested population at its southern limit (Galicia, NW Spain). *Mar. Biol.* 161, 2885–2895. doi: 10.1007/s00227-014-2553-0

Wahl, M., Schneider Covach,ã, S., Saderne, V., Hiebenthal, C., Müller, J., Pansch, C., et al. (2018). Macroalgae may mitigate ocean acidification effects on mussel calcification by increasing pH and its fluctuations. *Limnol. Oceanogr.* 63, 3–21. doi: 10.1002/lno.10608

Walters, L. J., and Wethey, D. S. (1996). Settlement and early post-settlement survival of sessile marine invertebrates on topographically complex surfaces: the importance of refuge dimensions and adult morphology. *Mar. Ecol. Prog. Ser.* 137, 161–171. doi: 10.3354/meps137161

Watt, C. A., and Scrosati, R. A. (2013a). Bioengineer effects on understory species richness, diversity, and composition change along an environmental stress gradient: experimental and mensurative evidence. *Estuar. Coast. Shelf Sci.* 123, 10–18. doi: 10.1016/j.ecss.2013.02.006

Watt, C. A., and Scrosati, R. A. (2013b). Regional consistency of intertidal elevation as a mediator of seaweed canopy effects on benthic species richness, diversity, and composition. *Mar. Ecol. Prog. Ser.* 491, 91–99. doi: 10.3354/meps10521

Weslawski, J. M., Wiktor, J., and Kotwicki, L. (2010). Increase in biodiversity in the arctic rocky littoral, Sorkappland, Svalbard, after 20 years of climate warming. *Mar. Biodivers.* 40, 123–130. doi: 10.1007/s12526-010-0038-z

Zawada, D. G., Piniak, G. A., and Hearn, C. J. (2010). Topographic complexity and roughness of a tropical benthic seascape. *Geophys. Res. Lett.* 37, 1–6. doi: 10.1029/2010GL043789

Conflict of Interest Statement: ML is employed by company Danish Center for Wild Salmon.

The remaining authors declare that the research was conducted in the absence of any commercial or financial relationships that could be construed as a potential conflict of interest.

frontiers in Marine Science

ORIGINAL RESEARCH
published: 26 October 2018
doi: 10.3389/fmars.2018.00397

Influence of the Seagrass, *Zostera marina*, on Wave Attenuation and Bed Shear Stress Within a Shallow Coastal Bay

Matthew A. Reidenbach and Emily L. Thomas*

Department of Environmental Sciences, University of Virginia, Charlottesville, VA, United States

OPEN ACCESS

Edited by:
François G. Schmitt, Laboratoire d'Océanologie et de Géosciences-UMR 8187 LOG, Centre National de la Recherche Scientifique (CNRS), France

Reviewed by:
Alejandro Orfila, Instituto Mediterráneo de Estudios Avanzados (IMEDEA), Spain
Ian Townend, University of Southampton, United Kingdom

****Correspondence:***
Matthew A. Reidenbach
reidenbach@virginia.edu

Specialty section:
This article was submitted to Coastal Ocean Processes, a section of the journal Frontiers in Marine Science

Received: *29 March 2018*
Accepted: *09 October 2018*
Published: *26 October 2018*

Citation:
Reidenbach MA and Thomas EL (2018) Influence of the Seagrass, Zostera marina, on Wave Attenuation and Bed Shear Stress Within a Shallow Coastal Bay. Front. Mar. Sci. 5:397. doi: 10.3389/fmars.2018.00397

Local effects of flow interaction with seagrass structure modify meadow scale hydrodynamics, resulting in lower current velocities and wave heights within a seagrass meadow. This attenuation promotes the deposition of suspended sediment, increasing the light available locally to benthic organisms. To elucidate the relationship between small-scale hydrodynamics that occur at the sea floor and the meadow scale effects of seagrass, high resolution velocity profiles were recorded adjacent to the sediment-water interface within a *Zostera marina* seagrass meadow in South Bay, Virginia. Additionally, instrumentation was deployed across the meadow to seasonally monitor corresponding changes in wave height across the seagrass meadow. Results show that wave height was reduced by 25–49% compared to an adjacent bare site, and by 13–38% compared to an analytical model of wave attenuation over an unvegetated seafloor with the same bathymetry. The greatest attenuation of wave height occurred during the spring and summer when seagrass biomass was greatest, while the lowest attenuation occurred in winter, corresponding to periods of minimal seagrass biomass. Significant wave height attenuation coefficients, α_w, calculated for the meadow ranged from $\alpha_w = 0.49$ in spring to 0.19 during winter, but were highly dependent on wave conditions, with greater α_w for larger wave heights and longer period waves. Within the seagrass meadow during summer, the highest measured bed shear stress was $\tau_{bed} = 0.034 \pm 0.022$ Pa, which occurred during peak wave conditions. This suggests that during high biomass conditions, the bed shear stress rarely exceeds the critical bed shear, $\tau_{crit} = 0.04$ Pa necessary to initiate sediment resuspension. This is in contrast to the bare site which showed elevated values of τ_{bed} above the critical threshold across all seasons. These findings suggest the seagrass meadow does exert significant control over both wave heights and the hydrodynamic conditions at the sediment-water interface, and this control is due to the attenuation of wave motion by drag induced from the seagrass over the expanse of the meadow.

Keywords: seagrass, waves, attenuation, turbulence, shear, canopy flow

INTRODUCTION

Coastal waters in which seagrasses exist often experience complex hydrodynamics containing both wind-driven wave motions and tide-driven currents. Seagrass beds have been shown to attenuate both oscillatory flows (Fonseca and Cahalan, 1992; Luhar et al., 2017) and current velocities (Koch and Gust, 1999; Lacy and Wyllie-Echeverria, 2011), impacting the flow structure above and within the canopy. Seagrasses are typically light limited, so their range and productivity is restricted by both the depth and clarity of the water column (Carr et al., 2016). Seagrasses reduce suspension of sediment due to the stabilizing effect of root structure and flow modification caused by the plant structure (Gacia and Duarte, 2001; Hansen and Reidenbach, 2013), creating a positive feedback loop that increases the light available at the sea floor and promotes primary productivity (Carr et al., 2010). Therefore, understanding flow within a combined wave-current boundary layer is critical to estimating local bed shear stress, which influences sediment suspension and light attenuation, which ultimately alters seagrass productivity and the ecosystem services provided by a healthy seagrass meadow.

Flow conditions adjacent to the sediment-water interface have the greatest implication for sediment suspension. Sediment grains are mobilized when the bed shear stress acting on a grain surpasses the critical shear stress necessary to initiate the grain's motion. Shear stress is a tangential force imparted to the sea floor by velocity gradients found in the boundary layer of the overlying water. As a result, the bottom boundary layer in shallow coastal waters is a combination of a thin wave boundary layer superimposed over a well-developed current boundary layer that may be orders of magnitude thicker (Grant and Madsen, 1979). This interaction between waves and currents is nonlinear, and the shear stresses created at the seafloor can be dramatically different than those expected under either condition independently (Jing and Ridd, 1996). For waves generated within fetch-limited shallow coastal bays, the magnitude of wave orbital motions decrease with depth and the amount of wave energy that reaches the seafloor depends on the wave height, wave period, and water depth (Chen et al., 2007; Fagherazzi and Wiberg, 2009) as well as the structure and density of vegetation (Zeller et al., 2014; Weitzman et al., 2015; Hansen and Reidenbach, 2017).

Drag is fundamentally a process of removing energy from a flow. The bulk drag coefficient (C_D) is a dimensionless measure of the resistance of an object to mean flow (Denny, 1988). This drag coefficient can be calculated in pure current environments (Rippeth et al., 2002) as well as in environments with waves and currents (Bricker et al., 2005), however is defined as a measure of momentum attenuation, and is not a measure of wave height reduction. In coastal environments, C_D is often estimated as the amount of energy dissipation caused by flow interaction with the seafloor, and historically has been computed from estimates of the bed shear velocity, u_*, through quantification of the mean velocity profile, turbulent Reynolds stresses, or rate of turbulent kinetic energy dissipation (e.g., Reidenbach et al., 2006). Due to the presence of vegetation, this drag can be due to interactions with the seafloor or with the seagrass blades themselves, therefore integrated drag through the water column must be taken in to account (Nepf, 1999). The relative magnitude of C_D can be impacted by the incident wave and current forcing, the characteristics of the seagrass canopy, and morphology and flexibility of the individual blades (Houser et al., 2015). C_D for a given canopy can range up to an order of magnitude or more due to variations in Reynolds number of the mean flow and Keuglan-Carpenter number of the oscillatory flow (Bradley and Houser, 2009; Zeller et al., 2014).

Although C_D is an important measure of the integrated drag by the canopy of the flow, often it is advantageous to determine canopy effects solely on the wave climate through a separate wave attenuation parameter. Wave attenuation, α_w, is typically calculated using the change in wave height or wave velocities measured at two or more locations along the direction of wave propagation. This method was first explored using wave height decay by Bretschneider (1954) and revised by Bretschneider (1958) for wind waves in shallow water with impermeable sediment, and has been applied to a variety of settings (Mazda et al., 1997; Quartel et al., 2007). Lowe et al. (2007) also calculated wave attenuation by comparing wave velocity spectra above and within a canopy. Using a similar method, Paul and Amos (2011) determined wave attenuation by comparing differences in wave spectra horizontally across a meadow. These methods are different in that the Bretschneider (1954) approach only considers energy dissipation across the mean of the highest 1/3 of the waves (the significant wave height), whereas Lowe et al. (2007) calculates the total energy dissipation across the entire wave spectra. However, it is the largest waves that are often most relevant to coastal erosion, so although only calculating energy loss at the significant wave frequency is a less complete measurement of attenuation, it may be a more practical metric for use in numerical models and to understand the dominant physical processes causing sediment resuspension, etc.

Over the past few decades, numerous field and laboratory studies have been performed to determine the effects of vegetation on wave attenuation. In a field study in a Florida bay, Bradley and Houser (2009) measured changes in wave height across a seagrass meadow using a linear array of pressure sensors. Wave height decayed at an exponential rate once within the meadow, with a total decrease of 30% across the 39 m transect. Dissipation was not uniform across all frequencies of wave motion; seagrasses acted as a low-pass filter for wave attenuation by selectively removing high frequency motions due to the slower oscillations of the seagrass blades. In flume studies, Fonseca and Cahalan (1992) compared attenuation of wave energy by four different seagrass species including *Zostera marina* over a 1 m section in a flume, and found an average wave energy reduction of 40% per meter of seagrass when the blade length was approximately equal to the water depth. The relation between leaf length and water depth was found to be the most important parameter for all four species studied. In another flume study, Paul et al. (2012) determined that seagrasses were less effective at attenuating wave energy in combined wave-current environments compared to environments with waves alone. Paul

et al. (2012) suggest that the reduction in attenuation in wave-current environments is a combination of decreased frontal area as seagrass blades are flattened by the current and a reduction in the amount of wave energy transferred to blade motion as individual blade are prevented from swaying with wave orbital motion in the presence of a strong current.

Within a shallow coastal bay in Virginia United States, Hansen and Reidenbach (2012) compared flow between vegetated sites of varying density at points above and below the seagrass canopy to assess the effect of seagrass on wave orbital motion, turbulence and sediment suspension. The seagrass canopy was found to reduce flow velocity, turbulence, and wave orbital velocities compared to measurements above the canopy. Significant wave heights were also observed to be lower compared to an adjacent unvegetated site. Hansen and Reidenbach (2013) continued this work with a seasonal comparison of hydrodynamics between a bare and vegetated site, and found that wave heights were reduced at the vegetated site in all seasons; however, wave orbital motions were still able to penetrate vertically through the canopy and induce bottom shear stress. However, no direct measurements of wave-current interactions within the fluid layer adjacent to the seafloor have yet been made within a seagrass meadow.

To determine the effects of a seagrass meadow on wave attenuation and wave-current interactions at the sediment-water interface, the same *Z. marina* meadow in South Bay, Virginia, was monitored seasonally across a 20-month time period. The two specific questions that are addressed are:

1. How does seagrass modify wave characteristics, including wave height and period, as waves propagate across a meadow?
2. How does seagrass alter wave-current boundary layer development and bed shear stress compared to an unvegetated (bare) site?

MATERIALS AND METHODS

Study Area

Research was conducted in South Bay, a shallow coastal lagoon located within the Virginia Coast Reserve Long Term Ecological Research site (VCR LTER) on the Delmarva Peninsula, Virginia (**Figure 1**). The VCR LTER consists of a system of barrier islands, lagoons, and salt marshes which are strongly influenced by semidiurnal tidal variations. Mean water depth in South Bay is 1.0 m, with an average tidal amplitude of 0.6 m, with winds primarily from the SSE-SSW and N-NE (Fagherazzi and Wiberg, 2009). Waves in the bay are primarily wind driven, as the barrier island system blocks larger ocean swell from propagating further inland.

The dominant vegetation in South Bay is the seagrass (eelgrass) *Z. marina*. Seagrasses, once a dominant feature in the coastal bays of the Delmarva Peninsula, disappeared in the 1930's due to a combination of a pandemic wasting disease and the 1933 Chesapeake-Potomac hurricane. South Bay was a site of eelgrass restoration that was reseeded with *Z. marina* from 2001–2005. As of summer 2010, the reseeded patches in South Bay had coalesced and grown to a meadow encompassing >6 km^2 (Orth et al., 2012). Three sites were chosen for the study within the restored seagrass meadow, named North, Center, and South sites, which were in an array spaced approximately 1 km apart (**Figure 1**). The fourth site was in a bare (unvegetated) portion of the bay adjacent to the meadow, approximately 0.5 km west of the Center site. Mean water depths at the four sites were North (1.21 m), Center (1.00 m), South (1.16 m), and bare (0.94 m). The fetch length at each site varied depending on wind angle due to the location of the marsh and barrier island system. South Bay is long and narrow, oriented with the long axis in a north to south direction, where the north and south fetch lengths were the longest (7.5 km), while east and west fetch lengths were typically between 1 and 2 km.

Data Collection

Hydrodynamics were measured at the four sites (North, Center, South, and bare) and a seasonal sampling regime was implemented between October 2011 and July 2013 to assess the impact of morphological changes of the seagrass on the meadow scale hydrodynamics. Wave motions were recorded simultaneously at each site using wave gauges (Richard Branker Research© TWR-1050), which were programmed to measure pressure in bursts of 1024 samples at 4 Hz every 10 min. These 1,024 samples were averaged to compute mean tidal height every 10 min. Significant wave height, the mean wave height of the highest third of waves, was determined from pressure data using spectral analysis (Wiberg and Sherwood, 2008). Wave gauge pressure data was corrected for atmospheric pressure fluctuations using measurements recorded at the nearby Wachapreague National Oceanographic and Atmospheric Administration (NOAA) meteorological station. Meteorological and wave data collected for this study is publicly available on the Virginia Coast Reserve, Long Term Ecological Research Data Repository (Thomas and Reidenbach, 2015; Porter et al., 2018).

Adjacent to the sediment-water interface, high resolution velocity profiles were recorded using a Nortek© Vectrino II acoustic Doppler profiler. Data were collected during July 2012 and July 2013 at the center seagrass site, and during July 2012, October 2012, and July 2013 at the bare site. The Vectrino profiler recorded velocity data over a 30 mm profile at 1 mm resolution at a rate of 20 Hz. Doppler pulses are emitted from a center transmitter and received by four passive transducers angled 30° toward the center, resulting in a sample volume 40–70 mm from the center transmitter. This high spatial and temporal resolution allowed for the resolution of wave and turbulence motions. The Vectrino profiler was positioned to record velocity measurements directly adjacent to the sediment-water interface to capture water motions associated with wave-current boundary layer development. To ensure measurements adjacent to the sediment were included in the data set, several bins were positioned below the interface, and the signal to noise ratio (SNR) was used to indicate the location of the bottom. If necessary, seagrass was removed from directly beneath the probe at the vegetated site to prevent blade interference. Velocity profiles were first rotated into the direction of the mean flow, using an average of the rotation required for the top three points. Each raw data record was then analyzed to see if the SNR and percent correlation

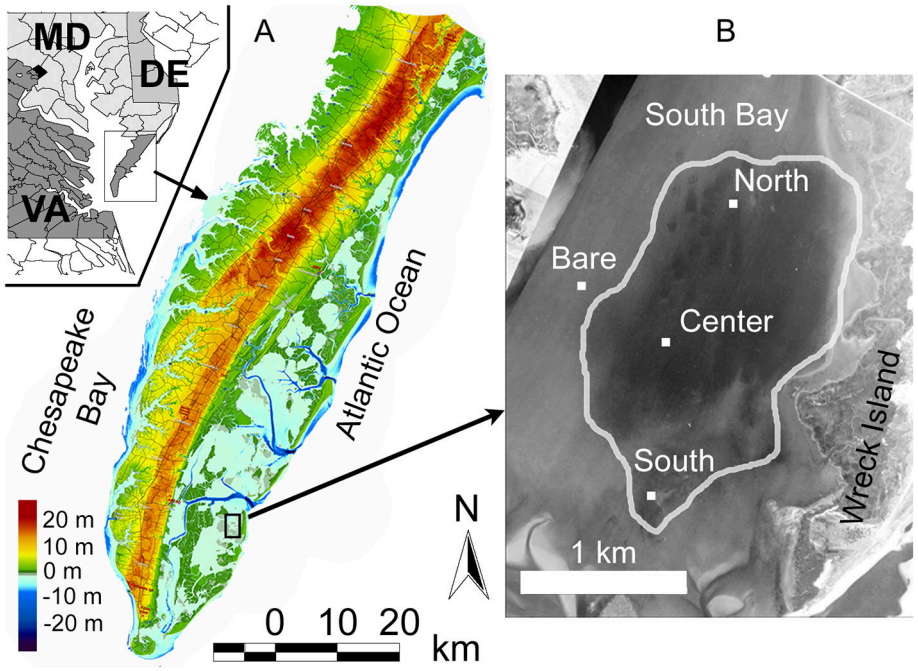

FIGURE 1 | (A) Location of study area off-shore of the Delmarva Peninsula, Virginia. Seagrass study site is in South Bay, indicated in the black box. Color-map shows the land elevation and bathymetry of the Delmarva Peninsula relative to the North American Vertical Datum of 1988 (NAVD88). **(B)** Site locations within South Bay, superimposed on an aerial photograph modified from Orth et al. (2012). The extent of the seagrass meadow as of 2010 is indicated by the area within the white line.

averaged across the 10-min record exceeded 20 dB and 80%, respectively, the recommended limits for velocity measurements. If these conditions were met, the raw data were used to compute velocity, wave, and turbulence statistics. In general, velocity data within approximately 5 mm from the seafloor did not meet these conditions, and therefore were not used in the analysis.

Seagrass Morphology and Biomass

Physical characteristics of the *Z. marina* bed (shoot density, blade length and width) were measured during each deployment at the Center site, which was considered representative of the established meadow area (**Table 1**). Density was determined *in situ* via 0.25 m^2 shoot counts, and shoots were brought to the laboratory to measure length and width. Lengths and widths were recorded for the longest three blades per shoot. The meadow was most dense with the longest and widest blades during the summer for both years sampled, with values that peaked during July 2013 with a density of 411 ± 33 shoots m^{-2} and were lowest during January 2012 at 100 ± 36 shoots m^{-2}. Summertime aboveground seagrass biomass has been measured in the South Bay seagrass meadow annually since 2009 (McGlathery, 2017), and was 107 ± 19 g m^{-2} in 2012 and 173 ± 52 g m^{-2} in 2013.

TABLE 1 | Seasonal morphometric data summarizing characteristics of *Z. marina* meadow in South Bay, Virginia across five sampling periods from April 2012 through July 2013.

	Blade length (cm)	Blade width (cm)	Density (shoots/m^2)
April 2012	27 ± 10	0.31 ± 0.05	140 ± 25
July 2012	47 ± 7	0.38 ± 0.06	347 ± 73
October 2012	23 ± 5	0.25 ± 0.05	115 ± 30
January 2013	19 ± 4	0.21 ± 0.04	100 ± 36
July 2013	53 ± 8	0.41 ± 0.03	411 ± 33

Density was determined as number of shoots per 0.0625 m^2 (25 cm by 25 cm) quadrat. Values presented below are mean ±1 SD. In each season, 10 randomly placed quadrats were measured.

Wave Attenuation

The effects of the seagrass meadow on wave development were made in three different ways. The first was by directly comparing the significant wave height at the Center site within the seagrass meadow to significant wave height measured simultaneously at the bare site. The second was through calculation of a wave attenuation coefficient (α_w) for attenuation of significant wave heights as waves propagated across the meadow, while the third was comparisons of wave heights at specific locations within the seagrass meadow to predicted wave heights using the commonly applied Young and Verhagen (1996) wave height model.

Wave data were first filtered to include only sampling periods during which the wind direction was nearly parallel to a line between the sites and significant wave heights were >3 cm. Because waves in South Bay are wind driven, wind direction can be used as an approximation for the direction of wave propagation. A range of 45° (22.5° to either side of the direction between two sites) was used in the filter to provide adequate

data for analysis of attenuation. After preliminary analysis, significantly lower wave heights were measured at the South site compared to the other two sites during periods when winds were blowing from the south. The South site has limited fetch for south winds with a distance of approximately 1 to 1.5 km. As a result of these short fetch lengths, waves are not fully developed when they reach the South site, and the processes of wave growth due to wind energy and decay due to seagrass induced drag compete in a way that cannot be easily predicted. Due to this limitation, only data for time periods of north winds (blowing north to south) was used in the computation of wave attenuation.

A wave attenuation coefficient, α_w, was calculated using the formulation from Bretschneider (1954) for waves propagating across an impermeable bottom with constant depth and no refraction:

$$H_2 = H_1 \left[\frac{f H_1 \phi_f \Delta x}{K_s T^4} + 1 \right]^{-1} \quad (1)$$

where H_1 and H_2 are the initial and final wave heights, f is the friction factor, Δx is the horizontal distance the wave traversed, T is the wave period, K_s is the shoaling factor, and ϕ_f is the bottom friction dissipation function [$s^4\ m^{-2}$], defined as:

$$\phi_f = \frac{64\pi^3}{3g^2} \left[\frac{K_s}{\sinh\left(\frac{2\pi h}{L}\right)} \right]^3 \quad (2)$$

where L is the wavelength and h is the water depth. Bretschneider (1954) describe f as a dimensionless "calibrated friction factor" which describes the reduction in wave height caused by bottom characteristics. This friction factor, f, can be rewritten as a measure of wave induced drag (Mazda et al., 1997), α_w, where Equation 1 then becomes:

$$\frac{H_2}{H_1} = \frac{1}{1 + \frac{\pi^5 K_s^2}{\sqrt{2} g^2 T^4} * \alpha_w H_1 \Delta x \left(\sinh \frac{2\pi h}{L}\right)^{-3}} \quad (3)$$

This method estimates flow resistance across the entire height of the plant structure as bottom friction. Equation 3 can be simplified for South Bay by setting the shoaling factor (K_s) equal to 1 because South Bay is roughly a constant depth (with mean water depths ranging between 1.0 and 1.2 m) and does not typically induce wave shoaling. Solving for α_w:

$$\alpha_w = \frac{g^2 \sqrt{2} T^4}{\pi^5} * \frac{\left(\sinh \frac{2\pi h}{L}\right)^3}{H_1 \Delta x} * \left(\frac{H_1}{H_2} - 1\right) \quad (4)$$

Mazda et al. (1997) called this α_w parameter a coefficient of drag (C_D), however in mixed wave-current dominated systems, it is not a true measure of integrated drag on the flow, but only the effects of the frictional resistance on waves. We therefore use α_w to indicate this parameter is solely a function of wave activity.

A wave height model, created by Young and Verhagen (1996), was applied to predict wave heights within South Bay assuming no seagrass is present. The Young and Verhagen (1996) model (abbreviated as YV) uses semi-empirical relationships that relate fetch length, wind velocity, and water depth to significant wave height and peak wave period. This commonly applied fetch-limited, finite-depth model was calibrated for fine-grained, cohesive mud within a 1–2 m depth shallow lake, and therefore is a good approximation for the sediment and physical conditions in South Bay in the absence of vegetation. In addition, this model has been previously validated for use in the coastal bay system of the VCR (Mariotti and Fagherazzi, 2013b; Mcloughlin et al., 2015). The significant wave H_s and peak wave period T_p were computed as:

$$\frac{g H_s}{(U_{wind})^2} = 0.2413 \left\{ \tanh A_1 \tanh \left[\frac{B_1}{\tanh A_1} \right] \right\}^{0.87} \quad (5)$$

$$\frac{g T_p}{U_{wind}} = 7.518 \left\{ \tanh A_2 \tanh \left[\frac{B_2}{\tanh A_2} \right] \right\}^{0.37} \quad (6)$$

with $A_1 = 0.493 \left(gh/[U_{wind}]^2\right)^{0.75}$, $B_1 = 3.13 \times 10^{-3} \left(g\chi/[U_{wind}]^2\right)^{0.57}$, $A_2 = 0.331 \left(gh/[U_{wind}]^2\right)^{1.01}$, and $B_2 = 5.215 \times 10^{-4} \left(g\chi/[U_{wind}]^2\right)^{0.73}$, where h is the depth, χ is the fetch, and U_{wind} is the reference wind speed. Fetch was determined from aerial photographs of the VCR LTER bays, wind velocity and direction were determined from the Wachapreague NOAA meteorological station, and water depth was determined from the wave gages following the atmospheric pressure correction. The model output, assuming no seagrass was present, was then compared to field data collected within the seagrass site to determine the effects of the seagrass meadow on wave attenuation. Model output was also compared to measured wave heights at the bare site.

Observed waves with significant wave heights below 3 cm were filtered from the data set to reduce contamination from small turbulent fluctuations that could artificially skew attenuation values. Small values below this cutoff may be the result of random non-wave motion, and are unlikely to be influenced by bottom drag (Wiberg and Sherwood, 2008). Model outputs were compared to observations collected in South Bay, and the percent difference between the modeled and measured values was calculated as follows:

$$Percent\ Difference = \frac{H_{s,\ model} - H_{s,\ observed}}{\left(\frac{(H_{s,\ model} + H_{s,\ observed})}{2}\right)} * 100 \quad (7)$$

Positive values indicate that the modeled wave heights predicted over an unvegetated seafloor were greater than the *in situ* observations of wave heights measured in the presence of seagrass. Modeled data was also computed and compared to observed wave heights measured at the bare site. In addition, Equation 7 was used to quantify the percent difference in observed wave heights measured simultaneously at the seagrass and bare sites to determine *in situ* values of wave height reduction.

Bed Shear and Friction Velocity

High resolution velocity measurements using a Nortek© Vectrino II acoustic Doppler profiler were used to quantify

bed shear and friction velocities at the bare and seagrass sites. In combined wave-current flow, both waves and currents can induce shear at the sediment-water interface. Bed shear is often estimated in current-dominated regimes by the magnitude of turbulent energy within the overlying boundary layer or through quantification of the logarithmic profile of the mean flow (Reidenbach et al., 2006). However, the presence of vegetation often disrupts the development of a logarithmic profile within the mean flow and alters the shear at the sediment-water interface (Hansen and Reidenbach 2013). In addition, wave orbitals induce large variances in the horizontal and vertical velocity components, which mask velocity variances due to turbulence, making it necessary to separate the wave and turbulence parts of the signal. For wave-current flows, the components of the total instantaneous velocity u (as well as for v and w, not shown) can be separated via Reynolds decomposition according to:

$$u = \overline{u} + \tilde{u} + u' \tag{8}$$

where $\overline{u}$ is the mean current velocity, $\tilde{u}$ is the instantaneous wave orbital velocity, and u' is the instantaneous turbulent velocity. Current, wave and turbulence perturbations were separated using a spectral decomposition technique called the Phase method (Bricker and Monismith, 2007), which converts the temporal velocity record into frequency space via Fourier transformation and isolates the wave stress using the phase lag between horizontal and vertical components of the velocity signal. Further details of the Phase method can be found in Bricker and Monismith (2007) and Stocking et al. (2016).

Bed shear stress τ_{bed} was calculated using the formulation of Wiberg and Smith (1983), defined as:

$$\tau_{bed} = \sqrt{\tau_c^2 + \tau_w^2} \tag{9}$$

where τ_c is bed shear due only to currents and τ_w is bed shear due only to wave orbital motions. The current-induced bed shear stress is estimated using near-bed turbulent kinetic energy (TKE) outside the wave boundary layer, according to Soulsby and Dyer (1981):

$$\tau_c = 0.19 \rho TKE^2 \tag{10}$$

where ρ is the density of seawater and:

$$TKE = \frac{1}{2}(\overline{u'^2} + \overline{v'^2} + \overline{w'^2}) \tag{11}$$

The wave-induced contribution is parameterized using the near-bottom wave orbital velocity, u_{orb}, computed by quantifying motions only within the wave band of the velocity spectra measured at z= 0.02 m above the seafloor, and a wave friction factor f_w (Jonsson, 1967):

$$\tau_{wave} = \frac{1}{2} f_w \rho u_{orb}^2 \qquad f_w = 0.04 \left[\frac{u_{orb} T}{2\pi k_b} \right]^{-0.25} \tag{12}$$

where ρ is the fluid density, and k_b is the characteristic roughness length (Fagherazzi and Wiberg, 2009). Lawson et al. (2007) estimated k_b as $3D_{84}$, where D_{84} is the sediment grain diameter (D) at which 84% of the sample is finer than D. D_{84} measured at the seagrass site ranged between 151 ± 1 μm and 158 ± 3 μm, while the unvegetated site ranged from 152 ± 4 μm to 162 ± 2 μm.

RESULTS

Wind speed for each deployment is shown in **Figure 2A**. Seasonal averages ranged from 2.1 m s^{-1} in July 2012 to 4.8 m s^{-1} in July 2013; however, the deployments captured enough variation that all seasonal means were within one standard deviation. The maximum 10-min averaged wind speed was 27.8 m s^{-1}. No seasonal trends were apparent in the data; although the second and third highest averages both occurred in April, possibly indicating stormier weather and the potential for larger wave development in the spring.

The seasonal average depth, measured at the Center site ranged between 0.93 m in January 2013 and 1.28 m in October 2011, with a standard deviation of 0.46 and 0.42 m, respectively (**Figure 2B**). A semi-diurnal tide drives the variation in water depth in South Bay, so the standard deviation is affected by the tidal range. At the bare site, the mean depth ranged from 0.82 m in January 2013 to 1.19 m in October 2012. The mean depths at the bare and seagrass sites were within one standard deviation for all seasons, with a maximum difference of 0.11 m in the mean seasonal values. Seasonal differences in mean water depth are a result of weather systems; including wind or barometric pressure variations which may force more water toward or away from the shoreline. Seasonally averaged mean water velocities ranged from 3.5 to 7.1 cm s^{-1} at the seagrass site, with significantly higher mean seasonal velocities (ANOVA, $p < 0.01$) at the bare site of 11.9–25.9 cm s^{-1}.

Wave Characteristics

Waves in South Bay are primarily wind driven, with seasonally averaged significant wave heights ranging from 0.02 m within the seagrass bed to 0.09 m at the bare site (**Figure 3A**). Seasonally averaged significant wave periods were between 1.6 and 2.4 s (**Figure 3B**). The distribution of significant wave height was highly skewed, with intermittent, large waves occurring during storm events. Consequently, the maximum 10-min significant wave heights for each season were much higher than the average value, with the largest H_s across all deployments reaching 0.55 m. In addition, significant wave height varied considerably as a function of wind direction due to altered fetch lengths.

Average H_s was statistically lower within the seagrass meadow compared to the bare site during all seasons (ANOVA, $p < 0.01$). As predicted by the seasonal mean wind values, the high wind speeds in April 2013 and July 2013 correspond to the largest mean significant wave heights at the bare site, however the mean significant wave height at the vegetated site follows a trend more aligned with the seasonal shoot density distribution, with maximum values when densities were low. Average significant wave period, T_s, was slightly higher at the vegetated site across all seasons except during October 2012, although the difference was not statistically significant. Controls on significant wave

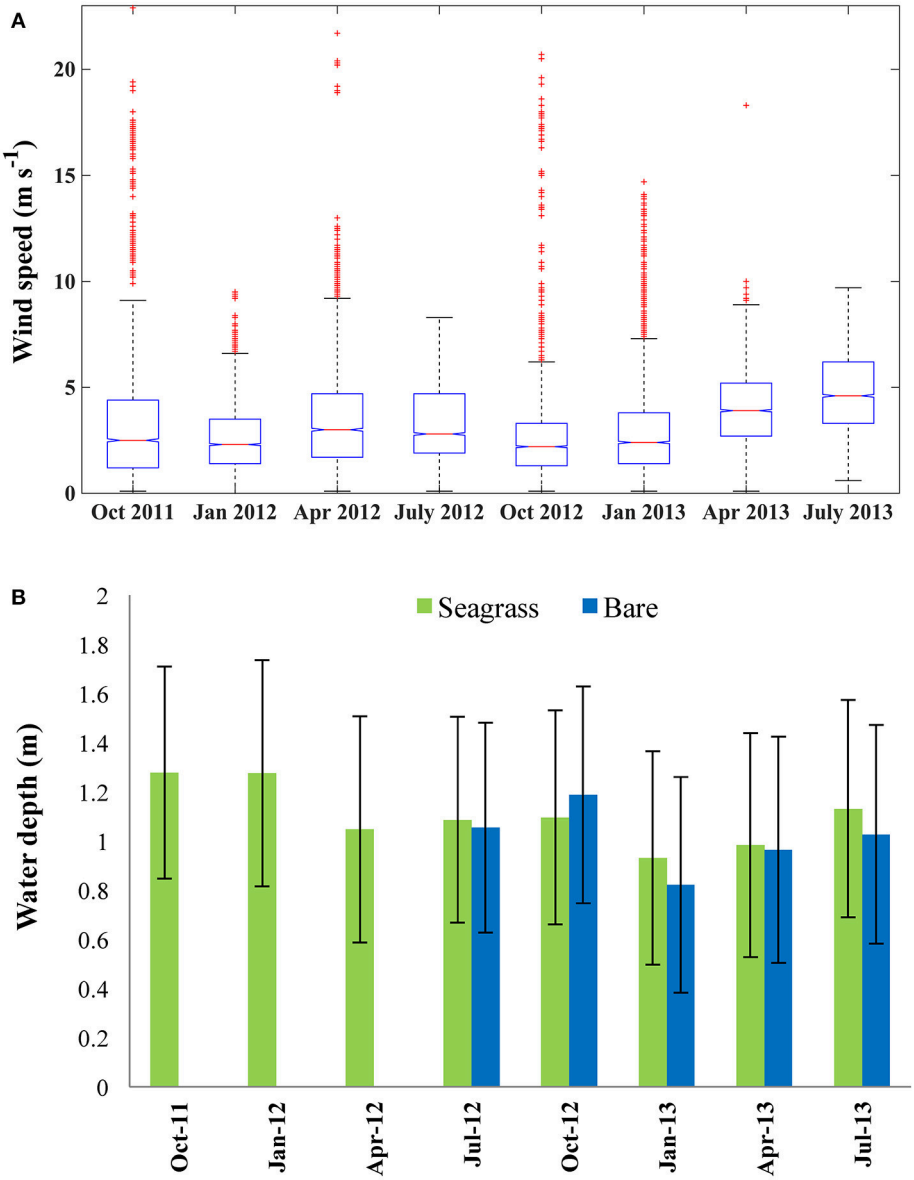

FIGURE 2 | (A) Wind speed measured at the Wachapreague NOAA Meteorological station for each sampling period. Horizontal red line within the box indicates median wind speed, lower and upper edges of the box represent the 25th and 75th percentiles respectively. Red crosses represent outliers. **(B)** Water depth at the bare (blue) and center seagrass (green) sites averaged across each sampling period. Error bars indicate ±1 SD.

height include; fetch length, wind speed, water depth, and wave attenuation, which varies as a property of meadow structure. The fetch length, wind speed, and water depth were all statistically similar at the bare and seagrass sites, and therefore the difference in apparent wave properties is primarily due to the presence of seagrass.

Wave Attenuation

Plots of significant wave height at the bare vs. vegetated site are displayed across four consecutive seasons (**Figure 4**). Data points that fall below the 1:1 line indicate wave attenuation at the seagrass site, and the slope of the regression line represents the degree to which wave height is attenuated by the seagrass bed (adapted from Koch 2006). Overall, significant wave height at the seagrass site was 51% of significant wave height at the bare site in the summer, 59% in the fall, 75% in the winter, and 53% in the spring. Mean water depths for these time periods are shown in **Figure 2B**, which range from 0.82 to 1.18 m across seasons. Although there is seasonal variability in the mean depths due to variability in tidal and atmospheric forcings, within each season mean water depths at the seagrass and bare sites are very similar. Data from the summer and fall 2012 show greater variation and therefore lower R^2-values (R^2 = 0.50 and 0.60, respectively), compared to winter and spring

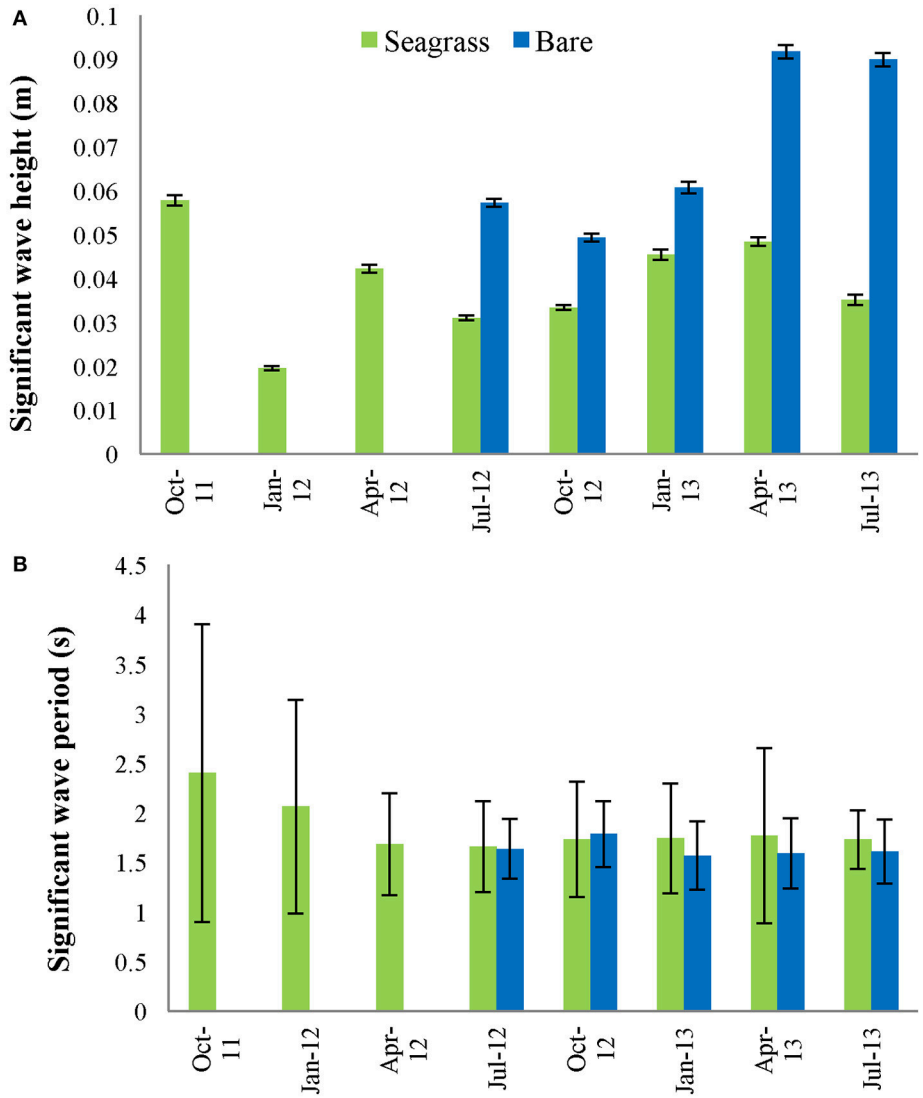

FIGURE 3 | (A) Average significant wave height (±1 SE) and **(B)** average significant wave period (±1 SD) for the center vegetated site and nearby bare site, across 8 seasonal deployments (ranging from 14 to 19 days). Bare data is missing for October 2011–April 2012.

2013 ($R^2 = 0.75$ and 0.70, respectively). This may be a result of the changes in seagrass cover during the sampling period due to growth or senescence of the seagrass. In the winter, the bed topography of the less dense meadow matches more uniformly with the surrounding unvegetated region, causing a line of best fit that better matches the 1:1 line of no attenuation ($R^2 = 0.75$, slope = 0.75).

Wave Attenuation Coefficients

Attenuation coefficients for South Bay averaged across seasonal deployments varied from $\alpha_w = 0.19$ to 0.49 (**Table 2**). The largest seasonally averaged wave attenuation coefficients occurred in spring, while the smallest occurred in winter when seagrass density was lowest. However, there is large variability in attenuation coefficients that are dependent upon the wave environment. Plots of wave frequency vs. α_w show a trend of higher attenuation coefficients for lower frequency waves during each season (**Figures 5A,B** shown for summer 2012 and winter 2013, respectively). Linear wave theory suggests that waves will attenuate prior to reaching the sea floor when the wave frequency (f) is greater than $\sqrt{g/(4\pi h)}$ (Wiberg and Sherwood, 2008). For the water depths typical in South Bay (1–2 m), this relationship suggests that waves with a frequency >0.63–0.88 s^{-1}, depending on the tidal conditions, will not interact with the seafloor. This is consistent with the decrease in attenuation coefficients observed as wave frequencies increase, approaching $\alpha_w = 0$ as frequencies surpass 0.75 s^{-1} (**Figures 5A,B**). Negative α_w values for large wave frequencies, indicate waves that were likely not interacting with the seafloor, and therefore represent waves that were still increasing in wave height due to wind energy input. Since winds are continually adding energy to the waves as they propagate across the shallow bay system, the actual wave energy dissipated

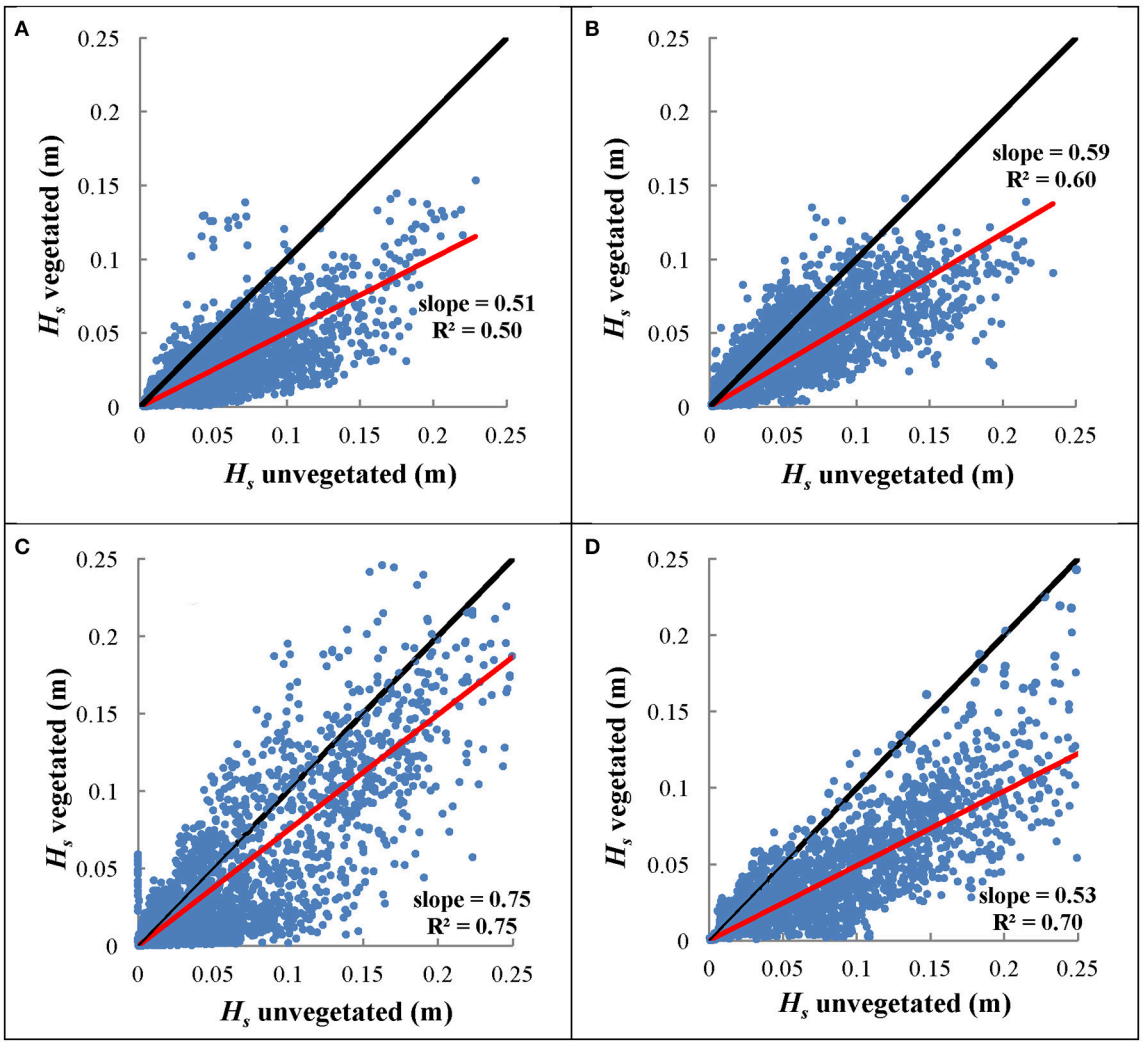

FIGURE 4 | Significant wave height at the center vegetated site compared to significant wave height at the nearby bare site over four seasons **(A)** summer 2012, **(B)** fall 2012, **(C)** winter 2013, and **(D)** spring 2013. The slope of the regression line represents the degree of wave height attenuation between these two sites, with shallower slopes indicating greater attenuation. The regression line was fit to pass through the origin. Black line represents 1:1 slope line, indicating a case with no attenuation between the bare and vegetated sites.

TABLE 2 | Seasonally averaged mean wave attenuation coefficients (± standard error) for north winds.

Season	Attenuation coefficient, α_w	*N*
Spring (2012, 2013)	0.49 ± 0.04	412
Summer (2012, 2013)	0.43 ± 0.08	301
Fall (2011, 2012)	0.38 ± 0.10	465
Winter (2012, 2013)	0.19 ± 0.04	145

The years indicate when data were collected and averaged. N is number of 10-min averaged values included in the seasonal average.

by the seafloor and seagrass canopy is likely greater than these wave attenuation coefficients suggest.

Wave attenuation increased with water depth (**Figures 5C,D** for summer 2012 and winter 2013, respectively), which was consistent across all seasons. Negative α_w values for small wave heights, similar to described above for small frequency waves, were likely not interacting with the bottom, and therefore represent waves that were still growing in wave height. Larger significant wave heights generally resulted in increased wave attenuation coefficients (**Figure 6**), however the scatter in these data were greater than those of wave frequency vs. α_w. Overall, there is a strong correlation between wave period and water depth in the seagrass meadow, as well as significant wave height and water depth (**Figure 7**). In general, these findings suggest that larger waves with longer wave periods can form when the water is deeper, and because of this wave orbitals penetrate deeper in to the water column and interact with the seagrass and seafloor to a greater extent. Although not directly computed, the wavelength, *L*, can be calculated according to linear wave theory for intermediate

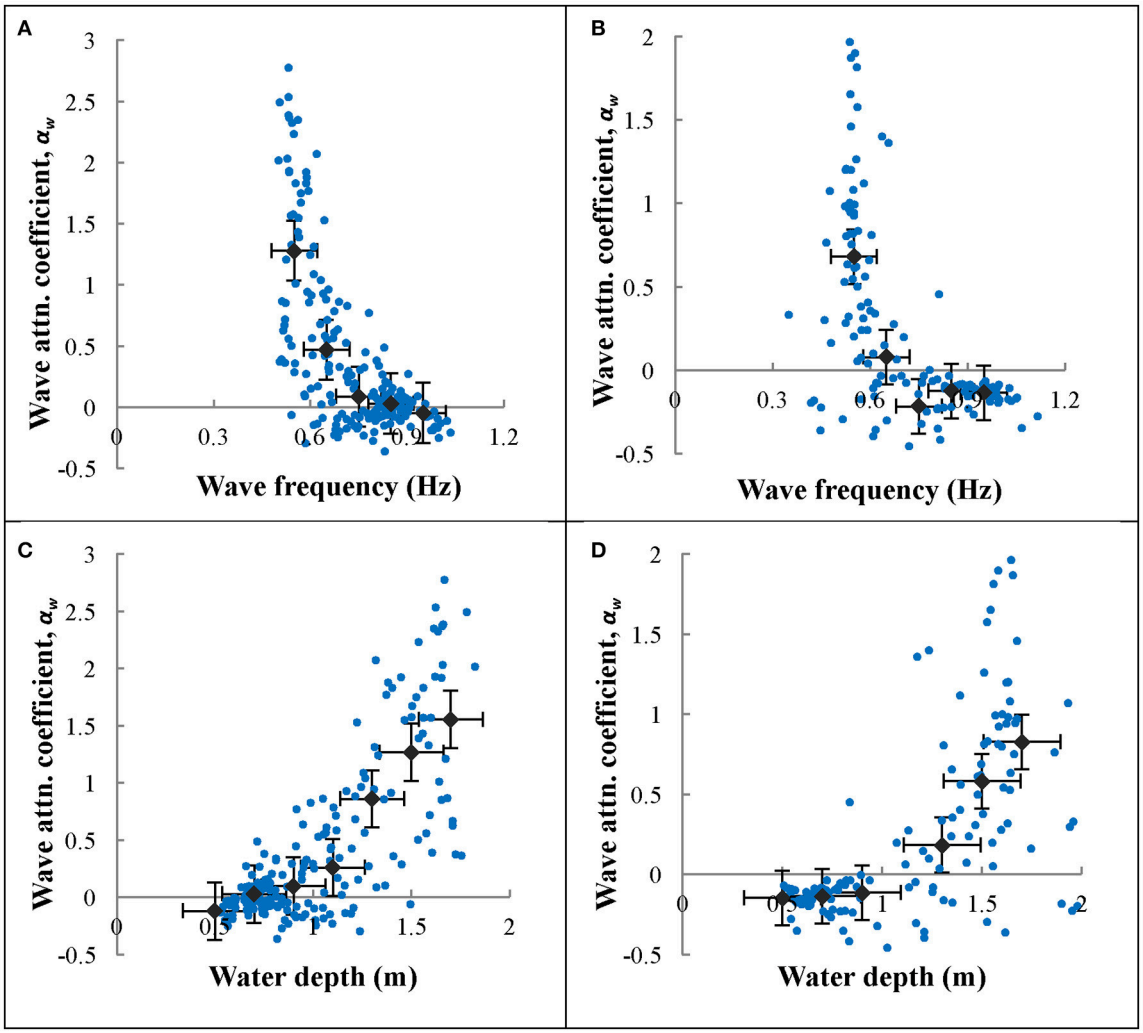

FIGURE 5 | Wave frequency vs. wave attenuation coefficient (α_w) for north winds during **(A)** summer 2012 and **(B)** winter 2013. Raw data are presented in green points. Data were averaged in 0.1 Hz bins and averages were plotted along with the raw data as gray diamonds. Water depth vs. wave attenuation coefficient (α_w) for north winds during **(C)** summer 2012 and **(D)** winter 2013. Raw data are presented as purple points. Depth data were averaged in 0.01 m bins and plotted along with the raw data as gray diamonds. Means that had fewer than 10 data points in a bin were excluded from the plots. Error bars on the averaged data show standard error.

waves as: $L = L_\infty \sqrt{\tanh(\frac{2\pi h}{L_\infty})}$, where $L_\infty = \frac{g}{2\pi} T^2$. This relationship suggests that with increases in wave period, waves with longer wavelengths also form in South Bay, and therefore increased wave attenuation occurs with larger wavelengths.

Comparison to Young and Verhagen Wave Height Model

An empirical model developed by Young and Verhagen (1996) was utilized to predict significant wave height in South Bay as a function of wind speed, water depth, and fetch length, assuming an unvegetated seafloor composed of fine-grained sediments. Model accuracy was verified by comparing model output values of wave height to the measured values at the bare site. Although there is inherent variability in model performance over short timescales when comparing modeled vs. observed wave heights at the bare site (**Figures 8A,B**), when seasonally averaged the model both over- and under- predicted wave heights within ±15% of observed values (**Table 3**). This suggests reasonably good agreement and calibration of the model to wave dynamics in South Bay given uncertainty in water depth and bathymetry across the bare site, changes in wind direction that impact fetch length, and the likely presence of some small amounts vegetation at the bare site. Young and Verhagen (1996) do not report a grain size for the sediment used to calibrate their model, but describe the bottom as "relatively fine grained but cohesive mud" in which "the bed is not mobile and ripples do not develop." This description is consistent with the fine-grained sediment in South Bay. Utilizing the same wind speed, water depth, and fetch length as that measured in South Bay, the difference between the model output and the recorded significant wave height was considered

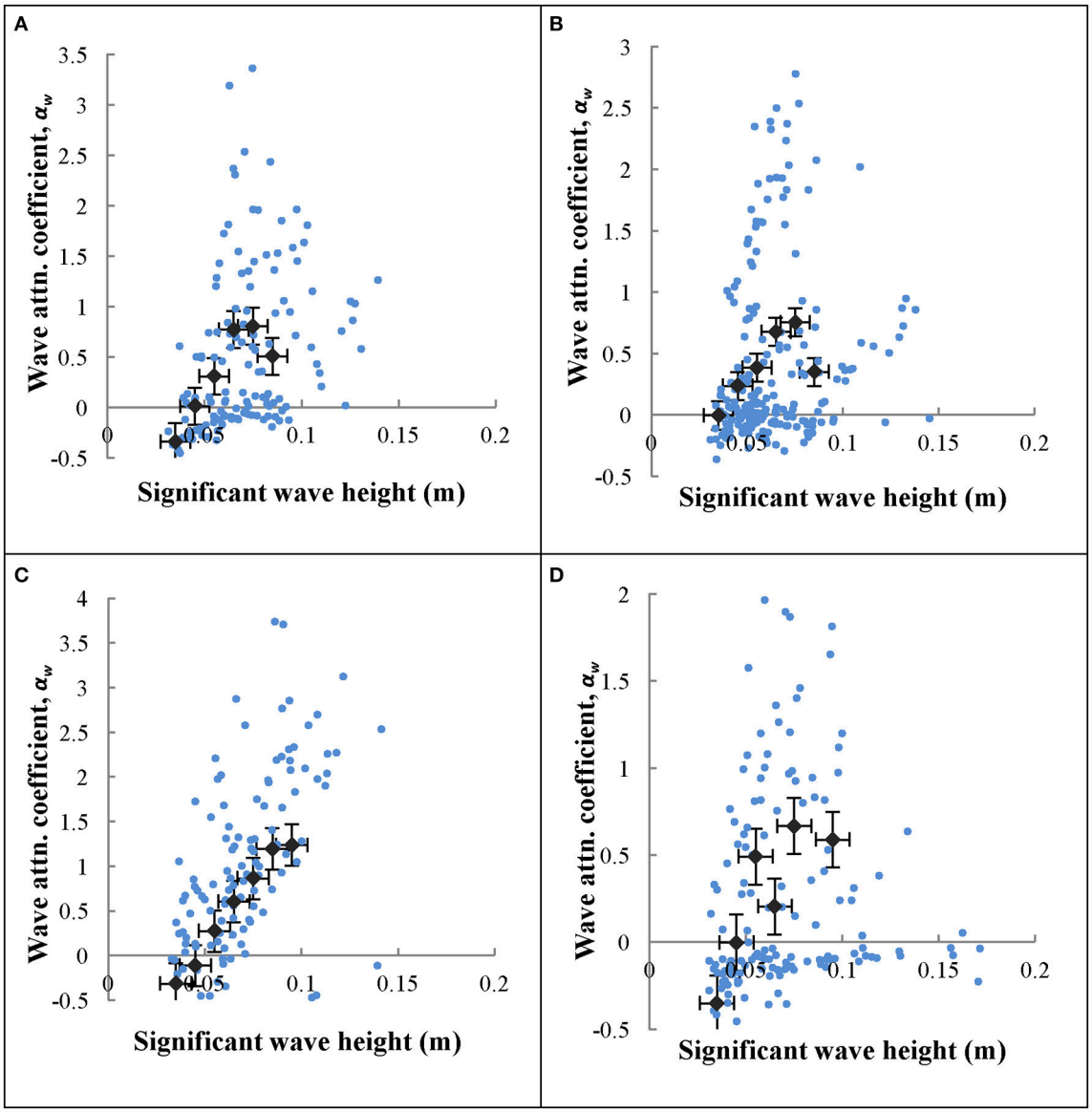

FIGURE 6 | Significant wave height (H_S) vs. wave attenuation coefficient (α_W) for north winds across **(A)** April 2012, **(B)** July 2012, **(C)** October 2012, **(D)** January 2013. Wave height data were averaged in 0.01 m bins and plotted along with the raw data as gray diamonds. Bins that had fewer than 10 data points were excluded. Error bars indicate standard error.

to represent the wave height attenuation caused by seagrass compared to a theoretical unvegetated site at the same physical location (**Figures 8C,D**). This comparison showed wave height attenuation caused by the seagrass of up to 44.8% at the Center site during summer, with minimum wave height attenuation of 12.3% during winter (**Table 3**). Seasonally averaged attenuation estimates from *in situ* measurements, model comparisons, and attenuation coefficients are summarized in **Table 4**.

Bed Shear and Friction Velocity

Near bed velocity profiles were collected over a range of flow conditions in nine separate deployments at the bare and center seagrass site. Measurements within the seagrass bed were performed during summer 2012 and 2013 months when the meadow was near peak biomass, with blade densities of 347 ± 73 shoots/m^2 and 411 ± 33 shoots/m^2, respectively. Bare site measurements were conducted during fall 2012 and summer 2013. Significant wave height averages at the bare site ranged from 0 to 0.11 m, and H_s values between 0 m and 0.08 m at the seagrass site. These wave heights were relatively small, but encompassed the average H_s range of 0.02 to 0.09 m observed during seasonal deployments in South Bay. Within each deployment, data was collected over approximately 3–4 h. However, to determine the effects of hydrodynamics on near bed boundary layer flows, the deployments with greatest and least

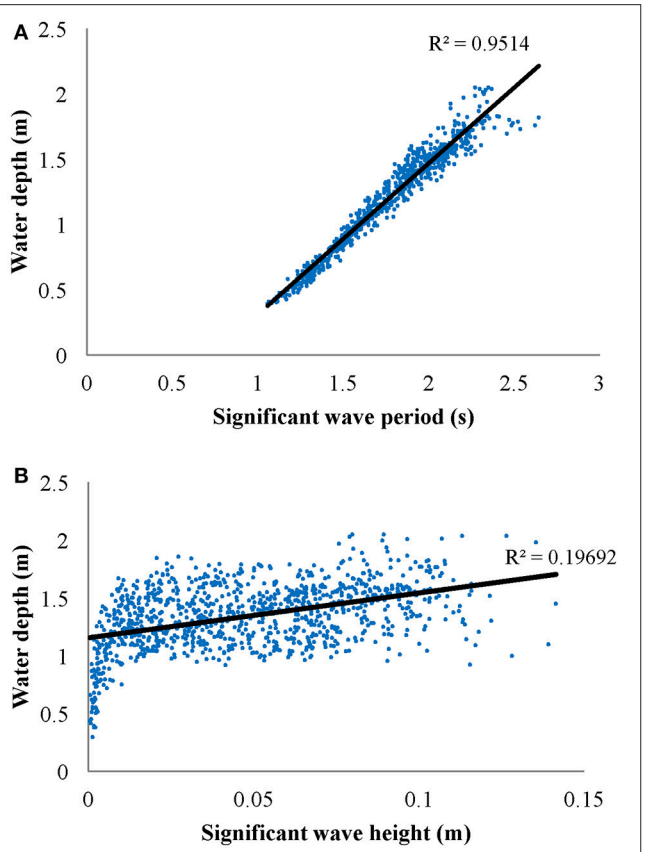

FIGURE 7 | (A) Significant wave period (s) vs. water depth (m) for waves with significant wave height >5 cm and **(B)** significant wave height (m) vs. water depth (m) for significant wave period <5 s. Data is from October 2012 recorded at the Center site.

measured bed shear stress were selected from both the bare and vegetated site for further analysis (**Table 5**).

At the bare site, the time period with the lowest bed shear stress, $\tau_{bed} = 0.019 \pm 0.008$ Pa, was recorded in fall 2012. This time period coincided with essentially no wave activity, with mean velocities across the 1 h deployment of 3.9 cm s^{-1} at 0.5 cm above the bed and 4.8 cm s^{-1} at 2.5 cm above the bed. The time period of highest $\tau_{bed} = 0.07 \pm 0.034$ Pa occurred at peak wave conditions with H_s= 0.11 m. The critical shear stress for sediment resuspension in South Bay was previously found to be $\tau_{crit} = 0.04$ Pa with a $D_{50} \approx 63\,\mu$m and sorting coefficient $\sqrt{D_{84}/D_{50}} \approx 2$ (Lawson et al., 2007; Fagherazzi and Wiberg, 2009), suggesting that sediment resuspension was actively occurring during higher wave conditions. In contrast, at the seagrass site, the lowest measured $\tau_{bed} = 0.004 \pm 0.003$ Pa, while the highest was $\tau_{bed} = 0.034 \pm 0.022$ Pa which occurred during peak wave conditions of H_s=0.08 m, suggesting that at no time during these summertime velocity measurements did the bed shear stress exceed τ_{crit} to initiate sediment resuspension. These findings suggest the seagrass meadow does exert significant control over the hydrodynamic conditions at the sediment-water interface, and this control is due to the attenuation of wave motion by drag induced from the seagrass over the expanse of the meadow.

DISCUSSION

This work presents several estimations of wave attenuation induced by a temperate *Z. marina* meadow across a range of seagrass density and morphologic variations. Wave height attenuation, both comparing a vegetated site to a bare site and comparing measured values to model predictions, showed large seasonal variations with the largest reduction occurring during spring and summer when the meadow was near peak density, and the lowest reduction during the winter (**Table 4**). Direct comparisons of wave heights showed reductions between 25 and 49% in the seagrass bed compared to an adjacent bare site. Results using the Young and Verhagen (1996) model showed similar seasonal trends, although model output consistently estimated less attenuation within the seagrass bed than direct *in situ* measurements would suggest. Seasonal estimates of wave heights predicted over the bare site using the YV model ranged between 12.7% lower and 14.7% greater than *in situ* wave heights (**Table 3**), with modeled significant wave heights being on average 5% greater than those measured *in situ* when averaged over annual timescales.

As expected, large variability in wave height attenuation was found within the seagrass canopy due to the seasonal variation in seagrass biomass, changes in water depth due to tidal fluctuations, and high variability in fetch length in response to changes in wind direction. Seagrass morphology varied from a minimum blade length of 19 ± 4 cm, blade width of 0.21 ± 0.04 cm, and shoot density of 100 ± 36 blades m^{-2} in winter, to peak blade length of 53 ± 8 cm, blade width of 0.41 ± 0.03 cm, and shoot density of 411 ± 33 blades m^{-2} in summer. Increased seagrass blade size and shoot density correlated directly with increased wave attenuation across the seagrass meadow.

The distance to the top of the seagrass bed, where waves will begin to feel drag, also decreases in the summer when the canopy is established with longer blades. For both the unvegetated and seagrass sites, wave theory predicts that waves with a wave frequency, $f > \sqrt{g/(4\pi h)}$ will be attenuated before reaching the bottom (Wiberg and Sherwood, 2008). For the range of depths found within the seagrass meadow and bare site, oscillatory motion will generally not reach the seafloor for wave frequencies ≥1 Hz. Although high frequency waves may interact with the vegetation, and experience drag even when the wave motions are too small to reach the sea floor, our results (**Figure 5**) suggest that wave attenuation when wave frequencies ≥1 Hz is minor. The maximum α_w value occurs at a wave frequency of approximately 0.55 Hz for every season, corresponding to a wave period of 1.8 s. The averaged α_w value for this wave period is as high as 1.3 during summer, and drops to 0.7 during winter. This suggests that variability in the seagrass biomass with season is a dominant contributor to wave attenuation. Unlike wavelength and wave period, which provides a length- and time-scale of a wave and results in a clear relationship for when waves will interact with the sea floor, there is no

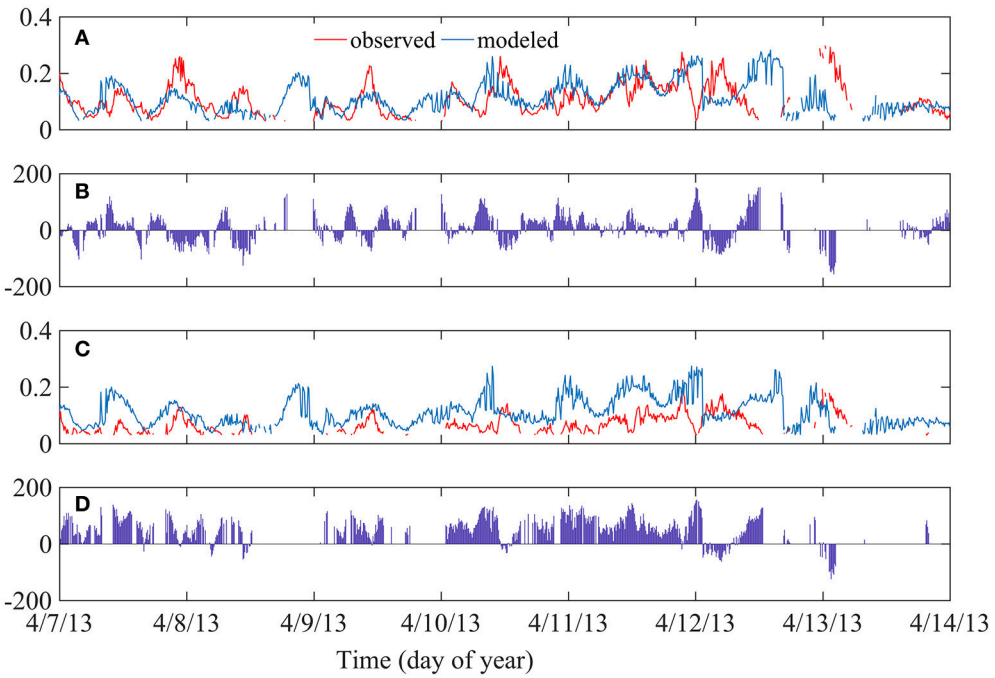

FIGURE 8 | (A) Significant wave height comparison between Young and Verhagen model output (blue) and *in situ* observation values (red) at the unvegetated site during April 2013. **(B)** Time series of percent attenuation (difference) between measured and modeled wave height at the unvegetated site. Positive attenuation signifies modeled wave heights were greater than observed wave heights. **(C)** Wave height comparison between model output (blue) and observed values (red) at the Center seagrass site during April 2013. **(D)** Time series of percent attenuation between measured and modeled wave height at the seagrass site.

TABLE 3 | Percent difference between observed significant wave heights and significant wave heights predicted by the Young and Verhagen (1996) model at each site for southward blowing winds, averaged across each season.

	North site (%)	Center site (%)	South site (%)	Bare site (%)
January 2012	−10.1	12.3	11.3	–
April 2012	31.0	29.9	9.6	12.9
July 2012	42.0	31.7	30.6	3.1
October 2012	29.1	22.8	6.3	11.5
January 2013	2.6	14.6	−9.5	−12.7
April 2013	53.1	43.3	21.8	−3.4
July 2013	56.5	44.8	31.3	14.7

theoretical relationship between wave height and when a wave of a certain height will experience bottom drag. However, there are theoretical limits to wave steepness, which define a maximum wave height for any given wave period (Dean and Dalrymple, 1991).

The relationship between water depth and wave attenuation coefficient first appears counterintuitive, showing an increase in α_w at greater depths (**Figure 5**). Since waves in South Bay are locally generated, wave development is controlled by a combination of water depth, wind speed, and fetch length (Young and Verhagen, 1996). The shallow water depth essentially limits the development of large waves, causing overall smaller significant wave heights and wave periods at low tides, with relatively larger waves formed during high tide or during storm events when storm surge increases water depths. During these periods of increased water depths, longer period waves are formed which can then interact with the seafloor and seagrass, causing greater attenuation coefficients. Although attenuation coefficients were estimated only for significant wave height and period, there is a range of wave heights and frequencies formed at any given time within coastal bay system. Results of Bradley and Houser (2009) found that seagrasses serve as a low-pass filter, where higher frequencies in the spectra tend to be more attenuated. Their results suggest that the rate of energy dissipation is not uniform over a range of wave frequencies, and waves at higher frequencies are attenuated, but waves at lower frequencies are less affected by the seagrass.

Velocity measurements adjacent to the sediment-water interface showed substantial reduction in bed shear stresses within the seagrass meadow compared to the bare site. Within the bare site, τ_{bed} ranged from 0.019 to 0.07, while in the seagrass bed τ_{bed} ranged from 0.004 to 0.034 Pa. The critical stress threshold to initiate sediment resuspension was found to be $\tau_{bed} = 0.04$ Pa (Lawson et al., 2007), suggesting that during summer, the seagrass canopy limits sediment from being suspended, although these measurements occurred over a limited time frame. The relative reduction of wave orbital motion caused by the canopy can be estimated using the ratio of wave orbital excursion length (A) to blade spacing (S), where $A = u_{orb}/\omega$, $\omega = 2\pi/T$, and S as the characteristic spacing between shoots (Lowe et al., 2005). For $A/S > 1$ orbital attenuation within the canopy is expected to be significant. Utilizing blade density and average blade width, blade spacing of the seagrass bed ranges from $S = 8.2$ cm in winter to 4.5 cm in summer, giving approximate estimates of $A/S = 0.1$ in winter to 0.2 in summer, assuming wave periods of $T = 1.5$ s and $u_{orb} = 2.9$ cm s^{-1} (**Table 5**). This indicates that orbital motions are not significantly altered due to direct interaction with the seagrass blades and oscillatory water motion is able to effectively penetrate the seagrass canopy, even though tidally-driven flows may be damped. This finding is similar to laboratory measurements within a model *Z. marina* meadow (Luhar et al., 2010), where it was found that unidirectional flows were reduced within the meadow but in-canopy orbital velocities were not significantly altered.

Complex bathymetry within the coastal bay and barrier island system provided a wide variety of fetch lengths to consider. Due to this variability, only north winds within a 45° wind range around true north were analyzed. The Young and Verhagen (1996) model predicted wave heights greater than those measured within the seagrass meadow during all seasons, indicating that actual wave heights were reduced compared to estimates of wave heights that would occur across an unvegetated South Bay. Although of comparable magnitude, direct *in situ* measurements of reductions in significant wave heights compared to the bare site were greater than wave height reductions compared to estimates from YV model predictions (**Table 3**). This deviation between *in situ* and modeled wave heights was consistent across seasons. Wave heights measured within the seagrass bed during winter were closest to YV model results, with an average reduction of 13%. This also corresponded with the lowest measured meadow density was lowest.

Overall, the YV model predicted wave heights that were within ±15% of those directly measured at the bare site in South Bay. Variations in model output compared to direct *in situ* measurements of wave height could be the result of multiple influences, including the coarseness of fetch distances input to the model, discrepancies in the magnitude of winds that occurred over South Bay from measured winds, or due to variations in sediment properties. Mariotti and Fagherazzi (2013a) found that the Young and Verhagen (1996) model under-predicted wave heights in a study in Willapa Bay, Washington. They attributed this to an underestimation of fetch-limited wave growth to the smooth mud substrate in the bay, which they hypothesize induced less drag on the flow than the sediment used in the formulation of the YV model. They found that a low friction coefficient for the sediment was necessary to match the observed wave dynamics. This highlights the importance of drag on wave attenuation, as even small differences in sediment characteristics can have a measurable effect on wave height, even in the absence of vegetation. Young and Verhagen (1996) do not report a grain size for the sediment used to calibrate the model, but describe the bottom as fine grained but cohesive mud. While the sediment in South Bay is fine-grained (Hansen and Reidenbach, 2012), it may not be as cohesive, as it was easily resuspended. This discrepancy could result in higher bottom friction in South Bay, and would explain wave height over-prediction by the model.

TABLE 4 | Summary of average attenuation statistics.

	Percent H_S reduction compared to bare site (%)	Percent H_S reduction compared to YV model (%)	α_w
Spring	47	37	0.49 ± 0.04
Summer	49	38	0.43 ± 0.08
Fall	41	23	0.38 ± 0.10
Winter	25	13	0.19 ± 0.04

Multiple seasons were sampled, however values from different years are averaged together to determine representative seasonal statistics. For consistency, both in situ and YV model average attenuation are computed at the Center seagrass site. α_w is listed as mean ± standard error.

CONCLUSION

A seagrass canopy within a shallow coastal bay was found to have a large impact on wave development, which varied seasonally in response to seagrass morphology and density. Although the largest wave attenuation compared to an adjacent

TABLE 5 | Wave properties and environmental conditions for Vectrino profiler deployments with lowest and highest wave activity at the bare and vegetated site.

Date	Temp (°C)	Depth (m)	H_S (m)	H_{max} (m)	T_S (s)	$\bar{u}$ @ 2.5 cm (cm s^{-1})	$\bar{u}$ @ 0.5 cm (cm s^{-1})	u_{orb} (cm s^{-1})	τ_{bed} (Pa)
BARE									
Oct 14, 2012	17.1	0.93	0.006	0.015	1.65	4.8	3.9	0	0.019 ± 0.008
Jul 01, 2013	24.9	0.61	0.114	0.191	1.48	16.0	12.5	5.7	0.070 ± 0.034
VEGETATED									
Jul 13, 2012	26.3	0.71	0.001	0.002	2.18	0.6	0.4	0.2	0.004 ± 0.003
Jul 24, 2012	29.1	0.85	0.077	0.149	1.50	4.4	3.0	2.9	0.034 ± 0.022

Temperature, water depth, H_S, H_{max}, and T_S data were obtained from wave gages, while velocities and τ_{bed} (±1 standard deviation) were obtained from the Vectrino profiler.

bare site occurred in summer when seagrass biomass was greatest, the largest wave attenuation coefficient, measured as wave decay as waves propagated across the seagrass canopy, occurred in spring, with $\alpha_w = 0.49$. This discrepancy is likely due to the large impact that physical conditions, including water depth and wind magnitude, has on wave development and attenuation and signifies that a single mean attenuation coefficient should be used with caution. α_w is highly variable with respect to water depth, wind speed, and seagrass biomass. During summer, Hansen and Reidenbach (2012) found a 45–70% reduction in wave height between a seagrass meadow and an unvegetated region in South Bay, with sites ranging from a seagrass density of 150 ± 80 shoots m^{-2} to 570 ± 70 shoots m^{-2}. The average reduction in wave height compared to a bare site of ∼50% for this study falls into this range, with summer densities of 347 ± 73 and 411 ± 33 shoots m^{-2}. Comparing a wide range of wave conditions, bed shear stresses measured at the sediment water interface were statistically lower at the vegetated compared to the unvegetated site, even though scaling of wave motions in the presence of seagrass suggest that wave orbitals should be locally unaffected by the seagrass blades, with waves being able to penetrate through the canopy. Since substantial net attenuation of wave energy as waves propagate across the meadow was found, this suggests that the integrated meadow-scale fluid drag controls the apparent decrease in bed shear within seagrass meadows compared to an unvegetated seafloor.

AUTHOR CONTRIBUTIONS

MR conceptualized the study. ET performed the experiments. MR and ET analyzed the data and wrote the manuscript.

ACKNOWLEDGMENTS

We thank A. Schwarzschild, C. Buck, and D. Boyd for field assistance. This research was funded by the National Science Foundation (NSF-DEB 1237733) to the Virginia Coast Reserve Long Term Ecological Research program and by NSF-OCE 1151314 to MR.

REFERENCES

Bradley, K., and Houser, C. (2009). Relative velocity of seagrass blades: implications for wave attenuation in low-energy environments. *J. Geophys. Res. Earth Surf.* 114, 1–13. doi: 10.1029/2007JF000951

Bretschneider, C. L. (1954). "Generation of wind waves over a shallow bottom," in *Beach Erosion Board Technical Memorandum No. 51*, (U. S. Corps of Engineers), 1–24. doi: 10.21236/AD0046517

Bretschneider, C. L. (1958). "Revisions in wave forecasting: deep and shallow water," in *Proceedings of the 6th International Conference on Coastal Engineering, American Society of Civil Engineers* (Fort Belvoir, VA), 30–67.

Bricker, J. D., Inagaki, S., and Monismith, S. G. (2005). Bed drag coefficient variability under wind waves in a tidal estuary. *J. Hydraulic Eng.* 131, 497–508. doi: 10.1061/(ASCE)0733-9429(2005)131:6(497)

Bricker, J. D., and Monismith, S. G. (2007). Spectral wave-turbulence decomposition. *J. Atmos. Ocean Technol.* 24, 1479–1487. doi: 10.1175/JTECH2066.1

Carr, J., D'odorico, P., Mcglathery, K., and Wiberg, P. (2010). Stability and bistability of seagrass ecosystems in shallow coastal lagoons: role of feedbacks with sediment resuspension and light attenuation. *J. Geophys. Res. Biogeosci.* 115:G03011. doi: 10.1029/2009JG001103

Carr, J. A., D'odorico, P., Mcglathery, K. J., and Wiberg, P. L. (2016). Spatially explicit feedbacks between seagrass meadow structure, sediment and light: habitat suitability for seagrass growth. *Adv. Water Resour.* 93, 315–325. doi: 10.1016/j.advwatres.2015.09.001

Chen, S. N., Sanford, L. P., Koch, E., Shi, F., and North, E. W. (2007). A nearshore model to investigate the effects of seagrass bed geometry on wave attenuation and suspended sediment transort. *Estuar. Coasts* 30, 296–310. doi: 10.1007/BF02700172

Dean, R. G., and Dalrymple, R. A. (1991). *Water Wave Mechanics for Engineers and Scientists*. Singapore: World Scientific. doi: 10.1142/1232

Denny, M. W. (1988). *Biology and the Mechanics of the Wave-Swept Environment.* Princeton, NJ: Princeton University Press.

Fagherazzi, S., and Wiberg, P. (2009). Importance of wind conditions, fetch, and water levels on wave-generated shear stresses in shallow intertidal basins. *J. Geophys. Res.* 114:F03022. doi: 10.1029/2008JF001139

Fonseca, M. S., and Cahalan, J. A. (1992). A preliminary evaluation of wave attenuation by four species of seagrass. *Estuar. Coast. Shelf Sci.* 35, 565–576. doi: 10.1016/S0272-7714(05)80039-3

Gacia, E., and Duarte, C. M. (2001). Sediment retention by a Mediteranean Posidonia oceanica meadow: the balance between deposition and resuspension. *Estuar. Coast. Shelf Sci.* 52, 505–514. doi: 10.1006/ecss.2000.0753

Grant, W. D., and Madsen, O. S. (1979). Combined wave and current interaction with a rough bottom. *J. Geophys. Res.* 84, 1797–1808. doi: 10.1029/JC084iC04p01797

Hansen, J. C., and Reidenbach, M. A. (2013). Seasonal growth and senescence of a *Zostera marina* seagrass meadow alters wave-dominated flow and sediment suspension within a coastal bay. *Estuar. Coasts* 36, 1099–1114. doi: 10.1007/s12237-013-9620-5

Hansen, J. C., and Reidenbach, M. A. (2017). Turbulent mixing and fluid transport within Florida Bay seagrass meadows. *Adv. Water Resour.* 108, 205–215. doi: 10.1016/j.advwatres.2017.08.001

Hansen, J. C. R., and Reidenbach, M. A. (2012). Wave and tidally driven flows in eelgrass beds and their effect on sediment suspension. *Mar. Ecol. Prog. Ser.* 448, 271–287. doi: 10.3354/meps09225

Houser, C., Trimble, S., and Morales, B. (2015). Influence of blade flexibility on the drag coefficient of aquatic vegetation. *Estuar. Coasts* 38, 569–577. doi: 10.1007/s12237-014-9840-3

Jing, L., and Ridd, P. V. (1996). Wave-current bottom shear stresses and sediment resuspension in Cleveland Bay, Australia. *Coast. Eng.* 29, 169–186. doi: 10.1016/S0378-3839(96)00023-3

Jonsson, I. G. (1967). "Wave boundary layers and friction factors," in *Proceedings of the 10th Annual Coastal Engineering Conference* (New York, NY), 127–148.

Koch, E., and Gust, G. (1999). Water flow in tide- and wave-dominated beds of the seagrass *Thalassia testudinum*. *Mar. Ecol. Prog. Ser.* 184, 63–72. doi: 10.3354/meps184063

Lacy, J. R., and Wyllie-Echeverria, S. (2011). The influence of current speed and vegetation density on flow structure in two macrotidal eelgrass canopies. *Limnol. Oceanogr. Fluids Environ.* 1, 38–55. doi: 10.1215/21573698-1152489

Lawson, S. E., Wiberg, P. L., Mcglatherty, K. J., and Fugate, D. C. (2007). Wind-driven sediment suspension controls light availability in a shallow coastal lagoon. *Estuar. Coasts* 30, 102–112. doi: 10.1007/BF02782971

Lowe, R. J., Falter, J. L., Bandet, M. D., Pawlak, G., Atkinson, M. J., Monismith, S. G., et al. (2005). Spectral wave dissipation over a barrier coral reef. *J. Geophys. Res. Oceans* 110, 5–20. doi: 10.1029/2004JC002711

Lowe, R. J., Falter, J. L., Koseff, J. R., Monismith, S. G., and Atkinson, M. J. (2007). Spectral wave flow attenuation within submerged canopies: Implications for wave energy dissipation. *J. Geophys. Res.* 112:C05018. doi: 10.1029/2006JC003605

Luhar, M., Coutu, S., Infantes, E., Fox, S., and Nepf, H. (2010). Wave-induced velocities inside a model seagrass bed. *J. Geophys. Res. Oceans* 115:C12005. doi: 10.1029/2010JC006345

Luhar, M., Infantes, E., and Nepf, H. (2017). Seagrass blade motion under waves and its impact on wave decay. *J. Geophys. Res. Oceans* 122, 3736–3752. doi: 10.1002/2017JC012731

Mariotti, G., and Fagherazzi, S. (2013a). Wind waves on a mudflat: the influence of fetch and depth on bed shear stresses. *Cont. Shelf Res.* 60, S99–S110. doi: 10.1016/j.csr.2012.03.001

Mariotti, G., and Fagherazzi, S. (2013b). Critical width of tidal flats triggers marsh collapse in the absence of sea-level rise. *Proc. Natl. Acad. Sci. U.S.A.* 110, 5353–5356. doi: 10.1073/pnas.1219600110

Mazda, Y., Magi, M., Kogo, M., and Hong, P. N. (1997). Mangroves as a coastal protection from waves in the Tong King delta, Vietnam. *Mangroves Salt Marsh.* 1, 127–135. doi: 10.1023/A:1009928003700

McGlathery, K. (2017). "Above- and below-ground biomass and canopy height of seagrass in Hog Island Bay and South Bay, VA 2007–2017," in *Virginia Coast Reserve Long-Term Ecological Research Project Data Publication knb-lter-vcr.183.17* (Oyster, VA). doi: 10.6073/pasta/09a0ce35bb3fc72113b5a16ad5b0d6bd

Mcloughlin, S. M., Wiberg, P. L., Safak, I., and Mcglathery, K. J. (2015). Rates and forcing of marsh edge erosion in a shallow coastal bay. *Estuar. Coasts* 38, 620–638. doi: 10.1007/s12237-014-9841-2

Nepf, H. M. (1999). Drag, turbulence, and diffusion in flow through emergent vegetation. *Water Resour. Res.* 35, 479–489. doi: 10.1029/1998WR900069

Orth, R., Moore, K., Marion, S., Wilcox, D., and Parrish, D. (2012). Seed addition facilitates eelgrass recovery in a coastal bay system. *Mar. Ecol. Prog. Ser.* 448, 177–195. doi: 10.3354/meps09522

Paul, M., and Amos, C. (2011). Spatial and seasonal variation in wave attenuation over *Zostera noltii*. *J. Geophys. Res. Oceans* 116:C08019. doi: 10.1029/2010JC006797

Paul, M., Bouma, T. J., and Amos, C. L. (2012). Wave attenuation by submerged vegetation: combining the effect of organism traits and tidal current. *Mar. Ecol. Prog. Ser.* 444, 31–41. doi: 10.3354/meps09489

Porter, J., Krovetz, D., Nuttle, W., and Spitler, J. (2018). "Hourly Meteorological Data for the Virginia Coast Reserve LTER 1989-present," in *Virginia Coast Reserve Long-Term Ecological Research Project Data Publication knb-lter-vcr.25.37* (Oyster, VA). doi: 10.6073/pasta/c87febba463a3ac63a64bdb484a197ce

Quartel, S., Kroon, A., Augustinus, P., Van Santen, P., and Tri, N. (2007). Wave attenuation in coastal mangroves in the Red River Delta, Vietnam. *J. Asian Earth Sci.* 29, 576–584. doi: 10.1016/j.jseaes.2006.05.008

Reidenbach, M. A., Monismith, S. G., Koseff, J. R., Yahel, G., and Genin, A. (2006). Boundary layer turbulence and flow structure over a fringing coral reef. *Limnol. Oceanogr.* 51, 1956–1968. doi: 10.4319/lo.2006.51.5.1956

Rippeth, T. P., Williams, E., and Simpson, J. H. (2002). Reynolds stress and turbulent energy production in a tidal channel. *J. Phys. Oceanogr.* 32, 1242–1251. doi: 10.1175/1520-0485(2002)032<1242:RSATEP>2.0.CO;2

Soulsby, R. L., and Dyer, K. R. (1981). The form of the near-bed velocity profile in a tidally accelerating flow. *J. Geophys. Res.* 81, 8067–8073. doi: 10.1029/JC086iC09p08067

Stocking, J. B., Rippe, J. P., and Reidenbach, M. A. (2016). Structure and dynamics of turbulent boundary layer flow over healthy and algae-covered corals. *Coral Reefs* 35, 1047–1059. doi: 10.1007/s00338-016-1446-8

Thomas, E., and Reidenbach, M. A. (2015). "Wave height and period in South Bay, VA 2011-2013," in *Virginia Coast Reserve Long-Term Ecological Research Project Data Publication knb-lter-vcr.235.3* (Oyster, VA). doi: 10.6073/pasta/8c1ce06a10283e3eb444111970674075

Weitzman, J. S., Zeller, R. B., Thomas, F. I., and Koseff, J. R. (2015). The attenuation of current-and wave-driven flow within submerged multispecific vegetative canopies. *Limnol. Oceanogr.* 60, 1855–1874. doi: 10.1002/lno.10121

Wiberg, P., and Smith, J. D. (1983). A comparison of field data and theoretical models for wave current interactions at the bed on the continental shelf. *Cont. Shelf Res.* 2, 147–162. doi: 10.1016/0278-4343(83)90013-4

Wiberg, P. L., and Sherwood, C. R. (2008). Calculating wave-generated bottom orbital velocities from surface-wave parameters. *Comput. Geosci.* 34, 1243–1262. doi: 10.1016/j.cageo.2008.02.010

Young, I., and Verhagen, L. (1996). The growth of fetch limited waves in water of finite depth. Part 1. Total energy and peak frequency. *Coast. Eng.* 29, 47–78. doi: 10.1016/S0378-3839(96)00006-3

Zeller, R. B., Weitzman, J. S., Abbett, M. E., Zarama, F. J., Fringer, O. B., and Koseff, J. R. (2014). Improved parameterization of seagrass blade dynamics and wave attenuation based on numerical and laboratory experiments. *Limnol. Oceanogr.* 59, 251–266. doi: 10.4319/lo.2014.59.1.0251

Conflict of Interest Statement: The authors declare that the research was conducted in the absence of any commercial or financial relationships that could be construed as a potential conflict of interest.

frontiers in Marine Science

BRIEF RESEARCH REPORT
published: 03 December 2018
doi: 10.3389/fmars.2018.00461

Canopy Functions of *R. maritima* and *Z. marina* in the Chesapeake Bay

*Emily French**† and Kenneth Moore*

Virginia Institute of Marine Science, College of William and Mary, Gloucester Point, VA, United States

Shoots in seagrass beds form canopies: structurally complex habitats that provide refuge for fauna and trap sediment particles by dampening water movement. Unfortunately, seagrasses are faced with continuing negative impacts to survival, including climate change and poor water quality. In areas where several seagrass species coexist, changing conditions may influence composition of beds so one species is favored over another. Two species found worldwide, *Zostera marina* and *Ruppia maritima*, are undergoing this shift: as *Z. marina* dies back, in some locations it is replaced by *R. maritima,* a smaller-form seagrass with shorter, thinner shoots. This process is occurring in Virginia, United States in the southern Chesapeake Bay, at intermediate depths where the species co-occur. Although changes in seagrass species abundance have previously been documented, few studies have measured the resulting effects on ecosystem functioning. We evaluated three sites to determine whether canopies of the two species displayed similar small epifaunal invertebrate animal assemblages and sediment properties, and found that *Z. marina* beds exhibited a greater amount of fine surface sediment than those of *R. maritima*, but found no effect of seagrass species on invertebrate assemblages. Epifaunal invertebrates were, however, more abundant and speciose with greater biomass, and more abundant with greater shoot density. This study provides baseline information from one summer for areas where the two seagrass species coexist. Although more research is needed, this study suggests in mixed beds, decline of *Z. marina* could result in coarsening of sediment, but dense *R. maritima* canopies could harbor similar small invertebrate assemblages.

Keywords: seagrass, eelgrass, Chesapeake, Chesapeake Bay, climate change, water quality, epifauna, widgeongrass

OPEN ACCESS

Edited by:
Susana Carvalho,
King Abdullah University of Science and Technology, Saudi Arabia

Reviewed by:
Juan Moreira Da Rocha,
Universidad Autónoma de Madrid, Spain
Marina Dolbeth,
Centro Interdisciplinar de Investigação Marinha e Ambiental (CIIMAR), Portugal

****Correspondence:***
Emily French
emily.d.french@gmail.com

†Present address:
Emily French,
Oak Ridge Institute for Science and Education, Environmental Protection Agency, Washington, DC, United States

Specialty section:
This article was submitted to Marine Ecosystem Ecology, a section of the journal Frontiers in Marine Science

Received: *01 September 2018*
Accepted: *15 November 2018*
Published: *03 December 2018*

Citation:
French E and Moore K (2018) Canopy Functions of R. maritima and Z. marina in the Chesapeake Bay. Front. Mar. Sci. 5:461. doi: 10.3389/fmars.2018.00461

INTRODUCTION

Seagrass canopies provide habitat for marine life, including small crustacean and gastropod invertebrates that are part of the diet of nearshore fishes (Orth et al., 1984; Valentine and Duffy, 2006). Seagrasses also attenuate waves and reduce currents, causing fine particles to be deposited and retained within beds, creating a positive feedback loop in which water clarity is improved for seagrass growth (Ward et al., 1984; Hansen and Reidenbach, 2013). Seagrasses are currently in decline due to decreased water quality and climate change (Cardoso et al., 2004; Orth et al., 2006), and beds in many areas could shift to being dominated by macroalgae or other seagrass species better able to cope with changing or degraded conditions (Armitage et al., 2011; van Tussenbroek et al., 2014). When a shift occurs between morphologically similar species, ecosystem functioning may not change (Christiaen et al., 2016), however, many co-occurring seagrasses have differing morphologies and life cycles. Several regions in the

United States have experienced seagrass habitats transitioning from larger-form, spatially stable species to more opportunistic, smaller-form species (Fourqurean et al., 1995; Johnson et al., 2003; Bologna et al., 2007; Cho et al., 2009; Lopez-Calderon et al., 2010; Micheli et al., 2014).

In Chesapeake Bay, two seagrasses co-occur: *Zostera marina* and *Ruppia maritima*. *Z. marina* has taller canopies, wider strap-like leaves and spatially stable populations (Orth and Moore, 1988; Moore et al., 2014); comparatively, *R. maritima* has shorter canopies, smaller leaf areas, and unpredictable annual abundances (Kantrud, 1991; Orth et al., 2016). These species coexist in other regions of the mid-Atlantic United States, and in California and Maine (Orth and Moore, 1988; Kantrud, 1991; Johnson et al., 2003). *Z. marina* in Chesapeake Bay is in decline and its recovery problematic (Moore et al., 2012; Lefcheck et al., 2017).

Seagrass canopy structure may play a role in epifaunal community composition and sediment deposition (Orth et al., 1984; Fonseca and Callahan, 1992), but these effects are incompletely understood. In this study we compared surface sediment characteristics and small invertebrate assemblages in canopies of each seagrass to determine whether a shift from *Z. marina* to *R. maritima* could result in changes in seagrass bed features. We hypothesized that *Z. marina* would have greater canopy biomass than *R. maritima* over the summer sampling took place, and that *Z. marina* areas would contain more fine sediment and organic matter and provide refuge for more abundant and speciose invertebrates.

MATERIALS AND METHODS

Study Locations

Three sites in the lower Chesapeake Bay (**Supplementary Figure S1**) with monotypic stands of *Ruppia maritima* and *Zostera marina* nearby to one another (50–300 m) in similar water depths (50 ± 10 cm MLLW) were sampled. The sites were physically diverse: one is located within an embayment with surrounding salt marsh, while the others are more exposed to prevailing winds and tidal currents, although all possess similar salinity and turbidity measurements[1]. Sites were within areas where an increase in *R. maritima* and decrease in *Z. marina* populations has occurred in recent years (Moore et al., 2014; Richardson et al., 2018).

Sample Collection Overview

Seagrass, sediment and invertebrate animal samples were taken in each of the habitat types (monospecific stands of *Z. marina* or *R. maritima*) during 2 months: June and August of 2013. Sampling timing was adapted from the NERRS (National Estuarine Research Reserve System) Vegetation Monitoring Protocols, which specify sampling within 2–3 weeks of peak biomass for seagrasses present (Moore, 2013). Here *Z. marina* increases in density during the late spring and senesces though mid-summer and into fall (Orth and Moore, 1986; Moore and Jarvis, 2008) and *R. maritima* has a similar trajectory, although it tends to peak in the fall (Moore et al., 2000). Replicate sampling areas were haphazardly chosen by throwing a meter-square quadrat within 10 m of a pole marking habitat type, samples were taken within the quadrat. HOBO temperature loggers (Onset Computer Corporation, Bourne, MA, United States) were anchored between the two habitat types at each site, where they recorded temperature every 15 min between 1 June and 26 August 2013.

Seagrass Biomass Sampling and Processing

Seagrass samples were taken with a 12 cm diameter acrylic core, sieved in the field to remove sediment, and transported back on ice to the laboratory where aboveground material was separated from roots and dried at 65°C until reaching a constant weight.

Sediment Sampling and Processing

Samples for grain size and sediment organic matter (SOM) were taken using a 7 cm diameter acrylic core, and transported back to the lab on ice, where the top (0–2 cm) layer of sediment was processed by homogenizing samples, separating sand from the sample, and using a pipetting method to determine fine (silt and clay) fractions (modification of Plumb, 1981). Silt and clay fractions were combined for a measurement of fine sediment, while the remaining sand represented coarse sediment. SOM was determined via the loss-on-ignition method (Erftemeijer and Koch, 2001) by drying samples at 65°C oven, then combusting at 500°C for 5 h.

Epifaunal Sampling and Processing

Samples were collected using a Virnstein grab (Virnstein and Howard, 1987), which closes over a 400 cm^2 area of sediment surface, collecting seagrass shoots, any overlying macroalgae, and epifauna without collecting sediment. During processing, epifauna were separated from seagrass shoots and macroalgae, shoots were counted, animals were sieved using 0.5 mm mesh, and all invertebrates were identified to species or genus levels. Seagrass and macroalgae was dried at 65°C until reaching a constant weight.

Data Analyses

Seagrass core samples were used to compare mean biomass between *Z. marina* and *R. maritima* habitats and mean biomass between the 2 months sampled. Separate mixed models were used to test for differences in fine sediment content, sediment organic matter content, invertebrate richness, and invertebrate abundance between *Z. marina* and *R. maritima* habitats and between the 2 months sampled. The habitat and month during which a sample was taken were used as fixed factors, and site where a sample was taken was used as a random factor in the models. Richness and abundance of epifauna were normalized to biomass from the grab samples from which they came: both to seagrass biomass and total biomass including macroalgae. A one-way ANOVA and Tukey's HSD test were used to determine the differences between daily means of temperature at the three sites. All data were inspected for normality and homogeneity of variance and transformed if assumptions were not met.

[1] http://www.vecos.org

Pearson's correlation was used to test relationships between seagrass biomass, total biomass including macroalgae, or shoot density within grab samples and the richness or abundance of invertebrates (6 comparisons). All analyses were considered significant at the $p < 0.05$ level and were performed in the R programming language (R Core Team, 2015).

RESULTS

Seagrass Biomass and Site Conditions

Water temperatures were higher in August than June, and mean temperatures were higher overall at the embayment site over the summer ($p < 0.001$ and $p < 0.001$, **Supplementary Figure S2**). Across sites, *Z. marina* had greater biomass than *R. maritima* during the months sampled (**Supplementary Table S1**), although at two sites in August, *R. maritima* biomass was greater. The greatest dieback of both *R. maritima* and *Z. marina* occurred at the embayment site, where seagrass biomass fell 90% between the beginning and end of the growing season.

Sediment Characterization

Zostera marina areas contained more fine sediment (silt and clay) than *R. maritima* areas ($p = 0.027$, **Figure 1**): *Z. marina* had an average of 86.8% sand and 13.2% fine sediment, compared to *R. maritima* with 89.4% sand and 10.6% fine sediment. The embayment site lost fine sediment from June to August, contrary to the other two sites, where the percentage of fine sediment increased. Mean organic content was greater, although not significantly so, in *Z. marina* sediments than *R. maritima* sediments in June, and means were similar in August (**Figure 1**). Mean organic content of sediments was greater in August than in June.

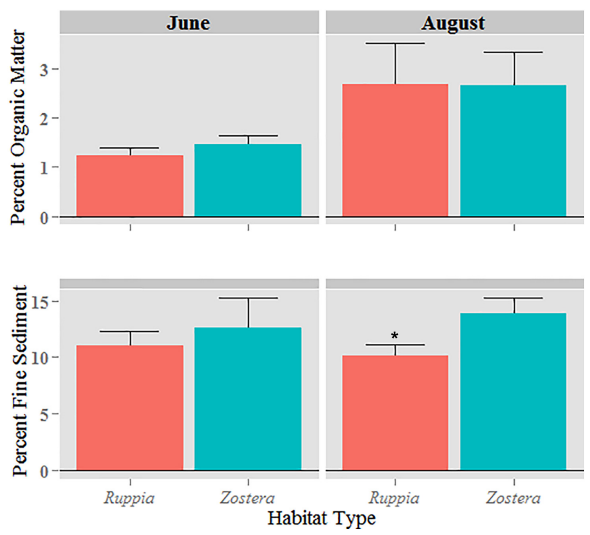

FIGURE 1 | Mean fine content of sediment and organic matter ± standard error at each habitat during the sampling periods. Asterisk indicates mean values are significantly different.

Invertebrate Abundance and Diversity

Thirteen species of small invertebrates (<3 cm) were found. There was no effect of seagrass species on abundance of invertebrates. There was a significant effect of month ($p = 0.001$); between June and August, mean abundance decreased from 165.6 to 28 individuals per sample. There was no effect of seagrass species on richness of invertebrates, though there was a significant effect of month ($p = 0.001$); a mean richness of 5.5 species per sample in June fell to 3 in August (**Supplementary Table S2**).

Greater seagrass biomass was strongly associated with both greater richness and abundance of invertebrates (**Table 1**). Several of the grabs included the macroalgal species *Gracilaria vermiculophylla*, where present, it was added to seagrass biomass for total biomass present, which resulted in stronger relationships. Higher invertebrate abundances were associated with higher shoot densities (**Table 1**), but the relationship was not significant between shoot density and invertebrate richness.

DISCUSSION

This study demonstrated that mean biomass of *Z. marina* across sites was greater than the biomass of *R. maritima*, as we hypothesized, during both June and August of the summer we sampled when *Z. marina* typically dies back. Biomass decline of *Z. marina* is typical between June and August, however, the decline demonstrated in *R. maritima* between June and August is somewhat uncharacteristic (Wetzel and Penhale, 1983; Orth and Moore, 1988; Kantrud, 1991; Moore et al., 2014). It is possible that *R. maritima* only declined in the areas sampled in this study, intermediate depths where the seagrasses cooccur, and not the shallow depths at which *R. maritima* is typically more abundant (Kantrud, 1991). When examining site data individually, the embayment site stands out: it lost the most biomass of the three sites between June and August, and had the highest temperatures over the summer, making it likely that high temperatures caused seagrass dieback.

Greater fine sediment content in *Z. marina* habitats compared to *R. maritima* suggests that *Z. marina* may possess a more enhanced capability to trap sediment than *R. maritima*. Because greater wave attenuation occurs when shoots occupy more of the water column (Fonseca and Callahan, 1992), the taller *Z. marina* canopy may trap more fine material than *R. maritima*.

TABLE 1 | Pearson's correlation matrix of relationships between invertebrate abundance and richness with biomass and shoot density.

	Invertebrate richness		Invertebrate abundance	
	p-value	*r*	*p-value*	*r*
Seagrass biomass	**0.010**	0.43	**<0.001**	0.54
Seagrass + macroalgal biomass	**0.002**	0.49	**<0.001**	0.66
Seagrass shoot density	0.084	0.29	**0.02**	0.38

Bold numbers indicate significant relationships.

Measuring sediment trapping by weighing the accumulation of fine vs. coarse sediments has limitations, thus the use of sediment traps would add valuable information to subsequent studies. However, fine-grained particles are more easily suspended than coarser particles (Ward, 1985); therefore, the increase of fine sediment from June to August in *Z. marina* beds is likely indicative of either settlement or retainment influenced by plant structure. The ubiquity of organic matter, including seagrass blade senescence and allochthonous sources, in the late summer could have contributed to the similar organic enrichment of sediments seen in August (Oreska et al., 2017).

Lack of differences in richness between seagrass species for small invertebrates (isopods, amphipods, decapods, and gastropods) could be attributable to their low richness in the lower Chesapeake Bay in general, and lack of differences in abundances could be attributable to the relative proximity of the habitat types in this study, or the mobility of invertebrates (Parker et al., 2001; Valentine and Duffy, 2006). Invertebrate richness and abundance were, however, greater in samples with higher shoot density, seagrass biomass, and total biomass including macroalgae. This intuitive relationship has been demonstrated in other studies (Orth et al., 1984 and sources therein; Douglass et al., 2010), and the present study supported this concept. Higher shoot density did not always correspond to higher biomass; most samples showed *R. maritima* had higher shoot density than *Z. marina*, while having less biomass. This suggests dense stands of *R. maritima* could harbor abundant epifauna. Abundance and richness of invertebrates decreased from June to August, this is likely due to the decrease in canopy biomass across all sites and both seagrasses.

This study highlights the need for further research in seagrass habitats transitioning from larger-form, stable species to smaller-form, opportunistic species. Recent research on seagrass populations in Chesapeake Bay show that *Z. marina* abundance is on a downward trajectory aligning in part with a warming climate (Lefcheck et al., 2017; Richardson et al., 2018), and the potential for long-term persistence of *R. maritima* populations warrants further research before concluding its canopies may provide ecosystem benefits comparable to that of *Z. marina*.

AUTHOR CONTRIBUTIONS

This research was completed when EF was a graduate student at the Virginia Institute of Marine Science, School of Marine Science, College of William and Mary and KM was her graduate advisor and mentor.

FUNDING

This study received financial support from the Chesapeake Bay National Estuarine Research Reserve and from the Virginia Institute of Marine Science, College of William and Mary (contribution number 3790).

ACKNOWLEDGMENTS

This manuscript was greatly improved through conversations with Andrew Johnson, Ashley Smyth, and Jonathan Lefcheck. We thank Erin Shields and Tavis Sparrer for assistance during field work and sample processing. We also thank the two reviewers whose comments significantly improved the manuscript.

SUPPLEMENTARY MATERIAL

The Supplementary Material for this article can be found online at: https://www.frontiersin.org/articles/10.3389/fmars.2018.00461/full#supplementary-material

FIGURE S1 | The three locations where the study took place in the lower Chesapeake Bay, VA, United States. Mobjack is the "embayment site" referred to in the methods section, and the two fringing marsh wave-exposed sites are Goodwin and Poquoson.

FIGURE S2 | Daily mean water temperatures at the three sites during the sampling events and throughout the summer. Mobjack is the "embayment site" referred to in the methods section, and the two fringing marsh wave-exposed sites are Goodwin and Poquoson.

TABLE S1 | Mean biomass of seagrass canopies ± standard error during the growing season. Mobjack is the "embayment site" referred to in the methods section, and the two fringing marsh wave-exposed sites are Goodwin and Poquoson.

TABLE S2 | Small epifaunal invertebrates (isopods, amphipods, gastropods and decapods) found in grab samples. Values are means (n = 3) ± standard error. G, M, and P correspond to the site names Goodwin, Mobjack and Poquoson. Mobjack is the "embayment site" referred to in the methods section, and the two fringing marsh wave-exposed sites are Goodwin and Poquoson.

REFERENCES

Armitage, A. R., Frankovich, T. A., and Fourqurean, J. W. (2011). Long-term effects of adding nutrients to an oligotrophic coastal environment. *Ecosystems* 14, 430–444. doi: 10.1007/s10021-011-9421-2

Bologna, P. A. X., Gibbons-Ohr, S., and Downes-Gastrich, M. (2007). Recovery of eelgrass (*Zostera marina*) after a major disturbance event in little egg harbor, new jersey, usa. *Bull. N. J. Acad. Sci.* 52, 1–6.

Cardoso, P. G., Pardal, M. A., Lillebø, A. I., Ferreira, S. M., Raffaelli, D., and Marques, J. C. (2004). Dynamic changes in seagrass assemblages under eutrophication and implications for recovery. *J. Exp. Mar. Biol. Ecol.* 302, 233–248. doi: 10.1016/j.jembe.2003.10.014

Cho, H. J., Biber, P., and Nica, C. (2009). "The rise of Ruppia in seagrass beds: changes in coastal environment and research needs," in *Handbook on Environmental Quality*, eds E. K. Drury and T. S. Pridgen (New York, NY: Nova Science), 1–15.

Christiaen, B., Lehrter, J. C., Goff, J., and Cebrian, J. (2016). Functional implications of changes in seagrass species composition in two shallow coastal lagoons. *Mar. Ecol. Prog. Ser.* 557, 111–121. doi: 10.3354/meps11847

Douglass, J. G., France, K. E., Richardson, J. P., and Duffy, J. E. (2010). Seasonal and interannual change in a chesapeake bay eelgrass community: insights into biotic

and abiotic control of community structure. *Limnol. Oceanogr.* 55, 1499–1520. doi: 10.4319/lo.2010.55.4.1499

Erftemeijer, P. L. A., and Koch, E. W. (2001). "Chapter 18: Sediment geology methods for seagrass habitat," in *Global Seagrass Research Methods*, eds F. T. Short and R. G. Coles (Berlin: Elsevier), 345–367. doi: 10.1016/B978-044450891-1/50019-0

Fonseca, M. S., and Callahan, J. A. (1992). A preliminary evaluation of wave attenuation by four species of seagrass. *Estuar. Coast. Shelf Sci.* 35, 565–576. doi: 10.1016/S0272-7714(05)80039-3

Fourqurean, J., Powell, G., Kenworthy, W., and Zieman, J. (1995). The effects of long-term manipulation of nutrient supply on competition between the seagrasses *Thalassia testudinum* and *Halodule wrightii* in florida bay. *Oikos* 72, 349–358. doi: 10.2307/3546120

Hansen, J. C. R., and Reidenbach, M. A. (2013). Seasonal growth and senescence of a *Zostera marina* seagrass meadow alters wave-dominated flow and sediment suspension within a coastal bay. *Estuar. Coast.* 36, 1099–1114. doi: 10.1007/s12237-013-9620-5

Johnson, M. R., Williams, S. L., Lieberman, C. H., and Solbak, A. (2003). Changes in the abundance of the seagrasses *Zostera marina* L. (eelgrass) and *Ruppia maritima L.* (widgeongrass) in san diego, california, following and El niño event. *Estuaries* 26, 106–115. doi: 10.1007/BF02691698

Kantrud, H. A. (1991). Wigeongrass (*Ruppia maritima*): a literature review. *Fish Wildl. Res.* 10, 1–58.

Lefcheck, J. S., Wilcox, D. J., Murphy, R. R., Marion, S. R., and Orth, R. J. (2017). Multiple stressors threaten the imperiled coastal foundation species eelgrass (*Zostera marina*) in chesapeake bay, usa. *Glob. Change Biol.* 23, 3474–3483. doi: 10.1111/gcb.13623

Lopez-Calderon, J., Riosmena-Rodríguez, R., Rodríguez-Baron, J. M., Carrión-Cortez, J., Torre, J., Meling-López, A., et al. (2010). Outstanding appearance of *Ruppia maritima* along baja california sur, méxico and its influence in trophic networks. *Mar. Biodivers.* 40, 293–300. doi: 10.1007/s12526-010-0050-3

Micheli, F., Bishop, M. J., Peterson, C. H., and Rivera, J. (2014). Alteration of seagrass species composition and function over two decades. *Ecol. Monogr.* 78, 225–244. doi: 10.1890/06-1605.1

Moore, K. A. (2013). NERRS SWMP vegetation monitoring protocol: long term monitoring of estuarine vegetation communities. *Veg. Monitor. Workgroup* 10–11.

Moore, K. A., and Jarvis, J. C. (2008). Eelgrass diebacks in the lower chesapeake bay: implications for long-term persistence. *J. Coast. Res.* 55, 135–147. doi: 10.2112/SI55-014

Moore, K. A., Shields, E. C., and Parrish, D. B. (2014). Impacts of varying temperature and light conditions on *Zostera marina* (Eelgrass) and its interactions with *Ruppia maritima* (Widgeongrass). *Estuar. Coasts.* 37, 20–30. doi: 10.1007/s12237-013-9667-3

Moore, K. A., Shields, E. C., Parrish, D. B., and Orth, R. J. (2012). Eelgrass survival in two contrasting systems: role of turbidity and summer water temperatures. *Mar. Ecol. Prog. Ser.* 448, 247–258. doi: 10.3354/meps09578

Moore, K. A., Wilcox, D. J., and Orth, R. J. (2000). Analysis of the abundance of submersed aquatic vegetation communities in the chesapeake bay. *Estuar. Coast.* 23, 115–127. doi: 10.2307/1353229

Oreska, M. P. J., Wilkinson, G. M., McGlathery, K. J., Bost, M., and Mckee, B. A. (2017). Non-seagrass carbon contributions to seagrass sediment blue carbon. *Limnol. Oceano* 63, S3–S18. doi: 10.1002/lno.10718

Orth, R. J., Carruthers, T. J. B., Dennison, W. C., Duarte, C. M., Fourqurean, J. W., Heck, K. L., et al. (2006). A global crisis for seagrass ecosystems. *Bioscience* 56, 987–996. doi: 10.1641/0006-3568(2006)56[987:AGCFSE]2.0.CO;2

Orth, R. J., Heck, K. L., and Montfrans, J. (1984). Faunal communities in seagrass beds: a review of the influence of plant structure and prey characteristics on predator-prey relationships. *Estuaries* 7, 339–350. doi: 10.2307/1351618

Orth, R. J., and Moore, K. A. (1986). Seasonal and year-to-year variations in the growth of *Zostera marina* L.(eelgrass) in the lower chesapeake bay. *Aquat. Bot.* 24, 335–341. doi: 10.1016/0304-3770(86)90100-2

Orth, R. J., and Moore, K. A. (1988). Distribution of *Zostera marina* and *Ruppia maritima* sensu lato along depth gradients in the lower chesapeake bay, usa. *Aquat. Bot.* 32, 291–305. doi: 10.1016/0304-3770(88)90122-2

Orth, R. J., Wilcox, D. J., Whiting, J. R., Nagey, L., Kenne, A. K., and Smith, E. R. (2016). *2015 Distribution of Submerged Aquatic Vegetation in Chesapeake Bay and Coastal Bays*. Availble at: http://web.vims.edu/bio/sav/sav15/index.html [accessed October 20, 2018]

Parker, J. D., Duffy, J. E., and Orth, R. J. (2001). Plant species diversity and composition: experimental effects on marine epifaunal assemblages. *Mar. Ecol. Prog. Ser.* 224, 55–67. doi: 10.3354/meps224055

Plumb, R. H. (1981). *Procedures for Handling and Chemical Analysis of Sediment and Water Samples*. Technical Report EPA/CE-81-1. Great Lakes Laboratory, State University College at Buffalo, Buffalo, NY, for the U.S. Environmental Protection Agency/Corps of Engineers Technical Committee on Criteria for Dredged and Filled Material: Environmental Laboratory, U.S. Army Waterways Experiment Station, Vicksburg, MS. 1–403.

R Core Team (2015). *R: A Language and Environment for Statistical Computing*. Vienna: R Foundation for Statistical Computing. Available at: http://www.r-project.org/

Richardson, J. P., Lefcheck, J. S., and Orth, R. J. (2018). Warming temperatures alter the relative abundance and distribution of two co-occuring foundaional seagrasses in chesapeake bay, usa. *Mar. Ecol. Porg. Ser.* 599, 65–74. doi: 10.3354/meps12620

Valentine, J. F., and Duffy, J. E. (2006). "Grazing in seagrass ecosystems," in *Seagrasses: Biology, Ecology and Conservation*, eds A. W. D. Larkum, R. J. Orth, and C. M. Duarte (Dordrecht: Springer), 463–501.

van Tussenbroek, B. I., Cortés, J., Collin, R., Fonseca, A. C., Gayle, P. M., Guzmán, H. M., et al. (2014). Caribbean-wide, long-term study of seagrass beds reveals local variations, shifts in community structure and occasional collapse. *PLoS One* 9:e90600. doi: 10.1371/journal.pone.0090600

Virnstein, R., and Howard, R. (1987). Motile epifauna of marine macrophytes in the indian river lagoon. *Bull. Mar. Sci.* 41, 1–12.

Ward, L. G. (1985). The influence of wind waves and tidal currents on sediment resuspension in the middle chesapeake bay. *Geo Mar. Lett.* 5, 71–75. doi: 10.1007/BF02629802

Ward, L. G., Kemp, W. M., and Boynton, W. R. (1984). The influence of waves and seagrass communities on suspended particulates in an estuarine embayment. *Mar. Geol.* 59, 85–103. doi: 10.1016/0025-3227(84)90089-6

Wetzel, R. L., and Penhale, P. A. (1983). Production ecology of seagrass communities in the lower chesapeake bay. *Mar. Technol. Soc. J.* 17, 22–31.

Conflict of Interest Statement: The authors declare that the research was conducted in the absence of any commercial or financial relationships that could be construed as a potential conflict of interest.

frontiers in Marine Science

ORIGINAL RESEARCH
published: 04 December 2018
doi: 10.3389/fmars.2018.00449

Predicting Current-Induced Drag in Emergent and Submerged Aquatic Vegetation Canopies

Arnold van Rooijen[1,2,3,4]*, *Ryan Lowe*[1,2,3,5], *Marco Ghisalberti*[2,5,6], *Mario Conde-Frias*[2,3,5] *and Liming Tan*[7]

[1] School of Earth Sciences, University of Western Australia, Perth, WA, Australia, [2] UWA Oceans Institute, University of Western Australia, Perth, WA, Australia, [3] ARC Centre of Excellence for Coral Reef Studies, University of Western Australia, Perth, WA, Australia, [4] Unit of Marine and Coastal Systems, Deltares, Delft, Netherlands, [5] Oceans Graduate School, University of Western Australia, Perth, WA, Australia, [6] Department of Infrastructure Engineering, University of Melbourne, Melbourne, VIC, Australia, [7] Institute of Port, Coastal and Nearshore Engineering, Ocean College, Zhejiang University, Zhoushan, China

Canopies formed by aquatic vegetation, such as mangroves, seagrass, and kelp, play a crucial role in altering the local hydrodynamics in rivers, estuaries, and coastal regions, and thereby influence a range of morphodynamic and biophysical processes. Prediction of the influence of canopies on these hydrodynamic processes requires a fundamental understanding of canopy drag, which varies significantly with both flow conditions and canopy properties (such as density and submergence). Although our knowledge on canopy drag has increased significantly in recent decades, a conclusive, physics-based description for canopy drag that can be applied to both emergent and submerged canopies is currently lacking. Here, we extend a new theoretical canopy drag model (that employs the velocity between canopy elements as the reference velocity) to submerged aquatic canopies. The model is validated for the first time with direct measurements of drag forces exerted by canopies across broad ranges of flow conditions and canopy density and submergence. The skill and broader applicability of the model are further assessed using a comprehensive set of existing experimental data, covering a broad range of natural conditions (including flexible vegetation). The resulting model provides a simple tool to estimate canopy drag forces, which govern hydraulic resistance, sediment transport, and biophysical processes within aquatic ecosystems.

Keywords: ecohydraulics, vegetated flows, flow-plant interaction, drag model, drag coefficient

OPEN ACCESS

Edited by:
Roshanka Ranasinghe, IHE Delft Institute for Water Education, Netherlands

Reviewed by:
Tomohiro Suzuki, Flanders Hydraulics Research, Belgium
Vanesa Magar, Centro de Investigación Científica y de Educación Superior de Ensenada (CICESE), Mexico

***Correspondence:**
Arnold van Rooijen
arnold.vanrooijen@research.uwa.edu.au

Specialty section:
This article was submitted to Coastal Ocean Processes, a section of the journal Frontiers in Marine Science

Received: *27 August 2018*
Accepted: *08 November 2018*
Published: *04 December 2018*

Citation:
van Rooijen A, Lowe R, Ghisalberti M, Conde-Frias M and Tan L (2018) Predicting Current-Induced Drag in Emergent and Submerged Aquatic Vegetation Canopies. Front. Mar. Sci. 5:449. doi: 10.3389/fmars.2018.00449

INTRODUCTION

It is widely recognized that aquatic vegetation, such as seagrass, reeds, kelp, and mangroves, greatly influences hydrodynamic processes within rivers, estuaries, and coastal regions (e.g., Nepf, 2012). The drag exerted by emergent and submerged vegetation impacts the local hydrodynamics, morphodynamics, and ecology over a range of spatial scales (Koch et al., 2007). The canopies formed by vegetation can affect the local flow environment at the smallest scale (i.e., the plant scale, mm to cm) to the larger-scale (>1 km) flows that occur across benthic ecosystems. Canopy drag forces contribute to reducing flow velocities within canopies (López and García, 2001) and enhancing local turbulence (Nepf and Vivoni, 2000). In areas with significant wave action, such as in coastal regions and large lakes, the rate of work done by canopy drag forces also results in

wave energy attenuation (e.g., Fonseca and Cahalan, 1992). The flow reduction induced by canopy drag can, in turn, influence a number of morphodynamic and biophysical processes (Koch et al., 2007). For example, canopies can modify local bed shear stresses (James et al., 2004), thereby affecting sediment transport, deposition (Hendriks et al., 2008, 2010) and resuspension (Widdows et al., 2008). Similarly, canopy drag also indirectly influences other particle dynamics, affecting pollination (Ackerman, 1995), establishment of seedlings (Balke et al., 2013), and recruitment and settlement of larvae, spores, and fauna (Kenyon et al., 1999). The effect of the reduced in-canopy flow on the diffusive boundary layer around plant leaves (Koch et al., 2007) also governs nutrient uptake (Morris et al., 2008) and can influence the growth of epiphytes (Cornelisen and Thomas, 2002). Under strong flow conditions, the drag forces exerted on canopy elements can result in their physical removal from the seabed (Duarte, 2002; Edmaier et al., 2011). Globally, aquatic ecosystems are under increasing pressure from anthropogenic and climate change impacts (Duarte, 2002), and it is crucial we increase our understanding of canopy drag as it directly influences many important biophysical processes in aquatic environments.

To be able to quantify the influence of aquatic canopies on the local hydrodynamics, a comprehensive understanding of the mechanics governing canopy drag is required. Given the diversity of plant morphologies in natural environments, individual plants are often schematized as uniform, rigid cylinders to establish a general knowledge framework for the processes governing drag (see review by Vargas-Luna et al., 2016). The drag force per unit length of a cylinder in isolation is given by:

$$f_d = \frac{1}{2}\rho d_c C_d {U_{ref}}^2 \tag{1}$$

where ρ is the water density, d_c is the cylinder diameter, C_d is the drag coefficient, and U_{ref} is a reference flow velocity (which, in the case of an isolated cylinder, is equal to the upstream velocity). For reference, a **Notation table** specifying all variables is provided at the end of this manuscript. Predicting the drag coefficient for a cylinder in isolation is historically well-established, and it can be robustly predicted as:

$$C_d = 1 + 10Re^{-2/3} \tag{2}$$

(White, 1991), where the Reynolds number is defined as $Re = U_{ref} d_c/\nu$, with ν is the kinematic viscosity. For real-world application, considering plants rather than cylinders, temporal fluctuations in the drag force (due to turbulence) and vertical variation of the drag are often of less interest than the mean drag force, which governs the range of biophysical processes described earlier. As the plant biomass and flow velocity may vary significantly over the height of the plant, the total mean drag force on the plant is usually defined as:

$$\overline{F_d} = \frac{1}{2}\rho \overline{\int_{z=0}^{h_v} d_v C_d {U_{ref}}^2 dz} \tag{3}$$

where the drag force is integrated over the vertical dimension (z) and averaged over time (denoted by the overbar), h_v is the vegetation (cylinder) height (with $z = 0$ at the bed), and d_v is the vegetation stem (cylinder) diameter.

In the case of a single plant, the upstream velocity is usually weakly vertically-varying over most of the water column and the depth-averaged velocity is an obvious choice for the reference velocity (U_{ref}) needed to estimate the drag force in Equation (3). However, in the case of multiple plants forming a canopy, the flow throughout the canopy (and therefore the "upstream" velocity for each plant) is spatially non-uniform. It is thus unclear which actual velocity governs drag and could be used as the appropriate reference velocity. In emergent canopies (denoted hereafter with the superscript "*em*"), previous studies have chosen the reference velocity to be either: (1) the bulk velocity (i.e., $U_b^{em} = Q/Wh$, where Q is the flow discharge, W is the channel width and h is water depth) (e.g., Wu et al., 1999) or, more commonly, (2) the pore velocity ($U_p^{em} = U_b^{em}/\left(1-\lambda_p\right)$, where λ_p is the canopy density that is equivalent to the canopy element plan area per unit bed area) (e.g., Tanino and Nepf, 2008), representing the spatially-averaged velocity inside the fluid spaces within a canopy. However, through Large Eddy Simulation, Etminan et al. (2017) found that the "constricted cross-section velocity," the average velocity in the constriction between adjacent canopy elements, is the velocity scale that actually governs wake pressure and thus canopy drag. The relationship between the pore velocity and the constricted cross-section velocity (U_c^{em}) is dependent on the arrangement of canopy elements, and is obtained through conservation of mass [*i.e.*, $U_c^{em}\left(1-\frac{d_v}{S_{v,l}}\right) = U_p^{em}\left(1-\lambda_p\right)$]. Here, $S_{v,l}$ is the lateral spacing between adjacent elements at the same streamwise (x) location, and can only be strictly defined for regular arrays (such as linear or staggered arrangements). This relationship between the constricted cross-section velocity and the pore velocity can be written as a function of the canopy density:

$$U_c^{em} = \frac{1-\lambda_p}{1-\sqrt{4\frac{\lambda_p}{\beta\pi}}} U_p^{em} \tag{4}$$

(Stone and Shen, 2002; Etminan et al., 2017). In Equation (4), β represents the ratio between $S_{v,l}$ and the distance between two rows of canopy elements in the streamwise direction ($S_{v,s}$). For random arrays, as can be found in nature, the constricted cross-section velocity can be computed from the bulk velocity:

$$U_c^{em} = \frac{1}{1-d_v\sqrt{N_v}} U_b^{em} = \frac{1-\frac{\pi}{4}N_v d_v^2}{1-d_v\sqrt{N_v}} U_p^{em} \tag{5}$$

where N_v is the total number of plants per unit area. Note that this will result in a canopy-average value of U_c^{em}, and local values may vary significantly.

In the case of submerged canopies, the shear layer present at the top of the canopy results in strong vertical variations in the spatially-averaged flow, further complicating canopy drag predictions. In many cases, the reference velocity used to predict the drag in submerged canopies is based on the bulk velocity ($U_b^{sub} = Q/Wh$, where the superscript "*sub*" refers to a velocity scale used for submerged canopies) (Wu et al., 1999; López

and García, 2001). However, this approach does not account for the attenuation of flow within the canopy that will significantly influence canopy drag. An exception is the study of Liu and Zeng (2017) who proposed a more representative in-canopy flow velocity that accounts for vertical variation in the spatially-averaged flow. However, their approach did not account for the local (horizontal) spatial variation in the mean flow inside the canopy.

In emergent canopies, experimental measurements of drag coefficients have most commonly been obtained by measuring the surface slope and assuming a force balance of canopy drag and hydraulic gradient (Liu et al., 2008; Tanino and Nepf, 2008). The drag force of an individual plant within the canopy is then given by:

$$\overline{F_d} = -\left(1-\lambda_p\right)\rho g \frac{d\eta}{dx} h_v N_v^{-1} \tag{6}$$

where g is the gravitational acceleration, and η is the (measured) water surface elevation. By combining Equations (3) and (6), the drag coefficient can be obtained when assuming a depth-uniform velocity profile. For emergent canopies, this is relatively straight-forward, although the choice of reference velocity may greatly affect the calculated C_d values (Etminan et al., 2017). A large range of empirical relations have been established to relate canopy drag coefficients to plant shape, the flow regime (i.e., Reynolds number) and canopy properties (e.g., density). The drag coefficient is generally found to decrease exponentially with increasing Reynolds number (e.g., Liu and Zeng, 2017), following a similar trend to the isolated cylinder case (Equation 2). In terms of canopy geometry, some studies have found that the drag coefficient decreases with increasing canopy density (e.g., Nepf, 1999), while many others obtained conflicting results (e.g., Wu et al., 1999; Tanino and Nepf, 2008; Wang et al., 2014). Relatively few studies have directly measured the forces on canopy elements using force sensors either mounted at the top (e.g., Kothyari et al., 2009) or at the base of a canopy element (e.g., Schoneboom et al., 2010).

Furthermore, the majority of studies have focused on emergent canopies, such that there are still significant knowledge gaps in predicting the drag of submerged canopies. This is largely due to the more complex vertical flow structure within submerged canopies. The in-canopy flow velocity is often significantly lower than the freestream velocity and, as for emergent canopies, horizontal variation in the flow field are expected to play a significant role in canopy drag. Even with accurate measurements of submerged canopy drag forces, it is still unclear how to predict the constricted cross-section velocity within a submerged canopy when velocity measurements are lacking. The main reason for this is that the in-canopy flow velocity is dependent on the drag itself (Lowe et al., 2005), so that C_d is a function of U_{ref}, and vice versa.

This paper aims to reduce the uncertainty in canopy drag estimation through direct measurements of the drag force in aquatic vegetation canopies subject to unidirectional flow. The experimental program includes both emergent and submerged canopies with varying densities, and a range of hydrodynamic conditions covering a broad range of natural conditions that can be found in aquatic systems. In addition, a theoretical canopy drag model for emergent canopies is extended to submerged canopies and validated for the first time using direct force measurements, and then more broadly assessed using a compilation of data reported in previous studies.

CANOPY DRAG MODEL

For both emergent and submerged canopies, the mean drag force exerted on a single plant or canopy element is governed by Equation (3). For emergent canopies, the mean horizontal flow velocity is often assumed to be depth-uniform. For submerged canopies, the horizontal flow profile can be approximated as a two-layer flow with depth-uniform velocities both above and inside the canopy (e.g., Lowe et al., 2005; Liu et al., 2008) (see **Figure 1** for a definition sketch and relevant velocity definitions).

Emergent Canopies

For emergent canopies, Etminan et al. (2017) proposed to use the theory of drag for isolated cylinders (i.e., Equation 2) as the basis to compute the drag coefficients associated with emergent canopy. Their model employs the constricted cross-section velocity (U_c^{em}) as the reference velocity (U_{ref}) to determine the drag coefficient through the Reynolds number (Equation 2) and to compute the drag force (Equation 3), and was validated through Large Eddy Simulation (Etminan et al., 2017).

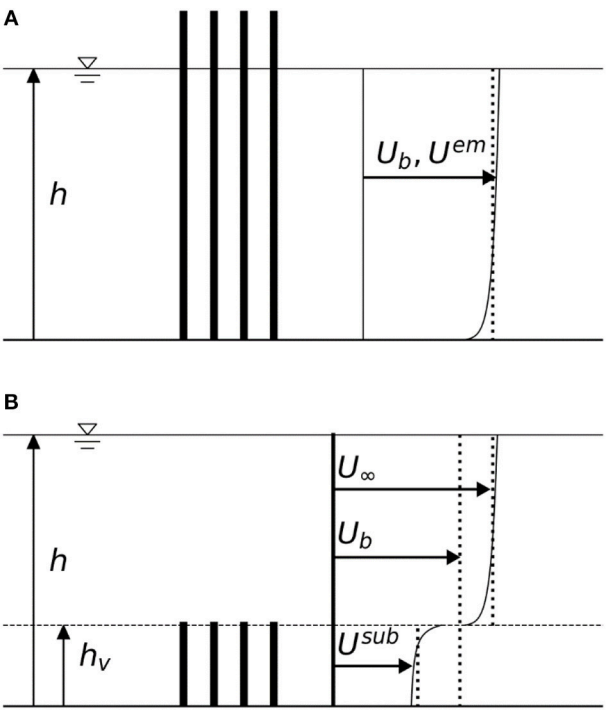

FIGURE 1 | Open channel flows with **(A)** an emergent canopy and **(B)** a submerged canopy. In emergent canopies, the depth-averaged velocity ($\overline{U}$) is often used as the representative in-canopy velocity scale (U^{em}). In submerged canopies, the depth-averaged velocity inside the canopy (U^{sub}) is often substantially reduced from the above-canopy (free stream) velocity (U_∞).

Submerged Canopies

For a given in-canopy flow, one can hypothesize that an analogous method to emergent canopies can be applied to submerged canopies, i.e., the in-canopy constricted cross-section velocity (U_c^{sub}) can be computed using Equation (4) or (5). However, as discussed in section Introduction, the estimation of U_p^{sub} is not straight-forward due to the vertical variation in the mean velocity profile (**Figure 1**); the magnitude of the in-canopy velocity both governs, and depends on, the canopy drag. Here, we propose to use a canopy flow model to predict the in-canopy pore velocity (U_p^{sub}) based on the (undisturbed) above-canopy flow velocity (U_∞). This model takes the form:

$$U_p^{sub} = U_\infty \sqrt{L_d / L_s} \tag{7}$$

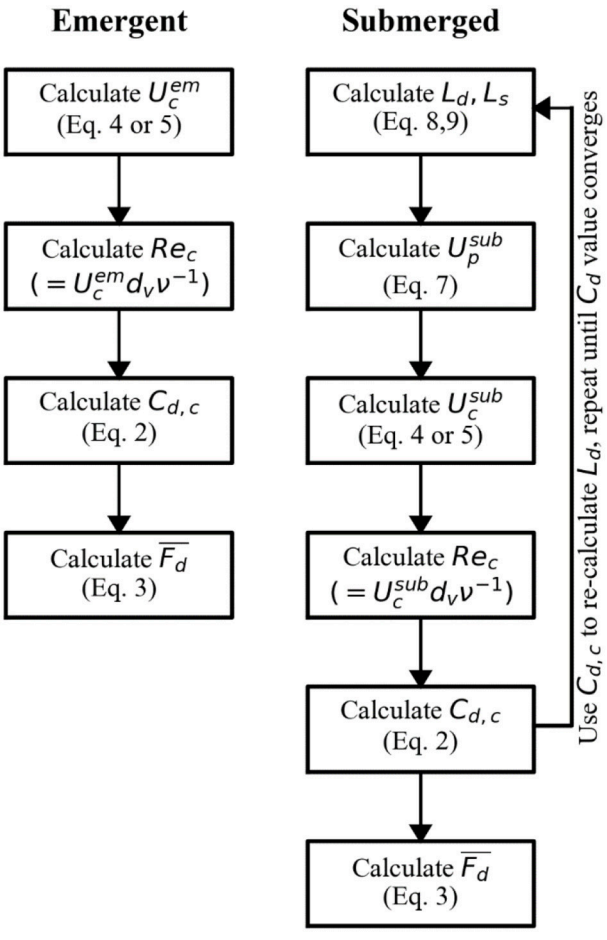

FIGURE 2 | Flow diagram for the canopy drag model. The model can be used to estimate the drag force on an individual element within an emergent or submerged canopy or the bulk canopy drag. As input, it requires above-canopy velocity (U_∞) that can be estimated from the flow rate (Q) or bulk velocity (U_b) for submerged and emergent canopies resp., local water depth (h), and the canopy properties: height (h_v), stem diameter (d_v), and canopy density (λ_p, N_v). For submerged canopies, an initial value of $C_d = 1$ (to calculate L_d) is suggested.

(Lowe et al., 2005). In Equation (7), L_d is the drag length scale, given by

$$L_d = \frac{2h_v\left(1-\lambda_p\right)}{C_d \lambda_f}, \tag{8}$$

(Lowe et al., 2005; Ghisalberti, 2009), and represents the flow resistance of the canopy. λ_f is the canopy element frontal area per unit bed area ($=h_v d_v N_v$). L_s is the shear length scale, given by

$$L_s = \frac{2h_v}{C_f} \tag{9}$$

(Lowe et al., 2005) (where C_f is a friction coefficient), which parameterizes the magnitude of the shear stress at the top of the canopy. This shear stress is generated by the velocity difference between the flow within and above the canopy. If velocity measurements are available, the friction coefficient can be estimated based on the peak in the Reynolds stress profile near the top of the canopy ($z \approx h_v$):

$$C_f = 2\frac{u_*^2}{U_\infty^2} = 2\frac{-\overline{u'w'}_{z\approx h_v}}{U_\infty^2} \tag{10}$$

(Lowe et al., 2005), where u_* is the friction velocity and u' and w' are the horizontal and vertical turbulent velocity fluctuations, respectively. Data from a wide range of canopies indicates that $\frac{u_*}{U_\infty}$ tends to be consistently $O(0.1)$, which corresponds to $C_f = O(0.01)$ (e.g., Harman and Finnigan, 2007; Lowe et al., 2008; Luhar et al., 2010; Moltchanov et al., 2011; Weitzman et al., 2015). Therefore, for a given canopy geometry and above-canopy flow velocity (U_∞), the in-canopy pore velocity U_p^{sub} can be estimated from Equations (7–10). Subsequently, the constricted cross-section velocity inside a submerged canopy can be obtained through Equations (4) or (5), and is used as the reference velocity (U_{ref}) to calculate the drag coefficient through the Reynolds number (Equation 2) and to compute the drag force (Equation 3).

In summary, the model that is proposed here relies on information on above-canopy flow velocity (U_∞) or bulk velocity (for emergent canopies), the local water depth (h), and the canopy properties: height (h_v), stem diameter (d_v), and canopy density (λ_p, N_v). It includes one empirical parameter (namely, C_f) in the case of a submerged canopy. It is important to emphasize that given the drag coefficient C_d is also needed in Equation (8) to predict the in-canopy flow (hence the drag forces and in-canopy flow are inherently coupled), for submerged canopies the model involves an iterative process. A flow diagram summarizing the model is provided in **Figure 2**. In the following sections, the model is validated using newly obtained velocity and drag force data, as well as a large dataset covering a broad range in canopy geometries and flow conditions obtained from literature.

EXPERIMENTAL METHODS

Experiments were carried out in a 20-m-long, 0.6-m-wide, and 0.6-m-deep recirculating flume using emergent (**Table 1**)

TABLE 1 | Experimental emergent vegetation conditions: canopy density (λ_p), canopy height (h_v), water depth (h), flow rate (Q), bulk velocity (U_b^{em}), pore velocity (U_p^{em}), constricted cross-section velocity (U_c^{em}), measured velocity averaged over the dowel height (U_m^{em}) and the measured time-averaged drag force acting on a single cylinder ($\overline{F_d}$).

Run	λ_p (%)	h_v (m)	h (m)	Q (L s^{-1})	U_b^{em} (m s^{-1})	U_p^{em} (m s^{-1})	U_c^{em} (m s^{-1})	U_m^{em} (m s^{-1})	$\overline{F_d}$ (mN)
E00-5	–	0.30	0.2	5.9	–	–	–	0.05	1.9
E00-10	–	0.30	0.2	10.2	–	–	–	0.08	5.9
E00-15	–	0.30	0.2	15.2	–	–	–	0.13	12.1
E00-20	–	0.30	0.2	20.5	–	–	–	0.17	19.1
E00-25	–	0.30	0.2	25.9	–	–	–	0.22	30.4
E00-30	–	0.30	0.2	31.5	–	–	–	0.26	41.3
E05-5	5	0.30	0.2	5.9	0.05	0.05	0.07	–	2.8
E05-10	5	0.30	0.2	10.2	0.08	0.09	0.11	–	8.6
E05-15	5	0.30	0.2	15.2	0.13	0.13	0.17	–	17.2
E05-20	5	0.30	0.2	20.5	0.17	0.18	0.23	–	32.1
E05-25	5	0.30	0.2	25.9	0.22	0.23	0.29	–	50.0
E10-5	10	0.30	0.2	5.9	0.05	0.05	0.07	–	3.6
E10-10	10	0.30	0.2	10.2	0.08	0.09	0.11	–	8.8
E10-15	10	0.30	0.2	15.2	0.13	0.14	0.17	–	17.8
E10-20	10	0.30	0.2	20.5	0.17	0.19	0.23	–	33.1

TABLE 2 | Experimental submerged vegetation conditions: canopy density (λ_p), canopy height (h_v), water depth (h), flow rate (Q), bulk velocity (U_b^{sub}), pore velocity (U_p^{sub}), constricted cross-section velocity (U_c^{sub}), measured in-canopy velocity averaged over the canopy/dowel height (U_m^{sub}) and the measured time-averaged drag force acting on a single cylinder ($\overline{F_d}$).

Run	λ_p (%)	h_v (m)	h (m)	Q (L s^{-1})	U_b^{sub} (m s^{-1})	U_p^{sub} (m s^{-1})	U_c^{sub} (m s^{-1})	U_m^{sub} (m s^{-1})	$\overline{F_d}$ (mN)
S3-00-10	–	0.09	0.27	10.2	–	–	–	0.05	1.0
S3-00-15	–	0.09	0.27	15.2	–	–	–	0.09	2.8
S3-00-20	–	0.09	0.27	20.5	–	–	–	0.12	4.0
S3-00-25	–	0.09	0.27	25.9	–	–	–	0.15	6.4
S3-00-30	–	0.09	0.27	31.5	–	–	–	0.18	9.6
S3-025-20	2.5	0.09	0.27	20.5	0.13	0.04	0.05	0.04	1.0
S3-025-25	2.5	0.09	0.27	25.9	0.16	0.06	0.07	0.05	1.3
S3-025-35	2.5	0.09	0.27	30.3	0.19	0.08	0.10	0.07	2.3
S3-05-15	5	0.09	0.27	15.2	0.09	0.02	0.03	0.03	0.7
S3-05-20	5	0.09	0.27	20.5	0.13	0.03	0.04	0.05	1.0
S3-05-25	5	0.09	0.27	25.9	0.16	0.04	0.05	0.06	1.5
S3-05-30	5	0.09	0.27	31.5	0.19	0.05	0.06	0.07	1.9
S3-05-35	5	0.09	0.27	36.7	0.23	0.06	0.07	0.08	2.1
S2-025-20	2.5	0.09	0.18	20.5	0.19	0.08	0.10	0.10	4.0
S2-025-25	2.5	0.09	0.18	25.9	0.24	0.10	0.12	0.13	6.8
S2-025-30	2.5	0.09	0.18	36.7	0.34	0.14	0.17	0.23	14.1
S2-05-10	5	0.09	0.18	10.2	0.09	0.03	0.03	0.05	0.8
S2-05-15	5	0.09	0.18	15.2	0.14	0.04	0.05	0.07	2.1
S2-05-20	5	0.09	0.18	20.5	0.19	0.06	0.07	0.09	3.1

and submerged (**Table 2**) model vegetation. To accommodate the drag force sensor, a 10-cm-high false bottom was placed over a length of 10 m. Model canopies were constructed using perforated PVC sheets and two sets of 6.4-mm-diameter dowels with heights of 30 cm (emergent) or 9 cm (submerged). Dowels were distributed in a staggered arrangement over the entire width of the flume. The dowel diameter used in this study has been used previously in numerous studies to represent a generic aquatic vegetation canopy (e.g., Nepf, 1999) and was originally based on actual observed stem diameters of cordgrass (*Spartina alterniflora*, see Zavistoski, 1994). An important design parameter for experimental studies with canopies is the canopy

length (L_v). Lowe et al. (2005) found a canopy flow adjustment length (x_0) of 3–5 times the drag length scale (L_d) in their experiments. Hence, to ensure fully-developed canopy flow, it was required that $L_v >> x_0$ resulting in L_v ranging between 2.4 m ($\lambda_p = 0.1$) and 3.6 m ($\lambda_p = 0.025$).

The drag force exerted on a representative aluminum dowel (canopy element) was measured using a load cell with 2 N capacity (Uxcell, Hong Kong) connected to a load cell amplifier (RW-ST01A, SMOWO, China). The load cell was mounted vertically onto the underside of the false bottom in the flume, ensuring the bottom end of the load cell was fixed but allowing the upper end to move slightly with the bending moment (M_Y) generated by the drag force acting on the dowel (**Figure 3**). Data was obtained from the load cell using a National Instruments data acquisition system (NI-DAQ PCI-6009) and LabVIEW software. This experimental setup relies on the linear relationship between drag force and the instrument voltage output. To confirm the load cell's linearity, the load cell was placed at the edge of a table and the voltage output recorded for cases with both no weight and a weight of (approximately) 1.9 N. The (linear) calibration coefficient was derived by calculating the ratio between the change in voltage output and the change in applied weight. The linear response was subsequently verified using 9 (smaller) weights ranging from 0.01 to 1.2 N ($R^2 > 0.99$). Prior to each individual experimental run, the load cell was re-calibrated using a set of three known weights ranging between 0 and ∼0.3 N.

For emergent canopies, the water level was measured using a point gauge at three locations both upstream and downstream of the canopy. The water level gradient ($d\eta/dx$) was then obtained by averaging the water level in time at the upstream and downstream locations and dividing by the canopy length. To calculate the flow rate, velocity measurements were obtained several meters upstream of the canopy using a Nortek Vectrino II Acoustic Doppler Velocity (ADV) profiler, resulting in 3-cm-tall velocity profiles with 1 mm resolution. The vertical position of the ADV was varied to obtain a full velocity profile extending from the bottom to ∼5 cm below the water surface. In a similar manner, the velocity profile in and above the canopy was obtained for the submerged cases, and extended from the base of the canopy up to ∼5 cm below the water surface. The ADV was positioned within the constricted cross-section in between two canopy elements at a lateral distance of $\sim 0.25 S_{v,l}$ from one of the elements. This was based on the modeling of Etminan et al. (2017), who found that the velocity at this point in a staggered canopy was similar to the constricted cross-section value. Experimental runs were repeated several times to obtain the full velocity profile over depth within and above the canopy. Both the load cell and ADV were placed at a distance of ∼2/3 of the canopy length downstream from the leading edge, which is at least 10 times the drag length scale (L_d) for all cases.

The experimental program included a range of canopy densities ($\lambda_p = 0.025$, 0.05, and 0.10), canopy submergence ratios ($h/h_v = 1$, 2, and 3, where h is the water depth at still water and h_v is the canopy height) and flow rates (**Tables 1**, **2**). The upstream flow velocity ranged between ∼0.05 and 0.35 m/s, which in combination with the range in canopy density and submergence ratio covers a broad range of conditions that can be found in aquatic canopies. The drag force and velocity data were processed and the drag coefficient was subsequently computed using Equation (3).

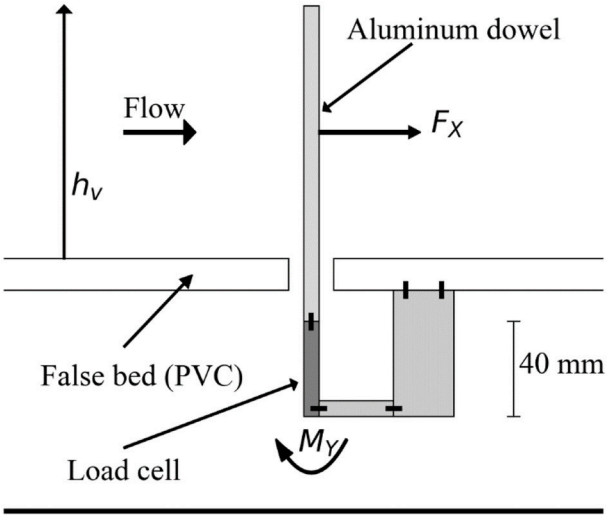

FIGURE 3 | Schematic view of the load cell, which was attached to a single aluminum dowel and placed under the false bed. The drag force (F_x) due to the flow acting on the dowel translates into a moment (M_y) around the base of the load cell.

Following Taylor (1997), measurement uncertainties were propagated, with an estimated velocity uncertainty of 0.1 cm/s and drag force uncertainty of 0.4 mN. For the model-data comparison the model skill was quantified using scatter index (*SCI*), and the relative bias. The scatter index is a relative measure of the scatter between computed (x_c) and measured data (x_m) and is computed by normalizing the root-mean-square error ($\sqrt{\overline{(x_c - x_m)^2}}$) with the maximum of the root-mean-square-value of the data ($\sqrt{\overline{(x_m)^2}}$) and the absolute value of the mean of the data ($|\overline{x_m}|$). The relative bias is a relative measure of the bias or mean error ($\overline{(x_c - x_m)}$) and is normalized in the same way as the scatter index.

To date only relatively few studies have used load cells to measure canopy drag, hence a comparison is made between the drag force measured directly using the current methodology ($F_{d,direct}$) and the drag force obtained through an indirect measuring method commonly used in previous studies [$F_{d,momentum}$, from Equation (6)]. The indirect estimate ($F_{d,momentum}$) for the emergent cases (E05 and E10, see **Table 1**) shows the same trend ($R^2 = 0.99$) as the drag force directly measured with the load cell ($F_{d,direct}$, see **Figure 4**). Although measured drag forces with magnitudes above 0.01 N are very similar for both methods (up to 8% difference), for drag forces <0.01 N the discrepancy between both methods increases (with an average 22% difference). For these low flow cases the percentage uncertainty associated with the measured water level gradient increases (with the water level dropping only ∼3 mm over the length of the canopy) leading to larger errors. Given

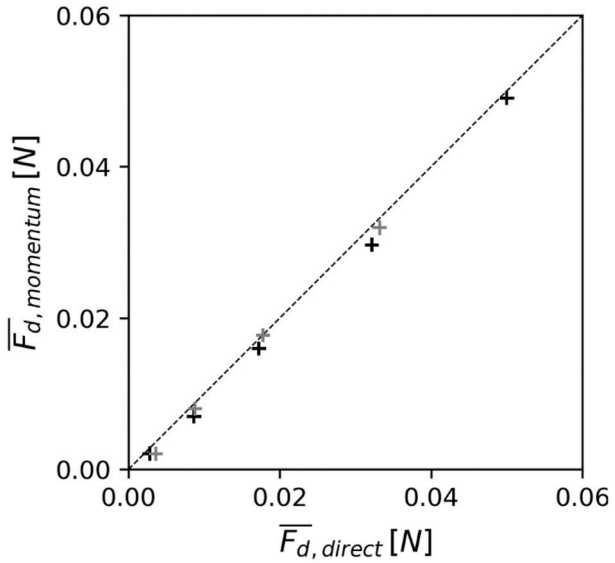

FIGURE 4 | The strong agreement in estimated drag forces on an individual element in an emergent canopy using two methods: (i) measured directly using the force sensor ($F_{d,direct}$) and (ii) derived indirectly from the water surface gradient ($F_{d,momentum}$). Marker color indicates canopy density (black: λ_p = 0.05; gray: λ_p = 0.10). The size of the markers indicates the associated measurement uncertainty. The dashed line represents the line of perfect agreement.

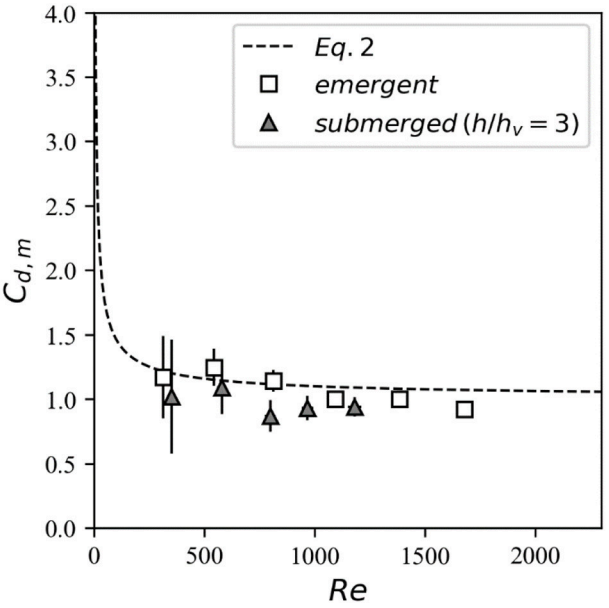

FIGURE 5 | Drag coefficients derived from the velocity and drag force measurements for the isolated cylinder cases.

the high instrument linearity, the force sensor is able to provide more accurate measurements for these cases and is therefore preferred.

RESULTS AND DISCUSSION

Measurement of Drag Coefficients

Isolated Cylinder

Although the focus in this study is on assessing canopy drag, a limited number of experiments were conducted with isolated emergent (**Table 1**) and submerged (**Table 2**) cylinders. The isolated cylinder drag coefficients were then compared to theory (Equation 2) to gain confidence in the experimental methodology (particularly the drag force data obtained from the load cell). For the emergent case, there is excellent agreement between the directly-measured drag on an isolated cylinder and Equation (2) (**Figure 5**, squares). For the submerged case (with same height as the submerged canopy), the value of C_d derived from the measured drag force and measured in-canopy velocity (averaged over the cylinder height) is consistent with isolated cylinder theory (**Figure 5**, triangles). In other words, despite the single vertical cylinder occupying a fraction of the water column in a boundary layer flow, its forces can be predicted by Equation (2) originally developed for a cylinder in a uniform cross-flow.

Emergent Canopies

As discussed in the Introduction, for emergent canopies, both the bulk velocity and pore velocity are often used as the reference velocity in Equation (3) to relate a given flow condition to the canopy drag force through a drag coefficient (i.e., $C_{d,b}$ and $C_{d,p}$, respectively). Here, when using both the bulk velocity (U_b^{em}) and pore velocity (U_p^{em}) are used as the drag reference velocity, there are large discrepancies with values for isolated cylinders (Equation 2), similar to results reported in other studies (e.g., Liu and Zeng, 2017). For the highest density canopies (λ_p =0.1), there is an exponential decrease in the drag coefficient with Reynolds number using both the bulk velocity U_b^{em} (**Figure 6A**, squares) and pore velocity U_p^{em} (**Figure 6B**). For the 5% density emergent canopies, the drag coefficient shows a slight decrease with *Re* using both reference velocities. When considering both U_b^{em} and U_p^{em}, the drag coefficient appears to take an approximately constant value at high *Re* (i.e., *Re* >1,000), consistent with other studies (e.g., Tang et al., 2014). Given that the pore velocity accounts for the volume of water being occupied by the canopy, $C_{d,p}$ is always smaller than $C_{d,b}$, but still deviates substantially from isolated cylinder values. To account for these discrepancies, previous studies have arrived at highly empirical $C_{d,p}$-Re_p relationships that are parameterized as a function of canopy density (Tanino and Nepf, 2008) and (sometimes) stem diameter (Sonnenwald et al., 2018).

The direct experimental measurements support the canopy drag model proposed by Etminan et al. (2017)–when the constricted cross-section velocity (U_c^{em}) is used as the reference velocity, calculated drag coefficients closely match the isolated cylinder values (**Figure 7**, squares). Therefore, while the drag coefficients derived using the bulk and pore velocities exhibit significant scatter (**Figure 6**), the use of U_c^{em} in the drag coefficient ($C_{d,c}$) calculations serves to collapse the data onto the isolated cylinder curve. For the range of Reynolds numbers investigated

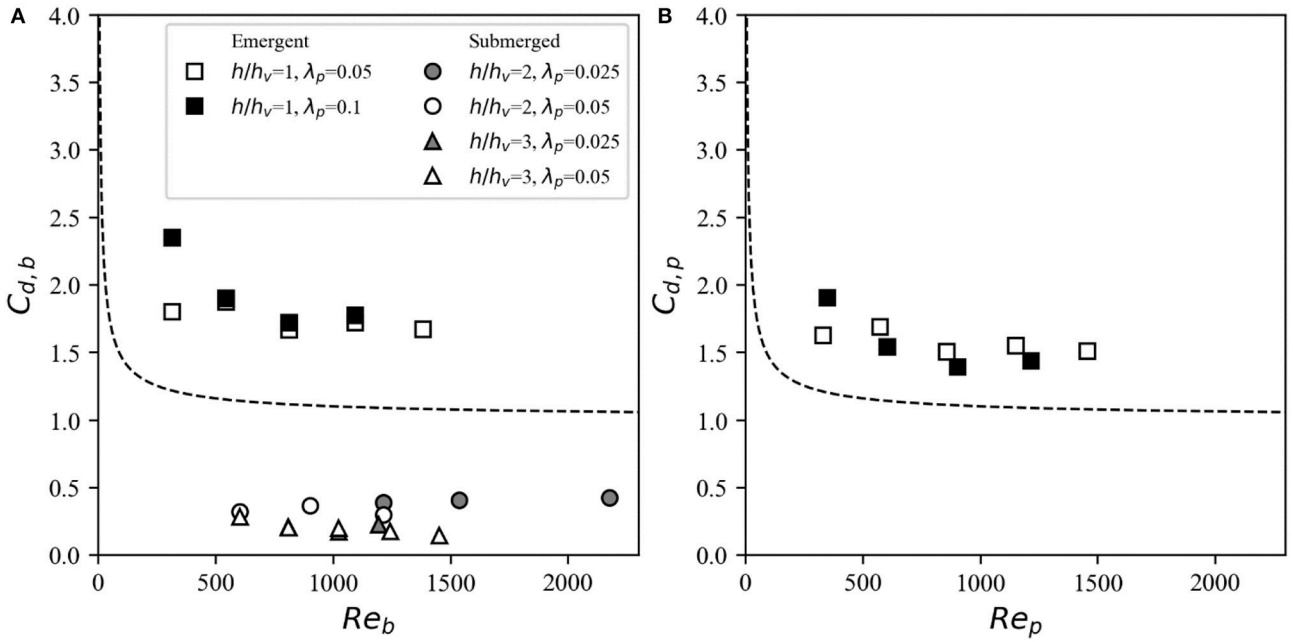

FIGURE 6 | Drag coefficients derived from the drag force measurements using **(A)** the bulk velocities U_b^{em} and U_b^{sub} and **(B)** the pore velocity U_p^{em} as the reference velocity for the emergent (squares) and submerged (circles: $h/h_v = 2$; triangles: $h/h_v = 3$) cases. The marker color represents the canopy density (black: $\lambda_p = 0.1$; white: $\lambda_p = 0.05$; gray: $\lambda_p = 0.025$), with theoretical values for an isolated cylinder (Equation 2) denoted by the dashed line.

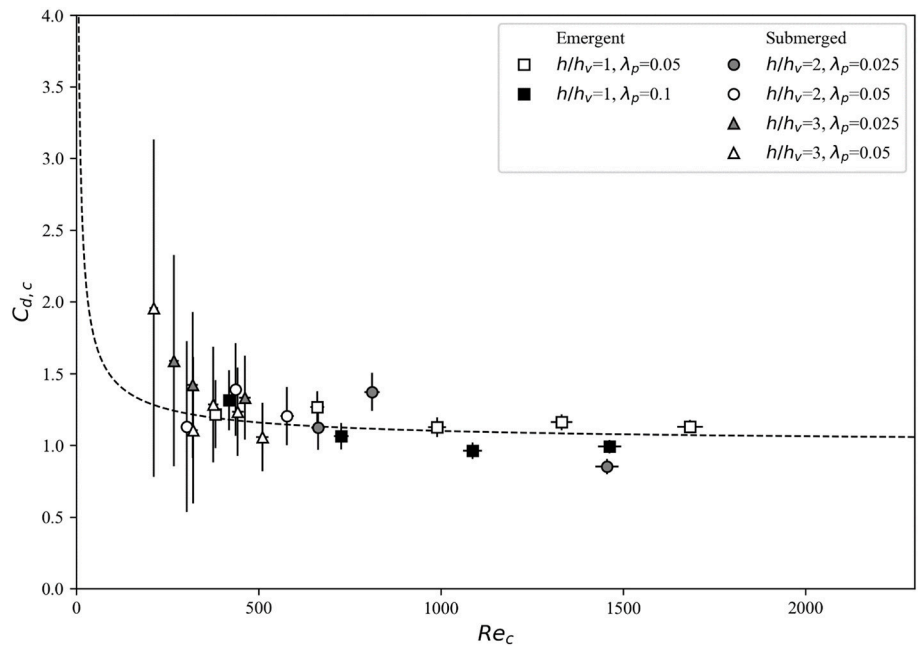

FIGURE 7 | Drag coefficients derived from the drag force measurements for all canopies using the constricted cross-section velocity U_C as the reference velocity for the emergent and submerged cases. Theoretical values for the drag coefficient of an isolated cylinder (Equation 2) are denoted by the dashed line.

(Re_c = 380–1,680), the drag coefficients for the emergent cases show relatively little scatter and approaches a canonical isolated cylinder value of $C_{d,c} \approx 1$.

Submerged Canopies

The velocity exhibits more vertical variation in submerged canopies than in emergent canopies due the drag discontinuity

and resulting shear layer present at the top of the canopy. When using the bulk velocity U_b^{sub} as the reference velocity to derive Re_b and $C_{d,b}$, relatively low drag coefficients (that substantially deviate from the isolated cylinder values) are obtained (**Figure 6A**, circles and triangles). This approach neglects the effect of canopy drag on reducing the in-canopy velocity, which is significant at higher canopy densities. Hence, we use measured U_c^{sub} obtained approximately within the constricted cross-section area and derive the associated drag coefficients. For the submerged canopy cases, the measured values of $C_{d,c}$ (i.e., evaluated using the constricted cross-section velocity U_c^{sub}) generally follows the isolated cylinder theory curve (**Figure 7**). There is more scatter at $Re_c < 500$, which can be attributed to the greater uncertainty associated with measuring flow and forces at such low Reynolds numbers. Therefore, analogous to the emergent canopy observations in **Figure 6**, where C_d evaluated using bulk and pore velocities deviates markedly from isolated cylinder theory, these results indicate that the constricted cross-section velocity U_c^{sub} is the optimal reference velocity for evaluation of drag of a submerged canopy (**Figure 7**).

Canopy Drag Model Assessment

Emergent Canopies

The canopy drag model for emergent canopies, based on Equations (2)–(4) using the computed constricted cross-section velocity U_c^{em} (see section Canopy Drag Model), was used to predict the drag force on a single canopy element in all experimental cases (**Table 1**). These predictions were then compared to the time-averaged drag force measured by the force sensor (**Figure 8**, squares). Using only the bulk flow velocity, which was derived from the known flow rate, and canopy geometry as model input, the canopy drag forces are accurately predicted over the full range of experimental cases. The results provide direct experimental validation of the finding of Etminan et al. (2017) that the constricted cross-section velocity U_c^{em} is the most appropriate reference velocity to parameterize canopy drag.

Submerged Canopies

To assess the ability of the model to predict the drag of submerged canopies, we first compared the predicted in-canopy velocities with the experimental measurements. Specifically, we compared the measured time-averaged constricted cross-section velocity integrated over the canopy height (U_m^{sub}) with predicted U_c^{sub} values, which generally reveals good agreement (**Figure 9**). The model (with above-canopy velocity and canopy geometry as input) is subsequently applied to calculate the drag force for all submerged canopy cases (**Table 2**). Canopy friction coefficient values were derived for each case through Reynolds stress profiles (Equation 10), resulting in a range of C_f values between 0.01 and 0.04. However, due to the experimental setup in this study, that used a downward facing ADV, the velocity measurement was limited to measuring only ∼6 cm below the water surface. The above-canopy velocity is therefore likely underestimated, particularly in the $h/h_v = 2$ cases, and actual C_f values are expected to be lower. Due to this uncertainty, here we opt to use a conventional value of 0.01 for all experimental cases (see section Canopy Drag Model). Compared to emergent canopies, there is greater scatter in the relationship between measured and predicted forces (particularly at low *Re*), but overall there is still relatively good agreement (**Figure 8**). Given the complexity

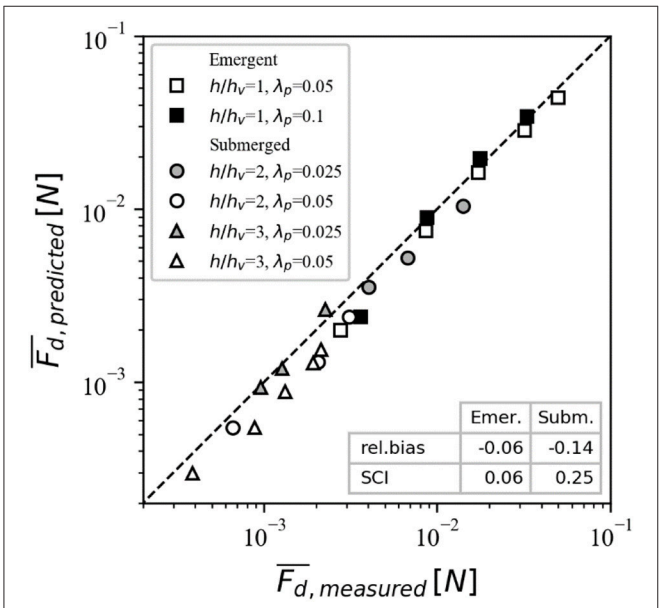

FIGURE 8 | The strong agreement between predicted and measured drag forces, including the line of perfect agreement (dashed). The predictive model skill is described by the relative bias and scatter index (bottom right corner).

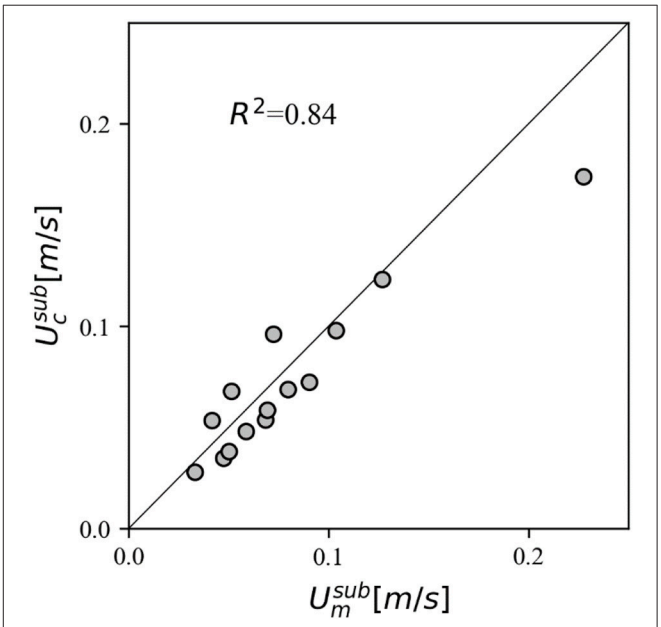

FIGURE 9 | Comparison between the measured depth-averaged in-canopy flow velocity (U_m^{sub}) and the estimated in-canopy constricted cross-section velocity (U_c^{sub}) in submerged canopies.

involved with submerged canopies (including the uncertainty involved with measurements under low *Re*), and the range in submergence ratio and density investigated, the model error averages about 11% ($SCI = 0.114$), and suggests that the whole model outlined in **Figure 2** can serve as a useful tool to obtain robust estimates of canopy drag forces.

Model Application to Other Submerged Canopy Data Sets

To date, the canopy drag model has been validated for *emergent* canopies (Etminan et al., 2017) (albeit using only numerical simulations); here we have provided direct experimental validation for both *emergent* and *submerged* canopies for the first time. Nevertheless, the experiments only covered a relatively small range of possible canopy geometry and flow conditions. To further assess the validity of the model across a large range of flow conditions and canopy properties (e.g., density, submergence ratio, flexibility), the model was tested against a large number of existing datasets. Experiments were limited to those with submerged canopies in which the energy slope was reported.

Rigid Vegetation

For rigid vegetation, experiments that employed either staggered (as in the present study), linear or random arrangements were selected here (**Table 3**). Although on the individual canopy element scale, the velocity distribution may vary significantly among these arrangements, we hypothesize that the model can still be used to estimate bulk canopy drag. Indeed, the

TABLE 3 | Overview of experimental studies on drag in submerged rigid canopies from which data was obtained.

References	d_v (mm)	h_v (cm)	h/h_v	λ_p (%)	Stem Type	Canopy Setup	Runs	U_b^{sub} (cm/s)	Re_b
Dunn et al., 1996	6.4	11.8	1.4–3.3	0.14–1.23	cyl.	Stag.	12	30–85	1890–5420
Stone, 1997; Stone and Shen, 2002	3.2–12.7	12.4	1.2–2.5	0.55–6.10	cyl.	Stag.	128	3–63	126–5400
Cheng, 2011	3.2–8.3	10	1.3–2	0.43–11.9	cyl.	Stag.	23	8–34	540–2,130
Shimizu et al., 1991	1–1.5	4.1–4.6	1.1–2.6	0.44–0.79	cyl.	Lin.	28	6–33	65–500
Poggi et al., 2004	4	12	5	0.08–1.35	cyl.	Lin.	5	~30	~1,200
Nezu and Sanjou, 2008	8	5	1.25–4	0.39–1.54	strips	Lin.	9	10–12	800–960
Murphy et al., 2007	6	7–14	1.3–4.3	1.18–3.77	cyl.	Rand.	24	1.5–18	90–1,060
This study	6.4	9	2–3	2.5–10	cyl.	Stag.	23	9–34	310–2,180
Overall	1–12.7	4.1–14	1.1–5	0.08–11.9			252	1.5–85	65–5,420

All experiments either used staggered (stag.), linear (lin.) or random (rand.) canopy setups.

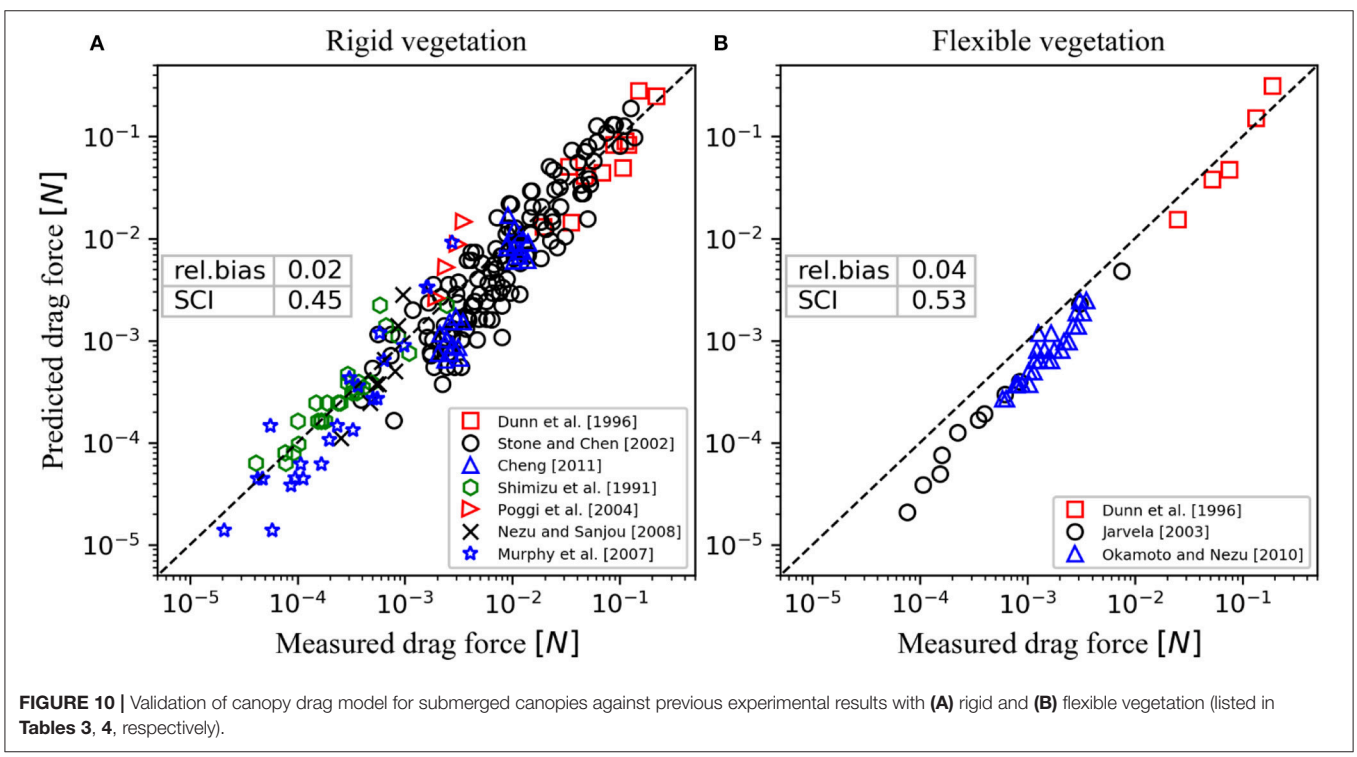

FIGURE 10 | Validation of canopy drag model for submerged canopies against previous experimental results with **(A)** rigid and **(B)** flexible vegetation (listed in **Tables 3**, **4**, respectively).

TABLE 4 | Overview of experimental studies on drag in submerged flexible canopies from which data was obtained.

References	d_v (mm)	h_v (cm)	h_{vd} (cm)	h/h_{vd}	λ_p (%)	Stem Type	Canopy Setup	Runs	U_b^{sub} (cm/s)	Re_b
Dunn et al., 1996	6.4	17	9.7–16	1.7–2.4	0.1–1.2	cyl.	stag.	6	30–85	1,950–5,430
Järvelä, 2003	2.8–3	28–30	16–29.5	1.4–3.3	0.4–7.4	real	stag.	12	7–33	200–990
Okamoto and Nezu, 2010	8	5–10.5	3–9.6	3–5.3	4.78	strip	lin.	28	10–35	800–2,800
Overall	2.8–8	5–30	3–29.5	1.4–5.3	0.1–7.4			46	7–85	200–5,430

work of Etminan et al. (2017) suggested that in the case of randomly-distributed canopy elements, the constricted cross-section velocity can still be considered as the velocity scale governing canopy drag, indicating that the model can be applied here without modification. Hence, using provided values of flow rate and canopy properties, the bulk drag was computed and compared with the measured drag (**Figure 10A**). Using a constant C_f value of 0.01 (as before), the model shows a similar trend as the measurements ($R^2 = 0.74$) with reasonably low bias and scatter (rel. bias = 0.02, $SCI = 0.45$). It should be emphasized that the main uncertainty is likely to be attributed to the schematization of relatively complex three-dimensional canopy hydrodynamics into a relatively simple (two-layer) model.

Flexible Elements

Although most studies so far have represented vegetation canopies using rigid elements, aquatic vegetation in natural systems is often flexible (e.g., seagrasses, kelp), adapting its shape and thereby frontal area in response to the flow. Hence, there is now increased experimentation with flexible mimics in hydraulic experiments (e.g., Abdolahpour et al., 2017). The canopy drag model presented in this study does not explicitly account for flexibility, but it is hypothesized that it could still be used as a tool provided the deflected vegetation height (i.e., the height of the vegetation under stationary flow condition) rather than the actual length of the element is used. Hence, data was obtained from three studies that investigated drag in submerged flexible canopies and reported the deflected canopy height (**Table 4**). From these studies, both Dunn et al. (1996) and Järvelä (2003) observed swaying motions of their flexible plants/(cylindrical) elements, resulting in a time-varying deflected canopy height. Okamoto and Nezu (2010) reported both swaying and the more organized monami-type motions (Ackerman and Okubo, 1993) in their experiments. Here, we use the time-averaged deflected canopy height as input for the model. Furthermore, for the experiments by Okamoto and Nezu (2010) we use the width of the flexible strip as a proxy for d_v given that it is equivalent to the frontal area.

For the flexible canopies, the model is able to predict the bulk drag relatively well (**Figure 10B**, $R^2 = 0.69$, rel. bias = 0.04, $SCI = 0.53$). This is surprising to some extent, as the complexity associated with flexible elements is only accounted for to some extent by the (deflected) plant height. Both the measurements by Järvelä (2003) and Okamoto and Nezu (2010) are consistently underpredicted, which may be related to the plant geometries that involved flat strips and real plants, respectively. Dunn et al. (1996), on the other hand, used flexible cylinders in their experiments which provide more similarity with rigid cylinders, and may therefore better be represented by model.

Overall, with limited information (above-canopy velocity derived from flow rate, canopy properties) the relatively simple canopy drag model is able to provide reasonably accurate estimates of the bulk canopy drag for both rigid and flexible vegetation canopies. Given the fact that the model performs well over such a broad range of hydrodynamic conditions ($U_b = 1.5$–85 cm/s, $Re = 65$–5,430) and canopies ($h/h_v = 1.1$–5, $\lambda_p = 0.08$–11.9%, both rigid and flexible vegetation), and is based on theory rather than empirical relations, it is thus expected the model can robustly predict hydraulic resistance of aquatic canopies, including in field setting with natural vegetation (e.g., where stem diameters are often of order 0.1–1 cm and current velocities of order 0.05–0.5 m/s, which translates to Re ranging between 50 and 5,000).

SUMMARY AND CONCLUSIONS

In this study we present new direct experimental measurements of canopy drag forces using emergent and submerged canopies with a broad range of flow conditions and canopy properties (i.e., density and submergence ratio). Drag coefficients were derived using direct measurements of the drag force on a dowel within the canopy. We found that if the constricted cross-section velocity is used as the reference velocity, the drag coefficient of both emergent and submerged canopies is equal to that of an isolated cylinder. Comparison between canopy drag model predictions and current and existing experimental data shows that the model is able to robustly and accurately predict canopy drag across the field range of flow conditions and canopy characteristics, including flexible canopies. The model can thus be used to predict drag forces in emergent and submerged canopies and is considered a simple and practical tool for estimating the hydraulic resistance of aquatic canopies.

DATA AVAILABILITY STATEMENT

The datasets analyzed for this study can be obtained by sending a written request to the corresponding author at arnold.vanrooijen@research.uwa.edu.au.

AUTHOR CONTRIBUTIONS

AvR designed the experiments, acquired the data, performed the data analysis, and wrote the manuscript. RL and MG provided support in the experimental design, data interpretation and the development of the manuscript. MC-F and LT provided support in data acquisition during the experiments. All authors revised the draft manuscript and approved the final version for submission.

FUNDING

This work was supported by an Australian Research Discovery Project Grant (DP170100802) to RL and MG.

ACKNOWLEDGMENTS

This research was undertaken by AvR as part of a Ph.D. at The University of Western Australia who was funded by a University Postgraduate Award for International Students (UPAIS) and an Australian Government Research Training Program (RTP) Scholarship. LT was supported by the China Scholarship Council (grant number: 201706320274). The authors would like to thank Mr. Carlin Bowyer, Ms. Dianne King, and Mr. Brad Rose for assistance in the lab, Dr. Guido Wager for providing support with the force sensor, Dr. Vahid Etminan for valuable discussions, and the reviewers for their constructive feedback that helped to improve the manuscript.

REFERENCES

Abdolahpour, M., Hambleton, M., and Ghisalberti, M. (2017). The wave-driven current in coastal canopies. *J. Geophys. Res. Oceans* 122, 3660–3674. doi: 10.1002/2016JC012446

Ackerman, J. D. (1995). Convergence of filiform pollen morphologies in seagrasses: functional mechanisms. *Evol. Ecol.* 9, 139–153.

Ackerman, J. D., and Okubo, A. (1993). Reduced mixing in a marine macrophyte canopy. *Funct. Ecol.* 7, 305–309. doi: 10.2307/2390209

Balke, T., Bouma, T. J., Herman, P. M. J., Horstman, E. M., Sudtongkong, C., and Webb, E. L. (2013). Cross-shore gradients of physical disturbance in mangroves: implications for seedling establishment. *Biogeosciences* 10, 5411–5419. doi: 10.5194/bg-10-5411-2013

Cheng, N. S. (2011). Representative roughness height of submerged vegetation. *Water Resour. Res.* 47, 1–8. doi: 10.1029/2011WR010590

Cornelisen, C. D., and Thomas, F. I. (2002). Ammonium uptake by seagrass epiphytes: isolation of the effects of water velocity using an isotope label. *Limnol. Oceanogr.* 47, 1223–1229. doi: 10.4319/lo.2002.47.4.1223

Duarte, C. M. (2002). The future of seagrass meadows. *Environ. Conserv.* 29, 192–206. doi: 10.1017/S0376892902000127

Dunn, C., Lopez, F., and Garcia, M. H. (1996). *Mean Flow and Turbulence in a Laboratory Channel with Simulated Vegetation.* Technical report, Hydraulic Engineering Series No. 51, University of Illinois.

Edmaier, K., Burlando, P., and Perona, P. (2011). Mechanisms of vegetation uprooting by flow in alluvial non-cohesive sediment. *Hydrol. Earth Syst. Sci.* 15, 1615–1627. doi: 10.5194/hess-15-1615-2011

Etminan, V., Lowe, R. J., and Ghisalberti, M. (2017). A new model for predicting the drag exerted by vegetation canopies. *Water Resour. Res.* 53, 3179–3196. doi: 10.1002/2016WR020090

Fonseca, M. S., and Cahalan, J. A. (1992). A preliminary evaluation of wave attenuation by four species of seagrass. *Estuar. Coast. Shelf Sci.* 35, 565–576.

Ghisalberti, M. (2009). Obstructed shear flows: similarities across systems and scales. *J. Fluid Mech.* 641, 51–61. doi: 10.1017/S0022112009992175

Harman, I. N., and Finnigan, J. J. (2007). A simple unified theory for flow in the canopy and roughness sublayer. *Boundary-Layer Meteorol.* 123, 339–363. doi: 10.1007/s10546-006-9145-6

Hendriks, I. E., Bouma, T. J., Morris, E. P., and Duarte, C. M. (2010). Effects of seagrasses and algae of the Caulerpa family on hydrodynamics and particle-trapping rates. *Mar. Biol.* 157, 473–481. doi: 10.1007/s00227-009-1333-8

Hendriks, I. E., Sintes, T., Bouma, T. J., and Duarte, C. M. (2008). Experimental assessment and modeling evaluation of the effects of the seagrass *Posidonia oceanica* on flow and particle trapping. *Mar. Ecol. Prog. Ser.* 356, 163–173. doi: 10.3354/meps07316

James, W. F., Barko, J. W., and Butler, M. G. (2004). Shear stress and sediment resuspension in relation to submersed macrophyte biomass. *Hydrobiologia* 515, 181–191. doi: 10.1023/B:HYDR.0000027329.67391.c6

Järvelä, J. (2003). "Influence of vegetation on flow structure in floodplains and wetlands," in *Proceedings of the 3rd Symposium on River, Coastal and Estuarine Morphodynamics (RCEM).* (Madrid), 845–856.

Kenyon, R. A., Haywood, M. D. E., Heales, D. S., Loneragan, N. R., Pendrey, R. C., and Vance, D. J. (1999). Abundance of fish and crustacean postlarvae on portable artificial seagrass units: daily sampling provides quantitative estimates of the settlement of new recruits. *J. Exp. Mar. Biol. Ecol.* 232, 197–216.

Koch, E. W., Ackerman, J. D., Verduin, J., and van Keulen, M. (2007). "Fluid dynamics in seagrass ecology—from molecules to ecosystems," in *Seagrasses: Biology, Ecology and Conservation*, eds A. Larkum, R. Orth, and C. C. Duarte, (Dordrecht: Springer), 193–225. doi: 10.1007/978-1-4020-2983-7_8

Kothyari, U. C., Hayashi, K., and Hashimoto, H. (2009). Drag coefficient of unsubmerged rigid vegetation stems in open channel flows. *J. Hydraulic Res.* 47, 691–699. doi: 10.3826/jhr.2009.3283

Liu, D., Diplas, P., Fairbanks, J. D., and Hodges, C. C. (2008). An experimental study of flow through rigid vegetation. *J. Geophys. Res. Earth Surf.* 113, 1–16. doi: 10.1029/2008JF001042

Liu, X., and Zeng, Y. (2017). Drag coefficient for rigid vegetation in subcritical open-channel flow. *Environ. Fluid Mech.* 17, 1035–1050. doi: 10.1007/s10652-017-9534-z

López, F., and García, M. H. (2001). Mean flow and turbulence structure of open-channel flow through non-emergent vegetation. *J. Hydraulic Eng.* 127, 392–402. doi: 10.1061/(ASCE)0733-9429(2001)127:5(392)

Lowe, R. J., Koseff, J. R., and Monismith, S. G. (2005). Oscillatory flow through submerged canopies: 1. Velocity structure. *J. Geophys. Res.* 110, 1–17. doi: 10.1029/2004JC002788

Lowe, R. J., Shavit, U., Falter, J. L., Koseff, J. R., and Monismith, S. G. (2008). Modeling flow in coral communities with and without waves: a synthesis of porous media and canopy flow approaches. *Limnol. Oceanogr.* 53, 2668–2680. doi: 10.4319/lo.2008.53.6.2668

Luhar, M., Coutu, S., Infantes, E., Fox, S., and Nepf, H. (2010). Wave-induced velocities inside a model seagrass bed. *J. Geophys. Res. Oceans* 115, 1–15. doi: 10.1029/2010JC006345

Moltchanov, S., Bohbot-Raviv, Y., and Shavit, U. (2011). Dispersive stresses at the canopy upstream edge. *Boundary-layer Meteorol.* 139, 333–351. doi: 10.1007/s10546-010-9582-0

Morris, E. P., Peralta, G., Brun, F. G., Van Duren, L., Bouma, T. J., and Perez-Llorens, J. L. (2008). Interaction between hydrodynamics and seagrass canopy structure: spatially explicit effects on ammonium uptake rates. *Limnol. Oceanogr.* 53, 1531–1539. doi: 10.4319/lo.2008.53.4.1531

Murphy, E., Ghisalberti, M., and Nepf, H. (2007). Model and laboratory study of dispersion in flows with submerged vegetation. *Water Resour. Res.* 43, 1–12. doi: 10.1029/2006WR005229

Nepf, H. M. (1999). Drag, turbulence, and diffusion in flow through emergent vegetation. *Water Resour. Res.* 35, 479–489. doi: 10.1029/1998WR900069

Nepf, H. M. (2012). Hydrodynamics of vegetated channels. *J. Hydraulic Res.* 50, 262–279. doi: 10.1080/00221686.2012.696559

Nepf, H. M., and Vivoni, E. R. (2000). Flow structure in depth-limited, vegetated flow. *J. Geophys. Res.* 105, 28547–28557. doi: 10.1029/2000JC900145

Nezu, I., and Sanjou, M. (2008). Turburence structure and coherent motion in vegetated canopy open-channel flows. *J. Hydro-Environ. Res.* 2, 62–90. doi: 10.1016/j.jher.2008.05.003

Okamoto, T. A., and Nezu, I. (2010). "Flow resistance law in open-channel flows with rigid and flexible vegetation," in *River flow, Proceedings of the International Conference on Fluvial Hydraulics* (Braunschweig), 261–268.

Poggi, D., Porporato, A., Ridolfi, L., Albertson, J. D., and Katul, G. G. (2004). The effect of vegetation density on canopy sub-layer turbulence. *Bound. Layer Meteorol.* 111, 565–587. doi: 10.1023/B:BOUN.0000016576.05621.73

Schoneboom, T., Aberle, J., and Dittrich, A. (2010). "Hydraulic resistance of vegetated flows: contribution of bed shear stress and vegetative drag to total hydraulic resistance," in *River flow, Proceedings of the International Conference on Fluvial Hydraulics* (Braunschweig), 269–276.

Shimizu, Y., Tsujimoto, T., Nakagawa, H., and Kitamura, T. (1991). Experimental study on flow over rigid vegetation simulated by cylinders with equi-spacing. *Doboku Gakkai Ronbunshu* 1991, 31–40. doi: 10.2208/jscej.1991.438_31

Sonnenwald, F., Stovin, V., and Guymer, I. (2018). Estimating drag coefficient for arrays of rigid cylinders representing emergent vegetation. *J. Hydraulic Res.* 1–7. doi: 10.1080/00221686.2018.1494050

Stone, B. M. (1997). *Hydraulics of Flow in Vegetated Channels*. MS thesis, Clarkson University, Potsdam, NY.

Stone, B. M., and Shen, H. T. (2002). Hydraulic resistance of flow in channels with cylindrical roughness. *J. Hydraulic Eng.* 128, 500–506. doi: 10.1061/(ASCE)0733-9429(2002)128:5(500)

Tang, H., Tian, Z., Yan, J., and Yuan, S. (2014). Determining drag coefficients and their application in modelling of turbulent flow with submerged vegetation. *Adv. Water Resour.* 69, 134–145. doi: 10.1016/j.advwatres.2014.04.006

Tanino, Y., and Nepf, H. M. (2008). Laboratory investigation of mean drag in a random array of rigid, emergent cylinders. *J. Hydraulic Eng.* 134, 34–41. doi: 10.1061/(ASCE)0733-9429(2008)134:1(34)

Taylor, J. (1997). *Error Analysis: The Study of Uncertainties in Physical Measurements*, *2nd Edn.* Sausalito, CA: University Science Books.

Vargas-Luna, A., Crosato, A., Calvani, G., and Uijttewaal, W. S. (2016). Representing plants as rigid cylinders in experiments and models. *Adv. Water Resour.* 93, 205–222. doi: 10.1016/j.advwatres.2015.10.004

Wang, H., Tang, H., Yuan, S., Lv, S., and Zhao, X. (2014). An experimental study of the incipient bed shear stress partition in mobile bed channels filled with emergent rigid vegetation. *Sci. China Technol. Sci.* 57, 1165–1174. doi: 10.1007/s11431-014-5549-6

Weitzman, J. S., Zeller, R. B., Thomas, F. I., and Koseff, J. R. (2015). The attenuation of current-and wave-driven flow within submerged multispecific vegetative canopies. *Limnol. Oceanogr.* 60, 1855–1874. doi: 10.1002/lno.10121

White, F. M. (1991). *Viscous Fluid Flow, 2nd Edn*. New York, NY: MacGraw-Hill Inc.

Widdows, J., Pope, N. D., Brinsley, M. D., Asmus, H., and Asmus, R. M. (2008). Effects of seagrass beds (*Zostera noltii* and *Z. marina*) on near-bed hydrodynamics and sediment resuspension. *Mar. Ecol. Prog. Ser.* 358, 125–136. doi: 10.3354/meps07338

Wu, F. C., Shen, H. W., and Chou, Y. J. (1999). Variation of roughness coefficients for unsubmerged and submerged vegetation. *J. Hydraulic Eng.* 125, 934–942. doi: 10.1061/(ASCE)0733-9429(1999)125:9(934)

Zavistoski, R. A. (1994). *Hydrodynamic Effects of Surface Piercing Plants*. MSc Thesis, Massachusetts Institute of Technology.

Conflict of Interest Statement: The authors declare that the research was conducted in the absence of any commercial or financial relationships that could be construed as a potential conflict of interest.

NOTATION

C_d = drag coefficient for an isolated cylinder
$C_{d,c}$ = canopy drag coefficient based on constricted cross-section velocity
$C_{d,b}$ = canopy drag coefficient based on bulk velocity
$C_{d,m}$ = canopy drag coefficient based on measured velocity
$C_{d,p}$ = canopy drag coefficient based on pore velocity
C_f = canopy friction coefficient
d_c = cylinder diameter
d_v = plant / canopy element diameter
f_d = drag force per unit length of a cylinder
F_d = plant / canopy element total drag force
g = gravitational acceleration
h = water depth
h_v = plant / canopy height
h_{vd} = deflected plant / canopy height
L_v = canopy length
L_d = canopy drag length scale
L_s = canopy shear length scale
N_v = number of plants / canopy elements per unit bed area
Q = flow rate / discharge
Re = Reynolds number for an isolated cylinder
Re_c = Reynolds number (canopy) based on constricted cross-section velocity
Re_b = Reynolds number (canopy) based on bulk velocity
Re_m = Reynolds number (canopy) based on measured velocity
Re_p = Reynolds number (canopy) based on pore velocity
$S_{v,l}$ = lateral distance between two canopy elements at the same streamwise (x) location
$S_{v,s}$ = streamwise distance between two canopy element rows
u' = turbulent velocity fluctuation in x direction
u_*= friction velocity based on canopy shear stress
U_∞ = free stream flow velocity
U_b^{em}, U_b^{sub}= bulk velocity for emergent or submerged canopy resp.
U_c^{em}, U_c^{sub}= constricted cross-section velocity for emergent or submerged canopy resp.
U_m^{em}, U_m^{sub}= measured depth-averaged velocity for emergent or submerged canopy resp.
U_p^{em}, U_p^{sub}= pore velocity for emergent or submerged canopy resp.
U_{ref} = reference velocity
w' = turbulent velocity fluctuation in z direction
W = channel width
x = streamwise direction
x_0 = canopy flow adjustment length
z = vertical elevation measured from bottom
β = ratio between lateral and streamwise canopy spacing ($S_{v,l}/S_{v,s}$)
η = water surface elevation
λ_f = canopy (frontal) density / element frontal area per unit bed area
λ_p= canopy (plan) density / element plan area per unit bed area
ρ = water density
ν = kinematic viscosity

frontiers in Marine Science

ORIGINAL RESEARCH
published: 08 February 2019
doi: 10.3389/fmars.2019.00008

Canopy-Mediated Hydrodynamics Contributes to Greater Allelic Richness in Seeds Produced Higher in Meadows of the Coastal Eelgrass *Zostera marina*

Elizabeth Follett[1]*, *Cynthia G. Hays*[2] *and Heidi Nepf*[1]

[1] Department of Civil and Environmental Engineering, Massachusetts Institute of Technology, Cambridge, MA, United States, [2] Department of Biology, Keene State College, Keene, NH, United States

OPEN ACCESS

Edited by:
Matthew Philip Adams, The University of Queensland, Australia

Reviewed by:
Maike Paul, Technische Universitat Braunschweig, Germany
Maryam Abdolahpour, University of Western Australia, Australia

***Correspondence:**
Elizabeth Follett
emf@alum.mit.edu

Specialty section:
This article was submitted to Marine Ecosystem Ecology, a section of the journal Frontiers in Marine Science

Received: *31 August 2018*
Accepted: *11 January 2019*
Published: *08 February 2019*

Citation:
Follett E, Hays CG and Nepf H (2019) Canopy-Mediated Hydrodynamics Contributes to Greater Allelic Richness in Seeds Produced Higher in Meadows of the Coastal Eelgrass Zostera marina. Front. Mar. Sci. 6:8. doi: 10.3389/fmars.2019.00008

Seagrass meadows, which mediate ocean acidity and turbidity, sequester carbon, and increase biodiversity by providing shelter for larvae and small fish, are among the fastest disappearing ecosystems worldwide. Seagrasses are ecosystem engineers, creating distinct regions of enhanced and diminished flow and turbulent mixing, dependent upon canopy physical parameters, such as canopy density and blade morphology, which in turn impact the transport of pollen, sediment, and nutrients. The health and resilience of seagrass meadows increase with intraspecies genetic diversity, which depends on successful sexual reproduction and the transport of pollen particles between reproductive shoots, which in turn depends on the hydrodynamic conditions created by the meadow. This paper explored the transport of pollen grains in seagrass meadows using a random walk model. The model was parameterized with profiles of mean velocity and eddy diffusivity derived as functions of shoot density, canopy height, canopy shear velocity, canopy drag coefficient, and blade width, and validated with experimental measurements of a tracer plume evolving in a submerged model canopy. Model results showed that release at the top of the canopy led to significantly greater dispersal than release within the canopy, which was consistent with observed patterns of genetic diversity in *Zostera marina* seeds collected from coastal Massachusetts meadows. Specifically, seeds produced from upper inflorescences had greater allelic richness than seeds from lower inflorescences on the same reproductive shoot, and were the product of a greater number of fathers, reflecting the greater in-canopy pollen movement farther from the bed. Pollen grains modeled with a realistic elongated shape experienced significantly higher rates of capture by the canopy relative to spherical grains of the same volume. The effect of submergence depth (the ratio of water depth to canopy height) on pollen dispersal depended on the nature of the surface boundary: when

pollen reflected off the water surface, the mean travel distance before pollen capture decreased with decreasing submergence depth. In contrast, when pollen accumulated at the water surface, surface transport increased pollen dispersal distances, especially at low submergence depths.

Keywords: seagrass, genetic diversity, pollen, particle transport, allelic richness

1. INTRODUCTION

Seagrasses are a foundation species in nearshore coastal ecosystems, forming highly productive meadows that provide structured habitat for many fish, invertebrate and bird species (Bruno and Bertness, 2001; Williams and Heck, 2001; Barbier et al., 2011). In addition to ecosystem services related to productivity and biodiversity (Unsworth et al., 2010), dense seagrass meadows also reduce bed shear stress, which increases sediment retention, and in some situations promote carbon sequestration (Duarte et al., 2013). Unfortunately, the area covered by seagrass meadows continues to decline, with an annual decrease of 7% since 1990 (Waycott et al., 2009; van Katwijk et al., 2016). A recent meta-analysis of meadow restoration found that only 37% of restoration efforts were successful, highlighting the importance of supporting existing meadows before collapse occurs (van Katwijk et al., 2016). Seagrasses are rhizomatous; like terrestrial grasses, they reproduce both clonally and sexually (i.e., from seeds). Seagrass pollination typically occurs without the use of an animal vector, with pollen release, transport, and capture all occurring within the water column (Ackerman, 1995; Kendrick et al., 2012). Sexual reproduction is critical for the establishment of new meadows and for genetic diversity, which improves meadow resilience (Hughes and Stachowicz, 2004; Hughes et al., 2008; Kendrick et al., 2012). Genetically diverse, outcrossed seeds are produced by pollen that travels beyond the area dominated by its parent clone and is captured by a mature flower of a separate genetic individual. Pollen that is captured on reproductive structures of its parent plant or vegetative blades may fail to produce viable seeds, while pollen that escapes the canopy and is transported downstream beyond the extent of the canopy will have a lower likelihood of successful pollination. Because hydrodynamic transport is a crucial link in this process, pollination depends on the canopy physical parameters that influence the velocity profile within and above the meadow, such as the canopy frontal area density, canopy height, and submergence depth (the ratio of water depth to canopy height).

The drag produced by seagrass blades attenuates flow within the canopy, creating a zone of low velocity close to the bed, with higher velocity above the canopy (Ackerman and Okubo, 1993; Ghisalberti and Nepf, 2002; Nepf, 2012). The magnitude of near-bed flow reduction depends on the canopy frontal area density (a) and the canopy height (h). Seagrass blades are flexible, and reconfigure (bend) in response to current, with meadow height decreasing with increasing current speed. The mean meadow height can be predicted from meadow morphology and current speed (see Equation 4 in Luhar and Nepf, 2013). When the canopy has sufficient non-dimensional density ($ah > 0.1$, ah = frontal area per bed area), the velocity profile resembles a mixing layer, with a hyperbolic tangent profile present between the vertical positions z_1 and z_2, defined by the canopy density (**Figure 1**, Ghisalberti and Nepf, 2002). In the temperate seagrass *Z. marina*, or eelgrass, the blade density falls within this high-density regime ($ah = 0.1$–3, based on data provided in Dennison and Alberte, 1982; Chandler et al., 1996; Moore, 2004; McKone, 2009; Lacy and Wyllie-Echeverria, 2011; Infantes et al., 2012; Hansen and Reidenbach, 2013; Reidenbach and Thomas, 2018). As the shoot density increases, the vertical extent of the mixing layer region inside the canopy is reduced (increasing z_1, **Figure 1**) and the thickness of the mixing layer ($t_{ml} = z_2 - z_1$) is also reduced. In the upper canopy ($z > z_1$ in **Figure 1**), the turbulence is dominated by canopy-scale vortices, which form in the shear layer at the top of the canopy. The canopy-scale vortices significantly enhance vertical turbulent diffusion in the upper canopy. For dense canopies, the canopy-scale vortices do not penetrate to the bed, and in the lower canopy ($z < z_1$, **Figure 1**) the turbulence is dominated by much smaller blade-generated vortices, which results in a much smaller vertical turbulent diffusion (Luhar et al., 2008; Nepf, 2012).

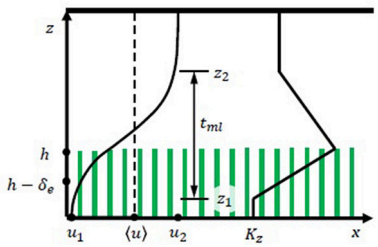

FIGURE 1 | Schematic of time-averaged mixing layer velocity profile $\overline{u}(z)$ within a submerged canopy. The canopy height is h. The time-mean velocity at the bed and far above the canopy are denoted u_1 and u_2, respectively, with $\Delta u = u_2 - u_1$. The mixing layer extends between z_1 and z_2 ($t_{ml} = z_2 - z_1$), with endpoints defined by $(\overline{u_{tml}} - u_1)/\Delta u = 0.01$ and $(u_2 - \overline{u_{tml}})/\Delta u = 0.01$, *with* $\overline{u_{tml}} = (u_1 + u_2)/2$.

Seagrass pollen has a filamentous shape, with *Z. marina* pollen length $L_p = 3$ to 5 mm and diameter $B_p = 7.5e-6$ m (Ackerman, 1997). The filamentous shape enhances the capture efficiency relative to spheroid pollen (de Cock, 1980; Ackerman, 2002). *Z. marina* is monoecious and self-compatible, producing spadices with both male and female flowers that develop acropetally along each reproductive stalk (Ackerman, 2006). Flowering shoots are slightly taller

than vegetative shoots (Ackerman, 2002). Within each spathe, flower development is protogynous, which prevents self-fertilization at the scale of the inflorescence, although geitonogamy may occur across flowering shoots that are part of the same clone (e.g., Reusch, 2001; Rhode and Duffy, 2004). Successful seed production requires pollen movement among spathes and flowering shoots, and the movement of pollen is expected to be highly dependent on the location of release within the canopy, and the canopy- and landscape-scale flow structure (Kendrick et al., 2012; Follett et al., 2016).

In this paper, we numerically simulated the trajectory of individual pollen grains to examine factors that impact pollen transport and capture in a seagrass canopy, focusing on the dominant seagrass species in the northern hemisphere, *Z. marina*, or eelgrass. Previous work has considered the dispersal of floating seagrass seeds and propagules, including rafted seeds of *Z. marina*, which are spread via large-scale coastal currents (Kallstrom et al., 2008; McMahon et al., 2014; Grech et al., 2016). Here we consider transport at the meadow scale, including the vertical turbulent diffusion that carries pollen out of and into a submerged meadow. The simulation was used to explore the impact of submergence depth and pollen release height. The effect of pollen shape was also investigated, building upon previous studies of the role of filiform pollen (Ackerman, 1995, 2000). Finally, the transport trends were related to observed genetic diversity in seeds produced from paired inflorescences located at higher and lower vertical positions on the same *Z. marina* reproductive shoot. Recruitment from seeds is increasingly recognized as important for seagrass population dynamics as well as genetic connectivity (Kendrick et al., 2012); thus a more detailed consideration of the hydrodynamic influences on pollen transport can improve our understanding of the processes underlying successful sexual reproduction in seagrasses, and in doing so enhance future investigations of meadow genetic diversity, clonal structure and demography.

2. METHODS

This study explored the dispersion of negatively buoyant particles (representing pollen) using a random displacement model (RDM) to simulate the trajectory of individual pollen grains. Within the model, the velocity profile $\overline{u}(z)$ and eddy diffusivity profile $K_z(z)$ were predicted from canopy physical properties, including the canopy height, shoot density, blade width, and shear velocity at the top of the canopy, which is equal to the square root of the Reynolds stress at the top of the canopy, $u_* = \sqrt{-\overline{u'w'}_h}$ (Follett et al., 2016). Experimental observations of velocity and turbulent diffusivity in a series of rigid and flexible submerged model canopies (Ghisalberti and Nepf, 2002, 2004, 2005, 2006; Lacy and Wyllie-Echeverria, 2011) were used to validate the modeled profiles of time-mean velocity and eddy diffusivity.

2.1. Vertical Profiles of Velocity and Eddy Diffusivity Used to Parameterize RDM

The model used coordinates (x, y, z) aligned with the current, in the cross-stream direction, and normal to the bed, respectively (**Figure 1**). The velocity vector $\overrightarrow{u} = (u, v, w)$ corresponded to the coordinates (x, y, z), respectively. An overbar denotes a time-average. The model only considered dense canopies ($ah \gtrsim 0.1$), representative of many *Z. marina* meadows (e.g., Dennison and Alberte, 1982; Chandler et al., 1996; Moore, 2004; McKone, 2009; Lacy and Wyllie-Echeverria, 2011; Infantes et al., 2012; Hansen and Reidenbach, 2013; Reidenbach and Thomas, 2018). For a dense canopy, the velocity profile within and above the canopy resembles a mixing layer, with a hyperbolic tangent profile centered slightly above the top of the canopy (Ghisalberti and Nepf, 2002):

$$\overline{u}(z) = 0.5\Delta u \tanh\left(\frac{z-(h+0.5\theta)}{2\theta}\right) + 0.5(u_1+u_2) \quad (1)$$

Here, u_1 and u_2 are the velocities at the limits of the mixing layer, z_1 and z_2, respectively, and $\Delta u = u_2 - u_1$ (**Figure 1**). The momentum thickness of the mixing layer, θ, is related to the physical thickness of the mixing layer $t_{ml} = z_2 - z_1 = 7.1\theta$ (Ghisalberti and Nepf, 2002). As summarized below, the empirical constants included in the mixing-layer profile (Equation 1) were estimated using measurements over nine rigid and six flexible canopies, with different frontal area density and depth-averaged velocity, the details of which are given in Ghisalberti and Nepf (2002, 2004, 2005, 2006). The height of the flexible canopies was defined as the maximum blade height as determined from video footage (Ghisalberti and Nepf, 2006). First, the velocity difference across the mixing layer ($\Delta u = u_2 - u_1$) is correlated with shear velocity at the top of the canopy, u_* Specifically, $\Delta u = \frac{u_*}{0.14}$ for rigid canopies (Ghisalberti and Nepf, 2005), and $\Delta u = \frac{u_*}{0.11}$ for flexible canopies (based on data presented in **Table 1**, Ghisalberti and Nepf, 2006). Second, the lower endpoint of the mixing layer, z_1/h, increases with canopy density, with $\frac{z_1}{h}$ dependent on the canopy drag parameter, $C_D ah$, with C_D the canopy drag coefficient. Specifically, $\frac{z_1}{h} = 0.39 - \frac{0.078}{C_D ah}$ for rigid canopies, and $\frac{z_1}{h} = 0.63 - \frac{0.29}{C_D ah}$ for flexible canopies, based on data presented in **Table 1**, Ghisalberti and Nepf (2006). Third, the extent of the mixing layer region $t_{ml} = \frac{h-z_1}{0.38}$. For submergence depths less than $H/h = 2$, the mixing layer is restricted by the water surface, and the penetration of the mixing layer into the canopy is limited to the distance $H-h$ from the top of the canopy (Nepf and Vivoni, 2000), so that for $H/h \leq 2$, the mixing layer extends from $z_1 = h - (H-h)$ to the water surface ($z_2 = H$). Fourth, the velocity in the lower canopy, u_1, is related to the velocity at the top of the meadow, u_h. Specifically, the ratio $\frac{u_1}{u_h}$ decreases with non-dimensional meadow density, ah. Specifically, $\frac{u_1}{u_h} = 0.38\left(C_D ah\right)^{-0.26}$ for rigid canopies; and $\frac{u_1}{u_h} = 0.21\left(C_D ah\right)^{-0.45}$ for flexible canopies (Ghisalberti and Nepf, 2006). Finally, the velocity difference across the mixing layer (Δu), normalized by the velocity at the top of the canopy u_h, is a function of the frontal area per canopy volume a and the stem diameter d ($\frac{\Delta u}{u_h} = 6.8\left(ad\right)^{0.42}$, Ghisalberti and Nepf, 2004). In order to construct velocity profiles using Equation (1), z_1 was first found using $C_D ah$. Next, u_* or Δu was chosen to define a

TABLE 1 | Equations describing the curves of **(A)** mean longitudinal velocity and **(B)** eddy diffusivity, which require the canopy shear velocity, canopy height, drag coefficient, frontal area, and blade width.

(A) $\bar{u}$ profile:

$\bar{u} = \frac{1}{2}\Delta u \tanh\left(\frac{z-((h+(h-z_1)))/4.73}{((h-z_1))/1.2}\right) + \frac{1}{2}(u_1 + u_2)$

Relations used to construct u profile for rigid canopies:

$\Delta u = \frac{u_*}{0.14}$ $\quad \frac{z_1}{h} = 0.39 - \frac{0.078}{C_D a h}$ $\quad \frac{u_1}{u_h} = 0.38(C_D a h)^{-0.26}$ $\quad \frac{\Delta u}{u_h} = 6.8(aL_v)^{0.42}$

Relations used to construct u profile for flexible canopies:

$\Delta u = \frac{u_*}{0.11}$ $\quad \frac{z_1}{h} = 0.63 - \frac{0.029}{C_D a h}$ $\quad \frac{u_1}{u_h} = 0.21(C_D a h)^{-0.45}$ $\quad \frac{\Delta u}{u_h} = 6.8(aL_v)^{0.42}$

Using these relations, $u = f(u_*,\ h,\ C_D,\ a,\ L_v)$

(B) K_z profile:

$K_z = (0.17 \pm 0.08)\, uL_v$ $\quad z/h < z_1/h$

$K_h = 0.096\Delta u(h - z_1)$ $\quad z/h = 1$

$K_z = 0.039\Delta u(h - z_1)$ $\quad z/h > z_2 h$

Using these relations, $K_z = f(u_*,\ h,\ C_D,\ a,\ L_v)$

(C) canopy parameters:

Study	u_* (cm/s)	Δu (cm/s)	h (m)	C_D	a (m^{-1})	L_v (mm)	H (m)
GN05 A	0.5	3.2	0.139	0.81	2.5	6.4	0.467
GN05 C	0.7	4.9	0.139	0.77	3.4	6.4	0.467
GN05 D	0.5	3.5	0.139	0.85	3.4	6.4	0.467
GN05 E	1.3	9.5	0.139	0.67	4.0	6.4	0.467
GN05 F	0.8	6.0	0.139	0.71	4.0	6.4	0.467
GN05 G	0.5	3.3	0.139	0.82	4.0	6.4	0.467
GN05 H	1.6	11.2	0.139	0.61	8.0	6.4	0.467
GN05 I	1.0	7.4	0.139	0.66	8.0	6.4	0.467
LW11	0.35 – 0.79	3.2–7.2	0.61–0.84	1.95	2.0	10	5

Physical parameters (C) of the canopies considered in this paper (Ghisalberti and Nepf, 2005, Lacy and Wyllie-Echeverria, 2011) are presented.

specific flow condition, and u_h, u_1, and u_2 were found using the fitted relations described above.

The vertical profile of eddy diffusivity is divided into two regions. In the lower canopy ($z < z_1$), the eddy diffusivity scales with the size of the vegetation elements, L_v, which here is the seagrass blade width. For conditions that produce turbulence in the blade wakes ($\frac{u_1 L_v}{\nu} > 100$, with ν the kinematic viscosity of water), the vertical eddy diffusivity is $K_z = (0.17 \pm 0.08)\, uL_v$ (Lightbody and Nepf, 2006). Within the mixing layer ($h \geq z \geq z_1$), canopy-scale vortices elevate K_z. The eddy diffusivity peaks at $z = h$ and scales with the mixing layer thickness, t_{ml}, and velocity difference, Δu ($K_h = 0.032\Delta u t_{ml}$, Ghisalberti and Nepf, 2005). When the submergence depth is low ($H/h \lesssim 5$), the eddy diffusivity has a constant value ($K_z = 0.013\Delta u t_{ml}$) above the mixing layer ($z > z_2$) (Ghisalberti and Nepf, 2005). The eddy diffusivity was assumed to follow a linear function between the regions of constant diffusivity ($z_1 > z > z_2$) and $z = h$. An example of a K_z profile is included in **Figure 1**. Lateral transport was assumed to be dominated by blade-scale turbulence, so that the lateral diffusivity was assumed to be equal to $K_y = (0.17 \pm 0.08)\, uL_v$. For validation of the method, the vertical profiles of velocity and diffusivity predicted from the above relationships across a range of canopy densities are compared to measured velocity and eddy diffusivity from experiments reported in Ghisalberti and Nepf (2005, **Figure 2**). On average, the predicted profiles agreed with the measurements to within 10%.

2.2. Random Displacement Model (RDM) for Particle Transport

Within the random displacement model (RDM), individual particles originated at a specific source height within the meadow ($0 < z < h$) and were tracked until they deposited on the canopy, settled to the bed, or left the model domain. The size of the model domain in the directions ($x, y,\ z$) was ($200h$, $20h$, H). In each time-step (Δt) the position of the particle (x_p, y_p, z_p) advanced longitudinally with the mean velocity $\bar{u}(z)$ and vertically due to both settling (w_s) and turbulent eddy velocity (w'). The equations used to model the particle position were (Wilson and Sawford, 1996):

$$x_{p,i+1} = x_{p,i} + \bar{u}(z_{p,i})\,\Delta t \quad (2)$$

$$y_{p,i+1} = y_{p,i} + R_y\sqrt{2K_y(z_{p,i})\,\Delta t} \quad (3)$$

$$z_{p,i+1} = z_{p,i} + \left(\frac{dK_z(z_{p,i})}{dz} - w_s\right)\Delta t + R_z\sqrt{2K_z(z_{p,i})\,\Delta t} \quad (4)$$

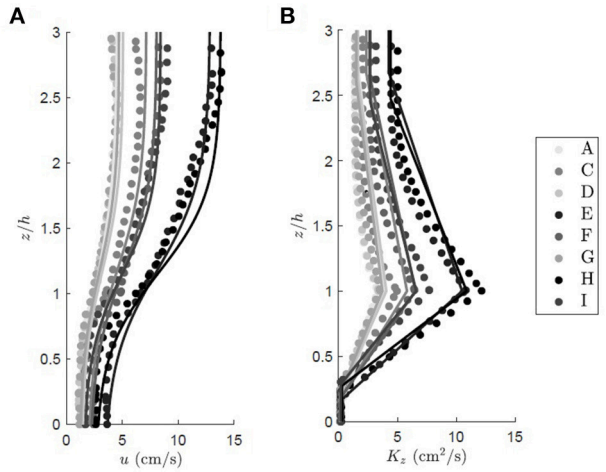

FIGURE 2 | Family of vertical profiles for the **(A)** time mean longitudinal velocity and **(B)** eddy diffusivity over a submerged rigid canopy of increasing shoot density. The circles represent the measured values from Ghisalberti and Nepf (2005), and the predicted profiles are shown with solid lines. The colors denote different experimental case. In alphabetical order of experimental run, $u_* = 0.45, 0.74, 0.53, 1.33, 0.84, 0.50, 1.57, 0.86, 0.55$ cm/s, $C_D = 0.81, 0.77, 0.85, 0.67, 0.71, 0.82, 0.61, 0.66, 0.79$, and $a = 0.025, 0.034, 0.034, 0.040, 0.040, 0.040, 0.080, 0.080, 0.080$ cm^{-1}. For all cases the canopy height was $h = 13.9$ cm and the plant width was $L_V = 0.64$ cm.

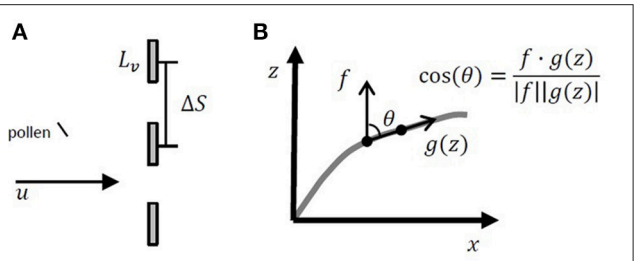

FIGURE 3 | (A) Diagram of pollen grain approaching three blades shown in cross-section. The blade width is L_V and the center-to-center spacing between blades is ΔS. **(B)** Diagram of blade posture and determination of projected area in the x direction. The curved blade posture was broken into a series of linear segments, such that the blade position was converted to a series of vectors. The cosine of the angle between the blade orientation $g(z)$ and the vertical vector f was found by dividing the dot product of f and $g(z)$ by the magnitudes of both vectors.

The last term in (3) and (4) represents transport by turbulent velocity $v' = R_y\sqrt{2K_y}/\sqrt{t}$ and $w' = R_z\sqrt{2K_z}/\sqrt{t}$, respectively, with R_y, R_z random numbers drawn from a normal distribution with mean 0 and standard deviation 1. The vertical transport (Equation 4) also included a drift correction, or pseudo-velocity, associated with the vertical variation in diffusivity (dK_z/dz). The pseudo-velocity term prevented the artificial accumulation of particles in regions of low diffusivity (Durbin, 1983; Wilson and Yee, 2007). The formulations for $\overline{u}(z)$, $K_y(z)$ and $K_z(z)$ were described in the section Vertical Profiles of Velocity and Eddy Diffusivity used to Parameterize RDM. The particle position was saved at every time-step. The constant model time-step, Δt, was constrained so that the vertical particle excursion within each time-step was much smaller than the scale of vertical gradients in the diffusivity and velocity (Israelsson et al., 2006). Within the canopy, both the velocity and diffusivity varied over length scales of approximately $0.1h$. Within each time-step, after a particle was moved, the position was assessed to determine if the particle had settled to the bed ($z_{p,i} = 0$), reached the water surface ($z_{p,i} = H$), traveled beyond the model domain ($x_{p,i} > 200h$, $|y_{p,i}| > 20h$), or deposited to the canopy.

Z. marina pollen contains a sticky coating, increasing adherence to surfaces contacted by the pollen grains (de Cock, 1980). Based on this, the canopy capture model used for this study assumed that all pollen particles contacting vegetation surfaces were captured and ceased further transport. Canopy deposition was described as the probability of capture of one particle in one time-step, found from the probability that the particle was located upstream of the projected area of a blade, multiplied by the capture efficiency, or the fraction of particles removed from the volume of water passing the projected area of the blade (Palmer et al., 2004). The probability that the particle was upstream of the projected area of a blade was equal to the blade width $L_v = 0.0055$ m (McKone, 2009) divided by the average center-to-center spacing between blades (ΔS) (**Figure 3A**). In addition, successful canopy capture required that the particle be located close enough to the blade so that it could impact the blade within one time-step, which was equal to the longitudinal particle excursion in one time-step ($\Delta x_{p,i} = \overline{u}(z_{p,i})\,t$) divided by the average longitudinal spacing between blades (ΔS). The capture efficiency (η) was based on the measured efficiency for particle impaction on rigid cylinders coated with Vaseline (Palmer et al., 2004), assuming that the blade width could be substituted for the cylinder diameter:

$$\eta = 0.224 {Re_c}^{0.718} {R_p}^{2.08} \quad (5)$$

with the collector Reynolds number $Re_c = \frac{\overline{u}L_v}{\nu}$. The particle ratio $R_p = \frac{d_p}{L_v}$ is the ratio of the particle diameter (d_p) to the blade width, so that Equation (5) indicates that the capture efficiency increases with increasing particle diameter. The impact of pollen grain shape was explored by simulating both filamentous and spherical pollen grains with the same settling velocity and volume. The filamentous pollen grains were given the following attributes based on Ackerman (2002): $w_s = 3.5e-6$ m/s, $L_p = 4e-3$ m, $B_p = 7.5e-6$ m. The spherical pollen grains were given the same settling velocity as the filamentous grains and diameter $d_p = 3.5e-5$ m. To adapt Equation (5) for the filamentous pollen, an effective pollen diameter was determined in the following way. The pollen filaments rotate continuously (Ackerman, 1997), with the pollen having equal probability of assuming any rotation angle (γ, ϕ) from the (x, y, z) axes, such that all possible pollen endpoints were evenly distributed over the surface of a sphere. Within each time-step, the effective pollen diameter was assumed to be the projected length of the pollen on the y-axis, so that a pollen grain with its long axis aligned with the y-axis would have an effective diameter equal to L_p and a pollen grain with its long axis aligned with the x-axis would have an effective diameter

equal to the diameter of the pollen, B_p. At each time step, a new particle rotation angle was chosen for each particle from a uniform distribution of all possible pollen positions. Specifically, j and k were chosen from a uniform distribution on (0, 1). Then

$$\gamma = 2\pi j \quad (6)$$

$$\phi = cos^{-1}(2k-1) \quad (7)$$

The effective pollen diameter was equal to the Cartesian transformation of the pollen position from spherical coordinates, $d_p = L_p sin\gamma \sin\phi$ (Edwards and Penney, 2002). Using this model, a pollen grain perpendicular to the y-axis would have diameter 0. In order to accommodate the finite width of real pollen grains, the minimum effective diameter was set equal to B_p.

Multiplying the capture efficiency by the probability that the particle is in the plane of the blade and close enough to contact the blade in one time-step, the probability of particle impaction on a blade surface in one time-step is:

$$dp_x = \eta \frac{L_v}{\Delta S^2} \Delta x_{p,i} = \eta a_x \Delta x_{p,i} \quad (8)$$

with (a_x) the component of the one-sided blade area projected in the x direction. Similarly, the probability of particle impaction on horizontal surfaces is $dp_z = min(0,\ \eta a_z \Delta z_{p,i})$, with the impact of gravitational settling and turbulent transport included in the vertical particle excursion $\Delta z_{p,i}$ (Equation 2). Particle impaction on lateral surfaces was neglected due to the relatively smaller blade thickness (1 mm).

We used equation 4 in Luhar and Nepf (2011) to describe the current-induced changes in seagrass blade position. To find the component of the blade area projected in the x and z directions at each vertical position, the curved blade posture was broken into linear segments, such that the blade surface was converted to a series of vectors (**Figure 3B**). The projected area in the x direction, $P_x(z)$, was found by multiplying the magnitude of the vector segment by the cosine of the angle ($\cos\theta$) between the vertical vector (f) and the blade position ($g(z)$) found by dividing the dot product of f and $g(z)$ by the magnitudes of both vectors ($\cos\theta\,(z) = \frac{f \cdot g(z)}{|f||g(z)|}$, **Figure 3B**). Similarly, the projected area in the z direction, $P_z(z)$, was found by multiplying the magnitude of the vector segment by the sine of the angle ($\sin(\theta)$) between the blade position and the vertical vector. The component of the blade area projected in the x and z directions was found by multiplying the one-sided blade area (a) by $P_x(z)$ and $P_z(z)$, respectively. The probability of particle deposition was the sum of the probability of particle impaction on both the vertical and horizontal surfaces $\left(dp = dp_x + dp_z\right)$. To determine if the particle deposited to the canopy during the time-step, a random number, R_c, was chosen from a uniform distribution between 0 and 1. If R_c was less than or equal to the probability of deposition, the particle deposited to the canopy.

The RDM model was validated using measured profiles of dye concentration along a rigid model canopy (case I in Ghisalberti and Nepf, 2004). The dye was released at $x/h = 0$ and $z/h = 1$ and measured at six downstream longitudinal locations ($x/h =$ 1.4, 3.9, 6.6, 10.8, 18.0, 27.3). To represent the neutrally buoyant tracer, the RDM particles were given neutral buoyancy ($w_s = 0$), retention on canopy elements was omitted, and the bed and water surface ($z = 0, H$) were treated as no-flux boundaries. In order to calculate simulated concentration and mass flux, a vertical column of interrogation boxes (0.02 m long × 0.01 m high) was defined, centered at the longitudinal measurement points. Particles were continuously released until a steady-state particle concentration was established in each box. The concentration, $C(z)$, was found by dividing the steady-state number of particles in each box by the box volume. The mass flux was found by integrating the flux at each box over the water depth, $Q_x = \int \overline{u}\,(z)\,C\,(z)\,dz$.

The validated transport model was used to explore the influence of several factors on pollen transport, including pollen release height within the canopy, pollen shape, interaction with the water surface, submergence depth ratio (H/h), and depth-average velocity. The flexible meadow parameterizations were used in order to represent the reconfiguration of real seagrass. The selected range of submergence, $H/h = 5, 4, 3, 2, 1.5$, represented the range observed for *Z. marina* canopies at our field sites near Nahant and Gloucester, MA, where $H/h = 1.5$ to 6.25 at the shallow and deep canopy edges. In the field, pollen grains have sometimes been observed to collect at the water surface, forming a connected floating layer that restricts future transport (de Cock, 1980), while in other instances pollen collected at the surface returned to the water column due to wave and wind action (Ducker et al., 1978; Ruckelshaus, 1996; Ackerman, 1997). These two conditions were represented in the simulation by different surface boundary conditions. On the one hand, the return of pollen from the water surface into the water column was represented as a no-flux, or reflecting, boundary. On the other hand, the collection of pollen on the water surface was represented as an absorbing (perfect sink) boundary condition. For all cases, the pollen was released at the top of the canopy ($z/h = 1$).

2.3. Genetic Diversity of Seeds Produced on Paired Upper and Lower Inflorescences

Flowering shoots were selected haphazardly, at least 5 meters apart at a depth of approximately 3 m MLLW, from the interior of two *Z. marina* meadows in northern Massachusetts (Dorothy Cove, Nahant, and Niles Beach, Gloucester). Canopy height (h) ranged from 85 to 135 cm, so that $H/h > 2$ for all samples. From each flowering shoot ($n = 7$; 3 from Nahant and 4 from Gloucester), we collected a leaf sample and 6–10 developing seeds from each of two spathes, one from the highest rhipidia and one from the lowest, and the location of those spathes were recorded as the distance above the substrate of the midpoint of the inflorescence. Maternal leaf tissue was frozen at −20°C until DNA extraction; seeds were frozen at −80°C. DNA was extracted from leaves by grinding each sample with a Retsch mixer mill MM400 and using the Omega Bio-Tek E.N.Z.A.® Plant DNA Kit. Individual seeds were ground by hand in microfuge tubes with micro-pestles and DNA was extracted with Chelex 100 (Bio-Rad); samples were incubated at 55°C for 8–24 h, gently mixed,

heated to 98°C for 10 min, vortexed, centrifuged at 14,000 rpm for 5 min, and the supernatant stored at −20°C until PCR.

Each seed and maternal shoot was genotyped using 8 microsatellite loci developed for *Z. marina* and known to be polymorphic for these populations, multiplexed in 3 11 μl PCR reactions (**Table 1**). Each reaction consisted of 1 μl DNA template, 5 μl 2X Type-It multiplex master mix (Qiagen), and 0.25 μl of each 10 μM primer. PCR cycling conditions included initial activation/denaturation at 95°C for 5 min, followed by 28 cycles of 95°C for 30 s, 60°C for 90 s, and 72°C for 30 s, and final extension at 60°C for 30 min. PCR products were separated on a 3730xl Genetic Analyzer (Applied Biosystems) and fragment analysis was performed using GeneMarker version 2.6 (SoftGenetics).

To compare seed diversity across samples that differed in size ($n = 6$ to 10 seeds per spathe), we calculated allelic richness (A_E) rarified to the smallest sample size (i.e., 12 alleles) using the program HP-RARE (Kalinowski, 2005). The program GERUD 2.0 (Jones, 2005) was used to determine the number of unique fathers contributing to each seed set. GERUD uses an exclusion approach to determine the minimum number of sires necessary to produce a given progeny array when the mother's genotype is known, as in our data set. If a progeny array was too complex to solve using all 8 loci, we removed the least informative locus until a solution could be found (Jones, 2005); pairs of inflorescences from the same maternal shoot were always analyzed with the same set of loci. We divided the minimum number of unique fathers by the number of seeds genotyped to standardize comparisons across inflorescences with different numbers of seeds and used paired *t*-tests to compare the diversity of seeds produced on high vs. low inflorescences on each flowering shoot.

3. RESULTS

3.1. Validation of RDM Model

The simulation was validated against vertical profiles of dye concentration measured along a rigid model canopy (case I in Ghisalberti and Nepf, 2004). To mimic the real tracer, the model particles were assumed to be neutrally buoyant ($w_s = 0$). The measured and modeled concentration fields displayed similar vertical dispersion for $x/h \geq 3.9$, where the measured and modeled observations agreed to within 7% (**Figure 4**). However, closer to the source, $x/H = 1.4$, the modeled concentration (**Figure 4**, open squares) exhibited greater vertical dispersion than the measured concentration (**Figure 4**, solid circles), as the modeled concentration spread over a larger vertical distance with a reduced peak magnitude relative to the measured concentration. The initially smaller rate of dispersion for the real tracer can be explained by the presence of multiple eddy scales within the real system. The vertical distribution of real tracer was initially influenced by turbulence scales smaller than the canopy-scale vortices, and thus experienced slower diffusion. The canopy-scale vortices did not contribute to the diffusion of the real tracer until the real tracer cloud grew to a size comparable to the canopy-scale vortices. In contrast, the simulation applied a constant diffusivity based on the canopy-scale vortices, so that the tracer was effectively influenced by the largest scale of turbulence from the point of release, and thus initially dispersed more rapidly than the real tracer.

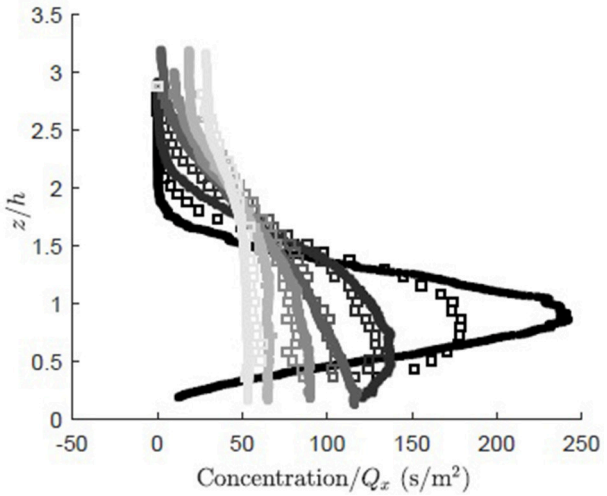

FIGURE 4 | Comparison of concentration normalized by total mass flux for RDM particles (open squares) and measured dye concentration (solid dots, case I, Ghisalberti and Nepf, 2005) at six longitudinal locations ($x/h = 1.4$, 3.9, 6.6, 10.8, 18.0, 27.3, dark to light gray). The concentration (g/m^2) was normalized by the longitudinal flux, $Q_x = \int \bar{u}(z)C(z)dz$ (g/s).

3.2. Validation of Velocity Model

The velocity model was also validated with field measurements in a *Z. marina* meadow, as reported in Lacy and Wyllie-Echeverria (2011, site ED3). The velocity profile was measured at 3 time points over a tidal cycle, resulting in different depth-average velocity and canopy height $h = 0.84$, 0.78, 0.61 m and $\Delta U = 0.032$, 0.050, 0.072 m/s (**Figure 5**, open circles, triangles, and squares). The frontal area per canopy volume $a = 2$ m^{-1} was computed for vertical blades from measurements of blade dimensions and shoot density, with blade width $L_v = 1$ cm. The frontal area per canopy volume was assumed to be constant over the reconfigured canopy height h. As a canopy composed of flexible blades reconfigures, there is decrease in drag predominantly because the pronated component of the blades contribute little to drag. Luhar and Nepf (2011) demonstrated that the drag imparted by a flexible blade can be represented as an equivalent rigid blade of shorter length, called the effective blade length, l_e. Since the effective blade is rigid, its imparted drag is described by the drag coefficient for a rigid blade, $C_D = 1.95$ (Luhar and Nepf, 2011). We assumed that the deflected meadow height (h) was a reasonable approximation for the effective blade length, but acknowledge that this may produce a slight over prediction, based on the comparison shown in Figure 2 in Luhar and Nepf (2013). The canopy was assumed to be deeply submerged ($H/h > 2$) based on the reported site elevation of −2 m MLLW. The modeled velocity profile (**Figure 5**, solid, dashed, and dash-dot lines) agreed with the measurements to within a maximum difference of 3.8%.

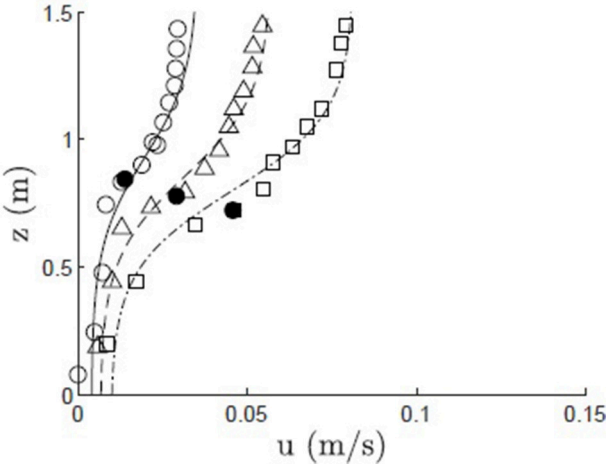

FIGURE 5 | Modeled (solid, dashed, and dash-dot lines) and measured (open circles, triangles, and squares) velocity profiles within a *Z. marina* canopy (Shaw Island, WA; Lacy and Wyllie-Echeverria, 2011) at three points during a tidal cycle, with canopy height $h = 0.84,\ 0.78,\ 0.61$ m, denoted by solid black dot, and $\Delta U = 0.032,\ 0.050,\ 0.072\ m/s$, $L_v = 1$ cm, $C_D = 1.95$, and $a = 2$ m^{-1}.

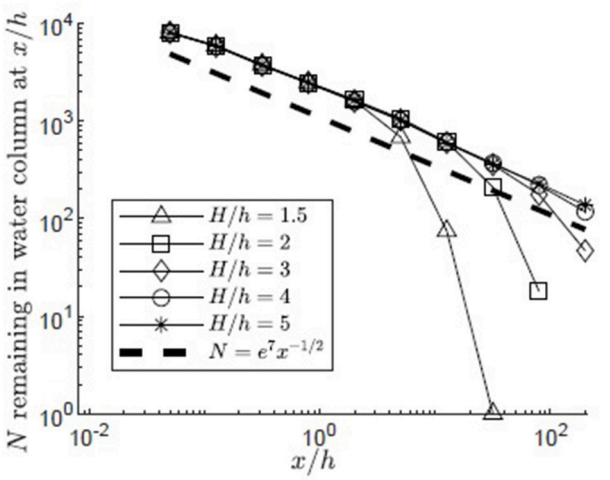

FIGURE 6 | Number of particles remaining in the water column with distance from the release point $x_{rel}/h = 0$ for 10,000 filamentous particles released at $z_{rel}/h = 1$ in a canopy ($u_* = 0.01$ m/s, $L_V = 1$ cm, $a = 2$ m^{-1}, $C_D = 1.95$, $h = 1$ m) with varied submergence depth, $H/h = 1.5,\ 2,\ 3,\ 4,\ 5$, respectively, represented by open triangles, squares, diamonds, circles, and asterisks. Particles were evaluated at 10 points spaced equally in log space, ($x/h = 0.05, 0.13, 0.32, 0.80, 2.0, 5.0, 13, 32, 80, 200$). Particles reaching the water surface ($z/h = H/h$) were reflected off of the surface boundary, remaining available for transport within the water column and the possibility of capture on canopy elements. A line illustrating a power law with decay constant −1/2 is plotted for reference (black dashed line).

The likelihood of outcrossing vs. selfing will depend on the relationship between mean clone size (i.e., the area covered by a given genotype) and the pollen dispersal kernel, both of which will vary among seagrass meadows. However, all else being equal, increased within-meadow pollen dispersal will increase opportunity for pollen to encounter non-self-flowers. Therefore, we are interested in what attributes of the meadow impact the maximum distance traveled before canopy capture. The validated model was used to explore the impact of different flow and morphology parameters on pollen transport. The effect of submergence depth, depth-average velocity, pollen shape, and pollen release height were explored, with canopy parameters $a = 2$ m^{-1}, $h = 1$ m, $L_v = 1$ cm, $C_D = 1.95$ remaining constant for all simulations.

3.3. Influence of Submergence Depth H/h on Pollen Transport

The simulation was used to understand the impact of submergence depth on long-distance pollen transport. Filamentous particles were released at $z_{rel}/h = 1$ for submergence depths $H/h = 1.5,\ 2,\ 3,\ 4,\ 5$ in a canopy with $u_* = 0.01$ m/s. As discussed in the methods, two surface boundary conditions were considered, particles rebounding off the water surface (**Figure 6**) and particles captured by the water surface (**Figure 7**). For all submergence depths and for both surface boundary conditions, the number of particles in the water column, N, most of which were above the canopy, decreased with the same dependence on distance, $N \sim x^{-1/2}$ (**Figures 6**, **7**). This dependence arose because the canopy was a strong sink for pollen, so that the in-water concentration of particles was close to zero within the canopy. Then, the loss of particles to the canopy, $\partial N/\partial x$, depends on the vertical turbulent flux of particles toward the canopy, which in turn depends on the vertical gradient of particle concentration, $\partial C/\partial z$, above the canopy, i.e., $\partial N/\partial x \sim \partial C/\partial z$. The remaining particles, N, are distributed above the canopy over the vertical length-scale for diffusion, $\delta_z \sim x^{-1/2}$, such that the mean concentration above the canopy is $C_{mean} \sim N/\delta_z$. Since the concentration is close to zero in the canopy, $\partial C/\partial z \sim C_{mean}/\delta_z \sim N/\delta_z^2 \sim Nx^{-1}$. Since $\partial N/\partial x \sim \partial C/\partial z$, we can also write $\partial N/\partial x \sim Nx^{-1}$, which has the solution $N \sim x^{-1/2}$.

The particle number (N) deviated from the $x^{-1/2}$ dependence when the particles began to interact with the water surface. For the reflecting boundary condition (**Figure 6**), the loss of particles to the canopy was accelerated, because the reflected particles were forced back toward the canopy. For example, for the smallest submergence depth, $H/h = 1.5$ (triangles in **Figure 6**), this transition occurred at $x/h = 5$, at which point a significant fraction of the particles (26%) had interacted with the surface. For the absorbing boundary condition (**Figure 7**), the transition in particle loss occurred at the same x-positions (i.e., $x/h = 5$ for $H/h = 1.5$), but once the particles were captured by the water surface, capture by the canopy ceased, so that the number of particles in the water column stopped decreasing. Particles trapped at the surface could remain in the water column until wave breaking or wind-generated turbulence knocked them free of the surface layer, making them available again for canopy capture. Although wavebreaking is not included in the model, this implied that capture at the water surface is a mechanism that enhanced long-distance dispersal.

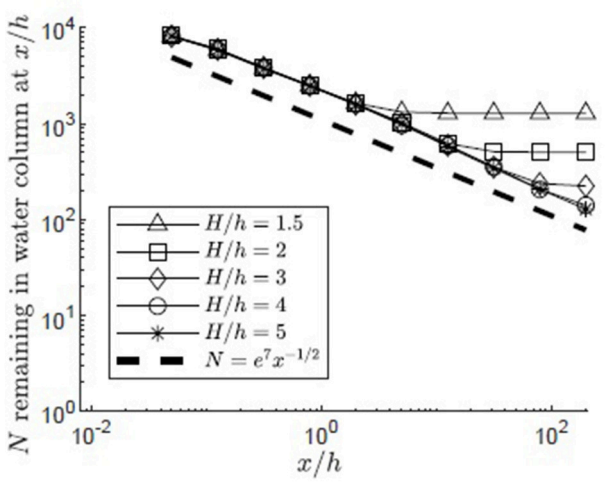

FIGURE 7 | Number of particles remaining in the water column with distance from the release point $x_{rel}/h = 0$ for 10,000 filamentous particles released at $z_{rel}/h = 1$ over a canopy ($u_* = 0.01$ m/s, $L_v = 1$ cm, $a = 2$ m^{-1}, $C_D = 1.95$, $h = 1$ m) with varied submergence depth, $H/h = 1.5$, 2, 3, 4, 5, respectively, represented by open triangles, squares, diamonds, circles, and asterisks. Particles were evaluated at 10 points spaced equally in log space, (x/h = 0.05, 0.13, 0.32, 0.80, 2.0, 5.0, 13, 32, 80, 200). Particles reaching the water surface ($z/h = H/h$) were considered to be adhered to that boundary, but remaining within the water column. A line illustrating a power law with decay constant −1/2 is plotted for reference (black dashed line).

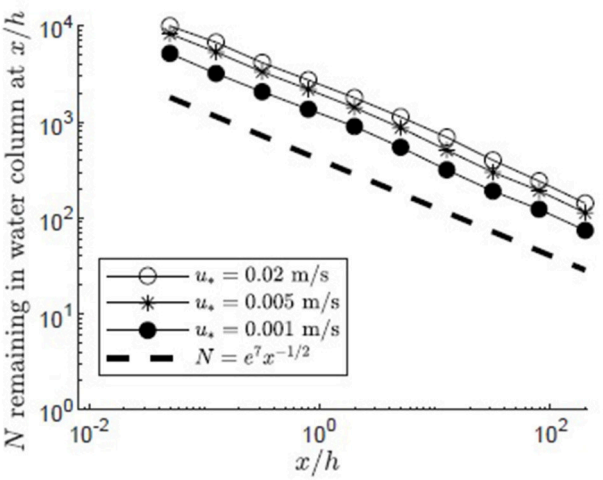

FIGURE 8 | Number of particles remaining in the water column with distance from the release point $x_{rel}/h = 0$ for 10,000 filamentous particles released at $z_{rel}/h = 1$ over a canopy ($H/h = 5$, $L_v = 1$ cm, $a = 2$ m^{-1}, $C_D = 1.95$, $h = 1$ m) with varied canopy shear velocity, $u_* = 0.001$, 0.005, 0.02 m/s, respectively, represented by black circles, asterisks, and open circles. Particles were evaluated at 10 points spaced equally in log space, (x/h = 0.05, 0.13, 0.32, 0.80, 2.0, 5.0, 13, 32, 80, 200). A line illustrating a power law with decay constant −1/2 is plotted for reference (black dashed line).

Note that the comparisons made in **Figures 6**, **7** assume the same depth-average velocity for all submergence ratios, whereas in the field, water depth and current speed are typically correlated through the tidal cycle. Therefore, the maximum transport of pollen in the field may not occur at high tide (maximum submergence ratio), but at some intermediate point in the tide with higher velocity. Nevertheless, the general trend of greater pollen transport at greater water depths (greater H/h) would be valid when comparing a meadow across a depth gradient.

3.4. Influence of Velocity Variation

The impact of variation in the depth-average velocity was considered by varying the canopy shear velocity between $u_* = 0.001$ and 0.02 m/s, based on the range of u_* found in four *Z. marina* meadows (Grizzle et al., 1996; Lacy and Wyllie-Echeverria, 2011). Filamentous particles were released in a canopy with $H/h = 5$, $z_{rel}/h = 1$, and a reflecting surface boundary condition. Increasing u_* was associated with an increase in depth-averaged velocity, U, which spanned 0.8 to 17 cm/s, respectively, for the u_* values given above. The vertical diffusivity within the mixing layer was linearly proportional to Δu and thus u_*, and for the range of u_* values spanned $K_{z,h} = 4$ to 80 cm^2/s^2, respectively. Because the velocity has higher values above the canopy and lower values within the canopy (**Figure 5**), particles that initially escaped the meadow and traveled for some distance above the meadow, where capture could not occur, had the greatest travel distances. The average distance traveled divided by the time spent above the canopy ($z/h \geq 1$) was 0.97, 4.8, 19 cm/s, which was close to the average longitudinal velocity above the canopy for each u_* condition ($\overline{u}|_{H-h} = 0.99$, 4.9, 20 cm/s), indicating that longitudinal transport predominantly occurred when particles were located above the canopy.

Particles released in canopies with higher depth-averaged velocity had only slightly greater travel distances. This is shown by a slightly higher number of particles remaining in the water column for larger values of u_* at each distance from the release (**Figure 8**). Similarly, increasing the depth-average velocity from 0.8 to 17 cm/s increased the number of particles reaching the end of the domain only slightly, from 86 to 146 (**Figure 8**). That is, increasing U by a factor of about 20 only increased the number of particles leaving the domain by a factor of about 2. The weak dependence of travel distance on depth-average velocity can be explained by the linear dependence of K_z on the velocity shear (Δu) and thus on the depth-average velocity (U). Specifically, the ratio K_z/U was roughly a constant. Therefore, although increasing U allowed particles above the meadow to advect more quickly away from the source, a comparable increase in K_z enhanced particle flux into the meadow, so that the spatial rate of particle capture by the meadow had little dependence on depth-average velocity.

3.5. Influence of Pollen Shape

Pollen shape significantly influenced the maximum distances traveled by pollen. Using the same meadow and release conditions ($H/h = 5$, $z_{rel}/h = 1$, reflecting surface boundary, $u_* = 0.01$ m/s), the transport of filamentous pollen ($L_p = 4e - 3$ m, $B_p = 7.5e - 6$ m) was compared to that of spherical

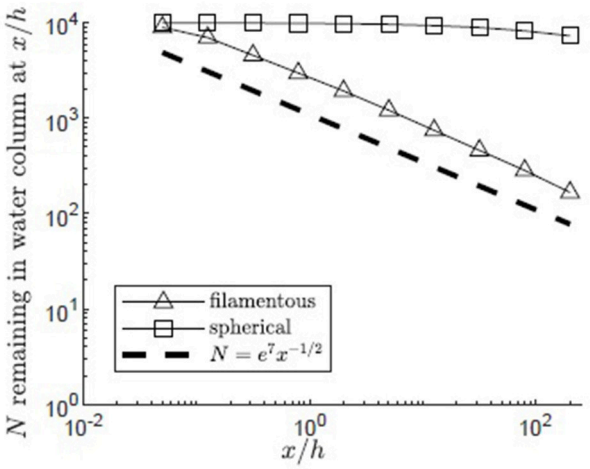

FIGURE 9 | Number of filamentous (open triangles) and spherical (open squares) particles remaining in the water column with distance from the release point $x_{rel}/h = 0$ for 10,000 particles released at $z_{rel}/h = 1$ over a canopy ($H/h = 5$, $u_* = 0.01$ m/s, $L_v = 1$ cm, $a = 2$ m^{-1}, $C_D = 1.95$, $h = 1$ m) with a reflecting water surface boundary. Particles were evaluated at 10 points spaced equally in log space, ($x/h = 0.05, 0.13, 0.32, 0.80, 2.0, 5.0, 13, 32, 80, 200$). A line illustrating a power law with decay constant −1/2 is plotted for reference (black dashed line).

pollen grains of the same volume and settling velocity, but diameter $d_p = 3.5e-5$ m (**Figure 9**). The filamentous pollen had significantly higher canopy capture rates, resulting in more of the filamentous pollen remaining closer to its release point. Specifically, for the filamentous pollen over 98% of the pollen was captured by the canopy before the end of the modeled domain, and no particles reached the bed ($z = 0$). In addition, the filamentous pollen remaining in the water column decays following the $x^{-1/2}$ dependence, which is consistent with the canopy behaving as a nearly perfect sink (see discussion in section Influence of Submergence Depth H/h on Pollen Transport). In contrast, the spherical pollen was not as efficiently captured by the canopy, and as a result the spatial decline in water column pollen was much slower and specifically did not follow the $x^{-1/2}$ dependence. Further, only 54% of the spherical pollen grains were captured by the canopy within the modeling domain, and 46% of particles traveled beyond the end of the modeling domain.

3.6. Influence of Pollen Release Height, z_{rel}/h

Vertical diffusivity was elevated by canopy-scale vortices within the canopy mixing layer, $z_1 \leq z \leq z_2$. The importance of this region of elevated diffusivity to pollen transport was explored by varying the pollen release height. The lowest release point ($z_{rel}/h = 0.25$, **Figure 10**) was below the mixing layer ($z_{rel}/h < z_1/h = 0.49$) in a region of reduced diffusivity dominated by blade-scale turbulence. The middle release point ($z_{rel}/h = 0.75$, **Figure 10**) was within the region affected by both blade-scale and canopy-scale turbulence, which significantly elevated the vertical diffusivity relative to the lower canopy region (**Figure 3**). The highest release point was $z_{rel}/h = 1$, reflecting the location of the highest inflorescences observed within coastal Massachusetts *Z. marina* canopies [Dorothy Cove, Nahant, MA; Niles Beach, Gloucester, MA; Woods Hole, MA (Ackerman, 1986)]. For the lowest release point ($z_{rel}/h = 0.25$), significant canopy capture (63%) occurred close to the release point ($x/h < 0.05$). Because the vertical diffusivity was low in this region and the release point was far from the top of the canopy, no pollen escaped the canopy from this release point. Specifically, none of the particles traveled more than $x/h = 0.43$, or roughly 0.43 m. Further, the maximum vertical position achieved by pollen released near the bed was only $z/h = 0.29$, indicating that pollen released below the mixing layer remained below the mixing layer. The fraction of particles remaining in the water column followed an exponential decay curve, reflecting first-order decay due to the distributed sink formed by the canopy elements. The capture of pollen over such small length-scales makes self-pollination likely. In contrast, at the highest release point ($z_{rel}/h = 1$), the pollen experienced both higher vertical diffusivity and proximity to the canopy top, both of which facilitated the particles being quickly carried above the canopy, allowing them to avoid canopy capture and experience higher current speeds. Together, this produced much greater travel distances. Specifically, 9% of the pollen released at $\frac{z_{rel}}{h} = 1$ traveled beyond $x/h = 5$ before canopy capture occurred, with 1.2% (120 particles) reaching the longitudinal extent of the model domain ($L = 200h$). The tendency to travel greater distances before capture reduces the probability of self-pollination and enhances the probability of genetically diverse, outcrossed seeds. The particles released within the upper canopy region initially followed an exponential decay curve due to the distributed canopy deposition sink, similar to the decay of the particles released at $z_{rel}/h = 0.25$ (**Figure 10**, open squares and diamonds). However, some particles were able to travel above $z = h$, after which particle deposition followed the pattern of diffusion to a boundary sink, similar to the release at $z_{rel}/h = 1$, with the number of particles decreasing with $x^{-1/2}$.

3.7. Genetic Diversity of Seeds Produced on Paired Upper and Lower Inflorescences

All eight loci used were polymorphic, displaying 3-7 alleles with a mean of 5.75 alleles locus^{-1}. We obtained complete multi-locus genotypes for 125 seeds from seven maternal half-sibling families. The majority of seeds showed Mendelian evidence of outcrossing (i.e., non-maternal alleles at one or more loci), with only 15 of 125 seeds (12%) possessing genotypes consistent with geitonogamous selfing; twice as many of these were found on lower inflorescences than on upper ones (10 vs. 5). Pooling data from both field sites and using a paired approach, we found that both measures of seed diversity tested were greater for inflorescences closer to the top of the canopy. Allelic richness (mean number of alleles per loci) was significantly greater for seeds produced in spadices close to the top of the canopy than those produced lower on the shoot (mean and standard deviation 2.87 ± 0.24 vs. 2.60 ± 0.41; one-tailed paired t-test, $p = 0.013$), and the difference in allelic richness between sibling seed cohorts tended to increase with increasing linear distance between spadices (**Figure 11**). Likewise, the minimum number of unique fathers was greater for

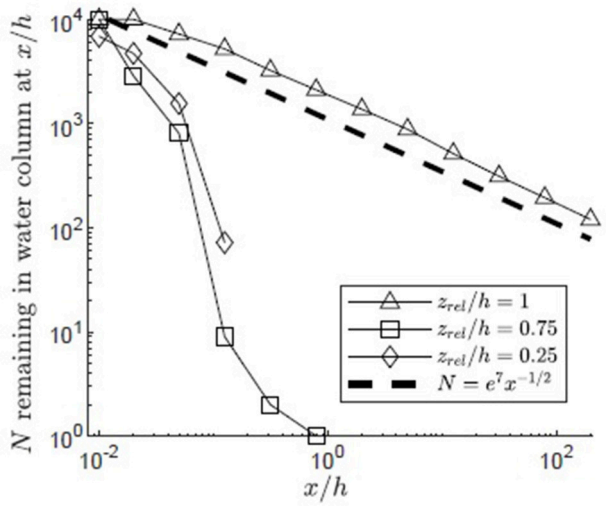

FIGURE 10 | Number of particles remaining in the water column with distance from the release point $x_{rel}/h = 0$ for 10,000 filamentous particles released in a canopy ($H/h = 5$, $u_* = 0.01$ m/s, $L_V = 1$ cm, $a = 2$ m^{-1}, $C_D = 1.95$, $h = 1$ m) with varied release heights ($z_{rel}/h = 1,\ 0.75,\ 0.25$) and a reflecting surface boundary. Particles were evaluated at two locations ($x/h = 0.01, 0.02$) chosen to occur before the location of first deposition of particles from the lower release points and 10 points spaced equally in log space, ($x/h = 0.05$, 0.13, 0.32, 0.80, 2.0, 5.0, 13, 32, 80, 200). A line illustrating a power law with decay constant −1/2 is plotted for reference (black dashed line).

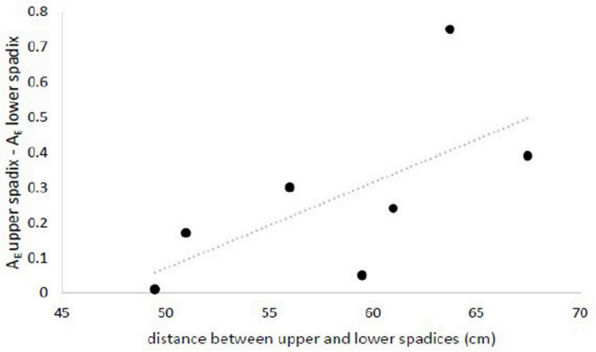

FIGURE 11 | Difference in allelic richness between seeds collected from upper- and lower-most spadices (rarified to the smallest sample size) increased with increasing distance between inflorescences. n_{seed} = (6 to 10 seeds/spadix) x (2 spadices/maternal shoot) x (7 maternal shoots). Data is available from the authors upon request.

seed families collected from upper spadices than from lower ones (3.52 vs. 2.93 fathers/10 seeds; one-tailed paired t-test, $p = 0.052$).

4. DISCUSSION

Although vegetative growth historically has been assumed to be the primary mode of reproduction in seagrasses, multiple lines of evidence suggest that recruitment from seed is both more common and more important than previously believed (Kendrick et al., 2012). For example, significant variation in genetic and genotypic diversity has been documented within and among natural seagrass beds (Williams and Orth, 1998; Olsen et al., 2004; Hughes and Stachowicz, 2009), and disturbed seagrass meadows often recover at a rate faster than could occur with vegetative propagation alone (Orth et al., 2006). Further, there is increasing evidence that the genetic diversity and relatedness of seeds influences resulting seedling performance, which highlights the importance of a diverse pollen supply. The fitness costs of self-pollination in *Z. marina* vary among populations, but experimentally selfed inflorescences often show significantly lower seed set (Ruckelshaus, 1995; Reusch, 2001; Rhode and Duffy, 2004) and reduced seed germination compared to outcrossed inflorescences (Ruckelshaus, 1995; Billingham et al., 2007). The positive effect of seed diversity can be seen beyond the dichotomy of selfed vs. outcrossed: increased allelic richness in seeds has been shown to increase both primary and secondary production in the field (Reynolds et al., 2012), and genetically diverse, non-sibling seeds outperformed sibling seeds in a greenhouse mesocosm experiment (Randall Hughes et al., 2016). Thus, the physical processes that affect pollen delivery in the nearshore environment impact both seed quantity and quality, and this can have important ramifications for population dynamics and genetic structure in eelgrass meadows.

The transport distances achieved by the simulated pollen in our model reflected the vertical structure of turbulence within the canopy. Specifically, longitudinal transport over distances greater than $x/h = 2$ was only possible for pollen released within the region of the upper canopy influenced by canopy-scale vortices ($z > z_1$). The elevated vertical diffusivity within this region carried pollen above the canopy where it experienced higher current speeds and avoided canopy capture until additional longitudinal transport had occurred (**Figure 10**). Observations in real eelgrass canopies suggest that *Z. marina* inflorescences are located in the vertical zone influenced by canopy scale vortices, suggesting that reproductive stalk resources were directed toward release points that can benefit from higher vertical diffusivity. For example, at our field site, the lowest spadices ranged from $z/h = 0.36$ to 0.64 in meadows for which the corresponding $z_1/h = 0.31$ to 0.53 was estimated based on the non-dimensional meadow density, $\frac{z_1}{h} = 0.63 - \frac{0.29}{C_D ah}$. That is, the spadices were all located within the zone influenced by canopy-scale vortices, $z > z_1$. Similarly, the vertical extent of inflorescences in a *Z. marina* canopy reported by Ackerman (1986) extended from $\frac{z}{h} = 0.3$ to 1, which corresponds with $z/h > z_1/h = 0.31$, estimated from the non-dimensional meadow density (ah). Over the range of reported dimensionless *Z. marina* meadow densities ($ah = 0.1$–3, based on data provided in Dennison and Alberte, 1982; Chandler et al., 1996; Moore, 2004; McKone, 2009; Lacy and Wyllie-Echeverria, 2011; Infantes et al., 2012; Hansen and Reidenbach, 2013; Reidenbach and Thomas, 2018), $z_1/h = 0$ to 0.6. This suggests that in some sparse canopies ($ah \lessapprox 0.5$), the canopy-scale vortices penetrate to the bed ($z_1 = 0$) and spadices over the entire meadow would experience elevated diffusivity. However, for dense canopies, inflorescences located

below z_1 would experience reduced diffusivity, resulting in much shorter distances for pollen transport.

The effect of vertical flow structure observed in the model can also be seen in our empirical data on seed diversity. Seeds collected from lower inflorescences had reduced allelic richness relative to seeds produced from higher inflorescences on the same flowering shoot (**Figure 11**), consistent with the significantly shorter travel distances for pollen released lower in the canopy in the simulation study. For particles released in the lower canopy, the maximum travel distance predicted was 0.43 m, vs. 5 m and higher for the upper canopy. This difference in travel distance implies that pollen released in the lower canopy is more quickly captured by the canopy and thus has a higher probability of self-pollination. Observed selfing rates in our genotyped seeds were low, as has been found in other eelgrass populations with polyclonal patches (Ruckelshaus, 1995; Reusch et al., 2000; Furman et al., 2015). However, more putatively selfed seeds were found on lower infloresences than upper ones, and upper inflorescences showed greater paternal diversity, suggesting greater access to diverse pollen sources higher in the canopy.

Overall, the simulated pollen travel distances exhibited a wide range, from essentially zero to distances that extended beyond the end of the model domain ($x > 200h = 200$ m) indicating that both short- and long-distance fatherhood is possible. Furman et al. (2015) similarly found genetic evidence of a range of father distances through genotyped single seeds from the tallest rhipidium on flowering shoots in a dynamic and patchy eelgrass meadow. Fathers were identified, with pollination found to occur from fathers located 0.57–74 m upstream. The lack of viable parents at distances shorter than 0.57 m was attributed to developmental synchrony of neighboring reproductive shoots. The measured pollen dispersal distance was limited by the study size, indicating the potential for pollen transport over further distances, similar to the fate of the modeled pollen grains that reached the longitudinal extent of the domain. Approximately 63% of modeled pollen particles would have been captured by the canopy within the first 0.57 m after release, suggesting that developmental synchrony would aid in the prevention of selfing over short distances. The model results showed a decrease in particles present in the water column with $x^{-1/2}$. Because the probability of pollination is directly related to particle density, the probability of pollination would also depend on $x^{-1/2}$, favoring long-distance fatherhood relative to a linear dependence. However, this dependence was also shown to depend on the proximity of the water surface (**Figures 6**, **7**). Once particles begin to interact with the water surface, which occurred closer to the source when submergence was lower (smaller H/h), then the capture to the canopy was either accelerated (when the water surface reflected the pollen) or shut-off (when the water surface absorbed the pollen).

Global declines in seagrass distributions may be accompanied by shifting depth distributions (e.g., loss in shallow regions due to high temperature episodes, loss at depth due to eutrophication and resulting light reduction). Modeled variation in submergence depth and pollen release height explored how such changes may impact pollen delivery. Particles that reflected off the water surface boundary displayed reduced longitudinal transport relative to the most deeply submerged canopy ($H/h = 5$) which was not affected by the water surface within the model domain, $L = 200h$. For the two most shallow cases considered, $H/h = 1.5,\ 2$, all particles were captured within the model domain ($x/h = 32,\ 80$). In these cases, long-distance fatherhood would be reduced relative to more deeply submerged canopies due to the influence of the surface boundary, which could weaken observed outcrossing rates in shallow canopies relative to more deeply submerged canopies. However, because the surface only affected particle transport after the vertical extent of the plume reached $z = H$, pollen traveling shorter distances would not be influenced by the surface boundary.

Z. marina produces elongated pollen with length comparable to blade width ($L_p = 3$–5 mm, Ackerman, 2002; $L_v = 5.5$ mm, McKone, 2009), with a pollen:ovule ration of approximately 10,000:1 (Ackerman, 2002).The high ratio of pollen length to blade width increased the capture efficiency (Equation 5) of the filamentous pollen grains relative to spherical grains of the same settling velocity. Previous observations (Ackerman, 1997) indicate that the elongated pollen shape increases capture efficiency on flowers as the pollen threads tumble through flower-generated velocity gradients toward the center of the flower, increasing the incidence of capture on stigmas. High canopy capture rates were reflected in the significantly reduced transport distance for filamentous pollen grains, compared to spherical grains (**Figure 9**). In all scenarios simulated in this study, $>$ 91% of the filamentous pollen was captured by the canopy within the model domain (**Figure 9**). The high rate of canopy capture and resulting short travel distances are consistent with previous observations suggesting that the elongated pollen is not optimized for long distance transport (Ackerman, 1986; Zipperle et al., 2011; Kendrick et al., 2012). The elongated dimension of the filamentous pollen increased the canopy capture rate, promoting successful capture by reproductive stalks, while maintaining a small settling velocity relative to canopy shear stress, $\frac{w_s}{u_*} = 0.0002 - 0.004$. Particles assigned the same settling velocity and an equivalent spherical diameter that conserved particle mass and density (section Influence of Pollen Shape) displayed reduced canopy deposition, with only 27% of spherical particles becoming captured by the canopy before the end of the modeling domain, $L = 200h$. Pollen with these characteristics would be expected to experience reduced pollination efficiency within a meadow ($L < 200h$), because over half the pollen released would exit the longitudinal extent of the meadow before becoming captured by the canopy. In contrast, larger particles with a higher settling velocity, as is seen in some terrestrial species such as ragweed ($\frac{w_s}{u_*} = 0.04$, Boehm et al., 2008) *Lycopodium* (clubmoss) spores ($\frac{w_s}{u_*} = 0.04$, Pan et al., 2014) could experience reduced longitudinal transport following periods of slack water as some particles could settle out of the water column. Recall that the canopy capture model used in this study was modified from a model based on observed capture of spherical particles on cylindrical collectors (Palmer et al., 2004). To improve the canopy capture model, future experiments should be done with filamentous pollen and flexible blade collectors. It is possible

that canopy capture on vegetative blades may be reduced due to interaction of the pollen coating and vegetative blade surface, as some sources note that pollen grains may slide off of vegetative blades under some conditions (Ackerman, 2002). These additional aspects should be considered in future research in order to improve characterizations of pollen transport.

To conclude, in this study, field samples of seeds on paired inflorescences and numerical simulations of pollen transport together demonstrated the connection between reduced in-canopy transport of pollen particles and reduced seed diversity. Pollen released in the lower canopy had significantly reduced longitudinal transport compared to pollen released in the upper canopy, which traveled for extended periods above the canopy. Consistent with this, seeds from lower inflorescences had reduced allelic richness relative to seeds produced from higher inflorescences. The transport distance of modeled pollen grains increased with increasing submergence depth, owing to the greater availability of flow space above the meadow in which pollen could travel without the likelihood of becoming captured by the canopy. Finally, paired simulations of filamentous and spherical pollen grains showed that filamentous grains were more rapidly captured by the blades, resulting in significantly shorter travel distances for most particles, consistent with conclusions drawn from previous field studies that filamentous pollen favors shorter dispersal distances (Ackerman, 1986). The results in this study highlight the importance of the physical processes of advection, diffusion, and interception in determining the travel distance of pollen grains and canopy genetic diversity.

AUTHOR CONTRIBUTIONS

EF and HN designed the model and analyzed the modeled data. EF implemented the model simulations. HN supervised model development. CH planned and carried out the genetic analyses. All authors discussed the results and contributed to the final manuscript.

FUNDING

This material is based on work supported by the National Science Foundation under Grant No. AGS-1005480 to HN; molecular analyses were conducted with support for STEM education from the USNH system to CH. Any opinions, findings, or recommendations expressed in this material are those of the authors and do not necessarily reflect the views of the National Science Foundation.

REFERENCES

Ackerman, J. (1997). Submarine pollination in the marine angiosperm, *Zostera marina*. II. Pollen transport in flow fields and capture by stigmas. *Am. J. Bot.* 84, 1110–1119. doi: 10.2307/2446154

Ackerman, J. D. (1986). Mechanistic implications for pollination in the marine angiosperm *Zostera marina*. *Aquat. Bot.* 24, 343–353. doi: 10.1016/0304-3770(86)90101-4

Ackerman, J. D. (1995). Convergence of filiform pollen morphologies in seagrasses: functional mechanisms. *Evol. Ecol.* 9, 139–153. doi: 10.1007/BF01237753

Ackerman, J. D. (2000). Abiotic pollen and pollination: Ecological, functional, and evolutionary perspectives. *Plant Syst. Evol.* 222, 167–185. doi: 10.1007/BF00984101

Ackerman, J. D. (2002). Diffusivity in a marine macrophyte canopy: implications for submarine pollination and dispersal. *Am. J. Bot.* 89, 1119–1127. doi: 10.3732/ajb.89.7.1119

Ackerman, J. D. (2006). "Sexual reproduction of seagrasses: pollination in the marine context," in *Seagrasses: Biology, Ecology, and Conservation*, eds. A. W. D. Larkum, R. J. Orth, and C. M. Duarte (Dordrecht: Springer), 89–109.

Ackerman, J. D., and Okubo, A. (1993). Reduced mixing in a marine macrophyte canopy. *Funct. Ecol.* 7, 305–309. doi: 10.2307/2390209

Barbier, E. B., Hacker, S. D., Kennedy, C., Koch, E. W., Stier, A. C., and Silliman, B. R. (2011). The value of estuarine and coastal ecosystem services. *Ecol. Monogr.* 81, 169–193. doi: 10.1890/10-1510.1

Billingham, M. R., Simoes, T., Reusch, T. B. H., and Serrao, E. A. (2007). Genetic substructure and intermediate outcrossing distance in the marine angiosperm *Zostera marina*. *Mar. Biol.* 152, 739–801. doi: 10.1007/s00227-007-0730-0

Boehm, M. T., Aylor, D. E., and Shields, E. J. (2008). Maize pollen dispersal under convective conditions. *J. Appl. Meteorol. Climatol.* 47, 291–307.

Bruno, J. F., and Bertness, M. D. (2001). *Positive Interactions, Facilitations, and Foundation Species*. Sunderland: Sinauer Associates.

Chandler, M., Colarusso, P., and Buchsbaum, R. (1996). *A study of Eelgrass Beds in Boston Harbor and northern Massachusetts Bays*. Narragansett, RI: Office of Research and Development, U.S. Environmental Protection Agency.

de Cock, A. W. A. M. (1980). Flowering, pollination, and fruiting in *Zostera marina* L. *Aquat. Bot.* 9, 201–220. doi: 10.1016/0304-3770(80)90023-6

Dennison, W. C., and Alberte, R. S. (1982). Photosynthetic responses of *Zostera marina* L. (eelgrass) to in situ manipulations of light intensity. *Oecologia* 55, 137–144. doi: 10.1007/BF00384478

Duarte, C. M., Losada, I. J., Hendriks, I. E., Mazarrasa, I., and Marbà, M. (2013). The role of coastal plant communities for climate change mitigation and adaptation. *Nat. Clim. Chang.* 3, 961–968. doi: 10.1038/nclimate1970

Ducker, S. C., Pettitt, J. M., and Knox, R. B. (1978). Biology of Australian seagrasses: pollen development and submarine pollination in *Amphibolis antarctica* and *Thalassodendron ciliatum* (Cymodoceaceae). *Aust. J. Bot.* 26, 265–285. doi: 10.1071/BT9780265

Durbin, P. A. (1983). *Stochastic Differential Equations and Turbulent Dispersion*. NASA Reference Publication 1103.

Edwards, C., and Penney, D. (2002). *Multivariable Calculus, 6th Edn*. New Jersey, NJ: Prentice Hall.

Follett, E., Chamecki, M., and Nepf, H. (2016). Evaluation of a random displacement model for predicting particle escape from canopies using a simple eddy diffusivity model. *Agri. Forest Meteorol.* 224, 40–48. doi: 10.1016/j.agrformet.2016.04.004

Furman, B. T., Jackson, L. J., Bricker, E., and Peterson, B. J. (2015). Sexual recruitment in *Zostera marina*: a patch to landscape-scale investigation. *Limnol. Oceanogr.* 60, 584–599. doi: 10.1002/lno.10043

Ghisalberti, M., and Nepf, H. (2002). Mixing layers and coherent structures in vegetated aquatic flows. *J. Geophys. Res.* 107, 1–11. doi: 10.1029/2001JC000871

Ghisalberti, M., and Nepf, H. (2004). The limited growth of vegetated shear layers. *Water Res. Res.* 40:W07502, doi: 10.1029/2003WR002776.

Ghisalberti, M., and Nepf, H. (2005). Mass transport in vegetated shear flows. *Environ. Fluid Mech.* 5, 527–551. doi: 10.1007/s10652-005-0419-1

Ghisalberti, M., and Nepf, H. (2006). The structure of the shear layer in flows over rigid and flexible canopies. *Environ. Fluid Mech.* 6, 277–301. doi: 10.1007/s10652-006-0002-4

Grech, A., Wolter, J., Coles, R., McKenzie, L., Rasheed, M., Thomas, C., et al. (2016). Spatial patterns of seagrass dispersal and settlement. *Divers. Distrib.* 22, 1150–1162. doi: 10.1111/ddi.12479

Grizzle, R. E., Short, F. T., Newell, C. R., Hoven, H., and Kindblom, L. (1996). Hydrodynamically induced synchronous waving of seagrasses: 'monami' and

its possible effects on larval mussel settlement. *J. Exp. Mar. Biol. Ecol.* 206, 165–177.

Hansen, J. C. R., and Reidenbach, M. A. (2013). Seasonal growth and senescence of a *Zostera marina* seagrass meadow alters wave-dominated flow and sediment suspension within a coastal bay. *Est. Coasts* 36, 1099–1114. doi: 10.1007/s12237-013-9620-5

Hughes, A. R., Inouye, B. D., Johnson, M. T., Underwood, N., and Vellend, M. (2008). Ecological consequences of genetic diversity. *Ecol. Lett.* 11, 609–623. doi: 10.1111/j.1461-0248.2008.01179.x

Hughes, A. R., and Stachowicz, J. J. (2004). Genetic diversity enhances the resistance of a seagrass ecosystem to disturbance. *Proc. Natl. Acad. Sci.U.S.A.* 101, 8998–9002. doi: 10.1073/pnas.0402642101

Hughes, A. R., and Stachowicz, J. J. (2009). Ecological impacts of genotypic diversity in the colonal seagrass *Zostera marina*. *Ecology* 90, 1412–1419. doi: 10.1890/07-2030.1

Infantes, E., Orfila, A., Simarro, G., Terrados, J., Luhar, M., and Nepf, H. (2012). Effect of a seagrass (*Posidonia oceanica*) meadow on wave propagation. *Mar. Ecol. Prog. Ser.* 456, 63–72. doi: 10.3354/meps09754

Israelsson, P. H., Kim, Y. D., and Adams, E. E. (2006). A comparison of three Lagrangian approaches for extending near field mixing calculations. *Environ. Model Softw.* 21, 1631–1649. doi: 10.1016/j.envsoft.2005.07.008

Jones, A. G. (2005). GERUD2.0: a computer program for the reconstruction of parental genotypes from half-sib progeny arrays with known or unknown parents. *Mol. Ecol. Notes* 5, 708–711. doi: 10.1111/j.1471-8286.2005.01029.x

Kalinowski, S. T. (2005). HP-Rare: a computer program for performing rarefaction on measures of allelic diversity. *Mol. Ecol. Notes* 5, 187–189. doi: 10.1111/j.1471-8286.2004.00845.x

Kallstrom, B., Nyqvist, A., Aberg, P., Bodin, M., and Andre, C. (2008). Seed rafting as a dispersal strategy for eelgrass (*Zostera marina*). *Aquat. Bot.* 88, 148–153. doi: 10.1016/j.aquabot.2007.09.005

Kendrick, G. A., Waycott, M., Carruthers, T. J. B., Cambridge, M. L., Hovey, R., Krauss, S. L., et al. (2012). The central role of dispersal in the maintenance and persistence of seagrass populations. *Bioscience* 62, 56–65. doi: 10.1525/bio.2012.62.1.10

Lacy, J. R., and Wyllie-Echeverria, S. (2011). The influence of current speed and vegetation density on flow structure in two macrotidal eelgrass canopies. *Limnol. Oceanogr.* 1, 38–55. doi: 10.1215/21573698-1152489

Lightbody, A., and Nepf, H. (2006). Prediction of velocity profiles and longitudinal dispersion in emergent salt marsh vegetation. *Limnol. Oceanogr.* 51, 218–228. doi: 10.4319/lo.2006.51.1.0218

Luhar, M., and Nepf, H. (2011). Flow-induced reconfiguration of buoyant flexible aquatic vegetation. *Limnol. Oceanogr.* 56, 2003–2017. doi: 10.4319/lo.2011.56.6.2003

Luhar, M., and Nepf, H. (2013). From the blade scale to the reach scale: a characterization of aquatic vegetative drag. *Adv. Water Resour.* 51, 305–316. doi: 10.1016/j.advwatres.2012.02.002

Luhar, M., Rominger, J., and Nepf, H. (2008). Interaction between flow, transport, and vegetation spatial structure. *Environ. Fluid Mech.* 8, 423–439. doi: 10.1007/s10652-008-9080-9

McKone, K. A. (2009). *Light Available to the Seagrass Zostera Marina When Exposed to Currents and Waves.* Ph.D. thesis, University of Maryland.

McMahon, K., Van Dijk, K. J., Ruiz-Montoya, L., Kendrick, G. A., Krauss, S. L., Waycott, M., et al. (2014). The movement ecology of seagrasses. *Proc. R. Soc. B* 281:20140878. doi: 10.1098/rspb.2014.0878

Moore, K. A. (2004). Influence of seagrasses on water quality in shallow regions of the lower Chesapeake Bay. *J Coast Res* 20, 162–178. doi: 10.2112/SI45-162.1

Nepf, H. (2012). Flow and transport in regions with aquatic vegetation. *Annu. Rev. Fluid Mech.* 44, 123–142. doi: 10.1146/annurev-fluid-120710-101048

Nepf, H., and Vivoni, E. (2000). Flow structure in depth-limited, vegetated flow. *J. Geophys. Res.* 105, 28547–28557. doi: 10.1029/2000JC900145

Olsen, J. L., Stam, W. T., Coyer, J. A., Reusch, T. B., Billingham, M., Boström, C., et al. (2004). North Atlantic phylogeography and large-scale population differentiation of the seagrass *Zostera marina* L. *Mol. Ecol.* 13, 1923–1941. doi: 10.1111/j.1365-294X.2004.02205.x

Orth, R. J., Carruthers, T. J. B., Dennison, W. C., Duarte, C. M., Fourqurean, J. W., Heck, K. L., et al. (2006). A global crisis for seagrass ecosystems. *Bioscience* 56, 987–996. doi: 10.1641/0006-3568(2006)56[987:AGCFSE]2.0.CO;2

Palmer, M. R., Nepf, H., and Pettersson, T. J. R. (2004). Observations of particle capture on a cylindrical collector: implications for particle accumulation and removal in aquatic systems. *Limnol. Oceanogr.* 49, 75–85. doi: 10.4319/lo.2004.49.1.0076

Pan, Y., Chamecki, M., and Isard, S. A. (2014). Large-eddy simulation of turbulence and particle dispersion inside the canopy roughness sublayer. *J. Fluid Mech.* 753, 499–534. doi: 10.1017/jfm.2014.379

Randall Hughes, A., Hanley, T. C., Schenck, F. R., and Hays, C. G. (2016). Genetic diversity of seagrass seeds influences seedling morphology and biomass. *Ecology* 97, 3538–3546. doi: 10.1002/ecy.1587

Reidenbach, M. A., and Thomas, E. L. (2018). Influence of the seagrass, *Zostera marina*, on wave attenuation and bed shear stress within a shallow coastal bay. *Front. Mar. Sci.* 5:397. doi: 10.3389/fmars.2018.00397

Reusch, T. B., Stam, W. T., and Olsen, J. L. (2000). A microsatellite-based estimation of clonal diversity and population subdivision in *Zostera marina*, a marine flowering plant. *Mol. Ecol.* 9, 127–140. doi: 10.1046/j.1365-294x.2000.00839.x

Reusch, T. B. H. (2001). Fitness-consequences of geitonogamous selfing in a clonal marine angiosperm (*Zostera marina*). *J. Evol. Biol.* 14, 129–138. doi: 10.1046/j.1420-9101.2001.00257.x

Reynolds, L. K., McGlathery, K. J., and Waycott, M. (2012). Genetic diversity enhances restoration success by augmenting ecosystem services. *PLoS ONE* 7:e38397. doi: 10.1371/journal.pone.0038397

Rhode, J. M., and Duffy, J. E. (2004). Seed production from the mixed mating system of Chesapeake Bay (USA) eel- grass (*Zostera marina; Zosteraceae*). *Am. J. Bot.* 91, 192–197. doi: 10.3732/ajb.91.2.192

Ruckelshaus, M. H. (1995). Estimates of outcrossing rates and inbreeding depression in a population of the marine angiosperm *Zostera marina*. *Mar. Biol.* 123, 583–593. doi: 10.1007/BF00349237

Ruckelshaus, M. H. (1996). Estimation of genetic neighborhood parameters from pollen and seed dispersal in the marine angiosperm *Zostera marina* L. *Evolution* 50, 856–864. doi: 10.1111/j.1558-5646.1996.tb03894.x

Unsworth, R. K. F., Cullen, L. C., Pretty, J. N., Smith, D. J., and Bell, J. J. (2010). Economic and subsistence values of the standing stocks of seagrass fisheries: potential benefits of no-fishing marine protected area management. *Ocean Coast. Manag.* 53, 218–224. doi: 10.1016/j.ocecoaman.2010.04.002

van Katwijk, M., Thorhaug, A., Núria, M., Orth, R., Duarte, C., Kendrick, G., et al. (2016). Global analysis of seagrass restoration: the importance of large-scale planting. *J. Appl. Ecol.* 53, 567–578. doi: 10.1111/1365-2664.12562

Waycott, M., Duarte, C., Carruthers, T., Orth, R., Dennison, W., Olya, S., et al. (2009). Accelerating loss of seagrass across the globe threatens coastal ecosystems. *Proc. Nat. Acad. Sci. U.S.A.* 106, 12377–12381. doi: 10.1073/pnas.0905620106

Williams, S. L., and Heck, K. L. J. (2001). "Seagrass community ecology," in *Marine Community Ecology,* eds. M. D. Bertness, S. D. Gaines, and M. E. Hay (Sunderland, MA: Sinauer Associates).

Williams, S. L., and Orth, R. J. (1998). Genetic diversity and structure of natural and transplanted eelgrass populations in the Chesapeake and Chincoteague Bays. *Est. Coasts* 21, 118–128. doi: 10.2307/1352551

Wilson, J. D., and Sawford, B. L. (1996). Review of Lagrangian stochastic models for trajectories in the turbulent atmosphere. *Boundary Layer Meteorol.* 78, 191–210. doi: 10.1007/BF00122492

Wilson, J. D., and Yee, E. (2007). A critical examination of the random displacement model of turbulent dispersion. *Boundary Layer Meterorol.* 125, 399–416. doi: 10.1007/s10546-007-9201-x

Zipperle, A. M., Coyer, J. A., Reise, K., Stam, W. T., and Olsen, J. L. (2011). An evaluation of small-scale genetic diversity and the mating system in *Zostera noltii* on an intertidal sandflat in the Wadden Sea. *Ann. Bot.* 107, 127–133. doi: 10.1093/aob/mcq214

Conflict of Interest Statement: The authors declare that the research was conducted in the absence of any commercial or financial relationships that could be construed as a potential conflict of interest.

frontiers in Marine Science

PERSPECTIVE
published: 24 April 2019
doi: 10.3389/fmars.2019.00217

Bridging the Separation Between Studies of the Biophysics of Natural and Built Marine Canopies

Craig Stevens[1,2]* *and David Plew*[3]

[1] National Institute of Water and Atmospheric Research, Wellington, New Zealand, [2] Department of Physics, The University of Auckland, Auckland, New Zealand, [3] National Institute of Water and Atmospheric Research, Christchurch, New Zealand

We argue that there is a separation between studies of the biophysics of natural and "built" marine canopies. Here, by "built" we specifically refer to floating, suspended aquaculture canopies. These structures, combining support infrastructure and crop, exhibit several unique features relative to natural marine canopies, in that they take a particular species, suspend them in spatially structured, mono-cultured arrangement and then induce a systematic harvest cycle. This is in contrast to natural canopies that are irregular and variable in form, have natural recruitment and growth, and sustain some level of biodiversity and more exposed to climate extremes. We synthesize published work to identify the points of difference and similarity with natural canopy studies. This perspective article identifies four main themes relating to (i) key scales, (ii) structural configuration, (iii) connections between biology and physics and (iv) connecting natural and built canopy science. Despite clear differences between natural and built canopies, they have more in common than not and we suggest that both sub-fields would benefit from better connection across the divide.

Keywords: canopies, stratification, mixing, biophysics, flow-structure interactions

OPEN ACCESS

Edited by:
Marco Ghisalberti,
The University of Western Australia, Australia

Reviewed by:
Rodrigo Riera,
Catholic University of the Most Holy Conception, Chile
Andrew William Mackay Pomeroy,
The University of Western Australia, Australia

***Correspondence:**
Craig Stevens
craig.stevens@niwa.co.nz

Specialty section:
This article was submitted to Marine Ecosystem Ecology, a section of the journal Frontiers in Marine Science

Received: *20 November 2018*
Accepted: *08 April 2019*
Published: *24 April 2019*

Citation:
Stevens C and Plew D (2019) Bridging the Separation Between Studies of the Biophysics of Natural and Built Marine Canopies. Front. Mar. Sci. 6:217. doi: 10.3389/fmars.2019.00217

INTRODUCTION

In the marine environment, natural canopies (kelp beds, seagrass meadows etc.) provide significant ecological value (Seitz et al., 2013). At the same time, "built" canopies provided by aquaculture installations have economic value (Troell et al., 2014). We argue that, in part because of these different high-level drivers, there is a separation in the marine canopy biophysics literature whereby it is rare to see studies make the connection between natural marine canopies and built aquaculture canopies. In this Perspective article we consider the nature of the two classes of canopy, explore key comparative themes and then make suggestions for how to build interconnections between the two sub-fields.

Natural canopies are irregular and variable in form, have natural recruitment and growth, and sustain some level of biodiversity. Studies on natural canopies tend to have objectives that are ecosystem function-centric, documenting ecosystem services like maintaining habitats, promoting biodiversity and sustaining pathways of nutrients and matter (e.g., Duarte, 2000). Aquaculture canopies are constructed, regular structures with a controlled mono-culture life-cycle (recruitment and harvesting) and an associated diverse transient fouling community and associated motile

fauna (Stevens et al., 2008). Restored natural canopies form an intersectional category (Fonseca and Fisher, 1986). Aquaculture-based studies have focused primarily on (i) how various natural processes affect crop production and (ii) the role of cultured stocks in controlling some coastal ecosystems; largely as a result of how their feeding activity interacts directly and indirectly with energy flow and nutrient cycling. Ecological studies on aquaculture systems have much in common with studies on natural canopies, except that they tend to have at least one anthropogenic objective (i.e., what is the local carrying capacity? e.g., Byron et al., 2011).

Despite these overarching differences, there is little to distinguish the two classes of canopies from hydrodynamic and even biophysical perspectives. Considering flow distortion, turbulence, waves and nutrient transport; natural and built marine canopies have more in common than not – so why are their respective literatures so distinct? This perspective article addresses several fundamental questions in the context similarities and differences between built and natural canopies. First, is the separation real? Assuming it is, what are the key differences in canopy-induced processes for determining feeding and scales of food depletion? Are the differing details of the canopy structural configuration important? Finally, in the two systems do biological aspects like productivity and physiology connect differently with physical processes like transport and turbulence?

DOES THE SEPARATION EVEN EXIST AND IS THERE BENEFIT TO CLOSING IT?

A consideration of selected papers from the reference list supports the argument that a separation exists as it is rare to see an aquaculture hydrodynamics paper referenced in a natural canopy study, although the reverse is somewhat more common. Built canopies have key attributes that differ from natural canopies (Stevens et al., 2008; Klebert et al., 2013), prime amongst these is structural regularity (**Figure 1**). For example, a shellfish long-line tethers a sequence of buoys at the water surface and then suspends the shellfish crop beneath. Multiple long-lines are laid out at regular intervals in parallel, occasionally with gaps of open water between lines to improve flushing and/or navigation, to form a "farm." Similarly, caged fish structures moor a sequence of cages side by side along with their operating infrastructure. The suspended cages or crop extend vertically anywhere from a few meters to nearly on the sea bed. The result, whatever the arrangement, is that a population finds itself constrained mid-water column, some distance from shore with its success depending on adequate food supply and waste removal. The literature on built canopies is clearly useful, in itself, for applied questions relating to crop production and environmental impact. However, some understanding can be transferred in either direction (see **Table 1**) when considering related processes in natural canopies. In other words, what discoveries from the built literature can aid in understanding natural canopies – and vice versa?

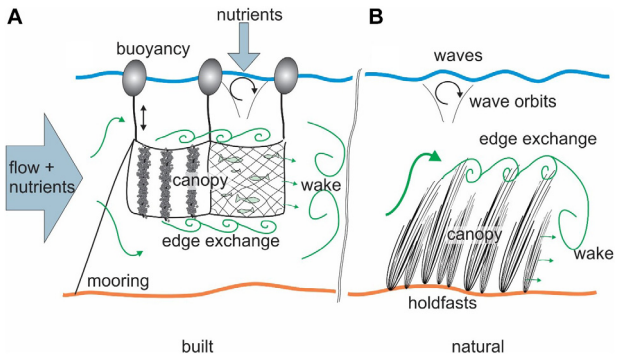

FIGURE 1 | Comparative synthesis diagram showing **(A)** built (showing both suspended longline shellfish and fish cage examples) and **(B)** natural (submerged used here as an example) canopies suggesting that while there are similarities in generalities (flow deformation, wakes, shear layers, etc.) there are substantial differences in the details like mooring/holdfast, buoyancy and nutrient supply. The decaying wave orbits in both panels indicate the approximate direct influence of surface waves.

WHAT ARE THE KEY SCALES FOR DETERMINING "FOOTPRINTS"?

When considering either canopy system, one can identify several key scales. The outer boundary conditions are set by (1) the far-field "embayment and inner continental shelf" scale which relates to the regional oceanography and meteorology. Depending on the scale of the canopy, this can reasonably be carried out in the absence of consideration of the effect of the canopy. If, however, the canopy is extensive it may well affect the wider circulation (Plew, 2011b). (2) The canopy/farm-scale is that at which crop feeding and effect is strongly influenced by the canopy and so representation of the details of the canopy is required. Focusing on the immediate region around the canopy provides information about the conditions that the population must live with. This highlights a common challenge at the canopy scale trying to separate the "canopy effect" from background variability. (3) The crop/organism scale is where the feeding takes place (**Figure 1**). This is likely influenced by the canopy-scale modulation of far-field drivers and needs detailed representation of the canopy and flow variability including waves.

At the regional to large scale, while models can have a vertical dimension (Wu et al., 2017), if the canopy is represented at all, it is typical to represent canopy drag as an enhanced bottom friction in 2D models (Grant and Bacher, 2001; Plew, 2011a,b; Shields et al., 2017). This approximation precludes detailed interaction between canopy and water column stratification (Plew et al., 2006) which can influence where food comes from as well as the fate of impacted water. This remains a challenge for both sub-disciplines.

Focus at the scale of the plant or crop forming the canopy brings the benefit that this is the scale at which biophysical interactions (photosynthesis, feeding, nutrient absorption, etc.) take place (e.g., Ackerman and Nishizaki, 2004). It is instructive to see approaches to determining useful scaling for natural

TABLE 1 | Comparison of key questions for built and natural canopy systems.

Context	Natural Canopy	Built Canopy
What are the key scales?		
Far-field scale	Likely same for both canopies	
Flow effect of canopy	Average enhanced drag coefficient	Structure provide scope for crop-scale representation
Footprint scale	Likely to be more diffuse as canopy boundaries not as well defined.	Of significant interest for impact studies
Are the details of the structural configuration important?		
Navigation	Only in that canopies may be removed as aid to navigation.	Yes, implicit in structural arrangement
Reduce or increased mixing	Density of canopy – difficult to estimate	Density of canopy – easier to estimate
In-out exchange	Scale of canopy and nature of canopy edges	Well-defined boundaries likely aid quantification
Surface waves	Well-studied with a range of impacts	Unexplored pathways due to buoyancy configuration
What are the key connections between biology and physics?		
Changing climate	Subject to natural migration strategies, i.e., limited and slow relative to rates of change.	Readily movable but controlled by socio-economic factors
Feeding strategies	Subject to nutrient availability	Readily variable but controlled by socio-economic factors
Resilience	Key science question especially in context of cumulative stressors and climate change.	Yes – within limits controlled by socio-economic factors
Canopy management	Restoration becoming more common.	Implicit in that an aquaculture installation is managed

canopy physical effects, like the laboratory experiments of Rosman et al. (2010), consider different physical representations for different scales. In a similar way, numerical models of built canopies move from highly resolved representations at fine scale (Delaux et al., 2011) to coarse representation at wider scales (Plew, 2011a; O'Donncha et al., 2015; Zhao et al., 2017) but the need to represent the canopy in a meaningful way remains. The same decisions need to be made when representing natural canopies (e.g., Mullarney and Henderson, 2018; van Rooijen et al., 2018).

The boundaries of any canopy are critical to quantifying fluxes of material in and out of the canopy region – and are often a key point of difference between built and natural canopies (**Figure 1**). Consequently, flow instability due to velocity shear is a key flux in both natural (Ghisalberti and Nepf, 2006) and built (Plew et al., 2006) systems. A suspended canopy can potentially sustain such boundaries both above and below the canopy. Adequately determining the mixing at the boundaries of the canopy is fundamental to understanding the canopy biomechanics. This is borne out when examining canopy retention times at larger scales in both natural and built canopies where any attempt at a nutrient budget requires estimation of boundary fluxes (e.g., Nepf et al., 2007; Venayagamoorthy et al., 2011; Lin et al., 2016). In addition, the leading and training edges form critical points whereby accelerated flow around the canopy (Tseung et al., 2016) or the recirculation in the trailing edge (Liu et al., 2017) perform a key mixing role in the near-field.

ARE THE DETAILS OF THE STRUCTURAL CONFIGURATION IMPORTANT?

It is important to consider if the details of the structural configuration have a bearing on the canopy effects – or if mixing or larger-scale variability dominate flows and transfer rates. Certainly, it has been long-established that substrate heterogeneity affects marine species (e.g., Menge, 1976). Shellfish long-line farming structures have a particular set of scales associated with their configuration (number of droppers, spacing, canopy size etc.). But this is not the only such arrangement to be found in built marine systems. Rafted shellfish structures tend to have quite dense aggregations of vertical lines beneath each raft (Newell and Richardson, 2014) but the rafts themselves are relatively well spaced to allow navigation and avoid line entanglement (Blanco et al., 1996). Fish cage installations take this to an extreme where several cages (more like flexible pens) are usually side by side and then the next installation is some distance away. A further complication with fish cages is they confine a free-swimming crop – sometimes in the tens of thousands per cage (He et al., 2018).

The ultimate cross-fertilization in canopy science is the improved understanding of the interaction of different types of canopies (O'Donncha et al., 2017). Abiological canopies are relevant in the discussion of built vs. natural canopies as they provide examples of flow evolution in the absence of any biological process. Marine renewable energy extraction arrays, while not common, are planned and in development in many places and offshore wind farms are already common (Broström, 2008). These would introduce what could be considered very large, sparse canopies. Wave energy devices, in particular, have much in common with early floating breakwaters which in turn were involved in some of the earliest canopy hydrodynamics studies (Elwany et al., 1995; Seymour, 1996). Non-canopy forming aquaculture such as on-bottom bivalve cultivation (e.g., Petersen et al., 2013; Saurel et al., 2013) provides extreme examples of structural configuration effects.

It is common for built canopies to be comprised of regular elements of crop (**Figure 1**) so that there are gaps in the canopy distribution affecting flow and in-out of canopy exchange (Stevens and Petersen, 2011). High resolution numerical

simulations found flow behavior very sensitive to flow-canopy orientation (Delaux et al., 2011). Mixing rates will affect the influence of any heterogeneity (Abdolahpour et al., 2017). Similarly, the role of gaps in canopy-flow exchange is a well-studied aspect of terrestrial canopies (e.g., Bohrer et al., 2008). Despite this, there has been less examination of this facet in the natural canopy literature (except e.g., Rosman et al., 2007; Kregting et al., 2011; El Allaoui et al., 2015; Hamed et al., 2017). Related to this point, most built canopies (aquaculture) are relatively sparse compared to natural canopies, and their dimensions commonly insufficient for a fully developed canopy flow to occur (the transition length is a function of the density of the canopy, Tseung et al., 2016). It is also important to recognize that the structural regularity actually makes some of the built canopy-scale observations possible. For example, it would not be possible to tow an undulator through most natural macroalgal canopies, whereas it is possible to work in the channels between shellfish rafts and long lines (Cranford et al., 2014).

An example of where built canopy understanding can benefit from natural canopy work is the role of surface waves (**Figure 1**). The macroalgal literature continues to make substantial advances in understanding of the response of individuals and canopies to wave forcing (e.g., Denny et al., 1997; Mullarney and Henderson, 2018). While some open-ocean studies exist (Plew et al., 2005; Gentry et al., 2017), aquaculture typically takes place in sheltered waters, where it is implicit that the farms will only be exposed to fetch-limited (i.e., short wavelength) waves. The influence of a surface wave decays exponentially with depth to zero, at half the wavelength (which is short). A consequence is that in aquaculture studies it is unusual to consider the influence of waves upon shellfish growth and behavior. However, it is clear that, as for a buoyant macroalgal frond, suspended canopy or raft shellfish culture structures directly link the crop to the surface wave field through the buoyancy of the supporting elements (Stevens et al., 2007). Therefore, even short wavelength waves can induce vertical velocities at depth in built canopies. This results in a relative velocity between crop and water – potentially with a strong vertical component. Again, relative motion in suspended natural canopies has been explored (Stevens et al., 2001; Lowe et al., 2005), along with waves associated with the canopy itself (monami – Ghisalberti and Nepf, 2009). So, it is not remarkable that this could affect shellfish and even caged fish and is a topic where the built canopy science stands to gain from the experiences of the macroalgal biophysics literature.

ARE THE CONNECTIONS BETWEEN BIOLOGICAL AND PHYSICAL PROCESSES UNDERSTOOD?

There are a range of connections between biology and physics – most of which will vary depending on canopy organism (e.g., Riisgård et al., 2011) and the in-canopy flow conditions. At the largest scale, the changing climate is central to natural canopy biophysical studies (e.g., Arias-Ortiz et al., 2018). Phenomenon like marine heat waves are impacting on both kinds of canopy and the associated ecosystems (Wernberg et al., 2016), but only the built canopy systems are in a position to rapidly adjust (Weatherdon et al., 2016).

Often these connections at the large scale, and the canopy differences, cascade to incorporate smaller scale interactions. For example, mussels generate feeding flows associated with their siphons (Riisgård et al., 2011), algae rely on diffusive processes (Hurd, 2000) and caged fish generate canopy-scale flows through their motility (Gansel et al., 2014; Johansson et al., 2014). The flow variability in the crop near-field suggests that any instantaneous snapshot of food depletion from a single point would fail to identify the effect of the feeding. This highlights the need when talking about scale to consider temporal scales also. For example, a "nutrient halo" whose scale is determined by time-averaging background turbulence and feeding rate as identified by Nielsen et al. (2016). Working at this crop-scale in natural (O'Riordan et al., 1995) and built (Plew et al., 2009) shellfish applications has a direct analogy with biophysics at the canopy-forming individual scale.

In a recent review of the magnitude and spatial extent of food depletion by bivalve aquaculture, Cranford (2018) emphasized the important role of the built canopy in limiting food depletion at all spatial scales. Canopy-induced flow reduction directly affects the degree of food depletion around individual mussel droppers as a result of the mussels re-filtering more of the same water instead of the feeding zone being sufficiently replenished by advection. This canopy effect at the scale of individual mussels ultimately limits the degree of depletion at canopy- and ecosystem-scales. Canopy-induced flow reduction has been shown to result in food depletion levels that are substantially lower than predicted by models that do not account for this physical effect (Cranford et al., 2014; Nielsen et al., 2016). Similar effects are seen in natural canopy studies (Boyle et al., 2004) but it would appear to be more difficult to achieve the depletion vs. distance measurements in a natural canopy as the crop elements are not so consistently spatially separated from one another.

Turbulence is a key quantity that influences transfer rates of material and energy both within, at the boundaries of, and in the background flow. One overarching question in all canopy mechanics is – "does the canopy generate more turbulence?" The answer is seemingly obvious – yes, due to the wakes of all the structural material in the water column. However, with the drag of the canopy and the slow-down of flow at the embayment scale (Plew et al., 2005), the system has the potential to produce less drag and wake at the individual element scale (Cranford et al., 2014). This is a demonstration of the multi-scale nature of flow-canopy interaction and seen equally in natural canopies (Ackerman and Okubo, 1993). Getting this balance right is fundamental to understanding mass fluxes in canopies (e.g., Pilditch et al., 2001; Strohmeier et al., 2005; Gaylord et al., 2007). Furthermore, the nature of the canopy edges has some bearing of how the wake develops as a more porous canopy with a relatively diffuse boundary will likely have a different wake than the abrupt end of a built canopy (**Figure 1**). The limited range of scales in built canopies lends itself to being more readily empirically quantified – the results of which are useful to both sub-disciplines.

CLOSING THE SEPARATION

Despite the various differences (**Figure 1** and **Table 1**) in canopy structure between built and natural systems, they have much in common. Furthermore, we suggest that studies of a particular approach (field observation, numerical simulations, physical model) have more in common with each other, regardless of being built or natural canopies, compared to the differences between approaches – which are substantial. It is not uncommon to see that studies designed to explore natural canopy behavior, especially where the approach involves physical or numerical modeling often appears as if it would have at least as relevant to built canopies as it does with the target natural canopy (e.g., Rosman et al., 2007; Qiao et al., 2016). Conversely, because they are constructed from a limited set of scales, built canopy studies seek to reduce, as much as is possible, the level of complexity when exploring flow-canopy interactions.

It is clear that the flow of information should be bi-directional. While debatable, we suggest that the natural canopy studies approach a problem with a more open perspective (e.g., Gaylord et al., 2007; Fram et al., 2008) than aquaculture studies which might have some focused targets (e.g., Maar et al., 2010; Newell and Richardson, 2014). This is in-part, we believe, due to the differing overarching drivers (economic vs. ecosystem) as well as the only partially overlapping research communities.

This perspective article is a call to better connect between the two fields of endeavor – so how do we do this? Certainly, it requires a better awareness of the various literature threads from both sides and cross-over of application of results. A common language should be possible relating in-water mixing processes to the canopy and substrate and the associated feedbacks (Nepf, 1999). It is likely that the research communities do not overlap sufficiently, so targeted combined special sessions at conferences would be one avenue of fostering better integration. A valuable result of such sessions would be an integrated review article. Ultimately, studies that seamlessly integrate across the separation to get at the best representation of bio-mechanics stand to generate the greatest advances.

AUTHOR CONTRIBUTIONS

CS and DP conceived the ideas. CS wrote the manuscript.

FUNDING

This work was supported by the National Institute for Water and Atmospheric Research (NIWA) Aquaculture Sustainability Program, the Danish Council for Strategic Research, research project "Production of Mussels: Mitigation and Feed for Husbandry (MuMiHus)" under grant agreement no. 09-066983 and the New Zealand Sustainable Seas National Science Challenge Project 4.2.2 Stressor Footprints.

ACKNOWLEDGMENTS

We would like to thank Pernille Nielsen, Peter Cranford, Jens K. Petersen, Barb Hayden, Joe O'Callaghan, and Niall Broekhuizen for support and advice. We would also like to thank two reviewers and the editor for their input and suggestions.

REFERENCES

Abdolahpour, M., Ghisalberti, M., Lavery, P., and McMahon, K. (2017). Vertical mixing in coastal canopies. *Limnol. Oceanogr.* 62, 26–42. doi: 10.1002/lno.10368

Ackerman, J. D., and Nishizaki, M. T. (2004). The effect of velocity on the suspension feeding and growth of the marine mussels *Mytilus trossulus* and *M. californianus*: implications for niche separation. *J. Mar. Sys.* 49, 195–208.

Ackerman, J. D., and Okubo, A. (1993). Reduced mixing in a marine macrophyte canopy. *Funct. Ecol.* 7, 305–309. doi: 10.3732/ajb.89.7.1119

Arias-Ortiz, A., Serrano, O., Masqué, P., Lavery, P. S., Mueller, U., Kendrick, G. A., et al. (2018). A marine heatwave drives massive losses from the world's largest seagrass carbon stocks. *Nat. Clim. Chang.* 8:338. doi: 10.1038/s41558-018-0096-y

Blanco, J., Zapata, M., and Moroño, Á. (1996). Some aspects of the water flow through mussel rafts. *Sci. Mar.* 60, 275–282.

Bohrer, G., Katul, G. G., Nathan, R., Walko, R. L., and Avissar, R. (2008). Effects of canopy heterogeneity, seed abscission and inertia on wind-driven dispersal kernels of tree seeds. *J. Ecol.* 96, 569–580. doi: 10.1111/j.1365-2745.2008.01368.x

Boyle, K. A., Kamer, K., and Fong, P. (2004). Spatial and temporal patterns in sediment and water column nutrients in a eutrophic southern California estuary. *Estuaries* 27, 378–388. doi: 10.1007/bf02803530

Broström, G. (2008). On the influence of large wind farms on the upper ocean circulation. *J. Mar. Syst.* 74, 585–591. doi: 10.1016/j.jmarsys.2008.05.001

Byron, C., Bengtson, D., Costa-Pierce, B., and Calanni, J. (2011). Integrating science into management: ecological carrying capacity of bivalve shellfish aquaculture. *Mar. Policy* 35, 363–370. doi: 10.1016/j.marpol.2010.10.016

Cranford, P. J. (2018). "Magnitude and extent of water clarification services provided by bivalve suspension feeding," in *Goods and Services of Marine Bivalves*, eds A. Smaal, J. Ferreira, J. Grant, J. Petersen, and Ø Strand (Cham: Springer).

Cranford, P. J., Duarte, P., Robinson, S. M., Fernández-Reiriz, M. J., and Labarta, U. (2014). Suspended particulate matter depletion and flow modification inside mussel (*Mytilus galloprovincialis*) culture rafts in the Ría de Betanzos, Spain. *J. Exp. Mar. Biol. Ecol.* 452, 70–81. doi: 10.1016/j.jembe.2013.12.005

Delaux, S., Stevens, C. L., and Popinet, S. (2011). High-resolution computational fluid dynamics modelling of suspended shellfish structures. *Environ. Fluid Mech.* 11, 405–425. doi: 10.1007/s10652-010-9183-y

Denny, M. W., Gaylord, B. P., and Cowen, E. A. (1997). Flow and flexibility II. The roles of size and shape in determining wave forces on the bull kelp Nereocystis luetkeana. *J. Exp. Biol.* 200, 3165–3183.

Duarte, C. M. (2000). Marine biodiversity and ecosystem services: an elusive link. *J. Exp. Mar. Biol. Ecol.* 250, 117–131. doi: 10.1016/s0022-0981(00)00194-5

El Allaoui, N., Serra, T., Soler, M., Colomer, J., Pujol, D., and Oldham, C. (2015). Modified hydrodynamics in canopies with longitudinal gaps exposed to oscillatory flows. *J. Hydrol.* 531, 840–849. doi: 10.1016/j.jhydrol.2015.10.041

Elwany, M. H. S., O'Rielly, W. C., Guza, R. T., and Flick, R. T. (1995). Effects of southern California kelp beds on waves. *J. Waterway Port Coast. Ocean Eng.* 121, 143–150. doi: 10.1061/(asce)0733-950x(1995)121:2(143)

Fonseca, M. S., and Fisher, J. S. (1986). A comparison of canopy friction and sediment movement between four species of seagrass with reference to their ecology and restoration. *Mar. Ecol. Prog. Ser.* 29, 15–22. doi: 10.3354/meps029015

Fram, J. P., Stewart, H. L., Brzezinski, M. A., Gaylord, B., Reed, D. C., Williams, S. L., et al. (2008). Physical pathways and utilization of nitrate supply to the

giant kelp, *Macrocystis pyrifera*. *Limnol. Oceanogr.* 53, 1589–1603. doi: 10.4319/lo.2008.53.4.1589

Gansel, L. C., Rackebrandt, S., Oppedal, F., and McClimans, T. A. (2014). Flow fields inside stocked fish cages and the near environment. *J. Offshore Mech. Arct. Eng.* 136, 031201. doi: 10.1115/1.4027746

Gaylord, B., Rosman, J. H., Reed, D. C., Koseff, J. R., Fram, J., MacIntyre, S., et al. (2007). Spatial patterns of flow and their modification within and around a giant kelp forest. *Limnol. Oceanogr.* 52, 1838–1852. doi: 10.4319/lo.2007.52.5.1838

Gentry, R. R., Froehlich, H. E., Grimm, D., Kareiva, P., Parke, M., Rust, M., et al. (2017). Mapping the global potential for marine aquaculture. *Nat. Ecol. Evol.* 1:1317. doi: 10.1038/s41559-017-0257-9

Ghisalberti, M., and Nepf, H. (2006). The structure of the shear layer in flows over rigid and flexible canopies. *Environ. Fluid Mech.* 6, 277–301. doi: 10.1007/s10652-006-0002-4

Ghisalberti, M., and Nepf, H. (2009). Shallow flows over a permeable medium: the hydrodynamics of submerged aquatic canopies. *Trans. Porous Media* 78:309. doi: 10.1007/s11242-008-9305-x

Grant, J., and Bacher, C. (2001). A numerical model of flow modification induced by suspended aquaculture in a Chinese bay. *Can. J. Fish. Aquat. Sci.* 58, 1003–1011. doi: 10.1139/f01-027

Hamed, A. M., Sadowski, M. J., Nepf, H. M., and Chamorro, L. P. (2017). Impact of height heterogeneity on canopy turbulence. *J. Fluid Mech.* 813, 1176–1196. doi: 10.1017/jfm.2017.22

He, Z., Faltinsen, O. M., Fredheim, A., and Kristiansen, T. (2018). The influence of fish on the mooring loads of a floating net cage. *J. Fluids Struct.* 76, 384–395. doi: 10.1016/j.jfluidstructs.2017.10.016

Hurd, C. L. (2000). Water motion, marine macroalgal physiology, and production. *J. Phycol.* 36, 453–472. doi: 10.1046/j.1529-8817.2000.99139.x

Johansson, D., Laursen, F., Fernö, A., Fosseidengen, J. E., Klebert, P., Stien, L. H., et al. (2014). The interaction between water currents and salmon swimming behaviour in sea cages. *PLoS One* 9:e97635. doi: 10.1371/journal.pone.0097635

Klebert, P., Lader, P., Gansel, L., and Oppedal, F. (2013). Hydrodynamic interactions on net panel and aquaculture fish cages: a review. *Ocean Eng.* 58, 260–274. doi: 10.1016/j.oceaneng.2012.11.006

Kregting, L. T., Stevens, C. L., Cornelisen, C. D., Pilditch, C. A., and Hurd, C. L. (2011). Effects of a small-bladed macroalgal canopy on benthic boundary layer dynamics: Implications for nutrient transport. *Aquat. Biol.* 14, 41–56. doi: 10.3354/ab00369

Lin, J., Li, C., and Zhang, S. (2016). Hydrodynamic effect of a large offshore mussel suspended aquaculture farm. *Aquaculture* 451, 147–155. doi: 10.1016/j.aquaculture.2015.08.039

Liu, C., Hu, Z., Lei, J., and Nepf, H. (2017). Vortex structure and sediment deposition in the wake behind a finite patch of model submerged vegetation. *J. Hydr. Eng.* 144:04017065. doi: 10.1061/(asce)hy.1943-7900.0001408

Lowe, R. J., Koseff, J. R., Monismith, S. G., and Falter, J. L. (2005).). Oscillatory flow through submerged canopies. Part 2. Canopy mass transfer. *J. Geophys. Res.* 110:C10017. doi: 10.1029/2004JC002789

Maar, M., Timmermann, K., Petersen, J. K., Gustafsson, K. E., and Storm, L. M. (2010). A model study of the regulation of blue mussels by nutrient loadings and water column stability in a shallow estuary, the Limfjorden. *J. Sea Res.* 64, 322–333. doi: 10.1016/j.seares.2010.04.007

Menge, B. A. (1976). Organization of the New England rocky intertidal community: role of predation, competition, and environmental heterogeneity. *Ecol. Monogr.* 46, 355–393. doi: 10.2307/1942563

Mullarney, J. C., and Henderson, S. M. (2018). "Flows within marine vegetation canopies," in *Advances in Coastal Hydraulics*, eds V. Panchang and J. Kaihatu (Singapore: World Scientific), 1–46. doi: 10.1142/9789813231283_0001

Nepf, H., Ghisalberti, M., White, B., and Murphy, E. (2007). Retention time and dispersion associated with submerged aquatic canopies. *Water Resourc. Res.* 43, 1–10. doi: 10.1029/2006WR005362

Nepf, H. M. (1999). Drag, turbulence, and diffusion in flow through emergent vegetation. *Water Resourc. Res.* 35, 479–489. doi: 10.1016/j.watres.2008.10.027

Newell, C. R., and Richardson, J. (2014). The effects of ambient and aquaculture structure hydrodynamics on the food supply and demand of mussel rafts. *J. Shellfish Res.* 33, 257–272. doi: 10.2983/035.033.0125

Nielsen, P., Cranford, P. J., Maar, M., and Petersen, J. K. (2016). Magnitude, spatial scale and optimization of ecosystem services from a nutrient extraction mussel farm in the eutrophic Skive Fjord. Denmark. *Aquac. Environ. Interact.* 8, 311–329. doi: 10.3354/aei00175

O'Donncha, F., Hartnett, M., and Plew, D. R. (2015). Parameterizing suspended canopy effects in a three-dimensional hydrodynamic model. *J. Hydr. Res.* 53, 714–727. doi: 10.1080/00221686.2015.1093036

O'Donncha, F., James, S. C., and Ragnoli, E. (2017). Modelling study of the effects of suspended aquaculture installations on tidal stream generation in Cobscook Bay. *Renew. Energy* 102, 65–76. doi: 10.1016/j.renene.2016.10.024

O'Riordan, C. A., Monismith, S. G., and Koseff, J. R. (1995). The effect of bivalve excurrent jet dynamics on mass transfer in a benthic boundary layer. *Limnol. Oceanogr.* 40, 330–344. doi: 10.4319/lo.1995.40.2.0330

Petersen, J. K., Maar, M., Ysebaert, T., and Herman, P. M. (2013). Near-bed gradients in particles and nutrients above a mussel bed in the Limfjorden: influence of physical mixing and mussel filtration. *Mar. Ecol. Prog. Ser.* 490, 137–146. doi: 10.3354/meps10444

Pilditch, C. A., Grant, J., and Bryan, K. R. (2001). Seston supply to scallops in suspended culture. *Can. J. Fish. Aquat. Sci.* 58, 241–253. doi: 10.1139/f00-242

Plew, D. R. (2011a). Depth-averaged drag coefficient for modeling flow through suspended canopies. *J. Hydr. Eng.* 137, 234–247. doi: 10.1061/(asce)hy.1943-7900.0000300

Plew, D. R. (2011b). Shellfish farm-induced changes to tidal circulation in an embayment, and implications for seston depletion. *Aquac. Environ. Interact.* 1, 201–214. doi: 10.3354/aei00020

Plew, D. R., Enright, M. P., Nokes, R. I., and Dumas, J. K. (2009). Effect of mussel bio-pumping on the drag on and flow around a mussel crop rope. *Aquac. Eng.* 40, 55–61. doi: 10.1016/j.aquaeng.2008.12.003

Plew, D. R., Spigel, R. H., Stevens, C. L., Nokes, R. I., and Davidson, M. J. (2006). Stratified flow interactions with a suspended canopy. *Environ. Fluid Mech.* 6, 519–539. doi: 10.1007/s10652-006-9008-1

Plew, D. R., Stevens, C. L., Spigel, R. H., and Hartstein, N. D. (2005). Hydrodynamic implications of large offshore mussel farms. *IEEE J. Ocean. Eng.* 30, 95–108. doi: 10.1109/joe.2004.841387

Qiao, J. D., Delavan, S. K., Nokes, R. I., and Plew, D. R. (2016). Flow structure and turbulence characteristics downstream of a spanwise suspended linear array. *Environ. Fluid Mech.* 16, 1021–1041. doi: 10.1007/s10652-016-9465-0

Riisgård, H. U., Jørgensen, B. H., Lundgreen, K., Storti, F., Walther, J. H., Meyer, K. E., et al. (2011). The exhalant jet of mussels *Mytilus edulis*. *Mar. Ecol. Progr. Ser.* 437, 147–164. doi: 10.3354/meps09268

Rosman, J. H., Koseff, J. R., Monismith, S. G., and Grover, J. (2007). A field investigation into the effects of a kelp forest (*Macrocystis pyrifera*) on coastal hydrodynamics and transport. *J. Geophys. Res. Oceans* 112:C2. doi: 10.1029/2005JC003430

Rosman, J. H., Monismith, S. G., Denny, M. W., and Koseff, J. R. (2010). Currents and turbulence within a kelp forest (*Macrocystis pyrifera*): Insights from a dynamically scaled laboratory model. *Limnol. Oceanogr.* 55, 1145–1158. doi: 10.4319/lo.2010.55.3.1145

Saurel, C., Petersen, J. K., Wiles, P. J., and Kaiser, M. J. (2013). Turbulent mixing limits mussel feeding: direct estimates of feeding rate and vertical diffusivity. *Mar. Ecol. Prog. Ser.* 485, 105–121. doi: 10.3354/meps10309

Seitz, R. D., Wennhage, H., Bergström, U., Lipcius, R. N., and Ysebaert, T. (2013). Ecological value of coastal habitats for commercially and ecologically important species. *ICES J. Mar. Sci.* 71, 648–665. doi: 10.1093/icesjms/fst152

Seymour, R. J. (1996). Discussion of Effects of southern California kelp beds on waves. *J. Waterway Port Coast. Ocean Eng.* 122, 207–208. doi: 10.1061/(asce)0733-950x(1996)122:4(207)

Shields, F. D. Jr., Coulton, K. G., and Nepf, H. (2017). Representation of vegetation in two-dimensional hydrodynamic models. *J. Hydr. Eng.* 143:02517002. doi: 10.1061/(ASCE)HY.1943-7900.0001320

Stevens, C., Plew, D., Hartstein, N., and Fredriksson, D. (2008). The physics of open-water shellfish aquaculture. *Aquac. Eng.* 38, 145–160. doi: 10.1016/j.aquaeng.2008.01.006

Stevens, C. L., Hurd, C. L., and Smith, M. J. (2001). Water motion relative to subtidal kelp fronds. *Limnol. Oceanogr.* 46, 668–678. doi: 10.4319/lo.2001.46.3.0668

Stevens, C. L., and Petersen, J. K. (2011). Turbulent, stratified flow through a suspended shellfish canopy: implications for mussel farm design. *Aquac. Environ. Interact.* 2, 87–104. doi: 10.3354/aei00033

Stevens, C. L., Plew, D. R., Smith, M. J., and Fredriksson, D. W. (2007). Hydrodynamic forcing of long-line mussel farms: observations. *J. Waterway Port Coast. Ocean Eng.* 133, 192–199. doi: 10.1061/(asce)0733-950x(2007)133:3(192)

Strohmeier, T., Aure, J., Duinker, A., Castberg, T., Svardal, A., and Strand, O. (2005). Flow reduction, seston depletion, meat content and distribution of diarrhetic shellfish toxins in a long-line blue mussel (*Mytilus edulis*) farm. *J. Shellfish Res.* 24, 15–23. doi: 10.2983/0730-8000(2005)24%5B15:frsdmc%5D2.0.co;2

Troell, M., Naylor, R. L., Metian, M., Beveridge, M., Tyedmers, P. H., Folke, C., et al. (2014). Does aquaculture add resilience to the global food system? *Proc. Natl. Acad. Sci. U.S.A.* 111, 13257–13263. doi: 10.1073/pnas.1404067111

Tseung, H. L., Kikkert, G. A., and Plew, D. (2016). Hydrodynamics of suspended canopies with limited length and width. *Environ. Fluid Mech.* 16, 145–166. doi: 10.1007/s10652-015-9419-y

van Rooijen, A., Lowe, R., Ghisalberti, M., Conde-Frias, M., and Tan, L. (2018). Predicting current-induced drag in emergent and submerged aquatic vegetation canopies. *Front. Mar. Sci.* 5:449. doi: 10.3389/fmars.2018.00449

Venayagamoorthy, S. K., Ku, H., Fringer, O. B., Chiu, A., Naylor, R. L., and Koseff, J. R. (2011). Numerical modeling of aquaculture dissolved waste transport in a coastal embayment. *Environ. Fluid Mech.* 11, 329–352. doi: 10.1007/s10652-011-9209-0

Weatherdon, L. V., Magnan, A. K., Rogers, A. D., Sumaila, U. R., and Cheung, W. W. (2016). Observed and projected impacts of climate change on marine fisheries, aquaculture, coastal tourism, and human health: an update. *Front. Mar. Sci.* 3:48. doi: 10.3389/fmars.2016.00048

Wernberg, T., Bennett, S., Babcock, R. C., De Bettignies, T., Cure, K., Depczynski, M., et al. (2016). Climate-driven regime shift of a temperate marine ecosystem. *Science* 353, 169–172. doi: 10.1126/science.aad8745

Wu, Y., Hannah, C. G., O'Flaherty-Sproul, M., and Thupaki, P. (2017). Representing kelp forests in a tidal circulation model. *J. Mar. Syst.* 169, 73–86. doi: 10.1016/j.jmarsys.2016.12.007

Zhao, F., Huai, W., and Li, D. (2017). Numerical modeling of open channel flow with suspended canopy. *Adv. Water Resourc.* 105, 132–143. doi: 10.1016/j.advwatres.2017.05.001

Conflict of Interest Statement: The authors declare that the research was conducted in the absence of any commercial or financial relationships that could be construed as a potential conflict of interest.

frontiers in Marine Science

REVIEW
published: 07 June 2019
doi: 10.3389/fmars.2019.00279

Biophysical Interactions in Fragmented Marine Canopies: Fundamental Processes, Consequences, and Upscaling

*Andrew M. Folkard**

Lancaster Environment Centre, Lancaster University, Lancaster, United Kingdom

Spatial fragmentation is a near-ubiquitous characteristic of marine canopies. Biophysical interactions with fragmented canopies are multi-faceted and have many significant implications at multiple scales. The aims of this paper are to review research on biophysical interactions in fragmented marine canopies, identify current gaps in knowledge and understanding, and propose ways forward. The review starts at the patch/gap scale and focuses initially on hydrodynamic interactions. It then considers the consequences of these interactions for particulate and dissolved material, and distributions of canopy-associated organisms. Finally, it addresses issues of upscaling to landscape-scale and ways in which this research can be applied to marine landscape management. Work on a broad range of canopy types is considered, including micro-algal biofilms and turf algae; macro-algae, seagrasses and coral reefs; saltmarsh vegetation and mangroves. Although the focus is on marine canopies, insights from studies of fragmented canopies in other contexts are drawn on where relevant. These include freshwater environments and terrestrial forests, grasslands, crop canopies, and urban areas. Specific areas requiring greater attention are highlighted. As a result of this meta-analysis, the following recommendations are made for further research. A lack of basic data is identified across all canopy types regarding the formation, fate and spatial and temporal characteristics of canopy patches, gaps, and spatial structure. Studies of hydrodynamics with fragmented canopies would benefit from shifting focus toward more non-uniform, realistic configurations, while ecological research in this area would benefit from a move toward configurations that are more controlled and tractable for quantitative modeling. More comparative studies across canopy types would enable understanding of their biophysical interactions and their consequences to be more fully tested and developed. A greater incorporation of chemical aspects of canopy systems into work that has hitherto focused on biophysical interactions would also be pertinent. Upscaling of patch and gap-scale phenomena to landscape-scale is identified as a crucial topic, since it is at the latter scale that management efforts are most readily carried out. Overall, an approach that balances hydrodynamics, marine canopy ecology, spatial analysis of landscapes, biogeochemistry, and socio-environmental interactions is recommended.

Keywords: marine canopies, biophysical interactions, hydrodynamics, fragmentation, upscaling, patches, gaps

OPEN ACCESS

Edited by:
Marco Ghisalberti,
The University of Western Australia, Australia

Reviewed by:
Mariana Mayer Pinto,
University of New South Wales, Australia
H. Nepf,
Massachusetts Audubon Society, United States

***Correspondence:**
Andrew M. Folkard
a.folkard@lancaster.ac.uk

Specialty section:
This article was submitted to Marine Ecosystem Ecology, a section of the journal Frontiers in Marine Science

Received: *13 August 2018*
Accepted: *13 May 2019*
Published: *07 June 2019*

Citation:
Folkard AM (2019) Biophysical Interactions in Fragmented Marine Canopies: Fundamental Processes, Consequences, and Upscaling. Front. Mar. Sci. 6:279. doi: 10.3389/fmars.2019.00279

INTRODUCTION

Aims, Methods, and Structure

Spatial fragmentation – which can range from apparently random distributions to strongly-ordered patterning – is a near-ubiquitous characteristic of biotic and biogenic marine canopies (Thomson et al., 2012; Folkard and Bouma, 2016). It is found in both newly-developing and damaged canopies, as well as in established canopies in equilibrium with their surroundings. It can indicate healthy, resilient ecosystem functioning (Pringle and Tarnita, 2017) or stress and increasing – often anthropogenic – pressures (Fraschetti et al., 2012). The effects of interactions between hydrodynamic processes and fragmented canopies are complex, and dependent on a variety of biotic and abiotic factors. They are of fundamental importance to the structure, functioning and services of canopy ecosystems, since hydrodynamic processes are primary causes of (mechanical) stresses and facilitations (e.g., nutrient supply) to canopies and the ecosystems they support (e.g., Folkard, 2016). The hydrodynamics of fragmented canopies are more spatially heterogeneous than the hydrodynamics of homogeneous canopies – because of the spatial heterogeneity of the canopies themselves – and this leads to heterogeneity in their stresses and facilitations, e.g., spatial variations in sheltering (e.g., Folkard, 2005) and nutrient supply (e.g., Morris et al., 2008). Fragmentation of canopies also leads to their becoming more vulnerable to external pressures (Gera et al., 2013). Understanding the large-scale impacts these effects have is therefore important for managing the many coastal areas where marine canopies are found, especially those affected by anthropogenic stresses and climate change (El Allaoui et al., 2016).

The term 'marine canopy' can cover a wide range of types of bed cover. These have been studied with different emphases, according to the priorities and drivers of the research communities working on them. This paper brings together research on spatial canopy fragmentation and its interactions with physical processes (primarily hydrodynamics, but also sediment transport and other phenomena driven by hydrodynamics) from this wide range of canopy types. From this collation, it creates a structured synthesis of work in this field. From this, it compares approaches and progress in work focused on different canopy types to determine what can be learnt about each one, and to identify ways of developing more universal understanding. To perform this collation of literature, searches were carried out using Web of Science[1]. Searches were made for articles that included in their title, abstract or keywords: words beginning with "patch," "gap," "fragment," or "heterogen"; one or more canopy-type name (seagrass, seaweed, macrophyte, macroalgae, kelp, mangrove, saltmarsh, alga, biofilm, coral) or the word "canopy" or "canopies"; and one or more word referring to hydrodynamic processes (flow, current, wave, turbulence, hydrodynamics). For each word, wildcard asterisks were added to the end so that plurals and other related words would be found (e.g., turbulen* was used to pick up turbulent, turbulence, turbulently etc.). This gave several thousand results, which were then filtered by date (the last 10 years – since 2008, as the initial search was completed in 2018) and for papers before that date, by number of citations (selecting only those papers with > 50 citations). The cutoffs for date and citation number were chosen semi-arbitrarily to reduce the number of papers to a sufficiently large, but manageable amount. The resulting sample of several hundred papers were then filtered by subjective analysis of their titles and, in cases where this did not produce a clear decision, by reading their abstracts. The resulting list was checked to ensure that it included key papers from the author's own knowledge of the literature. This resulted in a final set of approximately 300 papers on which this review was constructed, although not all of them survived the drafting process to appear in the final manuscript. Subsequently, smaller, more focused searches were used to identify papers on specific topics (approaches to habitat fragmentation in landscape ecology and flow-canopy interactions in terrestrial contexts) to fill gaps that arose in earlier drafts of the review. A small number (∼10) papers recommended by reviewers have also been added to the final form of the manuscript.

The remainder of the paper is structured as follows. I begin, in the next section, by justifying my use of patches and gaps as the 'unit elements' of canopy fragmentation, and identifying the types of canopies to be covered. The following sections then lay out the structured synthesis of research across canopy types mentioned above. This starts from fundamental processes and works up to their consequences at landscape-scale for restoration and management. Thus, firstly, the causes, formation and evolution of individual canopy patches and gaps are reviewed. I then focus on the hydrodynamics of individual patches and gaps. This is followed by a section reviewing current knowledge of the consequences of these hydrodynamics-patch/gap interactions in terms of the transport and deposition of particulates and solutes, and the distribution of organisms. I then consider the upscaling of these consequences, firstly via studies of interactions between multiple patches and gaps, and then from a landscape-scale perspective. I then consider application of this work to marine canopy landscape restoration and management. Finally, I take a comparative overview of all this work, identify key research questions and recommend possible ways forward. Although the focus here is on marine benthic canopies, throughout, insights from studies of fragmented canopies heterogeneity in other contexts will be drawn upon where they provide relevant insights. These include freshwater lentic and lotic environments and terrestrial environments, including forest, grassland and crop canopies and urban areas.

FRAMING: PATCHES, GAPS, AND CANOPY TYPES

Characterization of Canopy Fragmentation in Terms of Patches and Gaps

The landscape-scale spatial structure of the sea floor in the coastal zone is often made up of patches of biota of various different sizes within a larger abiotic matrix (Robbins and Bell, 1994). The

[1]https://clarivate.com/products/web-of-science/

inverse situation is also possible, in which the matrix made up of an approximately continuous biotic or biogenic canopy punctuated by gaps of relatively bare substrate or reduced canopy density (El Allaoui et al., 2016). Thus, these landscapes can be characterized spatially in terms of patches and gaps. There are many metrics associated with this perspective – for example, patch or gap size and density, edge length density (the mean length of canopy edge per unit area) – that have become widely used, particularly via earlier versions of the widely-used landscape ecology software package FRAGSTATS (McGarigal and Marks, 1995). As the field of landscape ecology has developed, alternative perspectives, in which fragmented landscapes are characterized by gradients, have been promoted (e.g., McGarigal and Cushman, 2005; McGarigal et al., 2009). More recently, there have been calls to re-think the conceptual foundations of landscape ecology, in light of better understanding of the non-linearity of relationships that determine the effects of fragmentation on ecosystems (e.g., Didham et al., 2012; Villard and Metzger, 2014; Liao et al., 2017). Thus, in some ways, research into canopy fragmentation has moved significantly beyond its characterization in terms of patches and gaps. Nevertheless, there are also many situations, where canopies are commonly organized into clearly delineated patches (e.g., salt marsh pioneer zones), or extended cover with clearly delineated gaps (e.g., seagrass meadows, mangroves). Therefore, the patch/gap conceptualization remains important. It also provides an idealized "unit element" of fragmentation for modeling studies of interactions between hydrodynamics and other physical processes, and fragmented canopies. Since this review starts from a focus on canopy-hydrodynamics interactions, therefore, it uses the patch/gap conceptualization.

This raises the question of how patches and gaps are defined. In many situations, this will be straightforward – as noted above, canopy patches and gaps are clearly delineated in many marine contexts. However, at times their edges are indistinct, and at others it is not clear whether a canopy distribution is a single but morphologically-complex patch, or a mosaic of several individual patches. For further discussion on this issue, the reader is directed toward Schoelynck et al. (2018). Hereinafter, I will assume that patch and gap edges are clearly defined.

Canopy Typology

In a marine context, a range of benthic canopies may be identified. They can be distinguished from each other in many ways. Given that this review starts with canopy-hydrodynamics interactions, they are distinguished here in terms of the main parameters that govern these interactions, namely: (i) their height compared to the surrounding substrate and water depth; and (ii) the rigidity or flexibility of the canopy-forming organisms. The choice of what to include and exclude from this typology is, inevitably, somewhat subjective. Because the intention of the paper is comparative, the choice of canopy types is deliberately broad. Moreover, what constitutes a patch of canopy, and what is deemed the surrounding matrix depends on the scale of interest. Thus, for example, when studying seagrass meadows, the matrix of "bare substrate" surrounding patches of seagrass is typically covered by lower-growing organisms. But if the lower-growing organisms are the community of interest, interest will focus on a smaller spatial scale, at which their vertical structure becomes relevant (e.g., Salta et al., 2013), and at which they can therefore be considered to be canopies. Hence, the smallest canopies included in this comparison are "micro-canopies" including micro-algal biofilms and turf algae. The second type of canopy is arguably the "classical" canopy, consisting of a permeable region whose elements rise significantly above the substrate. These include macro-algae beds, seagrass canopies and coral reefs. In the cases of macro-algae and seagrasses, these are made up of highly flexible elements, which pronate in the direction of flow, and oscillate back and forth in response to wave-forcing. The third category consists of pioneer saltmarsh vegetation but also includes pneumatophore roots of mangrove genera such as *Avicennia* and *Sonneratia*. These canopies are also permeable, but their elements tend to be more rigid than macro-algae and seagrasses. Moreover, they are found in inter-tidal regions, so that sometimes they fill the full water column depth and emerge above the water surface, while at others they may be fully submerged. Finally, mangrove genera with stilt roots such as *Rhizophora* form relatively rigid sub-aqueous canopies that are always emergent. Many of the areas of research reviewed herein are dominated by studies of one of these canopy categories, whereas others have been investigated in the context of several. Moreover, some of these types of canopy form patches or gaps more than others. For example, saltmarsh plants such as *Spartina anglica* typically form clearly defined patches in the pioneer zone, and canopy gaps are relatively common occurrences in seagrass meadows and mangroves. On the other hand, whilst coral reefs are highly spatially heterogeneous, they are not typically organized into clearly distinguished patches and gaps (Lowe and Falter, 2015). As a result, while there is an extensive literature on coral reef hydrodynamics (for reviews, see Monismith, 2007; Lowe and Falter, 2015), there is very little on the hydrodynamics of coral patches or gaps.

PATCHES AND GAPS: FORMATION AND CAUSES

Patches

Canopy patches are often found in areas that have been newly-colonized by the canopy-forming organism. The patches can grow from propagules or by clonal growth in clonal organisms such as seagrasses. Propagules can be dispersed widely, hence the creation of isolated patches. This dispersal can occur over very long distances, notably in seagrasses (Grech et al., 2016). and mangroves (Harwell and Orth, 2002).

Once they establish, the spatial structure of canopy patches is controlled by their growth strategy, which differs between species. For example, dense plant species can cause flow to deflect and accelerate around themselves, which militates against patch expansion because new shoots cannot survive in these faster flows. As a result, they tend to expand by releasing plant fragments which establish on bare substrate away from the parent patches and grow into new patches. On the other hand,

sparse species, which alter the flow less strongly, can grow more easily via expansion of existing patches (Verschoren, 2017). The distribution of patches is often affected by geology, topography and shelter from hydrodynamics stresses (e.g., energetic waves or strong tidal currents), although the underlying factor is usually access to sufficient nutrients and light (Koch, 2001). For example, Parnell (2015) found patches of giant kelp (*Macrocystis pyrifera*) and elk kelp (*Pelagophycus porra*) occurred preferentially on topographic highs, and Rinde et al. (2014) found that patches of the kelp *Laminaria hyperborea* established mainly on ridges. The higher elevation thus afforded to the kelp provides better access to water column nutrients and light. In contrast, Di Carlo et al. (2005) found that in shallow, well-lit waters, seagrass establishment was densest in topographic lows, because of the deeper layer of nutrient-rich sediment there. Similarly, Nardin et al. (2016) found that mangroves in a rapidly prograding area of the Mekong delta expanded as continuous coverage in areas of high sediment availability, but as sparse patches in areas of lower sediment supply. In both these cases, greater access to substrate nutrients is the determining factor. Patchy colonization may also be associated with preferential growth in areas where hydrodynamic stresses are lower, which may themselves be patchily distributed. For example, Francoeur et al. (1998) found that microform bed clusters provided refugia that allowed spatially-patchy establishment of periphyton in fast flowing rivers.

Canopy patchiness may also occur in post-disturbance areas, where canopies are damaged but recovering. The spatial pattern that this results in is affected by multiple factors. Underwood (1998) found that in an inter-tidal community of the macroalgae *Hormosira banksia*, post-storm patchiness was primarily caused by variations in the amount of damage sustained during the storm. Such recovery may also be subject to Allee effects (the weakening of individual plants' reproductive success with decreasing population density) leading to the canopy's accelerated decline, for example due to pollen limitation in sparse communities of intertidal *Zostera noltii*. This can impair their recovery even after environmental conditions have improved from those that caused their decline (van Tussenbroek et al., 2016).

As well as being indicative of newly-colonizing and post-disturbance canopies, patchiness can be a consequence of communities' spatial self-organization (Rietkerk and van de Koppel, 2008). This tends to result in pattern formation (Pringle and Tarnita, 2017), which can be complex and not just uniformly-spaced or -sized patches or stripes (van Wesenbeeck et al., 2008; van de Koppel et al., 2012). For example, it may be manifested as frequency distributions of patch size or separation distance which follow power law functions, i.e., where the probability that a patch's size (or distance from its nearest neighbor patch) is greater than some value s is proportional to $s^{-\beta}$, where β is a constant (Schoelynck et al., 2012). Spatial self-organization is defined as a process whereby large-scale ordered patterns emerge from disordered initial conditions due to small-scale interactions between organisms (Liu et al., 2014). It is generally considered to be due to scale-dependent feedbacks (Rietkerk and van de Koppel, 2008) – processes whereby organism interactions change from positive to negative as spatial scale is varied. For example, pioneer salt marsh vegetation shoots grow together in patches for mutual protection and sediment and nutrient retention. But this causes flow to accelerate around them, causing increased substrate scouring which militates against shoots establishing within a certain distance of an established patch. Thus, near-field positive effects combined with far-field negative effects create patches (van Wesenbeeck et al., 2008). In other cases, the positive effect of nutrient retention by patches is counterbalanced by reducing light availability for each shoot as patches get larger (Gera et al., 2013).

Gaps

Homogeneous canopies in which gaps may form tend to occur in regions where conditions are relatively uniform over wide areas, i.e., in the sub-tidal or in mangrove forests, rather than in transitional areas such as the inter-tidal, where canopies are often patchier. The main causes of gap formation include edaphic variations; damage or removal; burial and grazing. Edaphic variations result in canopy gaps where substrate is relatively poor or thin. Damage or removal can be due to natural forces – typically storms, but also mechanisms such as ice scouring (Cervin et al., 2004) – or anthropogenic causes, such as boat anchors, propellers, or infrastructure installation (e.g., Serrano et al., 2016). Likewise, burial can be caused by natural movements of bed material, usually during storms (Bell et al., 1999), or human activity such as deposition of dredging spoil. Herbivorous grazing can be relatively subtle, creating small scale mosaics of herbivore preferred and avoided patches, promoting plant biodiversity and resilience (Weerman et al., 2011; Howison et al., 2017), or more complete, leading to invasion by other species (e.g., Davies et al., 2007) or the creation of bioturbation pits (Yager et al., 1993). Grazing appears to be more important in some types of canopy (e.g., seagrass meadows, Townsend and Fonseca, 1998; Gera et al., 2013; periphyton biofilms, Gresens and Lowe, 1994; Holomuzki et al., 2006) than in others (e.g., macro-algae beds), although it may have a role in the persistence of gaps in the latter (Thomson et al., 2012). In some contexts, gap formation can be more complex. For example, in Argentinian salt marshes, Escapa et al. (2015) found salt pans formed gaps in *Sarcocornia*-dominated areas. They deduced that this was due to *Sarcocornia* growing in dense patches and providing shelter for crabs (*Neohelice granulata*). The crabs construct burrows, causing the *Sarcocornia* patch centers to die off. The patches then lose elevation relative to the surrounding marsh, and salt pans form within the depressions. Thus, the gaps are formed by interactions between biotic and abiotic processes.

Data on the extent, number and size of gaps in marine canopies is patchy. Bell et al. (1999) reported that gaps constituted 2.4–5.7% of a monospecific meadow of the seagrass *Halodule wrightii*. Gaps in algal canopies have been found to be larger at exposed sites than on sheltered coastlines, suggesting that a combination of exposure to external stresses and internal ecosystem context – e.g., canopy composition and grazing intensity – is fundamental to gap characteristics (Wernberg and Connell, 2008; Gera et al., 2013). Gap age appears to vary greatly. For example, Bell et al. (ibid.) found that most gaps in the

Halodule wrightii meadow they studied persisted for less than 6 months, whereas Thomson et al. (2012) inferred, from the ages of invertebrates within them, that gaps in the macroalgae canopies they studied had persisted for decades.

As is the case for patches, gaps are often in a dynamic state of evolution. Both seagrass (*Halodule wrightii*, Bell et al., 1999) and macrolagae (*Ascophyllum nodosum*, Cervin et al., 2004) canopy gaps have been observed to recover by re-growth or recruitment of the same species as the surrounding meadows. Jimenez-Ramos et al. (2017) noted that gaps and sparse areas of canopies have less self-shading, which should boost growth in them, homogenizing the canopy. Similarly, in a study of flow through seagrass meadow simulations made up of sparser and denser regions in various configurations, Adhitya et al. (2014) found that the flow tends to favor supply of water column resources to sparse areas, which may lead to homogeneity. In other cases, however, gaps are filled by other species. This can be caused by these invasive species being faster growing (e.g., Cervin et al., 2005) or having other advantageous species characteristics. For example, Vogt et al. (2012) observed that the regeneration of open patches after hurricanes in mangroves was dominated by flood-tolerant *Rhizophora*, which outcompeted the faster-growing, but less flood-tolerant pioneer *Laguncularia racemosa*), while Voerman et al. (2017) found that the ability of the invasive species *Caulerpa filiformis* to respond better to disturbance than native species allows it to outcompete them. Gap-filling mechanisms may also be affected by the clarity of gaps. For example, Wernberg and Connell (2008) found fucalean algae to be recruited into complete clearings in a macroalgae canopy, whereas turf algae cover was more prominent in less complete clearings. The relative competitiveness of re-growth of meadow immediately surrounding a gap versus invasion into the gap from outside the meadow is likely affected by gap geometry and the permeability of its surrounding meadow. This determines whether flow arriving from through the canopy (favoring the surrounding meadow) or over the canopy (favoring invasion from outside) dominates within the gap (Folkard, 2016).

HYDRODYNAMICS OF CANOPY PATCHES AND GAPS

Much work has been carried out in recent decades on the hydrodynamics of marine canopy patches, gaps, and their boundaries. Most of this work has been concerned with canopies of seagrass, saltmarsh plants or mangroves. These canopies are in many ways analogous to forest, crop or urban canopies in terrestrial settings, and much understanding has been developed by comparison of results from studies of aquatic and terrestrial canopies.

Significant contributions in this area have been made via analytical, numerical and physical modeling. The last of these has largely been carried out in laboratory flumes (or in wind tunnels for terrestrial canopies), often using artificial simulants – wooden dowels for rigid plants and plastic strips for flexible plants (see Thomas et al., 2014, for further discussion). These approaches are deliberately reductionist, the intention being to strip away complexity and focus on quantitative, mechanistic understanding of specific biophysical interactions, with the subsequent aim of inferring their wider implications and thus moving toward greater understanding in a "bottom–up" way. They have also tended to focus on uni-directional currents, rather than on waves. There has, however, been significant recent progress in understanding wave interactions with homogeneous canopies through studies of simulated canopies representing a range of flexible and rigid vegetation (Pujol and Nepf, 2012; Pujol et al., 2013a,b) and canopies of seagrass (e.g., Zhang et al., 2018), saltmarsh vegetation (Moeller et al., 2014; Maza et al., 2015) and coral reefs (Lowe and Falter, 2015). Moreover, El Allaoui et al. (2015, 2016) have analyzed wave interactions with canopy gaps aligned both parallel and perpendicular to the wave direction.

Measurements of flow velocity – the essential form of hydrodynamic data – are analyzed by separating them into a mean flow field – the long-term average velocity at each location – and a turbulent field – the time-varying aspect of the velocity that remains when the mean velocity is subtracted from the time series of measured velocity. In biophysical terms, the impact of hydrodynamics on canopies can be divided into positive processes (supply of nutrients, dispersion of propagules etc.) and negative processes (e.g., physical stresses, which may lead to damage or uprooting). The mean flow and turbulence fields play different roles in these processes. Canopy organisms respond by adjusting their physiology and growth strategies, which in turn alter their impacts on the hydrodynamics. Thus, there arises a non-linear interaction between hydrodynamics and canopy biology. This rest of this section reviews recent work aimed at understanding these interactions at the single patch or gap scale. Historically, research in this area focused first on simpler, more idealized two-dimensional configurations, and then proceeded to more complex and realistic three-dimensional configurations. Therefore, the following exposition adopts the same distinction.

Two-Dimensional Patch and Gap Simulations

The generic configuration under consideration here consists of a steady flow encounters a patch of a permeable canopy of obstacles with a uniform upstream edge. At the upstream edge of the patch, the flow adjusts to the presence of the canopy. If the canopy has non-negligible height and is permeable, it does this partly by flowing at an accelerated speed over the patch (the "overflow") and partly by flowing at a slower rate through the patch (the "throughflow"). If the canopy is flexible, the flow causes it to pronate, thus the canopy also adjusts to the hydrodynamics. Belcher et al. (2003) provided an idealized model of this situation and identified three stages of adjustment. In the first, pressure due to canopy drag decelerates the flow in an impact region upstream of the canopy. The second region is an adjustment region that extends a distance L_C into the canopy. Here, flow decelerates until there is a local balance between downward turbulent transport of momentum from the overflow and removal of momentum by canopy drag forces. L_C is inversely proportional to the canopy density (the frontal area of canopy elements per unit bed area), so the extent of edge effects varies

with canopy structure (Peterson et al., 2004). L_C may be longer than the patch itself, so the flow doesn't reach equilibrium within the patch. Indeed, in highly fragmented landscapes, the flow may always be under the influence of canopy edges (Dupont et al., 2011). The third region is where the flow reaches equilibrium with the canopy. Here, the flow structure within the canopy depends on canopy density variations: in general, flow will be faster at heights at which the canopy structure is sparser. Depending on the height and density of the canopy, the flow above the canopy in this region may resemble either a mixing layer (denser canopies) or a boundary layer (sparser canopies) (Sukhodolova and Sukhodolov, 2012).

For patches of other types of canopy, the adjustment will be similar. Micro-canopies, in which through flow will be very small in comparison with the overflow, can be idealized for hydrodynamic purposes as changes in bed roughness with no significant change in bed height. In these conditions, the overflow will adjust to the different roughness characteristics of the patch compared to the surrounding substrate (Chamorro and Porte-Agel, 2009). This increases both the generation of turbulence and the bed shear stress. The former is generally advantageous to canopy organisms, since it increases the supply of nutrients through vertical turbulent diffusion. The latter is generally deleterious, since it increases mechanical stress, which can lead to physical damage or removal. For emergent canopies, only the throughflow will occur. Its mean flow and turbulent characteristics are determined by the size, spacing and frontal area density of the canopy elements (Nepf, 1999, 2012; James et al., 2004).

In terms of the turbulent flow field, enhanced turbulent energy is found close to leading canopy patch edges (Folkard, 2005). Similar effects are seen in wind fields at rural-urban transitions and upwind forest edges (Cheng and Porte-Agel, 2016). In emergent aquatic canopies, such as mangroves, this may be partly due to wave breaking, but also to turbulence generation in canopy element wakes (Norris et al., 2017). As the flow develops into the patch, the turbulence evolves. The sharp gradient in flow speed between the patch and its surroundings creates strong shear layers, in which coherent turbulent structures are generated (Siniscalchi et al., 2012). In a terrestrial context, Dupont and Brunet (2009) found that Kelvin-Helmholtz instabilities develop at the top of forest canopies, where there is a quasi-discontinuous change in the drag conditions between the region within the forest and the clear air above. As they move along the canopy, they roll over, then form transverse vortices. Secondary instabilities then destabilize these vortices, and by nine canopy heights downstream, they have become complex coherent structures. Submerged aquatic canopies have similar effects on the flow, but there are differences because of the finite depth of the water above the canopy. In aquatic contexts, the growth of the coherent structures stops when the production of the turbulent kinetic energy that feeds them in the shear layer at the top of the canopy is balanced by dissipation of that energy within the canopy (Ghisalberti and Nepf, 2004). These structures, and thus influence of the canopy overflow, penetrate a significant depth into the canopy, vertically dividing the canopy into an upper region dominated by the overflow and a lower region dominated by throughflow (Nepf and Vivoni, 2000). These two layers often have very different flushing timescales, which can lead to their ecology and water quality also being different (Nepf and Ghisalberti, 2008).

Downstream of canopy patches in two-dimensional configurations, where the canopy edge geometry and flow velocity allow, recirculation zones form immediately behind the canopy which are similar to those found downstream of impermeable obstacles with a backward-facing step configuration (Detto et al., 2008). Whether this occurs or not, the shear layer at the top of the canopy extends downstream of the patch, forming a free shear layer "wake." In the wake, the turbulence increases first as the shear layer grows (the "near-wake"), then decreases as it decays (the "far-wake") (Folkard, 2005). At the same time, a new boundary layer starts to form above the bed downstream of the patch. As this grows, it comes to dominate the wake, which decays downstream. In the transition region from the canopy edge to the point where the wake is negligible and the bed boundary layer completely re-established, the flow structure is dynamic and multi-layered (Folkard and Bouma, 2016). This region often extends far downstream of the patch: Markfort et al. (2010) found that wind adjusting to a lake surface downstream of a tree canopy had reduced surface shear stress up to 50 canopy heights downwind of the transition, and in wind tunnel experiments, Markfort et al. (2014) found that mean turbulent quantities required at least 100 canopy heights to adjust to the new surface.

Less work has been done on the hydrodynamic influence of canopy gaps than on patches. Folkard (2011) compared flow in submerged canopy gaps to Morris's (1955) characterization of skimming flow, wake interference flow and isolated roughness flow, expanding the typology to five categories by separating wake interference flow into recirculation flow, boundary layer recovery, and canopy throughflow. He found that the type of flow that occurred could best be predicted using a Reynolds number based on overflow speed and gap depth, and the gap aspect ratio (i.e., the ratio of the gap length to its height). A Froude number based on the same speed and length scales was found to predict bed shear stress in the gaps well. Extending this work, Adhitya et al. (personal communication) found that longer leaves, lower shoot densities, deeper water and narrower gaps all led to dominance of throughflow over overflow in determining conditions in canopy gaps. In a study of wave interactions with canopies, Lowe et al. (2005) found that short wave orbital velocity is not significantly diminished in canopies compared to bare substrate, in contrast to canopies' significant attenuation of current velocities. As a result, Luhar et al. (2008) suggest that fragmented meadows are more likely to persist in current-dominated environments, because of the enhanced current feedback within canopy gaps, than in wave-dominated environments, where there will be a tendency toward homogeneity because of this lack of feedback. El Allaoui et al. (2015, 2016) reported flume experiments in which waves interacted with gaps aligned perpendicular and parallel to the wave direction, simulating sagittal channels that form perpendicular to coastlines in seagrass canopies due to

currents transporting waters mixed near the shoreline seaward. They found that, for both types of gap, wave velocity increased over the gap compared to the canopy and that denser canopies attenuated both wave velocity and turbulent kinetic energy within adjacent gaps, compared to sparser canopies. Modeling based on these results showed that, for the same total gap area, canopies with large gaps cause more mixing than canopies with small gaps.

Three-Dimensional Patch and Gap Simulations

As computer power and physical modeling facilities have developed, more hydrodynamic studies of three-dimensional patches have been carried out, although to date, there appear to have been no three-dimensional studies of canopy gap hydrodynamics. Most commonly, 3D patch experiments have used idealized, circular patches made up of uniform elements. The flow is diverted around their sides, as well as flowing over and through them. Horseshoe or necklace vortices form around the upstream patch edge (Chang and Constantinescu, 2015; Chang et al., 2017). The flow accelerates as it moves around the patch, the lateral distance from the patch where maximum flow occurs increasing with patch size (Vandenbruwaene et al., 2011). As at the top of the canopy, there is a strong velocity gradient across the lateral patch edges, causing coherent horizontal vortices to form (Yan et al., 2016). These enhance lateral transport across the patch edges (Zong and Nepf, 2011).

Downstream of three-dimensional patches, the wake structure is complicated in comparison to the two-dimensional case by the convergence of the flow around the patch with the overflow and throughflow. For dense patches where overflow dominates throughflow, the patch width-height ratio determines the orientation of wake vortices. If the height is less than the width, vortices form in the vertical plane within a few patch heights downstream of the patch. If the height is greater than the width, horizontal vortices form closest to the patch and control velocity recovery within the wake (Liu et al., 2018). In cases where the throughflow is significant compared to the overflow, there are two peaks of turbulent intensity behind a circular patch. The first is directly behind the patch and related to the wakes of the individual patch elements. The second is further downstream and related to the patch-scale wake (Chen et al., 2012; Chang and Constantinescu, 2015). As patches narrow, the horizontal shear layer becomes more important and there is a mix of horizontal and vertical shear layers, so wake recovery is slower (Chen et al., 2013).

CONSEQUENCES OF HYDRODYNAMIC INTERACTIONS WITH CANOPY PATCHES AND GAPS

Mineral and Organic Particulates

An important consequence of the hydrodynamic influences of canopy patches is their effects on sediment resuspension, transport and deposition. This involves highly non-linear interactions, since each element of the hydrodynamics-canopy-sediment triad influences the others. Enhanced sediment deposition creates new substrate, which provides nutrients and anchoring, encouraging enhanced canopy growth, and this positive feedback maintains spatial correlation between canopy and substrate distributions (Baattrup-Pedersen and Riis, 1999). Sediment resuspension reduces light levels, which reduce canopy growth rates, leading to sparser canopies, enabling further resuspension (Adams et al., 2016). Resuspension can occur because of enhanced turbulence or enhanced mean flow – thus sediment may be resuspended within patches even if mean flow speeds are below the threshold of sediment motion, due to stem wake turbulence (Lefebvre et al., 2010). Conversely, sediment deposition within patches may only be enhanced in the absence of stem wake turbulence (Liu and Nepf, 2016). Patches generally have two sources of sediment – from upstream and laterally. The relative contributions of each determine the spatial pattern of in-patch deposition (Zong and Nepf, 2011). Where advection from upstream dominates, net deposition initially increases as flow decelerates on entering a patch, then decreases as suspended sediment concentration decreases (Zong and Nepf, 2010), so there is a point of maximum sedimentation at some distance into a patch.

Sedimentation downstream of circular patches varies depending on the rigidity and density of the patch elements. For rigid elements, the patch throughflow shifts the patch-scale wake downstream, so there is a region of relatively stagnant flow and thus enhanced deposition immediately downstream of the patch (Chen et al., 2012). For flexible elements, the flow adjustment is more three-dimensional, and turbulence is enhanced immediately downstream of the patch so deposition is reduced there (Ortiz et al., 2013). In sparse patches of rigid elements, sediment is scoured from within the patch and deposited closer downstream than that from denser patches, because the latter divert flow more (Follett and Nepf, 2012). The spatial pattern of sediment deposition around and downstream of a circular patch of model vegetation varies primarily with the ratio of shear velocity to critical shear velocity. If this is < 0.7, there is high deposition in both the wake and adjacent zones. If it is 0.7–3, deposition is high in the wake only. If it is > 3, deposition is low everywhere. The deposition pattern correlates better with shear velocity than with settling velocity, implying that the patterns are driven by resuspension, not deposition (Shi et al., 2016). Again, there have been very few similar studies of the sedimentary consequences of canopy gap hydrodynamics, although Folkard (2011) provides some speculative inferences from a purely hydrodynamic flume study.

These effects in mineral particles are important, since they provide nutrients to canopy organisms and scale-up to affect landscape-scale geomorphology. Of greater importance ecologically, the influence on hydrodynamics of canopy patches and gaps also affects organic particles – including food, waste material, reproductive propagules and plankton. In transport, organic particles behave physically in many ways like mineral sediments. However, the timing of release of organic particles is governed by organism biology, and their deposition is governed by their varying buoyancy and morphology (Gurnell, 2007).

Therefore, the behavior of organic particles is more complex than that of mineral particles, so these complexities need to be taken into account in their modeling.

Solutes

Because of their influence on fluxes and budgets of solutes, aquatic canopies are important in determining the biogeochemistry of water bodies (Bal et al., 2013) and canopy fragmentation can have a significant effect on this. Canopy organisms can take up nutrients from the water column or, if they are rooted, from the substrate. Canopies of plants can also provide substrate for epiphytic biofilms, which also take up nutrients (Levi et al., 2015). Spatial patterns of in-canopy flow are highly correlated with solute uptake rates, which are enhanced by up to 20% at the leading edges of canopies (Morris et al., 2008; Bal et al., 2013). The hydrodynamic effects of seagrass canopy leading edges also drives nutrient exchange between the water column and the substrate; this is caused by pressure gradients arising from flow deceleration (Adhitya et al., 2016). Canopy patches often concentrate and store dissolved nutrients (Schoelynck et al., 2012). Tussocks of wetland sedges efficiently retain biogenic silica, giving them a competitive advantage (Opdekamp et al., 2012). In the Okavango delta, aquatic macrophytes accumulate and concentrate organic matter in sediments below patches, allowing high productivity in an otherwise oligotrophic environment (Schoelynck et al., 2017). Liu et al. (2017) also found this 'soil island' effect around isolated and clustered tamarisk (*Tamarix chinensis* Lour.) in a coastal wetland. However, the effect size was less for clustered tamarisks than for isolated ones, implying that the effect will be weakened by vegetation restoration or natural expansion. Solute retention can vary within patches: Hemminga et al. (1998) found that growth at *Spartina anglica* patch edges was dependent on nutrients in the local substrate, whereas in the (older) patch centers, this material had been depleted in previous years, and growth depended on nutrients bound to allochthonous organic particles.

Distribution of Canopy-Dwelling Organisms

Patch and gap interiors and edges can be very different environments, and strong gradients can exist in both environmental and canopy parameters across patches and gaps. This can alter ecological interactions even within single patches or gaps (Mota et al., 2015). In biological terms, differences between edges and interiors are found in the properties of the canopy-forming organism itself (e.g., Brun et al., 2003); in faunal abundances (e.g., Barbera-Cebrian et al., 2002; Bologna and Heck, 2002; Efird and Konar, 2014); in the levels of thermal (Jurgens and Gaylord, 2016) and mechanical (Folkard, 2005) stresses experienced by organisms; and in terms of sediment quality (e.g., Alves et al., 2017). Local diversity and distribution of benthic fauna is intimately associated with canopy type and distribution (e.g., Begin et al., 2004; Bouma et al., 2009). Macrophyte structural complexity plays an important role in determining differences in macroinvertebrate distribution between canopies of different species (O'Hare and Murphy, 1999). This is likely driven by differences in hydrodynamic stress attenuation and food availability rather than structural complexity *per se* (Bell et al., 2013). Canopies of macroalgae with greater structural complexity also promote spatial and temporal patchiness of microphytobenthos, with potential significant effects on the overall productivity of ecosystems (Umanzor et al., 2017). Fragmentation of seagrass canopies also alters their interactions with filter feeders. Within canopy patches, filter feeders' food supply is reduced, strongly restricting their growth (Reusch and Williams, 1999), but in the gaps between canopies, they can find greater protection from hydrodynamic forces and higher resource availability (Gonzalez-Ortiz et al., 2014). Thus the fragmentation allows the seagrass and filter feeders to co-exist compatibly.

UPSCALING TO LANDSCAPE-SCALE

An important aim of studies of fragmented canopies is to be able to quantify total or average parameter values at the whole-landscape scale. Whilst these require knowledge of inputs and characteristics at that scale, they also require understanding of structure and processes at smaller scales, i.e., patch and gap-scale. In part, this is born of necessity, since field measurements are generally made at patch and gap scales for logistical reasons, so landscape-scale measurements tend to have to be derived from their upscaling. Moreover, variability at patch and gap scale within fragmented canopies often has important effects on landscape-scale structures and processes, and this has given rise to many different approaches to upscaling (e.g., Bou-Zeid et al., 2004; Chesson et al., 2005; Denny and Gaylord, 2010; Nikora, 2010).

If parameters of interest scaled linearly with spatial scale, upscaling would be trivial – it would simply comprise of adding up the contributions of each patch or gap-scale area to give a total for a whole landscape. However, this is not the case. Most, if not all, parameters of interest in aquatic canopy ecosystems scale non-linearly with spatial scale (Chesson et al., 2005). In addition, emergent forms and processes often arise at larger scales that are not apparent at the individual patch of gap scale, due to the spatial distribution of patches and gaps. For example, the spatial density and distribution of patch or gap edges plays a large part in governing landscape-scale flow structure (Dupont et al., 2011; Folkard and Bouma, 2016), and in saltmarshes, regions of relatively dense vegetation deflect flow into more sparsely-vegetated regions, where drainage channels form. Thus, landscape-scale drainage rates are determined in part by the spatial distribution of vegetation patches (Temmerman et al., 2007; Vandenbruwaene et al., 2013). These issues provide the main challenges in upscaling of patch and gap-scale phenomena to enable derivation of landscape-scale parameter values.

These challenges are addressed in two general ways. Empirically, correlations can be sought between variations in metrics describing the patch/gap-scale structure of fragmented

canopy landscapes and variations in landscape-scale total or average parameter values. While this approach can provide evidence of these cross-scale relationships, they do little to provide causal, mechanistic insights to them. The alternative approach is to create spatially-distributed models into which the smaller scale processes are explicitly incorporated but which operate over domains covering entire landscapes. These can then be explored to elicit mechanistic understanding of the cross-scale relationships. They can also be used to infer correlative relationships between patch/gap-scale causes and landscape-scale effects of the type described above that are underpinned by that mechanistic understanding (e.g., Luhar and Nepf, 2013; Larsen et al., 2017). However, such models require detailed understanding, not only of the nature of processes at the smaller scale, but also of ways in which these interact with each other as spatial complexity and scale are increased. Therefore, there is a need for studies of these interactions and the ways in which they influence landscape-scale phenomena, as well as for development of robust and broadly-applicable techniques for their upscaling.

An ecological perspective on the problem of non-linearity in upscaling can be illustrated by the example of trying to estimate the growth rate of a canopy from knowledge of the percentage of algal cover. Because increased algal cover enhances algal growth rate due to mutual protection effects at the patch scale, applying the patch-scale relationship to calculate growth rate from percentage cover at landscape-scale will not give an accurate value. To address this type of problem, scale transition theory (Chesson et al., 2005; Benedetti-Cecchi et al., 2012; Chesson, 2012) quantifies the non-linear scale-dependence of interactions between parameters in terms of the variances and co-variances of their patch/gap-scale values across whole landscapes. Larsen et al. (2017) provide an illustration of how the problems of non-linearity and spatial distribution effects in upscaling are addressed in a hydrological context in a study of the flow through the vegetated ridge-and-slough landscape of the Florida Everglades. Following approaches that have been used previously in the groundwater literature (Cushman et al., 2002; Farmer, 2002), they calculate the landscape-scale average flow resistance as a non-linear spatial average of small scale roughness, using an approach based on the ergodic hypothesis (Lumley and Panofsky, 1964). They conceptualize the landscape as binary – being made up purely of patches and gaps of 'matrix' between them. The landscape-scale average of a parameter (flow resistance in the case of Larsen et al., 2017), H_{land}, is then calculated from values of the same parameter for the patches, h_p, and the gaps, h_g, and the fractional cover of patches, p, across the whole landscape as

$$H_{\text{land}} = [p h_{\text{p}}^{\omega} + (1-p) h_{\text{g}}^{\omega}]^{1/\omega} \quad (1)$$

The non-linearity and dependence on spatial distribution are incorporated in the exponent ω, which is calculated by fitting the data produced by repeat runs of a numerical model of the landscape, based on long-term field observations (see Larsen et al., 2017, for further details). They then, via this model, explore the dependence of ω on changes in various metrics describing the heterogeneity of the landscape.

In order to be able to test and develop upscaling approaches such as scale transition theory and non-linear spatial averaging, understanding is needed of ways in which all aspects of canopy ecosystems interact as spatial complexity and scale increase. The remainder of this section identifies progress that has been made in understanding these interactions, firstly via studies of interactions between two or more patches or gaps. It then covers interactions between patch-scale and landscape-scale processes, and finally identifies some landscape-scale consequences of these interactions in fragmented canopies. Because work in this area to date is at a relatively early stage of development, the coverage is necessarily illustrative, rather than comprehensive.

Hydrodynamically-Mediated Interactions Between Canopy Patches

Taking a bottom–up approach, the first stage in understanding how processes at patch/gap-scale scale up is consideration of the interactions between two patches or gaps. In an aquatic context, hydrodynamics is usually the dominant mediator in these interactions. For example, where a downstream patch is located in the hydrodynamic wake of an upstream patch, the wake's enhanced turbulence will alter the conditions in the downstream patch (Folkard, 2005). This can affect its nutrient uptake rate, due to changes in both the mean flow speed and the levels of turbulence (Cornacchia, 2018). Other interactions will involve hydrodynamically-mediated sediment processes. For example, when the two side-by-side patches are far apart, their wake interactions are weak, and each has its own region of sediment deposition behind it. If the transverse distance between them reduces, their wakes will start to interact and a depositional region will form further downstream where their wakes merge (Meire et al., 2014). This encourages formation of a new vegetation patch, which will slow the flow between the patches and allow them to merge (de Lima et al., 2015; Liu et al., 2018). Over time, this process may lead to continuous vegetation coverage (Kondziolka and Nepf, 2014). Because of the differences in their interactions with flow, these morphological feedbacks will be different for rigid and flexible vegetation (Ortiz et al., 2013). This leads to a different set of outcomes when patches of different species interact. For example, Cornacchia et al. (2019) found that when a patch of a vegetation species with a taller, denser canopy (*Callitriche*) was located upstream of a patch of a shorter, sparser species (*Groenlandia*), it generated a turbulent wake that enhanced nutrient uptake by the *Groenlandia*. At the same time, the uptake rate of the *Callitriche* benefited from being exposed to the higher mean velocity of the upstream flow, as its canopy was too dense for turbulence to penetrate.

Influence of Canopy Patch Interactions at Landscape-Scale

Interactions between canopy patches, hydrodynamics and sediment processes of the type described in the previous section can lead to landscape-scale structure in the spatial distribution of canopies. For example, in saltmarshes, regions of relatively dense vegetation can deflect flow into more sparsely-vegetated

regions, leading to preferential formation of drainage channels in the latter. As a result, the saltmarshes evolve with some regions characterized by dense vegetation, and others by drainage creek networks (Temmerman et al., 2007; Vandenbruwaene et al., 2013). Other examples of feedbacks between vegetation canopies, flow and sediment processes governing the evolution of landscapes have been found by Larsen et al. (2007) and Larsen and Harvey (2010, 2011) in studies of the ridge-and-slough patterning of vegetation distributions in the Florida Everglades.

In forming these spatial structures, ecological traits of the canopy species are often important. For example, rate of growth is an important determinant of canopy patches' contributions to landscape dynamics (Bertoldi et al., 2011). Where patches grow fast, they are more resilient due to their ability to recover from disturbance more quickly. Slower growing species also tend to decline more slowly, so are resistant to degradation (O'Brien et al., 2018). These differences will lead to differences in the evolution of canopy-hydrodynamics-sediment interactions and thus differences in spatial structure. Variations in establishment strategies amongst canopy-forming species (e.g., clonal extension, ruderal gap filling), variable spatial and temporal patterns of disturbance (van Hulzen et al., 2006), and the extent to which they change their physical structure and biomechanical properties over their growth-senescence cycles (Kleeberg et al., 2010) will also significantly modify their landscape-forming function. In general, canopies species' role in landscape dynamics is to act as ecosystem engineers (Jones et al., 1994) – they trap and stabilize sediments, organic matter and propagules of other species, modify local sediment and morphology, and drive development of landforms and habitats (Gurnell, 2007; Gurnell et al., 2012). Aboveground biomass modifies flow and retains sediment, while below ground biomass affects the hydraulics and mechanical properties of the substrate. Thus, their effects change as above and below ground biomass fractions change in response to climatic and hydrodynamic forcing (Gurnell, 2014).

The upscaled consequences of patch-scale interactions will also often interact with larger scale processes. Generally, the large-scale processes determine the overall extent of the fragmented canopy and can shape and orient the patches and gaps in the landscape, while small-scale interactions generate the patch/gap-scale structure (van de Koppel et al., 2012). For example, Fonseca et al. (2008) found that the spatial organization of *Halophila decipiens* (Caribbean seagrass) in an open ocean setting subject to hurricane damage was dictated first by large scale dispersal of propagules (over 100s of meters) then, within a growing season, by clonal organization of individual seagrass patches. The large-scale controls can include anthropogenic disturbance: in the Wadden Sea in NW Europe, the landscape-scale consequences of increased human disturbance of sediment (e.g., dredging of navigation channels and ports) has interfered with biological controls of sediment dynamics and have shifted the inter-tidal zone from a state of internal regulation (by the ecosystems within the zone) and spatial heterogeneity to external regulation (by anthropogenic impacts originating outside the zone) and spatially homogeneity (Eriksson et al., 2010).

Consequences of Patch-Scale Interactions at Landscape-Scale

Understanding of the landscape-scale consequences of interactions between canopy patches, hydrodynamics and hydrodynamically-mediated sediment processes is mainly focused on those particular elements of the ecosystem (i.e., the patches, hydrodynamics and sediment themselves). However, there have also been some studies of their influences on some of other physical, chemical and biological aspects of fragmented canopy ecosystems. For example, they have an important influence on solute diffusion coefficients and residence times (Nepf et al., 1997; Nepf, 1999). These can vary by an order of magnitude across fragmented canopies because of the great difference in flow speed between canopy throughflow, and flow over and around patches (Lightbody et al., 2008). This can affect the canopies themselves, for example by varying their exposure to pollution or their access to dissolved nutrients and gasses (Lara et al., 2012).

Another major landscape-scale ecological consequences of interactions between hydrodynamics and fragmented canopies is their effect on habitat diversity. However, the nature and direction of these effects (i.e., whether they increase or decrease habitat diversity, or leave it unchanged whilst changing the mox of habitats) remains unclear. The heterogeneous flow conditions created by fragmented canopies create a highly diverse mosaic of habitats (Sukhodolov and Sukhodolova, 2010; Verschoren, 2017). According to the long-established patch dynamics concept, high levels of spatial habitat variability imply high levels of species richness (Townsend, 1989). However, this is not always well-supported by data (Resh et al., 1994). In a meta-analysis of seagrass research, neither literature review nor field measurements suggested that habitat fragmentation has any consistent effect on fauna, and there was little evidence of fragmentation sensitivity in any taxonomic group (Bell et al., 2001). Lefcheck et al. (2016) found that abundance, species richness, Simpson and functional diversity and composition of faunal communities were invariant to fragmentation in experimental eelgrass landscapes. They concluded that this is likely a consequence of the fauna's rapid life histories and high mobility. In other studies, however, such relationships have been found: Matias et al. (2015) found that higher habitat complexity in fragmented macro-algae canopies promoted species colonization, so the higher the level of fragmentation, the more species were present. Thus, the relationship between hydrodynamic interactions with fragmented canopies and species richness of communities inhabiting those canopies requires further investigation.

APPLICATIONS TO MARINE CANOPY LANDSCAPE MANAGEMENT AND RESTORATION

As noted by Bell et al. (1997), there is a powerful mutualistic relationship between the practice of landscape restoration and the science of landscape ecology. Restoration can provide

experimental spatial distributions and opportunities for experiments over large spatial scales. Landscape ecology can provide insights into selecting reference sites and establishing restoration project goals, and appropriate spatial configurations to aim for. The same kind of mutualistic relationship is also evident between the practice of river restoration and the science of eco-hydromorphology and eco-hydraulics, which focus on interactions between ecology, catchment hydrology, river channel hydraulics and channel and floodplain geomorphology (e.g., Vaughan et al., 2009). Similar mutually beneficial links exist between the practices of coastal zone restoration, protection and management, and the science of biophysical (and chemical) interactions in coastal marine ecosystems – many of which have canopy organisms as keystone species. Some examples of ways in which understanding of canopy spatial distribution and fragmentation can be utilized in coastal zone management are given below.

Analysis of canopies' spatial distributions can be used effectively to describe the impacts of multiple human stressors in marine environments (Tamburello et al., 2012). van der Heide et al. (2010) found consistent responses of spatially self-organized patterns in seagrass meadows to changing abiotic conditions, and suggested that this could lead to the use of self-organized spatial patterns as stress indicators in these meadows. Even in inter-tidal diatom micro-canopies, spatial patterns can provide important clues about level of degradation of ecosystem (Weerman et al., 2012). However, interpretation of these patterns requires detailed knowledge of the nature of underlying feedbacks, including hydrodynamically-mediated feedbacks, as the patterns differ markedly between ecosystems. Of potentially greater value, understanding of the spatial distribution of canopy fragmentation can be used to predict the development of canopies and identify those that are at risk of catastrophic decline (Rietkerk et al., 2004). For example, the shape of *Spartina anglica* patches has been found to indicate the long-term development of salt-marsh pioneer zones, although the outcome is conditional on large scale morphodynamics and sediment grain size (Balke et al., 2012). Fraschetti et al. (2012) suggested that increasing spatial heterogeneity of both intertidal and subtidal assemblages probably represents an early warning of increasing human pressure in marine protected areas. In a model of seagrass meadow spatial patterning, Ruiz-Reynés et al. (2017) found that a transition to patches of vegetation arranged in approximately hexagonal formations indicates that the meadow is close to a tipping point where further increase in mortality may lead to catastrophic loss of the meadow.

Fragmentation of canopies at landscape-scales may also be used as a bio-indicator of loss of abundance amongst canopy-using organisms. For example, properties of fragmented landscapes at 10–100 m scales have been found to be effective indicators of nekton distributions, with lower nekton abundances correlating with higher degrees of canopy fragmentation and loss of habitat connectivity (Baillie et al., 2015; Favre-Bac et al., 2017).

Better understanding of the hydrodynamics of canopies at patch/gap and landscape-scales may also help attempts to re-establish or restore marine canopies. Attempts to re-seed and re-turf seagrass canopies have been made in marine environments but have had limited success (van Katwijk and Hermus, 2000; van Katwijk et al., 2009). Natural re-establishment of macrophyte patches has been somewhat more successful in streams (Larned et al., 2006). In these environments, the main bottleneck for re-colonization is the initial establishment of attached roots in the sediment from propagules or seedlings (Riis, 2008), therefore understanding of the hydrodynamic conditions that facilitate this process for different canopy types in different contexts would be valuable. Once they have established, patches of plant canopy are able to create interactions with the flow, leading to positive feedback that causes enhanced sediment deposition and allows the patches to expand (Sand-Jensen, 1998).

COMPARISON ACROSS CANOPY TYPES AND PROPOSED DIRECTIONS FOR RESEARCH

Having provided a structured synthesis of work on biophysical interactions with a wide range of canopy types in the preceding sections, this final section compares the approaches taken and progress made in work focused on different canopy types, and draws out what can be learnt about each one, and how we can develop more universal understanding of these interactions, their consequences and how they can be harnessed for management purposes.

In terms of patches and gaps themselves there appears to be a lack of basic data across all canopy types regarding how commonly they occur; their size, shape and orientation distributions; and how long they typically persist. This sort of information is important, as it allows models predicting their evolution and consequences to be developed on the basis of realistic data. Comparative studies of the modes of formation, maintenance and destruction of patches and gaps across different canopy types might also help to elucidate the relative importance of different factors (environmental gradients, biotic and abiotic stresses and facilitations, catastrophic events) for each one.

The study of fundamental hydrodynamic interactions with canopies has largely been carried out via laboratory flume or basin studies, numerical modeling and field experiments. These have typically used more-or-less idealized hydrodynamics (uniform flows or wave fields) and canopies in simplified two- or three-dimensional configurations. Often, the elements of the canopies have been idealized using simulants, which are uniformly rigid (e.g., wooden dowels) or flexible (e.g., plastic strips). These simulations have tended to be based on the essential biomechanical and morphological properties of seagrasses, saltmarsh vegetation, and mangroves. From this, a relatively detailed and thorough understanding of the hydrodynamics of these types of canopies has been built up. The review carried out suggests that less work has been done on the fundamental hydrodynamics of lower growing organisms – biofilms, turf algae etc. Moreover, the strongly reductionist, idealizing approach taken in this work to date suggests that moves toward greater realism in these experiments is needed. For example, this

would include studies of the hydrodynamics of patches or gaps with boundaries that are not quasi-discontinuous, which vary in height and density, and which have elements with variable morphology. Studies incorporating a wider range of configurations of patches and gaps – for example cases in which patch-gap edges are aligned at intermediate angles to the direction of the oncoming current or waves (rather than being parallel or perpendicular to it, as has almost universally been the case hitherto), or where edges are not either straight or circular – and less uniform hydrodynamic conditions might also elucidate non-linear interactions between variations in canopy and hydrodynamic characteristics.

Studies of the effects of hydrodynamic interactions with canopy patches and gaps on particulates, solutes and canopy-dwelling organisms appear from this review to have focused mainly on canopies of seagrasses, saltmarsh vegetation, macroalgae, and mangroves. This suggests that there is a need for further work in this area on low-growing canopies, where the focus hitherto appears to have been more biological (e.g., on patterns of grazing) than hydrodynamic. In general, as with studies of the hydrodynamic interactions with canopies, the physical aspects of this topic appear to have been studied largely through idealized configurations, whereas the biological aspects have been mainly studied through field measurements of *in situ* ecosystems. Moving the former toward more complex, realistic settings, and the latter toward more controlled focused conditions will help to bring understanding of biophysical interactions in these contexts from biological and physical perspectives closer together.

Arguably the most consequential motivation for studying these interactions is a desire to be able to predict how marine canopy landscapes will be affected by our actions, and how they can help us via their ecosystem services. This ability would enable us to guide our actions and harnessing of those services. This implies that landscape-scale is the scale at which the insights delivered by research may be applied most usefully. This is at odds with the fact that the most common scale for measurement and modeling – due to logistical and technological limitations – is the patch/gap scale. Therefore, upscaling from patch/gap scale to landscape-scale is arguably the most important current problem in fragmented marine canopy research. Although significant progress has been made in this area in recent years there still remains much to be done. Further studies are needed into the mechanics of interactions between multiple canopy patches and gaps at all scales – from interactions between two patches, through studies of patch mosaics (Schoelynck et al., 2018) and fragmented canopies with more complex spatial distributions, to whole-landscape scales. These need to take into account the roles of a wide range of different variables, including those related to hydrodynamics (waves, currents, turbulent mixing), sediment (erosion, resuspension, transport, deposition), and other physical variables such as light levels (e.g., Koch, 2001; Adams et al., 2016) and water temperature. From a chemical perspective, they need to include concentrations of nutrients, dissolved gasses, pollutants and a wide range of biogenic chemicals, as well as their flux rates, both in terms of physical movement between the substrate, water column, biota and atmosphere, and in terms of chemical changes, for example from dissolved to particulate form, or organic to inorganic form. From a biological perspective, they need to include rates of primary production, bulk biomass, species diversity and richness, and metrics of ecosystem structure, functioning and services. Clearly, no single study or model could incorporate all of these variables. They are listed here to emphasize the importance of considering the full range of factors that may be at play in determining the dynamics of fragmented marine canopies.

In summary, a number of general ways of progressing the science driving our ability to manage ecosystems and landscapes characterized by fragmented marine canopies approaches can be identified. Firstly, closer collaboration is required between researchers carrying out work aimed at improving our understanding of the fundamental processes of biophysical interactions with fragmented canopies, practitioners of landscape management and restoration, and policymakers concerned with coastal environments. Within the research community, traditionally reductionist, laboratory and numerical model-based hydrodynamics research would benefit from a move toward studying more non-uniform, varied and realistic configurations, and traditionally holistic, field-based ecological research would benefit from a move toward studying more controlled, idealized and quantitatively-modelable configurations. Moreover, a greater appreciation of the importance of chemical aspects of the systems studied needs to be incorporated into the current biophysical approach. Further development of techniques for upscaling understanding and predictions of bio-chemo-physical interactions at the patch/gap scale to the landscape-scale in the context of spatially complex canopies is required. All of these would benefit greatly from a globally distributed experiment approach (Borer et al., 2014) with a clear shared direction and aims. Finally, in attempting to interweave the fields of hydrodynamics, marine canopy ecology and spatial analysis of landscapes, whilst incorporating biogeochemistry and socio-environmental interactions, an approach that balances these disciplines, rather than viewing one as subordinately serving the other, would be the best way forward.

AUTHOR CONTRIBUTIONS

The author confirms being the sole contributor of this work and has approved it for publication.

ACKNOWLEDGMENTS

I am grateful to MG and the editorial team for this special issue for the opportunity to contribute this review article. I am also grateful to the two reviewers whose comments and suggestions helped greatly with the completion of this manuscript.

REFERENCES

Adams, M. P., Hovey, R. K., Hipsey, M. R., Bruce, L. C., Ghisalberti, M., Lowe, R. J., et al. (2016). Feedback between sediment and light for seagrass: where is it important? *Limnol. Oceanogr.* 61, 1937–1955. doi: 10.1002/lno.10319

Adhitya, A., Bouma, T. J., Folkard, A. M., van Katwijk, M. M., Callaghan, D., de Iongh, H. H., et al. (2014). Comparison of the influence of patch-scale and meadow-scale characteristics on flow within seagrass meadows: a flume study. *Mar. Ecol. Prog. Ser.* 516, 49–59. doi: 10.3354/meps10873

Adhitya, A., Folkard, A. M., Govers, L. L., van Katwijk, M. M., de Iongh, H. H., Herman, P. M. J., et al. (2016). The exchange of dissolved nutrients between the water column and substrate pore-water due to hydrodynamic adjustment at seagrass meadow edges: a flume study. *Limnol. Oceanogr.* 61, 2286–2295. doi: 10.1002/lno.10376

Alves, R. M. S., Vanaverbeke, J., Bouma, T. J., Guarini, J. M., Vincx, M., and Van Colen, C. (2017). Effects of temporal fluctuation in population processes of intertidal *Lanice conchilega* (Pallas, 1766) aggregations on its ecosystem engineering. *Estuar. Coastal Shelf Sci.* 188, 88–98. doi: 10.1016/j.ecss.2017.02.012

Baattrup-Pedersen, A., and Riis, T. (1999). Macrophyte diversity and composition in relation to substratum characteristics in regulated and unregulated danish streams. *Freshw. Biol.* 42, 375–385. doi: 10.1046/j.1365-2427.1999.444487.x

Baillie, C. J., Fear, J. M., and Fodrie, F. J. (2015). Ecotone effects on seagrass and saltmarsh habitat use by juvenile nekton in a temperate estuary. *Estuaries Coasts* 38, 1414–1430. doi: 10.1007/s12237-014-9898-y

Bal, K. D., Brion, N., Woule-Ebongue, V., Schoelynck, J., Jooste, A., Barron, C., et al. (2013). Influence of hydraulics on the uptake of ammonium by two freshwater plants. *Freshw. Biol.* 58, 2452–2463. doi: 10.1111/fwb.12222

Balke, T., Klaassen, P. C., Garbutt, A., van der Wal, D., Herman, P. M. J., and Bouma, T. J. (2012). Conditional outcome of ecosystem engineering: a case study on tussocks of the salt marsh pioneer *Spartina anglica*. *Geomorphology* 153, 232–238. doi: 10.1016/j.geomorph.2012.03.002

Barbera-Cebrian, C., Sanchez-Jerez, P., and Ramos-Espla, A. A. (2002). Fragmented seagrass habitats on the mediterranean coast, and distribution and abundance of mysid assemblages. *Mar. Biol.* 141, 405–413. doi: 10.1007/s00227-002-0852-3

Begin, C., Johnson, L. E., and Himmelman, J. H. (2004). Macroalgal canopies: distribution and diversity of associated invertebrates and effects on the recruitment and growth of mussels. *Mar. Ecol. Prog. Ser.* 271, 121–132. doi: 10.3354/meps271121

Belcher, S. E., Jerram, N., and Hunt, J. C. R. (2003). Adjustment of a turbulent boundary layer to a canopy of roughness elements. *J. Fluid Mech.* 488, 369–398. doi: 10.1017/S0022112003005019

Bell, N., Riis, T., Suren, A. M., and Baattrup-Pedersen, A. (2013). Distribution of invertebrates within beds of two morphologically contrasting stream macrophyte species. *Fundam. Appl. Limnol.* 183, 309–321. doi: 10.1127/1863-9135/2013/0517

Bell, S. S., Brooks, R. A., Robbins, B. D., Fonseca, M. S., and Hall, M. O. (2001). Faunal response to fragmentation in seagrass habitats: implications for seagrass conservation. *Biol. Conserv.* 100, 115–123. doi: 10.1016/S0006-3207(00)00212-3

Bell, S. S., Fonseca, M. S., and Motten, L. B. (1997). Linking restoration and landscape ecology. *Restor. Ecol.* 5, 318–323. doi: 10.1046/j.1526-100X.1997.00545.x

Bell, S. S., Robbins, B. D., and Jensen, S. L. (1999). Gap dynamics in a seagrass landscape. *Ecosystems* 2, 493–504. doi: 10.1007/s100219900097

Benedetti-Cecchi, L., Tamburello, L., Bulleri, F., Maggi, E., Gennusa, V., and Miller, M. (2012). Linking patterns and processes across scales: the application of scale-transition theory to algal dynamics on rocky shores. *J. Exp. Biol.* 215, 977–985. doi: 10.1242/jeb.058826

Bertoldi, W., Drake, N. A., and Gurnell, A. M. (2011). Interactions between river flows and colonizing vegetation on a braided river: exploring spatial and temporal dynamics in riparian vegetation cover using satellite data. *Earth Surf. Processes Landf.* 36, 1474–1486. doi: 10.1002/esp.2166

Bologna, P. A. X., and Heck, K. L. (2002). Impact of habitat edges on density and secondary production of seagrass-associated fauna. *Estuaries* 25, 1033–1044. doi: 10.1007/bf02691350

Borer, E. T., Harpole, W. S., Adler, P. B., Lind, E. M., Orrock, J. L., Seabloom, E. W., et al. (2014). Finding generality in ecology: a model for globally distributed experiments. *Methods Ecol. Evol.* 5, 65–73. doi: 10.1111/2041-210X.12125

Bouma, T. J., Ortells, V., and Ysebaert, T. (2009). Comparing biodiversity effects among ecosystem engineers of contrasting strength: macrofauna diversity in *Zostera noltii* and *Spartina anglica* vegetations. *Helgol. Mar. Res.* 63, 3–18. doi: 10.1007/s10152-008-0133-8

Bou-Zeid, E., Meneveau, C., and Parlange, M. B. (2004). Large-eddy simulation of neutral atmospheric boundary layer flow over heterogeneous surfaces: blending height and effective surface roughness. *Water Res. Res.* 40:W02505. doi: 10.1029/2003WR002475

Brun, F. G., Perez-Llorens, J. L., Hernandez, I., and Vergara, J. J. (2003). Patch distribution and within-patch dynamics of the seagrass *Zostera noltii* hornem. in los torunos salt-marsh, cadiz bay, natural park, Spain. *Botanica Marina* 46, 513–524. doi: 10.1515/BOT.2003.053

Cervin, G., Aberg, P., and Jenkins, S. R. (2005). Small-scale disturbance in a stable canopy dominated community: implications for macroalgal recruitment and growth. *Mar. Ecol. Prog. Ser.* 305, 31–40. doi: 10.3354/meps305031

Cervin, G., Lindegarth, M., Viejo, R. M., and Aberg, P. (2004). Effects of small-scale disturbances of canopy and grazing on intertidal assemblages on the Swedish west coast. *J. Exp. Mar. Biol. Ecol.* 302, 35–49. doi: 10.1016/j.jembe.2003.09.022

Chamorro, L. P., and Porte-Agel, F. (2009). Velocity and surface shear stress distributions behind a rough-to-smooth surface transition: a simple new model. *Boundary Layer Meteorol.* 130, 29–41. doi: 10.1007/s10546-008-9330-x

Chang, K., and Constantinescu, G. (2015). Numerical investigation of flow and turbulence structure through and around a circular array of rigid cylinders. *J. Fluid Mech.* 776, 161–199. doi: 10.1017/jfm.2015.321

Chang, W. Y., Constantinescu, G., and Tsai, W. F. (2017). On the flow and coherent structures generated by a circular array of rigid emerged cylinders placed in an open channel with flat and deformed bed. *J. Fluid Mech.* 831, 1–40. doi: 10.1017/jfm.2017.558

Chen, Z. B., Jiang, C., and Nepf, H. M. (2013). Flow adjustment at the leading edge of a submerged aquatic canopy. *Water Res. Res.* 49, 5537–5551. doi: 10.1002/wrcr.20403

Chen, Z. B., Ortiz, A., Zong, L. J., and Nepf, H. M. (2012). The wake structure behind a porous obstruction and its implications for deposition near a finite patch of emergent vegetation. *Water Res. Res.* 48:W09517. doi: 10.1029/2012WR012224

Cheng, W. C., and Porte-Agel, F. (2016). Large-eddy simulation of flow and scalar dispersion in rural-to-urban transition regions. *Int. J. Heat Fluid Flow* 60, 47–60. doi: 10.1016/j.ijheatfluidflow.2016.04.004

Chesson, P. (2012). Scale transition theory: its aims, motivations and predictions. *Ecol. Complex.* 10, 52–68. doi: 10.1016/j.ecocom.2011.11.002

Chesson, P., Donahue, M. J., Melbourne, B. A., and Sears, A. L. W. (2005). "Scale transition theory for understanding mechanisms in metacommunities," in *Metacommunities: Spatial Dynamics and Ecological Communities*, eds M. Holyoak, M. A. Leibold, and R. D. Holt (Chicago, IL: University of Chicago Press), 279–306.

Cornacchia, L. (2018). *Emergent Properties of Bio-Physical Self-Organization in Streams*. Ph.D. thesis. NIOZ/University of Groningen, Groningen.

Cornacchia, L., Licci, S., Nepf, H. M., Folkard, A. M., van der Wal, D., van de Koppel, J., et al. (2019). Turbulence-mediated facilitation of resource uptake in patchy stream macrophytes. *Limnol. Oceanogr.* 64, 714–727. doi: 10.1002/lno.11070

Cushman, J. H., Bennethum, L. S., and Hu, B. X. (2002). A primer on upscaling tools for porous media. *Adv. Water Res.* 25, 1043–1067. doi: 10.1016/S0309-1708(02)00047-7

Davies, A. J., Johnson, M. P., and Maggs, C. A. (2007). Limpet grazing and loss of ascophyllum nodosum canopies on decadal time scales. *Mar. Ecol. Prog. Ser.* 339, 131–141. doi: 10.3354/meps339131

de Lima, P. H. S., Janzen, J. G., and Nepf, H. M. (2015). Flow patterns around two neighboring patches of emergent vegetation and possible implications for deposition and vegetation growth. *Environ. Fluid Mech.* 15, 881–898. doi: 10.1007/s10652-015-9395-2

Denny, M. W., and Gaylord, B. (2010). Marine ecomechanics. *Annu. Rev. Mar. Sci.* 2, 89–114. doi: 10.1146/annurev-marine-120308-081011

Detto, M., Katul, G. G., Siqueira, M., Juang, J. Y., and Stoy, P. (2008). The structure of turbulence near a tall forest edge: the backward-facing step flow analogy revisited. *Ecol. Appl.* 18, 1420–1435. doi: 10.1890/06-0920.1

Di Carlo, G., Badalamenti, F., Jensen, A. C., Koch, E. W., and Riggio, S. (2005). Colonisation process of vegetative fragments of *Posidonia oceanica* (L.) Delile on rubble mounds. *Mar. Biol.* 147, 1261–1270. doi: 10.1007/s00227-005-0035-0

Didham, R. K., Kapos, V., and Ewers, R. M. (2012). Rethinking the conceptual foundations of habitat fragmentation research. *Oikos* 121, 161–170. doi: 10.1111/j.1600-0706.2011.20273.x

Dupont, S., Bonnefond, J. M., Irvine, M. R., Lamaud, E., and Brunet, Y. (2011). Long-distance edge effects in a pine forest with a deep and sparse trunk space: in situ and numerical experiments. *Agric. For. Meteorol.* 151, 328–344. doi: 10.1016/j.agrformet.2010.11.007

Dupont, S., and Brunet, Y. (2009). Coherent structures in canopy edge flow: a large-eddy simulation study. *J. Fluid Mech.* 630, 93–128. doi: 10.1017/S0022112009006739

Efird, T. P., and Konar, B. (2014). Habitat characteristics can influence fish assemblages in high latitude kelp forests. *Environ. Biol. Fishes* 97, 1253–1263. doi: 10.1007/s10641-013-0211-x

El Allaoui, N., Serra, T., Colomer, J., Soler, M., Casamitjana, X., and Oldham, C. (2016). Interactions between fragmented seagrass canopies and the local hydrodynamics. *PLoS One* 11:e0156264. doi: 10.1371/journal.pone.0156264

El Allaoui, N., Serra, T., Soler, M., Colomer, J., Pujol, D., and Oldham, C. (2015). Modified hydrodynamics in canopies with longitudinal gaps exposed to oscillatory flows. *J. Hydrol.* 531, 840–849. doi: 10.1016/j.jhydrol.2015.10.041

Eriksson, B. K., van der Heide, T., van de Koppel, J., Piersma, T., van der Veer, H. W., and Olff, H. (2010). Major changes in the ecology of the wadden sea: human impacts, ecosystem engineering and sediment dynamics. *Ecosystems* 13, 752–764. doi: 10.1007/s10021-010-9352-3

Escapa, M., Perillo, G. M. E., and Iribarne, O. (2015). Biogeomorphically driven salt pan formation in sarcocornia-dominated salt-marshes. *Geomorphology* 228, 147–157. doi: 10.1016/j.geomorph.2014.08.032

Farmer, C. L. (2002). Upscaling: a review. *Int. J. Numer. Methods Fluids* 40, 63–78. doi: 10.1002/fld.267

Favre-Bac, L., Lamberti-Raverot, B., Puijalon, S., Ernoult, A., Burel, F., Guillard, L., et al. (2017). Plant dispersal traits determine hydrochorous species tolerance to connectivity loss at the landscape scale. *J. Veg. Sci.* 28, 605–615. doi: 10.1111/jvs.12518

Folkard, A. M. (2005). Hydrodynamics of model *Posidonia oceanica* patches in shallow water. *Limnol. Oceanogr.* 50, 1592–1600. doi: 10.4319/lo.2005.50.5.1592

Folkard, A. M. (2011). Flow regimes in gaps within stands of flexible vegetation: laboratory flume simulations. *Environ. Fluid Mech.* 11, 289–306. doi: 10.1007/s10652-010-9197-5

Folkard, A. M., T. J. (2016). "Flow interactions with blue mussel patches: hydrodynamic and ecological implications," in *Proceedings of the 11th International Symposium on Ecohydraulics*, eds J. A. Webb, J. F. Costelloe, R. Casas Mulet, J. P. Lyon, and M. J. Stewardson (Melbourne: AU University of Melbourne).

Folkard, A. M., and Bouma, J. A. (2016). "Creating patches of comprehension and filling gaps in knowledge: physical modelling contributions to joined-up understanding of heterogeneous eco-scapes," in *Proceedings of the 11th International Symposium on Ecohydraulics*, eds J. F. Costelloe, R. Casas Mulet, J. P. Lyon, and M. J. Stewardson. (Melbourne: AU University of Melbourne).

Follett, E. M., and Nepf, H. M. (2012). Sediment patterns near a model patch of reedy emergent vegetation. *Geomorphology* 179, 141–151. doi: 10.1016/j.geomorph.2012.08.006

Fonseca, M. S., Kenworthy, W. J., Griffith, E., Hall, M. O., Finkbeiner, M., and Bell, S. S. (2008). Factors influencing landscape pattern of the seagrass *Halophila decipiens* in an oceanic setting. *Estuar. Coast. Shelf Sci.* 76, 163–174. doi: 10.1016/j.ecss.2007.06.014

Francoeur, S. N., Biggs, B. J. F., and Lowe, R. L. (1998). Microform bed clusters as refugia for periphyton in a flood-prone headwater stream. *N. Z. J. Mar. Freshw. Res.* 32, 363–374. doi: 10.1080/00288330.1998.9516831

Fraschetti, S., Bevilacqua, S., Guarnieri, G., and Terlizzi, A. (2012). Idiosyncratic effects of protection in a remote marine reserve. *Mar. Ecol. Prog. Ser.* 466, 21–34. doi: 10.3354/meps09937

Gera, A., Pages, J. F., Romero, J., and Alcoverro, T. (2013). Combined effects of fragmentation and herbivory on *Posidonia oceanica* seagrass ecosystems. *J. Ecol.* 101, 1053–1061. doi: 10.1111/1365-2745.12109

Ghisalberti, M., and Nepf, H. M. (2004). The limited growth of vegetated shear layers. *Water Res. Res.* 40:W07502. doi: 10.1029/2003WR002776

Gonzalez-Ortiz, V., Egea, L. G., Jimenez-Ramos, R., Moreno-Marin, F., Perez-Llorens, J. L., Bouma, T. J., et al. (2014). Interactions between seagrass complexity, hydrodynamic flow and biomixing alter food availability for associated filter-feeding organisms. *PLoS One* 9:e104949. doi: 10.1371/journal.pone.0104949

Grech, A., Wolter, J., Coles, R., McKenzie, L., Rasheed, M., Thomas, C., et al. (2016). Spatial patterns of seagrass dispersal and settlement. *Divers. Distrib.* 22, 1150–1162. doi: 10.1111/ddi.12479

Gresens, S. E., and Lowe, R. L. (1994). Periphyton patch preference in grazing chironomid larvae. *J. North Am. Benthol. Soc.* 13, 89–99. doi: 10.2307/1467269

Gurnell, A. M. (2007). Analogies between mineral sediment and vegetative particle dynamics in fluvial systems. *Geomorphology* 89, 9–22. doi: 10.1016/j.geomorph.2006.07.012

Gurnell, A. M. (2014). Plants as river system engineers. *Earth Surf. Process. Landf.* 39, 4–25. doi: 10.1002/esp.3397

Gurnell, A. M., Bertoldi, W., and Corenblit, D. (2012). Changing river channels: the roles of hydrological processes, plants and pioneer fluvial landforms in humid temperate, mixed load, gravel bed rivers. *Earth Sci. Rev.* 111, 129–141. doi: 10.1016/j.earscirev.2011.11.005

Harwell, M. C., and Orth, R. J. (2002). Long-distance dispersal potential in a marine macrophyte. *Ecology* 83, 3319–3330. doi: 10.1890/0012-9658(2002)083%5B3319:lddpia%5D2.0.co;2

Hemminga, M. A., van Soelen, J., and Maas, Y. E. M. (1998). Biomass production in pioneer spartina anglica patches: evidence for the importance of seston particle deposition. *Estuar. Coast. Shelf Sci.* 47, 797–805. doi: 10.1006/ecss.1998.0388

Holomuzki, J. R., Lowe, R. L., and Ress, J. A. (2006). Comparing herbivory effects of stream macroinvertebrates on microalgal patch structure and recovery. *N. Z. J. Mar. Freshw. Res.* 40, 357–367. doi: 10.1080/00288330.2006.9517427

Howison, R. A., Olff, H., van de Koppel, J., and Smit, C. (2017). Biotically driven vegetation mosaics in grazing ecosystems: the battle between bioturbation and biocompaction. *Ecol. Monogr.* 87, 363–378. doi: 10.1002/ecm.1259

James, C. S., Birkhead, A. L., Jordanova, A. A., and O'Sullivan, J. J. (2004). Flow resistance of emergent vegetation. *J. Hydraulic Res.* 42, 390–398. doi: 10.1080/00221686.2004.9641206

Jimenez-Ramos, R., Mancilla, M., Villazan, B., Egea, L. G., Gonzalez-Ortiz, V., Vergara, J. J., et al. (2017). Resistance to nutrient enrichment varies among components in the cymodocea nodosa community. *J. Exp. Mar. Biol. Ecol.* 497, 41–49. doi: 10.1016/j.jembe.2017.09.008

Jones, C. G., Lawton, J. H., and Shachak, M. (1994). *Organisms as Ecosystem Engineers in Ecosystem Management*. New York, NY: Springer.

Jurgens, L. J., and Gaylord, B. (2016). Edge effects reverse facilitation by a widespread foundation species. *Sci. Rep.* 6:37573. doi: 10.1038/srep37573

Kleeberg, A., Kohler, J., Sukhodolova, T., and Sukhodolov, A. (2010). Effects of aquatic macrophytes on organic matter deposition, resuspension and phosphorus entrainment in a lowland river. *Freshw. Biol.* 55, 326–345. doi: 10.1111/j.1365-2427.2009.02277.x

Koch, E. W. (2001). Beyond light: physical, geological, and geochemical parameters as possible submersed aquatic vegetation habitat requirements. *Estuaries* 24, 1–17. doi: 10.2307/1352808

Kondziolka, J. M., and Nepf, H. M. (2014). Vegetation wakes and wake interaction shaping aquatic landscape evolution. *Limnol. Oceanogr.* 4, 106–119. doi: 10.1215/21573689-2846314

Lara, M., Peralta, G., Alonso, J. J., Morris, E. P., Gonzalez-Ortiz, V., Rueda-Marquez, J. J., et al. (2012). Effects of intertidal seagrass habitat fragmentation on turbulent diffusion and retention time of solutes. *Mar. Pollut. Bull.* 64, 2471–2479. doi: 10.1016/j.marpolbul.2012.07.044

Larned, S. T., Suren, A. M., Flanagan, M., Biggs, B. J. F., and Riis, T. (2006). Macrophytes in urban stream rehabilitation: establishment, ecological effects, and public perception. *Restor. Ecol.* 14, 429–440. doi: 10.1111/j.1526-100X.2006.00151.x

Larsen, L. G., and Harvey, J. W. (2010). How vegetation and sediment transport feedbacks drive landscape change in the everglades and wetlands worldwide. *Am. Nat.* 176, E66–E79. doi: 10.1086/655215

Larsen, L. G., and Harvey, J. W. (2011). Modeling of hydroecological feedbacks predicts distinct classes of landscape pattern, process, and restoration potential in shallow aquatic ecosystems. *Geomorphology* 126, 279–296. doi: 10.1016/j.geomorph.2010.03.015

Larsen, L. G., Harvey, J. W., and Crimaldi, J. P. (2007). A delicate balance: ecohydrological feedbacks governing landscape morphology in a lotic peatland. *Ecol. Monogr.* 77, 591–614. doi: 10.1890/06-1267.1

Larsen, L. G., Ma, J., and Kaplan, D. (2017). How important is connectivity for surface water fluxes? A generalized expression for flow through heterogeneous landscapes. *Geophys. Res. Lett.* 44, 10349–10358. doi: 10.1002/2017GL075432

Lefcheck, J. S., Marion, S. R., Lombana, A. V., and Orth, R. J. (2016). Faunal communities are invariant to fragmentation in experimental seagrass landscapes. *PLoS One* 11:e0156550. doi: 10.1371/journal.pone.0156550

Lefebvre, A., Thompson, C. E. L., and Amos, C. L. (2010). Influence of zostera marina canopies on unidirectional flow, hydraulic roughness and sediment movement. *Cont. Shelf Res.* 30, 1783–1794. doi: 10.1016/j.csr.2010.08.006

Levi, P. S., Riis, T., Alnoe, A. B., Peipoch, M., Maetzke, K., Bruus, C., et al. (2015). Macrophyte complexity controls nutrient uptake in lowland streams. *Ecosystems* 18, 914–931. doi: 10.1007/s10021-015-9872-y

Liao, J. B., Bearup, D., and Blasius, B. (2017). Diverse responses of species to landscape fragmentation in a simple food chain. *J. Anim. Ecol.* 86, 1169–1178. doi: 10.1111/1365-2656.12702

Lightbody, A. F., Avener, M. E., and Nepf, H. M. (2008). Observations of short-circuiting flow paths within a free-surface wetland in Augusta. Georgia, USA. *Limnol. Oceanogr.* 53, 1040–1053. doi: 10.4319/lo.2008.53.3.1040

Liu, C., Hu, Z. H., Lei, J. R., and Nepf, H. M. (2018). Vortex structure and sediment deposition in the wake behind a finite patch of model submerged vegetation. *J. Hydraulic Eng.* 144:04017065. doi: 10.1061/(ASCE)HY.1943-7900.0001408

Liu, C., and Nepf, H. M. (2016). Sediment deposition within and around a finite patch of model vegetation over a range of channel velocity. *Water Res. Res.* 52, 600–612. doi: 10.1002/2015WR018249

Liu, J. T., Rong, Q. Q., and Zhao, Y. Y. (2017). Variations in soil nutrients and salinity caused by tamarisk in the coastal wetland of the laizhou bay, China. *Ecosphere* 8:e01672. doi: 10.1002/ecs2.1672

Liu, Q. X., Herman, P. M. J., Mooij, W. M., Huisman, J., Scheffer, M., Olff, H., et al. (2014). Pattern formation at multiple spatial scales drives the resilience of mussel bed ecosystems. *Nat. Commun.* 5:5234. doi: 10.1038/ncomms6234

Lowe, R. J., and Falter, J. L. (2015). Oceanic forcing of coral reefs. *Annu. Rev. Mar. Sci.* 7, 43–66. doi: 10.1146/annurev-marine-010814-015834

Lowe, R. J., Koseff, J. R., and Monismith, S. G. (2005). Oscillatory flow through submerged canopies: 1. velocity structure. *J. Geophys. Res.* 110:C10016.

Luhar, M., and Nepf, H. M. (2013). From the blade scale to the reach scale: a characterization of aquatic vegetative drag. *Adv. Water Res.* 51, 305–316. doi: 10.1016/j.advwatres.2012.02.002

Luhar, M., Rominger, J., and Nepf, H. M. (2008). Interaction between flow, transport and vegetation spatial structure. *Environ. Fluid Mech.* 8, 423–439. doi: 10.1007/s10652-008-9080-9

Lumley, J. L., and Panofsky, H. A. (1964). *The Structure of Atmospheric Turbulence*. New York, NY: John Wiley.

Markfort, C. D., Perez, A. L. S., Thill, J. W., Jaster, D. A., Porte-Agel, F., and Stefan, H. G. (2010). Wind sheltering of a lake by a tree canopy or bluff topography. *Water Res. Res.* 46:W03530. doi: 10.1029/2009WR007759

Markfort, C. D., Porte-Agel, F., and Stefan, H. G. (2014). Canopy-wake dynamics and wind sheltering effects on earth surface fluxes. *Environ. Fluid Mech.* 14, 663–697. doi: 10.1007/s10652-013-9313-4

Matias, M. G., Arenas, F., Rubal, M., and Pinto, I. S. (2015). Macroalgal composition determines the structure of benthic assemblages colonizing fragmented habitats. *PLoS One* 10:e0142289. doi: 10.1371/journal.pone.0142289

Maza, M., Lara, J. L., Losada, J., Ondiviela, B., Trinogga, J., and Bouma, T. J. (2015). Large-scale 3-D experiments of wave and current interaction with real vegetation. *Part* 2: experimental analysis. *Coast. Eng.* 106, 73–86. doi: 10.1016/j.coastaleng.2015.09.010

McGarigal, K., and Cushman, S. (2005). "The gradient concept of landscape structure," in *Issues and Perspectives in Landscape Ecology*, eds J. A. Wiens and M. R. Moss (Cambridge: Cambridge University Press), 112–119. doi: 10.1017/cbo9780511614415.013

McGarigal, K., and Marks, B. J. (1995). *FRAGSTATS: Spatial Pattern Analysis Program for Quantifying Landscape Structure*. Gen. Tech. Rep. PNW-GTR-351. Portland, OR: U.S. Department of Agriculture.

McGarigal, K., Tagil, S., and Cushman, S. A. (2009). Surface metrics: an alternative to patch metrics for the quantification of landscape structure. *Landsc. Ecol.* 24, 433–450. doi: 10.1007/s10980-009-9327-y

Meire, D. W. S. A., Kondziolka, J. M., and Nepf, H. M. (2014). Interaction between neighboring vegetation patches: impact on flow and deposition. *Water Res. Res.* 50, 3809–3825. doi: 10.1002/2013WR015070

Moeller, I., Kudella, M., Rupprecht, F., Spencer, T., Paul, M., van Wesenbeeck, B. K., et al. (2014). Wave attenuation over coastal salt marshes under storm surge conditions. *Nat. Geosci.* 7, 727–731. doi: 10.1038/NGEO2251

Monismith, S. G. (2007). Hydrodynamics of coral reefs. *Annu. Rev. Fluid Mech.* 39, 37–55. doi: 10.1146/annurev.fluid.38.050304.092125

Morris, E. P., Peralta, G., Brun, F. G., van Duren, L., Bouma, T. J., Perez-Llorens, J. L., et al. (2008). Interaction between hydrodynamics and seagrass canopy structure: spatially explicit effects on ammonium uptake rates. *Limnol. Oceanogr.* 53, 1531–1539. doi: 10.4319/lo.2008.53.4.1531

Morris, H. M. (1955). Flow in rough conduits. *Trans. Am. Soc. Civil Eng.* 120, 373–398. doi: 10.1088/1748-3190/10/1/016015

Mota, C. F., Engelen, A. H., Serrao, E. A., and Pearson, G. A. (2015). Some don't like it hot: microhabitat-dependent thermal and water stresses in a trailing edge population. *Funct. Ecol.* 29, 640–649. doi: 10.1111/1365-2435.12373

Nardin, W., Locatelli, S., Pasquarella, V., Rulli, M. C., Woodcock, C. E., and Fagherazzi, S. (2016). Dynamics of a fringe mangrove forest detected by landsat images in the mekong river delta. Vietnam. *Earth Surf. Process. Landf.* 41, 2024–2037. doi: 10.1002/esp.3968

Nepf, H. M. (1999). Drag, turbulence, and diffusion in flow through emergent vegetation. *Water Res. Res.* 35, 479–489. doi: 10.1029/1998WR900069

Nepf, H. M. (2012). Hydrodynamics of vegetated channels. *J. Hydraulic Res.* 50, 262–279. doi: 10.1080/00221686.2012.696559

Nepf, H. M., and Ghisalberti, M. (2008). Flow and transport in channels with submerged vegetation. *Acta Geophys.* 56, 753–777. doi: 10.2478/s11600-008-0017-y

Nepf, H. M., Sullivan, J. A., and Zavistoski, R. A. (1997). A model for diffusion within emergent vegetation. *Limnol. Oceanogr.* 42, 1735–1745. doi: 10.4319/lo.1997.42.8.1735

Nepf, H. M., and Vivoni, E. R. (2000). Flow structure in depth-limited, vegetated flow. *J. Geophys. Res.* 105, 28547–28557. doi: 10.1029/2000jc900145

Nikora, V. (2010). Hydrodynamics of aquatic ecosystems: an interface between ecology, biomechanics and environmental fluid mechanics. *River Res. Appl.* 26, 367–384. doi: 10.1002/rra.1291

Norris, B. K., Mullarney, J. C., Bryan, K. R., and Henderson, S. M. (2017). The effect of pneumatophore density on turbulence: a field study in a sonneratia-dominated mangrove forest, Vietnam. *Cont. Shelf Res.* 147, 114–127. doi: 10.1016/j.csr.2017.06.002

O'Brien, K. R., Waycott, M., Maxwell, P., Kendrick, G. A., Udy, J. W., Ferguson, A. J. P., et al. (2018). Seagrass ecosystem trajectory depends on the relative timescales of resistance, recovery and disturbance. *Mar. Pollut. Bull.* 134, 166–176. doi: 10.1016/j.marpolbul.2017.09.006

O'Hare, M. T., and Murphy, K. J. (1999). Invertebrate hydraulic microhabitat and community structure in *Callitriche stagnalis* scop patches. *Hydrobiologia* 415, 169–176. doi: 10.1023/A:1003827000258

Opdekamp, W., Teuchies, J., Vrebos, D., Chormanski, J., Schoelynck, J., van Diggelen, R., et al. (2012). Tussocks: biogenic silica hot-spots in a riparian wetland. *Wetlands* 32, 1115–1124. doi: 10.1007/s13157-012-0341-5

Ortiz, A. C., Ashton, A., and Nepf, H. M. (2013). Mean and turbulent velocity fields near rigid and flexible plants and the implications for deposition. *J. Geophys. Res.* 118, 2585–2599. doi: 10.1002/2013JF002858

Parnell, P. E. (2015). The effects of seascape pattern on algal patch structure, sea urchin barrens, and ecological processes. *J. Exp. Mar. Biol. Ecol.* 465, 64–76. doi: 10.1016/j.jembe.2015.01.010

Peterson, C. H., Luettich, R. A. Jr., Micheli, F., and Skilleter, G. A. (2004). Attenuation of water flow inside seagrass canopies of differing structure. *Mar. Ecol. Prog. Ser.* 268, 81–92. doi: 10.3354/meps268081

Pringle, R. M., and Tarnita, C. E. (2017). Spatial self-organization of ecosystems: integrating multiple mechanisms of regular-pattern formation. *Annu. Rev. Entomol.* 62, 359–377. doi: 10.1146/annurev-ento-031616-035413

Pujol, D., and Nepf, H. M. (2012). Breaker-generated turbulence in and above a seagrass meadow. *Cont. Shelf Res.* 49, 1–9. doi: 10.1016/j.csr.2012.09.004

Pujol, D., Casamitjana, X., Serra, T., and Colomer, J. (2013a). Canopy-scale turbulence under oscillatory flow. *Cont. Shelf Res.* 66, 9–18. doi: 10.1016/j.csr.2013.06.012

Pujol, D., Serra, T., Colomer, J., and Casamitjana, X. (2013b). Flow structure in canopy models dominated by progressive waves. *J. Hydrol.* 486, 281–292. doi: 10.1016/j.jhydrol.2013.01.024

Resh, V. H., Hildrew, A. G., Statzner, B., and Townsend, C. R. (1994). Theoretical habitat templets, species traits, and species richness - a synthesis of long-term ecological research on the upper rhone river in the context of concurrently developed ecological theory. *Freshw. Biol.* 31, 539–554. doi: 10.1111/j.1365-2427.1994.tb01756.x

Reusch, T. B. H., and Williams, S. L. (1999). Macrophyte canopy structure and the success of an invasive marine bivalve. *Oikos* 84, 398–416. doi: 10.2307/3546420

Rietkerk, M., Dekker, S. C., de Ruiter, P. C., and van de Koppel, J. (2004). Self-organized patchiness and catastrophic shifts in ecosystems. *Science* 305, 1926–1929. doi: 10.1126/science.1101867

Rietkerk, M., and van de Koppel, J. (2008). Regular pattern formation in real ecosystems. *Trends Ecol. Evol.* 23, 169–175. doi: 10.1016/j.tree.2007.10.013

Riis, T. (2008). Dispersal and colonisation of plants in lowland streams: success rates and bottlenecks. *Hydrobiologia* 596, 341–351. doi: 10.1007/s10750-007-9107-0

Rinde, E., Christie, H., Fagerli, C. W., Bekkby, T., Gundersen, H., Norderhaug, K. M., et al. (2014). The influence of physical factors on kelp and sea urchin distribution in previously and still grazed areas in the NE Atlantic. *PLoS One* 9:e100222. doi: 10.1371/journal.pone.0100222

Robbins, B. D., and Bell, S. S. (1994). Seagrass landscapes: a terrestrial approach to the marine subtidal environment. *Trends Ecol. Evol.* 9, 301–304. doi: 10.1016/0169-5347(94)90041-8

Ruiz-Reynés, D., Gomila, D., Sintes, T., Hernández-García, E., Marbà, N., and Duarte, C. M. (2017). Fairy circle landscapes under the sea. *Sci. Adv.* 3:e1603262. doi: 10.1126/sciadv.1603262

Salta, M., Wharton, J. A., Blache, Y., Stokes, K. R., and Briand, J. F. (2013). Marine biofilms on artificial surfaces: structure and dynamics. *Environ. Microbiol.* 15, 2879–2893. doi: 10.1111/1462-2920.12186

Sand-Jensen, K. (1998). Influence of submerged macrophytes on sediment composition and near-bed flow in lowland streams. *Freshw. Biol.* 39, 663–679. doi: 10.1046/j.1365-2427.1998.00316.x

Schoelynck, J., Creelle, S., Buis, K., De Mulder, T., Emsens, W. J., Hein, T., et al. (2018). What is a macrophyte patch? Patch identification in aquatic ecosystems and guidelines for consistent delineation. *Ecohydrol. Hydrobiol.* 18, 1–9. doi: 10.1016/j.ecohyd.2017.10.005

Schoelynck, J., De Groote, T., Bal, K., Vandenbruwaene, W., Meire, P., and Temmerman, S. (2012). Self-organised patchiness and scale-dependent bio-geomorphic feedbacks in aquatic river vegetation. *Ecography* 35, 760–768. doi: 10.1111/j.1600-0587.2011.07177.x

Schoelynck, J., Schaller, J., Murray-Hudson, M., Frings, P. J., Conley, D. J., van Pelt, D., et al. (2017). The trapping of organic matter within plant patches in the channels of the okavango delta: a matter of quality. *Aquatic Sci.* 79, 661–674. doi: 10.1007/s00027-017-0527-2

Serrano, O., Ruhon, R., Lavery, P. S., Kendrick, G. A., Hickey, S., Masqué, P., et al. (2016). Impact of mooring activities on carbon stocks in seagrass meadows. *Sci. Rep.* 6:23193. doi: 10.1038/srep23193

Shi, Y., Jiang, B. H., and Nepf, H. M. (2016). Influence of particle size and density, and channel velocity on the deposition patterns around a circular patch of model emergent vegetation. *Water Res. Res.* 52, 1044–1055. doi: 10.1002/2015WR018278

Siniscalchi, F., Nikora, V. I., and Aberle, J. (2012). Plant patch hydrodynamics in streams: mean flow, turbulence, and drag forces. *Water Res. Res.* 48:W01513. doi: 10.1029/2011WR011050

Sukhodolov, A. N., and Sukhodolova, T. A. (2010). Case study: effect of submerged aquatic plants on turbulence structure in a lowland river. *ASCE J. Hydraulic Eng.* 136, 434–446. doi: 10.1061/(ASCE)HY.1943-7900.0000195

Sukhodolova, T. A., and Sukhodolov, A. N. (2012). Vegetated mixing layer around a finite-size patch of submerged plants: 1. Theory and field experiments. *Water Res. Res.* 48:W10533. doi: 10.1029/2011WR011804

Tamburello, L., Benedetti-Cecchi, L., Ghedini, G., Alestra, T., and Bulleri, F. (2012). Variation in the structure of subtidal landscapes in the NW mediterranean sea. *Mar. Ecol. Prog. Ser.* 457, 29–41. doi: 10.3354/meps09703

Temmerman, S., Bouma, T. J., van de Koppel, J., van der Wal, D. D., De Vries, M. B., and Herman, P. M. J. (2007). Vegetation causes channel erosion in a tidal landscape. *Geology* 35, 631–634. doi: 10.1130/G23502A.1

Thomas, R. E., Johnson, M. F., Frostick, L. E., Parsons, D. R., Bouma, T. J., Dijkstra, J. T., et al. (2014). Physical modelling of water, fauna and flora: knowledge gaps, avenues for future research and infrastructural needs. *J. Hydraulic Res.* 52, 311–325. doi: 10.1080/00221686.2013.876453

Thomson, D. P., Babcock, R. C., Vanderklift, M. A., Symonds, G., and Gunson, J. R. (2012). Evidence for persistent patch structure on temperate reefs and multiple hypotheses for their creation and maintenance. *Estuar. Coast. Shelf Sci.* 96, 105–113. doi: 10.1016/j.ecss.2011.10.014

Townsend, C. R. (1989). The patch dynamics concept of stream community ecology. *J. North Am. Benthol. Soc.* 8, 36–50. doi: 10.2307/1467400

Townsend, E. C., and Fonseca, M. S. (1998). Bioturbation as a potential mechanism influencing spatial heterogeneity of north carolina seagrass beds. *Mar. Ecol. Progress. Ser.* 169, 123–132. doi: 10.3354/meps169123

Umanzor, S., Ladah, L., and Zertuche-Gonzalez, J. A. (2017). The influence of species, density, and diversity of macroalgal aggregations on microphytobenthic settlement. *J. Phycol.* 53, 1060–1071. doi: 10.1111/jpy.12565

Underwood, A. J. (1998). Crazing and disturbance: an experimental analysis of patchiness in recovery from a severe storm by the intertidal alga *Hormosira banksii* on rocky shores in New South wales. *J. Exp. Mar. Biol. Ecol.* 231, 291–306. doi: 10.1016/S0022-0981(98)00091-4

van de Koppel, J., Bouma, T. J., and Herman, P. M. J. (2012). The influence of local- and landscape-scale processes on spatial self-organization in estuarine ecosystems. *J. Exp. Biol.* 215, 962–967. doi: 10.1242/jeb.060467

van der Heide, T., Bouma, T. J., van Nes, E. H., van de Koppel, J., Scheffer, M., Roeloefs, J. G. M., et al. (2010). Spatial self-organized patterning in seagrasses along a depth gradient of an intertidal eco-system. *Ecology* 91, 362–369. doi: 10.1890/08-1567.1

van Hulzen, J. B., van Soelen, J., Herman, P. M. J., and Bouma, T. J. (2006). The significance of spatial and temporal patterns of algal mat deposition in structuring salt marsh vegetation. *J. Veg. Sci.* 17, 291–298. doi: 10.1111/j.1654-1103.2006.tb02448.x

van Katwijk, M. M., Bos, A. R., de Jonge, V. N., Hanssen, L. S. A. M., Hermus, D. C. R., and de Jong, D. J. (2009). Guidelines for seagrass restoration: importance of habitat selection and donor population, spreading of risks, and ecosystem engineering effects. *Mar. Pollut. Bull.* 58, 179–188. doi: 10.1016/j.marpolbul.2008.09.028

van Katwijk, M. M., and Hermus, D. C. R. (2000). Effects of water dynamics on *Zostera marina*: transplantation experiments in the intertidal dutch wadden sea. *Mar. Ecol. Prog. Ser.* 208, 107–118. doi: 10.3354/meps208107

van Tussenbroek, B. I., Soissons, L. M., Bouma, T. J., Asmus, R., Auby, I., Brun, F. G., et al. (2016). Pollen limitation may be a common allee effect in marine hydrophilous plants: implications for decline and recovery in seagrasses. *Oecologia* 182, 595–609. doi: 10.1007/s00442-016-3665-7

van Wesenbeeck, B. K., van de Koppel, J., Herman, P. M. J., and Bouma, T. J. (2008). Does scale-dependent feedback explain spatial complexity in salt-marsh ecosystems? *Oikos* 117, 152–159. doi: 10.1111/j.2007.0030-1299.16245.x

Vandenbruwaene, W., Bouma, T. J., Meire, P., and Temmerman, S. (2013). Bio-geomorphic effects on tidal channel evolution: impact of vegetation establishment and tidal prism change. *Earth Surf. Process. Landf.* 38, 122–132. doi: 10.1002/esp.3265

Vandenbruwaene, W., Temmerman, S., Bouma, T. J., Klaassen, P. C., de Vries, M. B., Callaghan, D. P., et al. (2011). Flow interaction with dynamic vegetation patches: implications for biogeomorphic evolution of a tidal landscape. *J. Geophys. Res.* 116:F01008. doi: 10.1029/2010JF001788

Vaughan, I. P., Diamond, M., Gurnell, A. M., Hall, K. A., Jenkins, A., Milner, N. J., et al. (2009). Integrating ecology with hydromorphology: a priority for river science and management. *Aquatic Conserv.* 19, 113–125. doi: 10.1002/aqc.895

Verschoren, V. (2017). *Spatial Pattern Formation of Macrophytes: An Integrated Model for the Management of Lowland Rivers*. Ph.D. thesis, University of Antwerp, Antwerpen.

Villard, M. A., and Metzger, J. P. (2014). Beyond the fragmentation debate: a conceptual model to predict when habitat configuration really matters. *J. Appl. Ecol.* 51, 309–318. doi: 10.1111/1365-2664.12190

Voerman, S. E., Glasby, T. M., Gladstone, W., and Gribben, P. E. (2017). Habitat associations of an expanding native alga. *Mar. Environ. Res.* 131, 205–214. doi: 10.1016/j.marenvres.2017.09.019

Vogt, J., Skora, A., Feller, I. C., Piou, C., Coldren, G., and Berger, U. (2012). Investigating the role of impoundment and forest structure on the resistance and resilience of mangrove forests to hurricanes. *Aquatic Bot.* 97, 24–29. doi: 10.1016/j.aquabot.2011.10.006

Weerman, E. J., van Belzen, J., Rietkerk, M., Temmerman, S., Kefi, S., Herman, P. M. J., et al. (2012). Changes in diatom patch-size distribution and degradation in a spatially self-organized intertidal mudflat ecosystem. *Ecology* 93, 608–618. doi: 10.1890/11-0625.1

Weerman, E. J., van der Geest, H. G., van der Meulen, M. D., Manders, E. M. M., van de Koppel, J., Herman, P. M. J., et al. (2011). Ciliates as engineers of phototrophic biofilms. *Freshw. Biol.* 56, 1358–1369. doi: 10.1111/j.1365-2427.2011.02574.x

Wernberg, T., and Connell, S. D. (2008). Physical disturbance and subtidal habitat structure on open rocky coasts: effects of wave exposure, extent and intensity. *J. Sea Res.* 59, 237–248. doi: 10.1016/j.seares.2008.02.005

Yager, P. L., Nowell, A. R. M., and Jumars, P. A. (1993). Enhanced deposition to pits: a local food source for benthos. *J. Mar. Res.* 51, 209–236. doi: 10.1357/0022240933223819

Yan, X. F., Wai, W. H. O., and Li, C. W. (2016). Characteristics of flow structure of free-surface flow in a partly obstructed open channel with vegetation patch. *Environ. Fluid Mech.* 16, 807–832. doi: 10.1007/s10652-016-9453-4

Zhang, Y. H., Tang, C. H., and Nepf, H. M. (2018). Turbulent kinetic energy in submerged model canopies under oscillatory flow. *Water Res. Res.* 54, 1734–1750. doi: 10.1002/2017WR021732

Zong, L. J., and Nepf, H. M. (2010). Flow and deposition in and around a finite patch of vegetation. *Geomorphology* 116, 363–372. doi: 10.1016/j.geomorph.2009.11.020

Zong, L. J., and Nepf, H. M. (2011). Spatial distribution of deposition within a patch of vegetation. *Water Res. Res.* 47:W03516. doi: 10.1029/2010WR009516

Conflict of Interest Statement: The author declares that the research was conducted in the absence of any commercial or financial relationships that could be construed as a potential conflict of interest.

frontiers in Marine Science

ORIGINAL RESEARCH
published: 09 July 2019
doi: 10.3389/fmars.2019.00376

Effect of Seagrass on Current Speed: Importance of Flexibility vs. Shoot Density

Mark S. Fonseca[1], James W. Fourqurean[2] and M. A. R. Koehl[3]*

[1] CSA Ocean Sciences Inc., Stuart, FL, United States, [2] Department of Biological Sciences, Center for Coastal Oceans Research, Florida International University, Miami, FL, United States, [3] Department of Integrative Biology, University of California, Berkeley, Berkeley, CA, United States

Water flow through seagrass beds transports nutrients, affects sediment stability and chemistry, and imposes hydrodynamic forces on shoots that alter canopy configuration. Past studies done under diverse conditions yielded conflicting results about the effects of shoot density on flow through seagrass bed canopies. We used eelgrass, *Zostera marina*, to study how the density of flexible shoots affect the hydrodynamics of seagrass beds in unidirectional water flow. By exposing randomly-arranged shoots of uniform length to current velocities controlled in a flume, the effects of shoot density and distance downstream from the bed edge could be determined without confounding factors. Comparison of velocity profiles within beds to those upstream of beds showed that flow was slower in the beds. However, shoot density, downstream distance, and current velocity did not affect the percent reduction in flow velocity in a bed. Turbulence enhances mixing of substances carried in the water. Here, turbulence intensity (index of the importance of turbulent velocity fluctuations relative to average current velocity) was lower when ambient flow was faster, but was not affected by shoot density or downstream position, Drag (hydrodynamic force on a shoot that bends it over in the flow direction) provides another measure of how the canopy affects flow experienced by a shoot. Drag was not affected by current velocity, shoot density, or downstream position in the bed. Gaps between shoots can enhance light and flow penetration into the canopy, but when shoots are bent over by flow, they can cover gaps. Faster ambient currents caused greater gap closure, which at each current speed was greater for high shoot densities. Thus, canopy gap closure did not correlate with percent flow reduction in grass beds or with drag on individual shoots, both of which were independent of shoot density and ambient current velocity. Since changing shoot density does not affect the flow in a grass bed exposed to a given ambient current, our results are inconsistent with the hypothesis that the high shoot densities observed in grass beds in habitats exposed to rapid flow are due to a direct, adaptive response of the grass to the flow environment.

Keywords: seagrass, current speed, shoot density, flexibility, canopy, gaps

OPEN ACCESS

Edited by:
Virginia B. Pasour, Army Research Office, United States

Reviewed by:
Lucy Gwen Gillis, Leibniz Centre for Tropical Marine Research (LG), Germany
Jennifer Joan Verduin, Murdoch University, Australia
Free Espinosa Torre, University of Seville, Spain

****Correspondence:***
Mark S. Fonseca
mfonseca@conshelf.com

Specialty section:
This article was submitted to Marine Ecosystem Ecology, a section of the journal Frontiers in Marine Science

Received: *06 September 2018*
Accepted: *17 June 2019*
Published: *09 July 2019*

Citation:
Fonseca MS, Fourqurean JW and Koehl MAR (2019) Effect of Seagrass on Current Speed: Importance of Flexibility vs. Shoot Density. Front. Mar. Sci. 6:376. doi: 10.3389/fmars.2019.00376

INTRODUCTION

Studies of water flow through seagrass beds have been carried out under different conditions (e.g., unidirectional currents vs. waves, field sites vs. laboratory flumes, various species vs. physical mimics or mathematical models), and thus have yielded conflicting results about the effects of shoot density on flow within and above seagrass beds. Even though focusing on the numerous studies that have examined the behavior of unidirectional water flow in and around seagrass canopies (e.g., Fonseca et al., 1982, 1983, 2007; Fonseca and Fisher, 1986; Fonseca and Kenworthy, 1987; Gambi et al., 1990; Ackerman and Okubo, 1993; Worcester, 1995; Koch and Gust, 1999; Verduin and Backhaus, 2000; Abdelrhman, 2003; Newell and Koch, 2004; Peterson et al., 2004; Fonseca and Koehl, 2006; Lacy and Wyllie-Echeverria, 2011; Lei and Nepf, 2016) consistently reveals that seagrass beds reduce flow velocity within the canopy, the effect of (seagrass[1]) shoot density on this velocity reduction is not clear.

Effects of Shoot Density on Water Flow in Seagrass Beds

The discrepancies between various empirical studies of shoot density effects on flow may be due to differences between studies in the range of densities compared, the flow conditions, the position within a seagrass bed that the flow was measured, and the morphology of the seagrass. For example, Lacy and Wyllie-Echeverria (2011) found for eelgrass (*Zostera marina*) that flow speed was attenuated more by beds with higher shoot densities. However, their shoot densities were low (44–63 shoots m^{-2}) and the plants they studied were from water depths of 3–4 m and thus had longer leaves (∼1.5 m leaf length) than do *Z. marina* from shallower sites (e.g., plants used in this study taken from seagrass beds of <2 m water depth; Fonseca et al., 2002). Likewise, Worcester (1995) considered the lower end of the shoot density range in an open, natural system and under very low ambient current speeds. She found that in a natural setting with current speeds of only 0.05 m s^{-1} and shoot density (with very large plants) of <200 shoots m^{-2}, found there was still significant reduction in currents within as opposed to above the canopy, whereas the turbulence of the flow was unaffected. In contrast Adhitya et al. (2014) studied seagrass beds with higher shoot densities (400 and 1100 shoots m^{-2}) and found that shoot density affected the flow dynamics at a very low ambient current speed (0.10 m s^{-1}), which is so slow that it does not fully deflect a seagrass canopy (Fonseca and Kenworthy, 1987). However, Adhitya et al. (2014) also found the spatial organization of seagrass shoots at the meadow scale was more important than shoot density within a patch in explaining hydrodynamic effects of seagrass beds. Paul and Gillis (2015) also found an effect of shoot density on flow reduction by beds of *Z. noltii*. They visually compared velocity profiles and concluded that canopy bending, and waving did not affect the flow-reduction capacity of their grass beds. In contrast, Fonseca et al. (1982, 2007), Fonseca and Fisher (1986), and Gambi et al. (1990) found little influence of shoot density on the degree of current speed reduction within beds of *Z. marina*. Interestingly, while Gambi et al. (1990) found no statistically significant difference in shear velocity or turbulence intensity in seagrass beds as a function of shoot density, they concluded "*More replicates in each position probably would reveal statistically significant differences between densities.*" Their assumption that shoot density affects flow was compelling, and their paper has been interpreted by others as having demonstrated that shoot density affects flow (e.g., Koch et al., 2006).

Various mathematical models have explored whether shoot density affects water flow within grass beds. Dijkstra and Uittenbogaard (2010) simulated the effect of shoot density and flexibility and found that turbulence intensity was decreased as shoot density increased (up to 10,000 shoots per m^{-2}), and that the drag force on stiff shoots was greater than on more flexible shoots. Their model suggests that both high shoot density and increased flexibility could be mechanisms that enable seagrass to withstand rapid ambient currents. Abdelrhman (2003) used shoot density as a factor influencing in-canopy flow in a model and found that high shoot density reduced transport through the canopy by increasing the tortuosity of the paths of water moving around seagrass shoots. However, Abdelrhman's model did not clarify the hydrodynamic conditions under which these different shoot densities may occur in the field. The model of Newell and Koch (2004) assumed critical shoot-density thresholds for wave attenuation by seagrass beds, and the model of Koch et al. (2006) also assumed that higher shoot density produced lower in-bed flow velocities. Thus, shoot density effects have become codified in models and perception, in spite of the conflicting empirical results. One way to resolve this issue would be to measure the hydrodynamic effects of shoot density at known positions in beds of actual plants of one species (rather than physical mimics) when they are exposed to the same unidirectional flow conditions, and to compare the effects of shoot densities using conventional statistics that directly consider the variability of each effect.

Effects of Seagrass Flexibility on Canopy Structure and Water Flow

Seagrass shoots, particularly those of strap-leaved species, are extremely flexible (Fonseca and Koehl, 2006; Fonseca et al., 2007), as anyone who has handled these plants can attest. Flexible seagrasses are bent over by the drag force imposed by flowing water (Bouma et al., 2005), while the buoyancy of grass blades resists their downward bending (Luhar and Nepf, 2011), as has also been demonstrated for macroalgae (e.g., Stewart, 2004). The magnitude of drag on a sessile organism depends on the projected area of the organism normal to the flow direction, thus bending over in flowing water is a mechanism of reducing drag (e.g., Charters et al., 1969; Koehl, 1976, 1977, 1986; Denny et al., 1985; Denny, 1988; Koehl and Alberte, 1988; Carrington, 1990; Abdelrhman, 2003). Increasing the ambient flow velocity encountered by a sessile organism causes higher drag. Therefore, the drag on a shoot within a grass bed is a measure of how the other plants in the canopy affect the flow experienced by that shoot.

[1]Hereafter "shoot density" is in reference to seagrass unless otherwise stated.

When a group of flexible seagrass shoots bend in response to flowing water, they can form a compact, interwoven structure that intensifies the reduction of water velocity within the compressed canopy and simultaneously redirects the flow over the canopy (Fonseca et al., 1982; Gambi et al., 1990), thereby shifting high shear stresses from the sediment surface to the top of the canopy (Fonseca et al., 1982). Such a reduction in flow-induced shear on the substratum should enhance both rhizosphere stability and carbon accumulation on the sediment (*sensu* Kenworthy et al., 1982).

Flexible and compressible grass canopies pose a challenge to understanding the effects of shoot density on flow. The relationship between shoot density and water-speed reduction in canopies composed of stiff macrophytes (e.g., marsh grass communities composed of upright shoots with relatively high flexural stiffness) has been determined via experiments using arrays of rigid rods in a flume (e.g., Nepf, 1999). In contrast, the degree of bending and canopy compression of flexible plants like seagrasses can depend on ambient current velocity and presumably on shoot density as well. Therefore, the effects of shoot density on flow through flexible canopies should be determined for the same sets of grass arrays at a range of different ambient flow speeds.

Fonseca et al. (2007) suggested that the arrangement of shoots in a seagrass bed might affect both water flow and light transmission into the bed. Seagrass shoots sometimes are arranged in rows (Fonseca et al., 2007) that can create anisotropic gaps in the canopy, and random arrangements of shoots can also create gaps in grass beds. Canopy gaps in terrestrial systems have long been recognized as local regions of higher light intensity and as initiation points of disturbance propagation (e.g., Sprugel, 1976; Veblen, 1985; Iwasa et al., 1991), and similar effects have been postulated for seagrasses (Fonseca et al., 1983; Valentine et al., 1994). Folkard (2011) studied how gaps within an array of flexible vegetation introduce flow into the canopy and described the likely role of gaps on various depositional process. The effects of shoot density on the formation or closure of gaps in seagrass canopies as these flexible plants are bent over by ambient water flow should be determined for different current speeds, and the effects of these gaps on flow velocities and turbulence should be measured. This would provide useful information to assess various mechanisms that have been proposed for how shoot density in a seagrass bed might be changed in response to ambient water flow.

Does Ambient Current Speed Affect Shoot Density in Seagrass Beds?

It has long been suggested that faster ambient water flow might lead to an increase in shoot density in seagrass beds (e.g., Conover, 1964; Short, 1975; Peterson et al., 2004). Subsequent work showing that shoot density of *Z. marina* was positively correlated with current speed (Kenworthy et al., 1982) was consistent with this prediction. However, a number of other factors are known to affect shoot density. For example, in light-limited environments, shoot density varies positively with light intensity (Short et al., 1995; Ruiz and Romero, 2001; Krause-Jensen et al., 2003). Furthermore, increasing sediment organic content or nutrient availability can lead to increases in shoot density (e.g., Koch, 2001; Holmer et al., 2008; Howard et al., 2016; Ceccherelli et al., 2018). These factors are in turn affected by the deformation of shoots by hydrodynamic drag, the formation or closure of gaps in the canopy in flowing water, and the transport of dissolved nutrients and sediment by water moving around and through a grass canopy. Therefore, determining whether current speed drives a shoot density response in seagrasses is complicated by the dynamic canopy architecture of most seagrasses in response to water motion.

Objectives of This Study

The goal of this study was to determine whether shoot density in a seagrass bed exposed to unidirectional ambient water flow affects the hydrodynamics and canopy architecture of the bed. We avoided the contradictory results of earlier studies conducted under diverse conditions by focusing on one species of seagrass (*Z. marina*) with very flexible shoots exposed to unidirectional currents of different velocities that we controlled in a laboratory flume. For all shoot density and flow treatments, we held shoot size constant and measured water flow, forces on shoots, and gaps in the canopy at the same defined positions in the grass bed. The specific questions that we addressed using this system were:

1. How does shoot density affect the reduction in water speed and the change in turbulence intensity within a seagrass bed as a function of distance from the upstream edge of the canopy when seagrass beds are exposed to ambient unidirectional currents of different speeds?
2. How do shoot density and ambient current velocity affect the hydrodynamic forces on shoots in a seagrass bed at different distances downstream from the upstream edge of the bed?
3. Does reduction in seagrass shoot density by random removal of plants affect the formation of gaps in the canopy, and how are those gaps affected by the speed of the ambient current that bends the shoots?

Answers to these questions can be used to address the issue of whether differences in seagrass shoot density observed in the field represent a direct adaptive response to ambient flow regime. For example, if seagrass shoots in a bed of a given density experience the same hydrodynamic forces and gap structure irrespective of downstream distance in the bed, and if those forces and gaps are not affected by shoot density, then the speed of the ambient unidirectional current flow should not be considered a direct driver of shoot density. Consequently, other factors (e.g., nutrients, light) could alone explain the large range in seagrass shoot densities often seen for *Z. marina* over small geographic distances.

MATERIALS AND METHODS

Seagrass Used in the Flume

Healthy (i.e., intact, minimally epiphytized) shoots of *Zostera marina* were collected near Beaufort, NC, in July from two sites described by Fonseca and Bell (1998): Middle Marsh [site mmnl1], and southern Core Sound [site hih2]). Shoots were kept in flowing seawater in tanks (40 l) at ambient temperature (∼24°C) and salinity (∼34) under flood lamps (Philips 250 W model: K250PARFL) that exposed them to ∼250 μE m^{-2} s^{-1} for 24 h per day to stimulate photosynthesis and stabilize flexural stiffness.

A seagrass shoot attached to the substratum and exposed to unidirectional water flow parallel to the substratum is bent by the hydrodynamic drag like a cantilevered beam is bent by an applied force. The flexural stiffness (*EI*) of a beam, its resistance to being bent by a force, depends on the stiffness (*E*, elastic modulus) of the material from which it is made, and on the distribution of material around its axis of bending (*I*, second moment of area of a beam cross-section) (e.g., Wainwright et al., 1976). Because one focus of our study was the role that seagrass flexibility plays in affecting gaps in seagrass canopies and thus flow through the canopies, we measured the flexural stiffness of grass from both field collection sites. Using methods described in Fonseca and Koehl (2006), the *EI* of both leaf and sheath samples from randomly selected seagrass shoots from each site were measured by being bent like a cantilevered beam by a point load, where:

$$EI = (F \times L^3)/8\delta \quad (1)$$

where, *F* is the force (N) applied at a point along the cantilever at distance *L* (m) from the attached end of the cantilever, and δ is the linear deflection distance (m) in the direction of force application of the point on the beam where the force was applied. Deflection was always $\delta < 0.10\ L$ so that small-deflection beam equation (Equation 1) would apply. Differences among the plants from the two field sites were tested by one-way analysis of variance (ANOVA) after natural log +1 transformation to determine if there were differences in flexural stiffness among plant sources that could influence subsequent trials.

Flume and Experimental Seagrass Beds

The seawater flume (8 m long × 1 m wide × 0.75 m deep) used for this study is described in Fonseca and Koehl (2006) and Fonseca et al. (2007). Consistent with past studies in this flume, the constructed seagrass bed was 0.25 m wide by 1.0 m long, and the water depth was 0.3 m. Shoots were held in place in holes in a clear acrylic plate (0.25 × 1.0 m) that was fit into a recessed portion of flume floor to be flush with the main floor of the flume. Random shoot arrangements were used to avoid the flow artifacts measured in beds of shoots arranged in unnatural, evenly-spaced rows (see Fonseca et al., 2007). Random arrangements of shoots were created in the plate by overlaying it with a clear plastic grid (25 × 100 cm) on which each point where lines intersected was numbered (1–2500). A random-number generator (produced by a HP-11c calculator) was used to select the points where shoots should be placed for the highest shoot density desired (1246 shoots m^{-2}). Holes (6.25 mm diameter) were drilled through the plate at these points. The shoot of a *Z. marina* was wedged through each hole so that the upper surface of the plate intersected the shoot at the same position as the sediment surface intersected the shoot in the field. The shoots were held in natural upright positions and the orientation of the shoots with respect to the direction of water flow in the flume was arbitrary. Shoots were kept moist when in air and were not exposed to air for more than 3 min between the time collected and when installed in the flume.

Seagrass-flow interactions were tested for seven different shoot densities (1246, 1046, 846, 646, 448, and 246 shoots m^{-2}) that were chosen to approximate the normal range of densities of monotypic stands of *Z. marina* in the Beaufort, NC, area (natural observed range of 185–1133 shoots m^{-2}; Fonseca and Bell, 1998). As described above, shoots were randomly arranged at the highest shoot density. After the flow trials were run at the highest density, some shoots were selected using the random-number generator to be removed to achieve the next lower density, and so on.

Drag Measurements

The hydrodynamic force pushing a shoot downstream (drag) was measured for shoots in grass beds of different densities. For each shoot density tested, a seagrass shoot was arbitrarily selected from those collected in the field and this single shoot was attached to a force transducer as described in Fonseca and Koehl (2006) and Fonseca et al. (2007). The force transducer and attached shoot were placed in the grass bed at the flume midline, first at the position 0.50 m downstream from the leading edge of the grass bed, and then at the position 1.00 m downstream from the leading edge. At each position, drag force was measured to the nearest 0.01 N at a sampling rate of 5 Hz for a period of 5 min, and the mean force was calculated. Such drag measurements were repeated 9 times at each position for each shoot density and freestream current velocity.

Flow Measurements

Three freestream water speeds representative of currents measured just upstream of beds of *Z. marina* at sites near Beaufort, NC (Fonseca and Bell, 1998), were tested in the flume: 21, 32, and 63 cm s^{-1}. Following protocols developed in Fonseca and Koehl (2006) and Fonseca et al. (2007), a Marsh-McBirney Model 523 electromagnetic current flow meter was used to record horizontal water velocities at the midline of the flume at heights of 2, 5, 8, 11, 14, 17, 20, and 23 cm above the substratum. Water velocities were recorded for 30 s at 5 Hz at each height. Examples of the velocity profiles measured in this way are shown in **Figure 1**. Velocity profiles were measured at three sampling locations along the midline of the flume: over bare substratum at a position 25 cm upstream of the leading edge of the constructed grass bed, and in the grass bed at distances of 50 and 100 cm downstream from the leading-edge.

The height of the seagrass canopy above the substratum was measured through a glass panel in the side of the flume. Canopy heights were measured at both the 50 and 100 cm positions downstream of the leading edge of the grass bed for every shoot

density and water speed tested. A ruler was set against the glass panel and the time averaged height of the deflected canopy visually estimated to the nearest cm. The canopy heights were used to determine which positions above the substratum in each velocity profile were within or above the canopy. In every case, the heights at which flow was measured that were within the canopy were 2, 5, 8, and in some lower velocities, 11–13 cm above the substratum, while all the other heights at which flow was measured were above the canopy.

For each shoot density and freestream current speed tested, the reduction in flow velocity within the grass bed canopy was determined at the positions 50 and 100 cm downstream from the leading edge of the bed. The mean flow velocity at each height within the canopy was determined for each treatment, as was the mean velocity at the same height at the position 25 cm upstream from the canopy. The percent reduction in flow within the canopy was then calculated for each height at each downstream position as described by Fonseca and Koehl (2006) and Fonseca et al. (2007). The mean % reduction in velocity for all the heights within the canopy was then determined for each downstream position (50 and 100 cm) in the canopy.

Turbulent eddies stir the water, thereby enhancing mixing of substances carried by the water and reducing their local depletion or accumulation in the water around organisms. Turbulence intensity is a dimensionless number that is a measure of the importance of velocity fluctuations (due to turbulence) relative

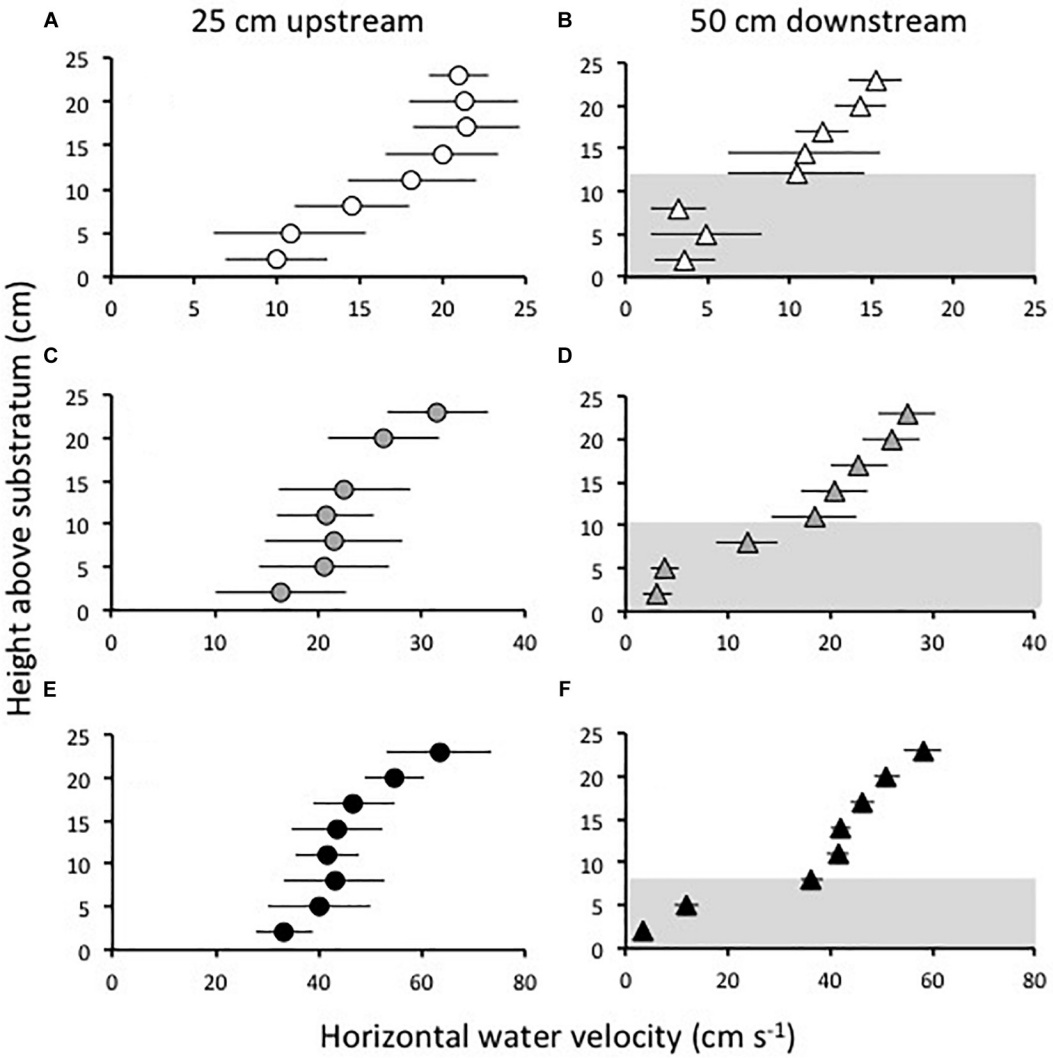

FIGURE 1 | Examples of velocity profiles measured in the flume at a position 25 cm upstream from the leading edge of a grass bed **(A,C,E)** with a density of 646 shoots m^{-2}, and at a position 50 cm downstream of the leading edge of the bed **(B,D,F)**, when the current velocity in the flume was "slow" (21 cm s^{-1}) **(A,B)**, "intermediate" (32 cm s^{-1}) **(C,D)**, and "fast" (63 cm s^{-1}) **(E,F)**. Symbols show mean horizontal velocities measured at different heights above the substratum and error bars show one standard deviation. The velocities measured above the substratum within the grass canopy are indicated in gray at the position 50 cm downstream from the leading edge of the bed. Shoots are bent over farther in faster flow, compressing the canopy. Evidence of this canopy compression is the reduction of canopy height at higher ambient current velocities (compare **B,D,F**).

to the average current velocity. Arrays of plants can decrease turbulence intensity of ambient flow by damping out fluid motion, or can increase turbulence intensity by shedding vortices or fluttering as the water flows past them. Comparison of the turbulence intensity of the ambient water flow outside of arrays of macrophytes with that of the flow inside the canopies has long been used to assess the effects of those canopies on the level of turbulence in the water (e.g., Anderson and Charters, 1982; Koehl and Alberte, 1988; Gambi et al., 1990; Worcester, 1995). So that we could compare our results to those of such earlier studies, we used our measurements of flow velocity as a function of time at each height (h) within the canopy to calculate the turbulence intensity at that height (I_h), as defined in Gambi et al. (1990):

$$I_h = (rmsU_h/\hat{u}_h) \times 100 \quad (2)$$

where $rmsU_h$ is the root mean square of the velocity at height h (in our study velocities were measured at 0.02 s intervals for a duration of 30 s, and $rmsU_h$ was computed using the RMSE function in Sas Institute Inc, 2002), and $\hat{u}_h$ is the mean of the velocities measured over that 30 s period at height h. We calculated the I_h 's for each of the heights at the positions in a grass bed that were 0.50 and 1.00 m downstream from the leading edge of the bed.

Canopy Deflection and Gap Area

For each experimental grass bed tested, the lengths of 10 arbitrarily selected shoots were measured to the nearest millimeter to determine mean grass length. For each current speed tested, the ratio of canopy height to mean shoot length was used as a measure of canopy deflection.

When shoots are randomly arranged in a seagrass bed, there can be gaps in the canopy. However, when flexible grass canopies are bent over in flowing water, the blades can cover gaps in the canopy and separate the slower flow within the canopy from the faster flow above it. We evaluated the gaps in the test grass beds at each shoot density and freestream current velocity by taking digital images of the entire test bed from above the flume. A downward-facing digital camera was positioned at a fixed point above the middle of the grass bed while the current was flowing and the entire bed was captured in a single digital image. Point Count software (Kohler and Gill, 2006) was utilized to randomly select 100 points in each image. The number of points on seagrass (as opposed to gaps, i.e., flume floor visible between regions of grass) grass were tallied for each photograph and used to calculate the percent canopy gap closure (PCG) as the percent of points falling on seagrass.

TABLE 1 | Flexural stiffness (EI) for seagrass shoots collected from different sites.

Region of seagrass shoot	Site	Mean (N m^{-2})	d.f.	*F*	*P*-value
Leaves	Middle Marsh	$3.38 \cdot 10^{-7}$	1	1.83	0.1902
	Core Sound	$2.30 \cdot 10^{-7}$			
Sheaths	Middle Marsh	$1.93 \cdot 10^{-6}$	1	0.01	0.9224
	Core Sound	$1.86 \cdot 10^{-6}$			
Leaves	(Sites pooled)	$2.84 \cdot 10^{-7}$	1	47.51	<0.0001
Sheaths	(Sites pooled)	1.89×10^{-6}			

TABLE 2 | Drag force on shoots as a function of shoot density, distance downstream into the canopy, and freestream current speed.

		Drag (range or mean) (N)	d.f.	*F*	*P*-value
Shoot density m^{-2}	246, 446, 646, 846, 1046, 1246	0.0107–0.018	5	0.93	0.4776
Distance (cm downstream into canopy)	50 100	0.0111 0.0132	1	0.92	0.3433
Current speed cm s^{-1}	21 32 63	0.0145 0.0109 0.0109	2	1.13	0.3352

Data Analysis

At each ambient freestream flow velocity (21, 32, or 63 cm s^{-1}) and position in the grass bed (0.50 or 1.00 m downstream from the leading edge of the bed), we tested whether shoot density or percent canopy closure affected three dependent variables: (1) percent reduction in current velocity within the canopy, (2) turbulence intensity within the canopy, and (3) drag force exerted on a shoot. For each flow velocity and shoot density, we also tested whether downstream position in the grass bed affected these three dependent variables.

One-way ANOVAs were performed after log transformation to satisfy assumptions of normality in order to test the effects of current speed, shoot density, PCG, and distance into the test canopy on percent flow reduction, turbulence intensity and force on individual shoots. Because of flow continuity, there can be no expectation of independence among measurements in the flume, thus freeing us to use this statistic as a tool to determine the change in velocities specifically as the result of non-independent factors (Fonseca and Koehl, 2006). Because we were interested in flow conditions within the entire canopy, our statistical tests of percent flow reduction and turbulence intensity utilized means of these parameters at each discrete elevation within the canopy as replicates. Percentages were arcsine transformed prior to application of ANOVA. Differences among means were determined by Duncan's multiple range test [DMRT] to guard conservatively against Type I error.

RESULTS

Shoot Characteristics

Average leaf length from five randomly selected *Z. marina* shoots was 103.8 mm (s.d. 40.7), sheath length was 25.6 mm (s.d. 6.2), and leaf and sheath width were 3.2 mm (s.d. 0.45). There was no significant difference in shoot total length (sheath + leaf) between shoots collected from the two field sites (ANOVA, $df = 1$, $F = 0.03$, $p = 0.861$).

The flexural stiffness (EI) of sheaths of *Z. marina* shoots (mean = 1.89×10^{-6} N m^{-2}, s.d. = 1.13×10^{-6}, n = 12 shoots) was approximately seven times higher than the EI of individual leaves (mean = 2.84×10^{-7} N m^{-2}, s.d. = 1.99×10^{-7}, n = 24 leaves, each from a different shoot) This difference in stiffness was significant (ANOVA, df = 1, F = 47.51, $p < 0.0001$). Flexural stiffnesses of both leaves and sheaths were not significantly different between the two field sites (**Table 1**), indicating that all plants used in this study should have responded similarly to water flow.

Force on Shoots

There were no significant difference in the force exerted on shoots across current speeds as a function of shoot density (1246, 1046, 846, 646, 448, and 246 shoots m^{-2}), nor was there a suggestion of a trend (**Table 2**). There was no significant difference in drag force exerted on shoots as a function either of distance into the canopy or of current speed (**Table 2**).

Percent Reduction in Current Speed

There were no significant differences in the effect of shoot density on percent current speed reduction among distances downstream into the canopy if all current speeds were pooled ($p > 0.05$) (**Figures 2A,B**). Similarly, there was no effect of shoot density on percent current speed reduction for any of the three current velocities tested (**Figures 3A–C**). There was some indication that the lowest shoot density (246 shoots m^{-2}) was tending toward a diminished capacity to reduce current velocity at the 32 and 63 cm s^{-1} speeds, but the variability of percent current velocity

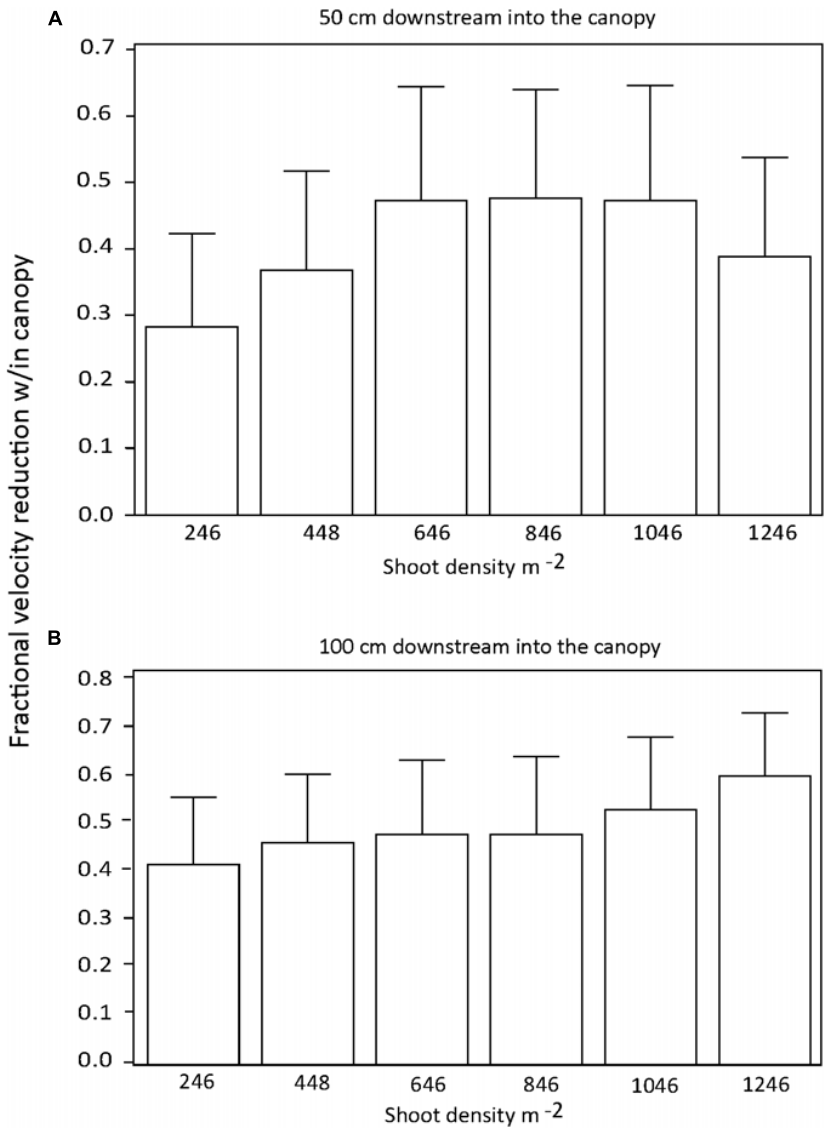

FIGURE 2 | Percent (fractional) reduction in current speed within the seagrass canopy as compared to an upstream location (−25 cm) for 50 **(A)** and 100 cm **(B)** downstream into test canopies.

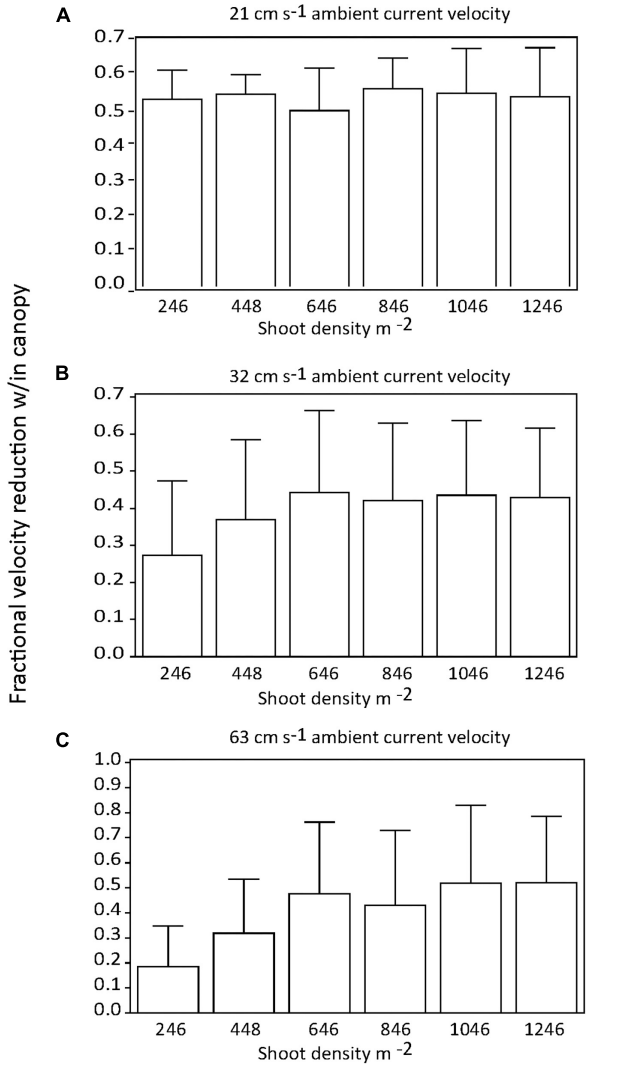

FIGURE 3 | Percent (fractional) reduction in current speed within the seagrass canopy as compared to an upstream location (−0.25 m) for each shoot density by current regime tested; **(A)** = 21, **(B)** = 32, and **(C)** = 63 cm s^{-1}.

reduction within the canopy environment resulted in a non-significant difference.

Turbulence Intensity

There were no significant differences in the effect of shoot density on turbulence intensity among distances downstream into the canopy ($p > 0.05$; **Figures 4A,B**). Similarly, there was no consistent effect of shoot density on turbulence intensity for any of the three current velocities tested (**Figures 5A–C**). At the mid-range current speed (32 cm s^{-1}), some shoot densities were significantly different from others, but there was no systematic (with shoot density) pattern to these differences (**Figure 5B**). The faster the current speed, the lower the turbulence intensity within the canopy (**Figures 5A–C**).

Canopy Gap Closure

Percent canopy gap closure (PCG; shown as a fractional change) increased with shoot density irrespective of current regime (**Figure 6A**); however, there was no significant difference in PCG among the five lowest shoot densities and limited overlap in non-significant differences among the highest shoot densities, despite increased shoot bending and canopy compression (**Figure 1**, compare **Figures 1B,D,F**). There was a stepwise increase in canopy closure with both shoot density and increased current speed, with similar proportions of PCG occurring among current speeds (**Figure 6B**). Current speed resulted in significant ($p < 0.05$) differences in PCG only among the highest and lowest speeds tested (mean PCG at 21 cm s^{-1} was 20.3% [$n = 6$; s.d. 10.4], at 32 cm s^{-1} was 32% [$n = 6$; s.d. 15.9], and at 63 cm s^{-1} was 41% [$n = 6$; s.d. 23.9]).

DISCUSSION

Canopies of aquatic plants play important roles in marine and freshwater ecosystems, such as providing food and habitat for animals, and stabilizing and altering the chemistry of sediments. The performance of these functions by canopies of seagrasses or macroalgae depends on their interaction with the ambient water flow. We have focused on seagrass beds exposed to unidirectional water currents to examine the roles of shoot density and flexibility in affecting the hydrodynamics of submerged aquatic plant canopies.

Shoot Density

Many studies have revealed that the vertical velocity profile and turbulence structure of a unidirectional water current are altered upon encounter with a seagrass bed, where a zone of rapid flow above the canopy and a zone of slower flow within the bed develop (Fonseca et al., 1982, 1983, 2007; Fonseca and Kenworthy, 1987; Gambi et al., 1990; Ackerman and Okubo, 1993; Worcester, 1995; Koch and Gust, 1999; Verduin and Backhaus, 2000; Abdelrhman, 2003; Peterson et al., 2004; Chen et al., 2013; **Figure 1**). If a seagrass bed is composed of flexible shoots, they are bent over by flowing water and overlap, thereby forming a compressed canopy. The roles of shoot density and of canopy deflection in determining the degree to which water flow is slowed within and re-directed above a bed of flexible seagrasses has been unclear. Our study of flow through beds of very flexible *Zostera marina* plants showed that shoot density had little influence on flow reduction and turbulence intensity at each downstream position in the bed and at each current velocity that we tested. Although our data hinted that the capacity of a grass bed to reduce flow velocity might be lower for the sparsest shoot densities we tested when exposed to the most rapid ambient currents we imposed, this result was not significant. Our data do not show the dramatic reductions in flow within a canopy as shoot density increases that were predicted by Abdelrhman (2003), who assumed that the simple displacement of water by shoots would limit water movement within the canopy. Instead, our data suggest that the effect of shoot density

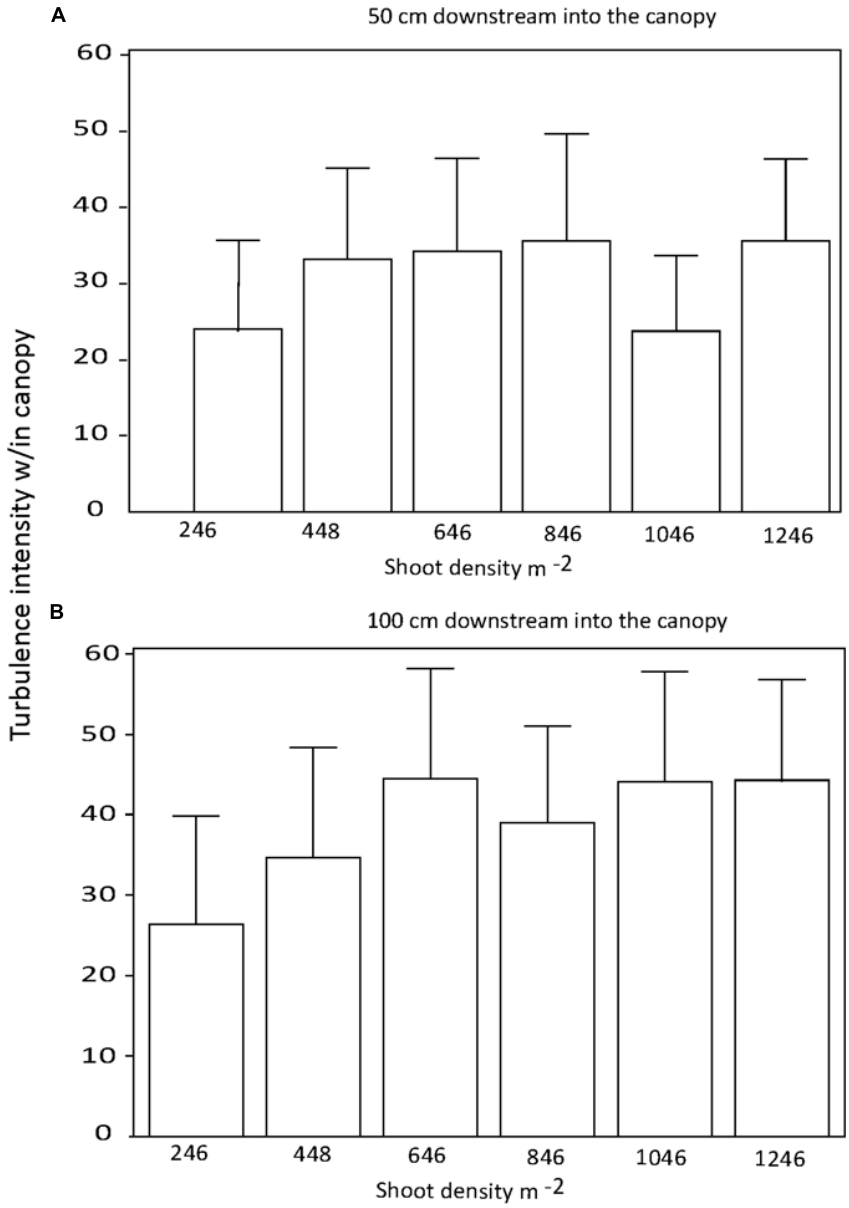

FIGURE 4 | Turbulence intensity within the seagrass canopy for 0.5 **(A)** and 1.0 m **(B)** downstream into test canopies.

on velocity reduction was largely eclipsed by other changes in the canopy architecture due to flow-induced bending of flexible shoots and the resulting canopy compression. Furthermore, our data suggests that the sedimentation that occurs in the slowed flow in a grass bed, and thus carbon deposition and sediment organic content, would be facilitated across much of the range of *Z. marina* shoot densities observed in nature.

Shoot Flexibility

The inconsistent results of different studies of the effects of shoot density on the hydrodynamics of seagrass beds exposed to unidirectional currents can be explained in part by differences in the flexibility of the shoots or physical models composing the canopy. For example, Chen et al. (2007) adopted Nepf's (1999) approach of using arrays of rigid cylinders to evaluate the effects of shoot density on flow through and around submerged plant canopies and found that increasing shoot density decreased water velocities in the canopy. In contrast, we found that shoot density had little effect on flow reduction in canopies of flexible seagrass. Dijkstra and Uittenbogaard (2010), who used both mathematical modeling and flume experiments with plastic mimics of shoots of different stiffness to determine water flow in canopies, discovered that shoot stiffness had a bigger effect on flow reduction in the canopy than did shoot density.

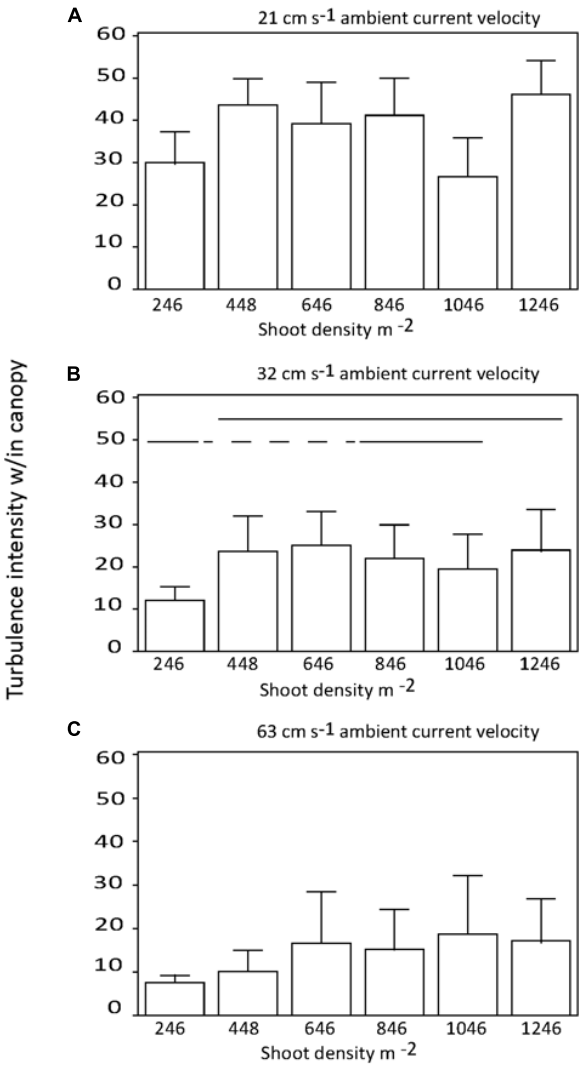

FIGURE 5 | Turbulence intensity within the seagrass canopy for each shoot density by current regime tested; **(A)** = 21, **(B)** = 32, and **(C)** = 63 cm s^{-1}. Horizontal solid lines show treatments that are not significantly different; dashed lines cross significantly different treatments to join equivalent treatments.

When a flexible organism attached to the substratum is bent over by ambient water flow, its projected area normal to the flow direction is reduced and the drag it experiences is lower than drag on a stiff organism of the same size and shape. This drag-reducing function of flexibility has been measured for macroalgae and sessile aquatic animals (e.g., Koehl and Wainwright, 1977; Koehl, 1984, 1986; Koehl et al., 2001), and for seagrass shoots and physical models (e.g., Bouma et al., 2005; Fonseca et al., 2007; Dijkstra and Uittenbogaard, 2010). Such drag reduction enhances the ability of a flexible organism to avoid being ripped off the substratum by ambient water motion. Another advantage of flexibility occurs when groups of attached organisms form canopies. Fonseca and Fisher (1986) found that canopies composed of species of seagrass that had flexible shoots compressed more in flowing water, and thereby provided greater protection from sediment erosion, than did canopies of species with stiffer shoots. Because faster flow causes greater deflection and streamlining of flexible shoots, and thus more canopy compression, it is not surprising that the drag we measured on flexible *Z. marina* shoots within grass beds was independent of ambient current velocity.

Canopy Configuration and Gap Closure

Gaps between shoots in a canopy can enhance light and flow penetration into the canopy, but when flexible shoots are bent over by flowing water, they can cover gaps. Not unexpectedly, we found that gap closure was greater when canopies of flexible *Z. marina* were exposed to fast ambient currents than when they experienced slower flow. Furthermore, at each current speed, gap closure was more pronounced in canopies with high shoot densities than in those with low densities. However, canopy gap closure did not correlate with the percent velocity reduction in grass beds or with drag on individual shoots, both of which were independent of ambient current velocity and shoot density. A possible explanation is that the effects of canopy closure on the flow above and through a flexible seagrass canopy were manifested at very low levels of gap closure (∼20% PCG) and at low ambient current speeds (e.g., Fonseca and Kenworthy, 1987). Our result that downstream position had no effect on flow reduction, turbulence intensity, drag on a shoot, and gap closure suggests that the flow structure in a flexible canopy develops quickly with distance as water moves into the canopy, as has been seen in other studies (Fonseca et al., 1982, 2007; Fonseca and Fisher, 1986; Gambi et al., 1990; Abdelrhman, 2003).

The lack of an effect of shoot density on velocity reduction and turbulence intensity in seagrass canopies could help explain why experiments in which shoot density was manipulated on a local patch scale in one hydrodynamic environment did not alter sediment characteristics in seagrass beds (Armitage and Fourqurean, 2016; Howard et al., 2016). This could explain the lack of a relationship between sediment stores of organic carbon and seagrass density that has been observed on a regional scale (Campbell et al., 2015).

Does Ambient Current Speed Affect Shoot Density in Seagrass Beds?

High shoot densities have been observed in grass beds in habitats exposed to rapid water flow (e.g., Conover, 1964; Kenworthy et al., 1982; Fonseca and Bell, 1998). We found that changing the density of flexible shoots does not affect the flow in a grass bed exposed to a given ambient current. Therefore, our results are inconsistent with the hypothesis that high shoot density is due to a direct, adaptive response of the grass to rapid water flow.

Rather than current speed providing some signal that stimulates an increase in shoot density, water flow might affect shoot spacing indirectly via a variety of mechanisms. For example, the accumulation of sediment and its content of nutrients and organic matter all are functions of the depositional environment, and all are drivers of seagrass shoot density

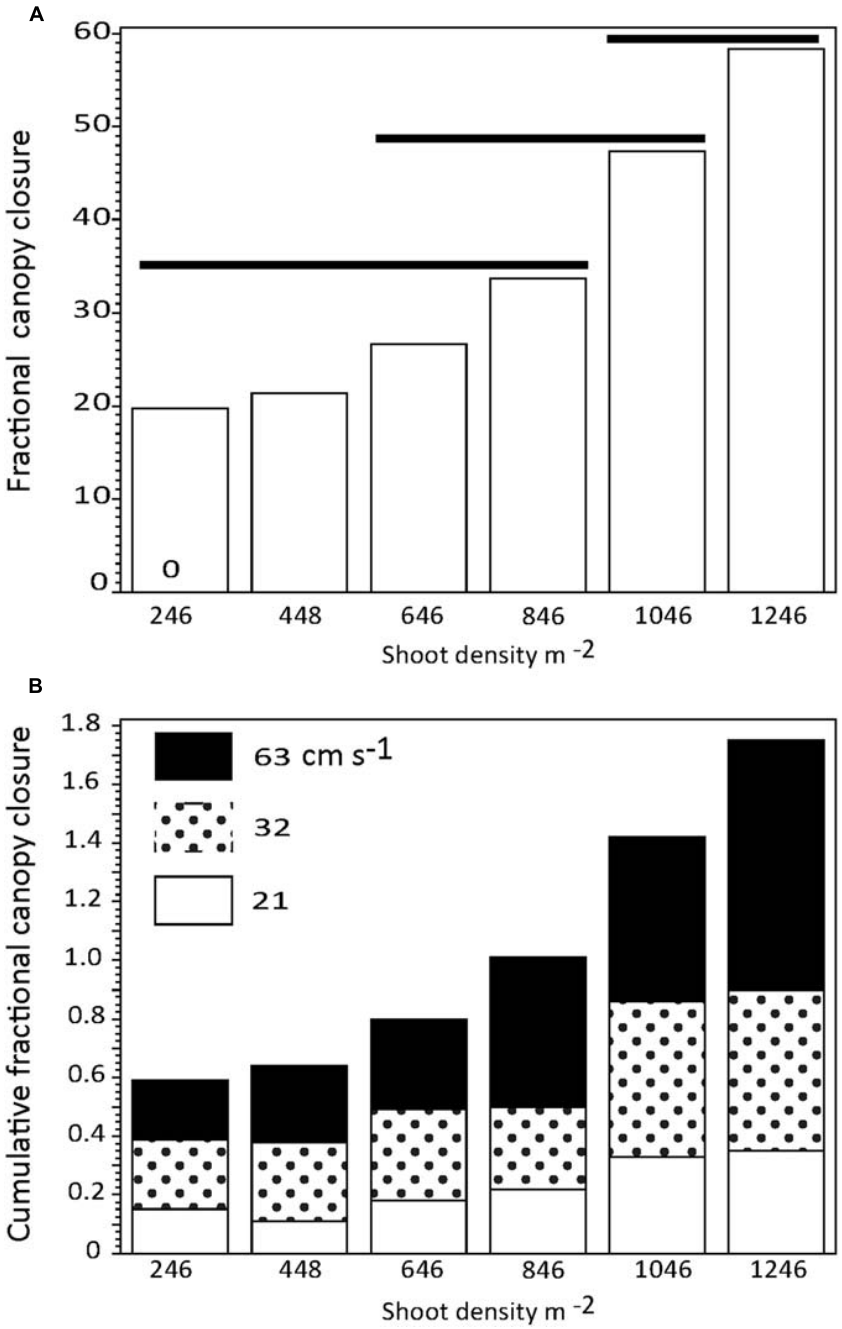

FIGURE 6 | (A) Percent canopy closure as a function of *Z. marina* shoot density irrespective of current speed. **(B)** Cumulative percent canopy closure by *Z. marina* shoot density showing the relative effects ofcurrent speed. Horizontal solid lines show treatments that are not significantly different.

(Holmer et al., 2008; Howard et al., 2016; Ceccherelli et al., 2018). In very oligotrophic environments, high nutrient supply increases shoot density (e.g., Fourqurean et al., 1995; Agawin et al., 1996). Similarly, in such resource-limited habitats where nutrients are taken up through seagrass leaves rather than the roots, high flow velocities increase nutrient delivery by making the diffusion boundary layer around the leaves thinner (e.g., Koch, 2001). In contrast, at eutrophic sites where sediment anoxia induces plant stress, slow flow regimes can result in reduced shoot density (e.g., Borum et al., 2005; Holmer et al., 2008; Brodersen et al., 2015). Feedback between a number of interacting environmental factors can also affect the light reaching seagrass, and thus their growth patterns, as described by van der Heide et al. (2011). For example, in habitats exposed to rapid water flow, seagrass canopies trap suspended particles, thereby improving water clarity and enhancing light. In contrast,

in estuaries with slow water flow, eutrophication reduces the light reaching the seagrass.

Our data are consistent with the view that the high shoot densities of seagrass canopies in habitats exposed to rapid water flow can be due to the effects of water motion on other factors, such as light and nutrients, that affect seagrass growth.

AUTHOR CONTRIBUTIONS

MF led the research and oversaw the experimental process and drafted the original manuscript. MK reviewed and revised the manuscript with regard to flow dynamics and interaction with the flexible seagrass shoots. JF reviewed and revised the manuscript with regard to environmental feedbacks and alternative mechanisms influencing seagrass shoot density.

FUNDING

Support was provided early and in part by the NOAA, Beaufort Laboratory (to MF) and later by CSA Ocean Sciences Inc. (to MF) and by National Science Foundation Grant IOS-1655318 (to MK). This is contribution #123 from the Center for Coastal Oceans Research in the Institute of Water and Environment at Florida International University.

ACKNOWLEDGMENTS

Thanks to L. Rose for providing technical support of the study at the NOAA, Beaufort Laboratory. Early review of this work by the late E. M. Koch and subsequently, G. Piniak, A. Uhrin and three reviewers greatly improved the manuscript.

REFERENCES

Abdelrhman, M. A. (2003). Effect of eelgrass *Zostera marina* canopies on flow and transport. *Mar. Ecol. Prog. Ser.* 248, 67–83. doi: 10.3354/meps248067

Ackerman, J. D., and Okubo, A. (1993). Reduced mixing in a marine macrophyte canopy. *Funct. Ecol.* 7, 305–309. doi: 10.3732/ajb.89.7.1119

Adhitya, A. T., Bouma, J., Folkard, A. M., van Katwijk, M. M., Callaghan, D., de Iongh, H. H., et al. (2014). Comparison of the influence of patch-scale and meadow-scale characteristics on flow within seagrass meadows: a flume study. *Mar. Ecol. Prog. Ser.* 516, 49–59. doi: 10.3354/meps10873

Agawin, N. S. R., Duarte, C. M., and Fortes, M. D. (1996). Nutrient limitation of Philippine seagrasses (Cape Bolinao, NW Philippines): in situ experimental evidence. *Mar. Ecol. Progr. Ser.* 138, 233–243. doi: 10.3354/meps138233

Anderson, S. M., and Charters, A. C. (1982). A fluid dynamic study of seawater flow through *Gelidium nudifrons*. *Limnol. Oceanogr.* 27, 399–412. doi: 10.4319/lo.1982.27.3.0399

Armitage, A. R., and Fourqurean, J. W. (2016). Carbon storage in seagrass soils: long-term nutrient history exceeds the effects of near-term nutrient enrichment. *Biogeosciences* 13, 313–321. doi: 10.5194/bg-13-313-2016

Borum, J., Pedersen, O., Greve, T. M., Frankovich, T. A., Zieman, J. C., Fourqurean, J. W., et al. (2005). The potential role of plant oxygen and sulphide dynamics in die-off events of the tropical seagrass, *Thalassia testudinum*. *J. Ecol.* 93, 148–158. doi: 10.1111/j.1365-2745.2004.00943.x

Bouma, T. J., De Vries, M. B., Low, E., Peralta, G., Tanczos, I. C., van de Koppel, J., et al. (2005). Trade-offs related to ecosystem engineering: a case study on stiffness of emerging macrophytes. *Ecology* 86, 2187–2199. doi: 10.1890/04-1588

Brodersen, K. E., Nielsen, D. A., Ralph, P. J., and Kühl, M. (2015). Oxic microshield and local pH enhancement protects *Zostera muelleri* from sediment derived hydrogen sulphide. *New Phytol.* 205, 1264–1276. doi: 10.1111/nph.13124

Campbell, J. E., Lacey, E. A., Decker, R. A., Crooks, S., and Fourqurean, J. W. (2015). Carbon storage in seagrass beds of Abu Dhabi, United Arab Emirates. *Est. Coasts* 38, 242–251. doi: 10.1007/s12237-014-9802-9

Carrington, E. (1990). Drag and dislodgment of an intertidal macroalga, consequences of morphological variation in *Mastocarpus papillatus*. Kutzing. *J. Exp. Mar. Biol. Ecol.* 139, 185–200. doi: 10.1016/0022-0981(90)90146-4

Ceccherelli, G., Oliva, S., Pinna, S., Piazzi, L., Procaccini, G., Marin-Guirao, L., et al. (2018). Seagrass collapse due to synergistic stressors is not anticipated by phenological changes. *Oecologia* 186, 1137–1152. doi: 10.1007/s00442-018-4075-9

Charters, A. C., Neushul, M., and Barilotti, C. (1969). The functional morphology of *Eisenia arborea*. *Proc. Intl. Seaweed Symposium* 6, 89–105.

Chen, S., Sanford, L., Koch, E. W., Shi, F., and North, W. W. (2007). A nearshore model to investigate the effects of seagrass bed geometry on wave attenuation and suspended sediment transport. *Est. Coasts* 30, 296–310. doi: 10.1007/bf02700172

Chen, Z., Jiang, C., and Nepf, H. (2013). Flow adjustment at the leading edge of a submerged aquatic canopy. *Water Resour. Res.* 49, 5537–5551. doi: 10.1002/wrcr.20403

Conover, J. T. (1964). *Environmental Relationships of Benthos in Salt Ponds (plant Relationships)*. Tech. Rep. No. 3, Univ. R.I. Grad. School Oceanogr. Kingston, RI: University of Rhode Island.

Denny, M. W. (1988). *Biology and the Mechanics of the Wave-Swept Environment*. Princeton, NJ: Princeton University Press.

Denny, M. W., Daniel, T., and Koehl, M. A. R. (1985). Mechanical limits to the size of wave-swept organisms. *Ecol. Monogr.* 55, 69–102. doi: 10.2307/1942526

Dijkstra, J. T., and Uittenbogaard, R. E. (2010). Modeling the interaction between flow and highly flexible aquatic vegetation. *Water Resour. Res.* 46:W12547.

Folkard, A. M. (2011). Flow regimes in gaps within stands of flexible vegetation: laboratory flume simulations. *Environ. Fluid. Mech.* 11, 289–306. doi: 10.1007/s10652-010-9197-5

Fonseca, M. S., and Bell, S. S. (1998). The influence of physical setting on seagrass landscapes near Beaufort North Carolina, USA. *Mar. Ecol. Prog. Ser.* 171, 109–121. doi: 10.3354/meps171109

Fonseca, M. S., and Fisher, J. S. (1986). A comparison of canopy friction and sediment movement between four species of seagrass with reference to their ecology and restoration. *Mar. Ecol. Prog. Ser.* 29, 15–22. doi: 10.3354/meps029015

Fonseca, M. S., Fisher, J. S., Zieman, J. C., and Thayer, G. W. (1982). Influence of the seagrass *Zostera marina* (L.) on current flow. *Est. Coast. Shelf Sci.* 15, 351–364. doi: 10.1016/0272-7714(82)90046-4

Fonseca, M. S., and Kenworthy, W. J. (1987). Effects of current on photosynthesis and distribution of seagrasses. *Aquat. Bot.* 27, 59–78. doi: 10.1016/0304-3770(87)90086-6

Fonseca, M. S., and Koehl, M. A. R. (2006). Modeling flow in seagrass canopies: the influence of patch width. *Est. Coastal Shelf Sci.* 67, 1–9. doi: 10.1016/j.ecss.2005.09.018

Fonseca, M. S., Koehl, M. A. R., and Kopp, B. S. (2007). Biomechanical factors contributing to self-organization in seagrass landscapes. *J. Exp. Mar. Biol. Ecol.* 340, 227–246. doi: 10.1016/j.jembe.2006.09.015

Fonseca, M. S., Whitfield, P. E., Kelly, N. M., and Bell, S. S. (2002). Modeling seagrass landscape pattern and associated ecological attributes. *Ecol. Appl.* 12, 218–237. doi: 10.1890/1051-0761(2002)012%5B0218:mslpaa%5D2.0.co;2

Fonseca, M. S., Zieman, J. C., Thayer, G. W., and Fisher, J. S. (1983). The role of current velocity in structuring seagrass meadows. *Est. Coast. Shelf Sci.* 17, 367–380. doi: 10.1016/0272-7714(83)90123-3

Fourqurean, J. W., Powell, G. V. N., Kenworthy, W. J., and Zieman, J. C. (1995). The effects of long-term manipulation of nutrient supply on competition between the seagrasses *Thalassia testudinum* and *Halodule wrightii* in Florida Bay. *Oikos* 72, 349–358.

Gambi, M. C., Nowell, A. R. M., and Jumars, P. A. (1990). Flume observations on flow dynamics in *Zostera marina* (eelgrass) beds. *Mar. Ecol. Prog. Ser.* 61, 159–169. doi: 10.3354/meps061159

Holmer, M., Argyrou, M., Dalsgaard, T., Danovaro, R., Diaz-Almela, E., Carlos, M. D. E., et al. (2008). Effects of fish farm waste on *Posidonia oceanica* meadows: synthesis and provision of monitoring and management tools. *Mar. Pollut. Bull.* 56, 1618–1629. doi: 10.1016/j.marpolbul.2008.05.020

Howard, J. L., Perez, A., Lopes, C. C., and Fourqurean, J. W. (2016). Fertilization changes seagrass community structure but not blue carbon storage: results from a 30-year field experiment. *Est. Coasts* 39, 1422–1434. doi: 10.1007/s12237-016-0085-1

Iwasa, Y., Kazunori, S., and Nakashima, S. (1991). Dynamic modeling of wave regeneration (Shimagare) in subalpine *Abies* forests. *J. Theor. Ecol.* 152, 143–158. doi: 10.1016/s0022-5193(05)80448-5

Kenworthy, W. J., Zieman, J. C., and Thayer, G. W. (1982). Evidence for the influence of seagrasses on the benthic nitrogen cycle in a coastal plains estuary near Beaufort, North Carolina. *Oecologia* 54, 152–158. doi: 10.1007/BF00378387

Koch, E. W. (2001). Beyond light: physical, geological and geochemical parameters as possible submersed aquatic vegetation habitat requirements. *Estuaries* 24, 1–17.

Koch, E. W., Ackerman, J., Verduin, J., van Keulen, M., Larkum, A., Orth, R., et al. (2006). "Fluid dynamics in seagrass ecology—from molecules to ecosystems," in *Seagrasses: Biology, Ecology and Conservation*, ed. R. Joseph Orth (Dordrecht: Springer).

Koch, E. W., and Gust, G. (1999). Water flow in tide- and wave-dominated beds of the seagrass *Thalassia testudinum*. *Mar. Ecol. Prog. Ser.* 184, 63–72. doi: 10.3354/meps184063

Koehl, M. A. R. (1976). "Mechanical design in sea anemones," in *Coelenterate Ecology and Behavior*, ed. G. O. Mackie (Boston, MA: Springer), 22–31.

Koehl, M. A. R. (1977). Mechanical organization of cantilever-like sessile organisms, sea anemones. *J. Exp. Biol.* 69, 127–142.

Koehl, M. A. R. (1984). How do benthic organisms withstand moving water? *Am. Zool.* 24, 57–70. doi: 10.1093/icb/24.1.57

Koehl, M. A. R. (1986). "Seaweeds in moving water: form and mechanical function," in *On the Economy of Plant Form and Function*, ed. T. J. Givnish (London: Cambridge University Press), 603–634.

Koehl, M. A. R., and Alberte, R. S. (1988). Flow, flapping and photosynthesis of *Nereocystis luetkeana*: a functional comparison of undulate and flat blade morphologies. *Mar. Biol.* 99, 435–444. doi: 10.1007/bf02112137

Koehl, M. A. R., Helmuth, B., and Carpenter, R. (2001). "Growing and flowing," in *The Algorithmic Beauty of Seaweeds, Sponges and Corals*, eds J. A. Kaandorp and J. E. Kubler (Heidelberg: Springer-Verlag).

Koehl, M. A. R., and Wainwright, S. A. (1977). Mechanical adaptations of a giant kelp. *Limnol. Oceanogr.* 22, 1067–1071. doi: 10.4319/lo.1977.22.6.1067

Kohler, K. E., and Gill, S. M. (2006). Coral point count with excel extensions (CPCe): a visual basic program for the determination of coral and substrate coverage using random point count methodology. *Comp. Geosci.* 32, 1259–1269. doi: 10.1016/j.cageo.2005.11.009

Krause-Jensen, D., Pedersen, M. F., and Jensen, C. (2003). Regulation of eelgrass (*Zostera marina*) cover along depth gradients in Danish coastal waters. *Estuaries* 26, 866–877. doi: 10.1007/bf02803345

Lacy, J. R., and Wyllie-Echeverria, S. (2011). The influence of current speed and vegetation density on flow structure in two macrotidal eelgrass canopies. *Limnol. Oceanogr. Fluids Environ.* 1, 38–55. doi: 10.1215/21573698-1152489

Lei, J., and Nepf, H. (2016). Impact of current speed on mass flux to a model flexible seagrass blade." *J. Geophys. Res.* 121, 4763–4776. doi: 10.1002/2016jc011826

Luhar, M., and Nepf, H. M. (2011). Flow-induced reconfiguration of buoyant and flexible aquatic vegetation. *Limnol. Oceanogr.* 56, 2003–2017. doi: 10.4319/lo.2011.56.6.2003

Nepf, H. M. (1999). Drag, turbulence and diffusion in flow through emergent vegetation. *Wat. Res. Res.* 35, 470–489.1999. doi: 10.1016/j.watres.2008.10.027

Newell, R. I. E., and Koch, E. W. (2004). Modeling seagrass density and distribution in Response to changes in turbidity stemming from bivalve filtration and seagrass sediment stabilization. *Estuaries* 27, 793–806. doi: 10.1007/bf02912041

Paul, M., and Gillis, L. G. (2015). Let if flow: how does an underlying current affect wave propagation over a natural seagrass meadow? *Mar. Ecol. Prog. Ser.* 523, 57–70. doi: 10.3354/meps11162

Peterson, C. H., Luettich, R. A., Micheli, F., and Skilleter, G. A. (2004). Attenuation of water flow inside seagrass canopies of differing structure. *Mar. Ecol. Prog. Ser.* 268, 81–92. doi: 10.3354/meps268081

Ruiz, J. M., and Romero, J. (2001). Effects of *in situ* experimental shading on the Mediterranean seagrass *Posidonia oceanica* (l.) Delile. *Mar. Ecol. Prog. Ser.* 215, 107–120. doi: 10.3354/meps215107

Sas Institute Inc. (2002). *SAS 9.2 Software Package*. Cary: SAS Institute, Inc.

Short, F. T. (1975). *Eelgrass Production in Charlestown Pond: An Ecological Analysis and Simulation Model*. M.S. Thesis, University of Rhode Island, Kinston, RI, 180.

Short, F. T., Burdick, D. M., and Kaldy, J. E. (1995). Mesocosm experiments quantify the effects of eutrophication on eelgrass, Zostera marina. *Limnol. Oceanogr.* 40, 740–749. doi: 10.4319/lo.1995.40.4.0740

Sprugel, D. G. (1976). Dynamic structure of wave-regenerated *Abies balsamea* forests in the north-eastern United States. *J. Ecol.* 64, 889–911.

Stewart, H. L. (2004). Hydrodynamic consequences of maintaining an upright posture by different magnitudes of stiffness in buoyancy in the tropical alga *Turbinaria ornata*. *J. Mar. Syst.* 49, 157–167. doi: 10.1016/j.jmarsys.2003.05.007

Valentine, J. F., Heck, K. L., Harper, P., and Beck, M. (1994). Effects of bioturbation in controlling turtlegrass *Thalassia testudinum* (Banks ex Konig) abundance: evidence from field enclosures and observations in the Northern Gulf of Mexico. *J. Exp. Mar. Biol. Ecol.* 178, 181–192. doi: 10.1016/0022-0981(94)90035-3

van der Heide, T., van Nes, E. H., van Katwijk, M. M., Olff, H., and Smolders, A. J. P. (2011). Positive feedbacks in seagrass ecosystems – evidence from large-scale empirical data. *PLoS One* 6:e16504. doi: 10.1371/journal.pone.0016504

Veblen, T. T. (1985). "Stand dynamics in Chilean *Nothofagus* forests," in *The Ecology of Natural Disturbance and Patch Dynamics*, eds P. S. White and S. T. A. Pickett (Cambridge, MA: Academic Press), 35–51. doi: 10.1016/b978-0-08-050495-7.50008-9

Verduin, J. J., and Backhaus, J. O. (2000). Dynamics of plant-flow interactions for the seagrass *Amphibolis antarctica*: field observations and model simulations. *Est. Coast. Shelf Sci.* 50, 185–204. doi: 10.1006/ecss.1999.0567

Wainwright, S. A., Biggs, W. D., Currey, J. D., and Gosline, J. M. (1976). *Mechanical Design in Organisms*. New York: John Wiley and Sons.

Worcester, S. E. (1995). Effects of eelgrass beds on advection and turbulent mixing in low current and low shoot density environments. *Mar. Ecol. Prog. Ser.* 126, 223–232. doi: 10.3354/meps126223

Conflict of Interest Statement: MF was employed by NOAA during the collection of the data and by CSA Ocean Sciences Inc. during the analysis and writing of the manuscript.

The remaining authors declare that the research was conducted in the absence of any commercial or financial relationships that could be construed as a potential conflict of interest.

Advantages of publishing in Frontiers

OPEN ACCESS
Articles are free to read for greatest visibility and readership

FAST PUBLICATION
Around 90 days from submission to decision

HIGH QUALITY PEER-REVIEW
Rigorous, collaborative, and constructive peer-review

TRANSPARENT PEER-REVIEW
Editors and reviewers acknowledged by name on published articles

Frontiers
Avenue du Tribunal-Fédéral 34
1005 Lausanne | Switzerland

Visit us: www.frontiersin.org
Contact us: info@frontiersin.org | +41 21 510 17 00

REPRODUCIBILITY OF RESEARCH
Support open data and methods to enhance research reproducibility

DIGITAL PUBLISHING
Articles designed for optimal readership across devices

FOLLOW US
@frontiersin

IMPACT METRICS
Advanced article metrics track visibility across digital media

EXTENSIVE PROMOTION
Marketing and promotion of impactful research

LOOP RESEARCH NETWORK
Our network increases your article's readership